Woods Hole Oceanographic Institution **WHOI-97-02**

Technical Report
March 1997

Acquisition, Description and Evaluation of Atmospheric Model Products for the Coastal Mixing and Optics Experiment

by

Mark F. Baumgartner
Steven P. Anderson

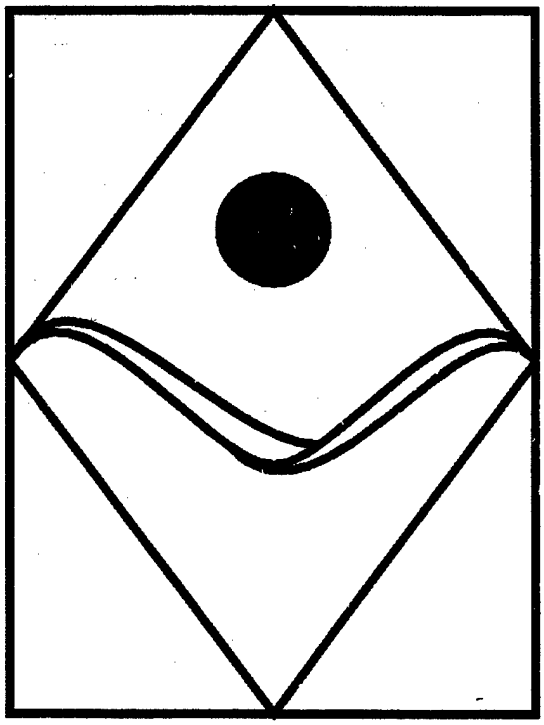

Upper Ocean Processes Group
Woods Hole Oceanographic Institution
Woods Hole, Massachusetts 02543

UOP Technical Report 97-01

WHOI-97-02
UOP Report 97-01

Acquisition, Description and Evaluation of Atmospheric Model Products for the Coastal Mixing and Optics Experiment

by

Mark F. Baumgartner
Steven P. Anderson

Upper Ocean Processes Group
Woods Hole Oceanographic Institution
Woods Hole, Massachusetts 02543-1541

March 1997

Technical Report

Funding provided by the Office of Naval Research under
Contract No. N00014-95-1-0339

Approved for Distribution:

Philip L. Richardson, Chair
Department of Physical Oceanography

Abstract

Numerical weather forecasting model products were acquired for use in the Coastal Mixing and Optics (CMO) Experiment to augment in situ observations of meteorological parameters (e.g., wind speed and direction, air temperature and relative humidity) at a moored array of buoys in the Middle Atlantic Bight. In this report, the Eta and Rapid Update Cycle (RUC) regional models are described and the two methods of acquisition via the Internet, the Internet Data Distribution (IDD) system and file transfer (FTP) from the NOAA Information Center's data server, are discussed. Processing and archival of the model data are also addressed. Data from the CMO central mooring and six National Data Buoy Center (NDBC) buoys in the Middle Atlantic Bight were used to evaluate the accuracy of the model products. Comparisons between model and in situ wind speed, wind direction, barometric pressure, air temperature and sea surface temperature were possible for all seven of the buoys. Since no moisture measurement was made from the NDBC buoys, comparisons of relative and specific humidity were only possible at the CMO buoy. Sensible and latent heat fluxes and global (net) radiation from the models were compared to estimates of heat fluxes and net radiation from the CMO central buoy.

Table of Contents

List of Figures

List of Tables

Section 1: Introduction

The scientific objective of the moored array component of the ONR Coastal Mixing and Optics (CMO) Experiment is to identify and understand the oceanic mixing processes influencing the evolution of the vertical temperature stratification on the continental shelf. To address this objective, four moorings were deployed at mid-shelf in the Middle Atlantic Bight; a central mooring on the 70m isobath and three surrounding moorings located ~10km inshore along the 60m isobath, ~10km offshore along the 80m isobath and ~25km alongshore to the east in 70m of water. These buoys were deployed in August 1996 and will be recovered in June of 1997. This observing period spans the destruction of the thermal stratification in fall and redevelopment of the thermal stratification in spring. The moorings support instrumentation to measure the ocean temperature, salinity and velocity structure and variability as well as the surface meteorology. The observations from this moored array will be used to investigate changes in the stratification in response to atmospheric forcing, surface gravity wave variability, surface and bottom boundary layer mixing, current shear, internal waves and advection.

The oceanic variability on the continental shelf is closely tied to temporal and spatial variability in the atmospheric forcing. To characterize the local atmospheric forcing, a surface buoy at the central mooring site contains redundant Vector Averaging Wind Recorder (VAWR) meteorological instrumentation (Weller *et al.*, 1990). Both VAWR packages measure wind speed and direction, incoming short-wave and long-wave radiation, relative humidity, air temperature, sea-surface temperature, barometric pressure. In addition, two stand-alone, internally logging precipitation gauges are on the buoy. The buoy observations will provide the various parameters necessary for estimating the local surface momentum, heat and buoyancy fluxes. The three surrounding mooring sites each support a WeatherPak 2000 meteorological package (Coastal Environmental Systems, Seattle, Washington) which records wind speed and direction, air temperature, relative humidity and barometric pressure.

The surface meteorological observations from the moored array provide limited information about the remote atmospheric forcing. Gridded products from numerical weather forecasting models can offer more complete descriptions of the spatial variability over the ocean. Surface flux estimates from European Centre for Medium-Range Weather Forecasts (ECMWF) and National Centers for Environmental Prediction (NCEP) global numerical models are commonly used by oceanographers to force basin-scale ocean models. However, the resolutions of these global analysis fields are too low both in time and space to be useful in understanding the

oceanic response on the continental shelf. In addition, the accuracy of these flux fields near the coast is questionable.

The regional numerical weather models, such as NCEP's Eta and Rapid Update Cycle (RUC) models, offer surface fields with higher spatial and temporal resolutions. The domain of these two models in particular covers much of the U.S. continental shelf. The coastal ocean community does not typically use the surface fields from these weather forecasting models and little work has been done to validate these surface fields over the ocean. The CMO program provides a good opportunity to both validate and utilize these surface fields.

The first part of this report (Sections 2, 3 and 4) briefly describes the Eta and RUC numerical weather prediction models and the methods by which the model and in situ data were acquired and archived. The final section (Section 5) provides a preliminary comparison of the surface model products with the meteorological observations from the CMO central site and six National Data Buoy Center (NDBC) buoys located in the Middle Atlantic Bight.

Section 2: Model Descriptions

Data from two regional NCEP models, the Eta and Rapid Update Cycle (RUC), were acquired for the CMO experiment. Each model's native domain is shown in Figure 1 and the features of each, including domain parameters, model run and forecast times and surface data availability, are provided in Tables 1 and 2. Although the RUC model is run on the 87 grid (Table 2), it is interpolated to the 211 grid by NCEP so that it can be compared to other models. Note that the list of variables in Table 1 are a subset of the variables available in each model. References for documentation of all the model products are given in Appendices D and E.

Table 1. Model products acquired for the CMO experiment. A "D" denotes the variable can be derived from other variables.

	Eta	RUC	RUC Analysis	RUC Hourly
Data Source	IDD	IDD	NIC	NIC
Native Domain	211	87	87	87
Distributed Domain	211	211	87	87
Model Run Interval (hours)	12	3	3	3
Forecast Hours	0–48	0–12	-	0–12
Forecast Interval (hours)	6	3	-	1
Variables				
East Wind ($m\ s^{-1}$)	X	X	X	X
North Wind ($m\ s^{-1}$)	X	X	X	X
Air Temperature (°C)	X	X	D	D
Relative Humidity (%)	X	X	D	D
Surface Pressure (mbar)	X	X		
Mean Sea Level Pressure (mbar)	X	X	X	X
Condensation Pressure (mbar)			X	X
Potential Temperature (°C)			X	X
Convective Inhibition ($J\ kg^{-1}$)	X	X		X
Convective Available Potential Energy ($J\ kg^{-1}$)	X	X		X
Precipitation over Accumulation Interval ($kg\ m^{-2}$)	X	X		
Large Scale Precipitation (non-convective) ($kg\ m^{-2}$)				X
Convective Precipitation ($kg\ m^{-2}$)				X
Precipitable Water ($kg\ m^{-2}$)				X
Latent Heat ($W\ m^{-2}$)				X
Sensible Heat ($W\ m^{-2}$)				X
Global Radiation ($W\ m^{-2}$)				X
Sea Surface Temperature (°C)				X
Precipitation Rate ($kg\ m^{-1}\ s^{-1}$)				X

The Eta model (also known as the Early Eta) is a 38-level eta-coordinate model run on the 211 grid. It is run every 12 hours and produces forecasts up to 48 hours into the future. The

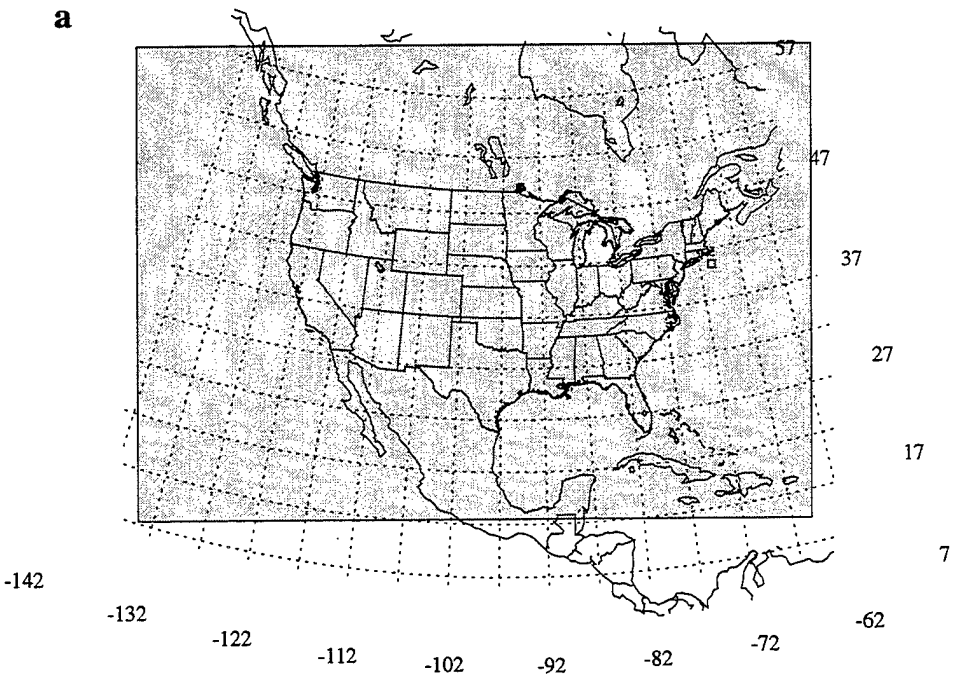

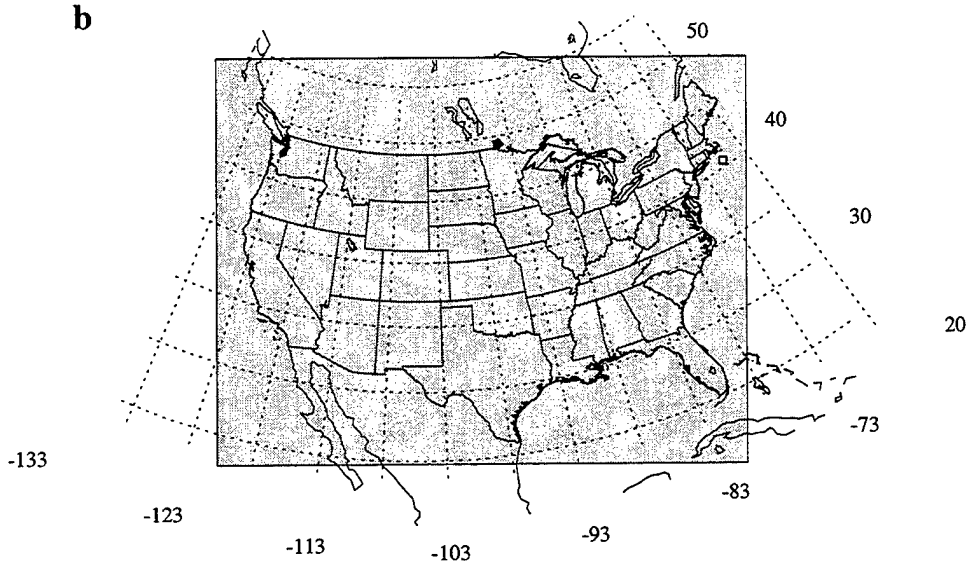

Figure 1. Domains of the (a) 211 and (b) 87 grids.

Eta model is initialized with output from the Global Data Assimilation System (GDAS) and the Eta optimal interpolation (OI) scheme. The 0 (initialized), 6, 12, 18, 24, 30, 36, 42 and 48 hour forecasts from this model are available from the Internet Data Distribution (IDD) system on the native 211 grid in GRIB format.

Table 2. Model domain parameters.

	Grid 87	Grid 211
Projection	Polar stereographic	Lambert Conformal Conic
Horizontal Resolution	60km (at 40°N)	80km (at 35°N)
Dimensions	81 x 62	93 x 65
NW Corner	52.489°N, 136.546°W	54.536°N, 152.856°W
NE Corner	46.017°N, 60.828°W	57.290°N, 49.385°W
SW Corner	22.876°N, 120.491°W	12.190°N, 133.459°W
SE Corner	20.128°N, 81.243°W	14.335°N, 65.091°W

The RUC model is the operational version of the Mesoscale Analysis and Prediction System (MAPS) developed by the Forecast Systems Laboratory (FSL) of the National Oceanic and Atmospheric Administration (NOAA). This model is a 25-level, hybrid isentropic-sigma coordinate analysis and forecast system which is run on the 87 grid. The model is run every three hours and produces forecasts up to 12 hours into the future. Data from rawinsonde, commercial aircraft, profilers and surface stations are assimilated in an analysis before each model run. The model is initialized at the start of each three hour run with a filtered product of the analysis. This filtered product is distributed as the 0 hour forecast.

Data from the RUC model are available from both the IDD and the NOAA Information Center (NIC) server in GRIB format. The data from the IDD are available on the 211 grid and consist of the 0 (initialized), 3, 6, 9 and 12 hour forecasts only. Model data from the NIC server are available both on the native 87 grid and the 211 grid. These data include analysis, initialized and hourly (1–12 hour) forecasts fields.

Section 3: Data Acquisition

NCEP and ECMWF model data are available through Unidata's Internet Data Distribution (IDD) system of which the Woods Hole Oceanographic Institution (WHOI) is a licensed member. The IDD is a distributed system, meaning that the data is not accessed at a single centralized server. There are three ways a computer can interact with the IDD; as a source, a relay or a sink. A source is a computer that inserts data into the system for use by an authorized group of computers called downstream hosts, a sink is a computer that accepts data from a source or a relay (i.e., its upstream host), and a relay is a computer that accepts data from its upstream host and then inserts that same data back into the system for its authorized group of downstream hosts (Figure 2). A workstation at WHOI is a sink, receiving data only from one upstream host. The flow of data within the IDD is managed by software on each computer in the system called the Local Data Manager (LDM) software.

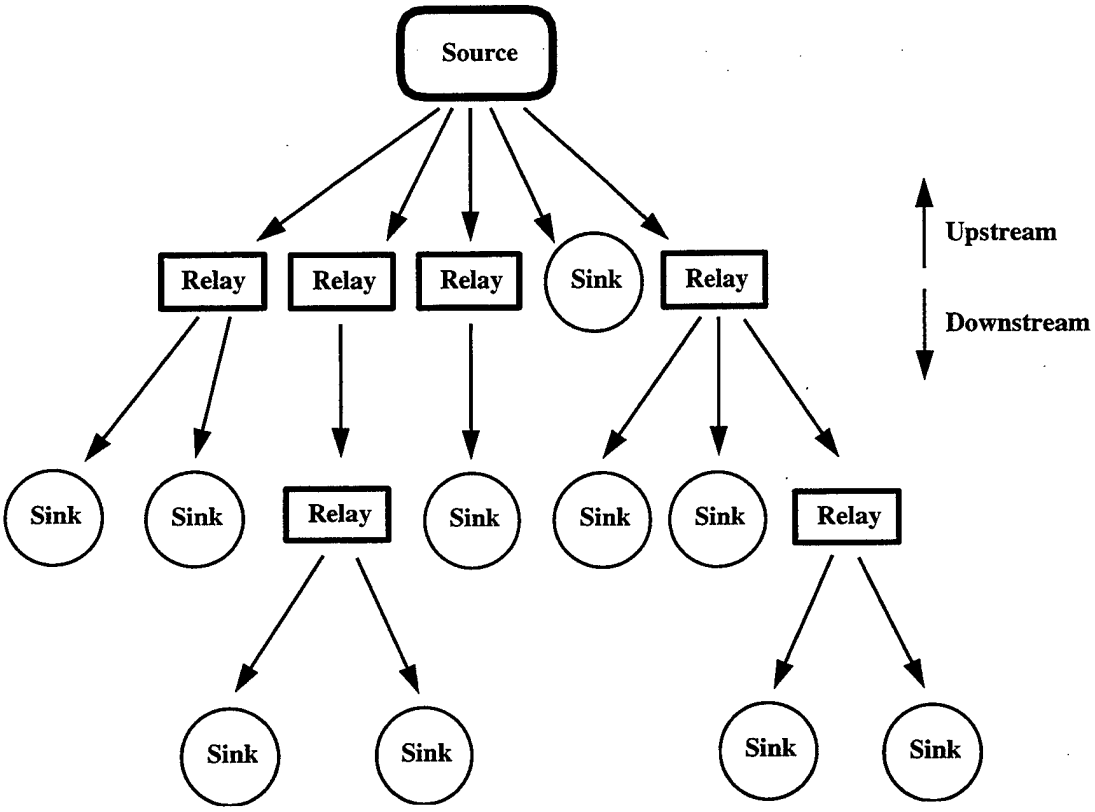

Figure 2. Conceptual distribution scheme of the Internet Data Distribution (IDD) system.

The LDM software is a daemon that runs in the background on a workstation. After initial configuration, the software requires no user input. For a source or a relay, the LDM

coordinates the delivery of data to downstream hosts. On a relay or sink computer, the LDM delivers requests for data to an upstream host and then coordinates delivery and any additional processing of the data. Data requests sent from sinks to sources or relays specify the type of data the sink wishes to acquire from its upstream host. The entire National Weather Service (NWS) Family of Services (FOS) are available through the IDD, including weather bulletins, surface station observations, upper-air data, atmospheric model products and buoy reports. Also available are ECMWF model products, GOES imagery, NEXRAD radar mosaics and data from the National Lightning Detection Network, although some services require additional licensing agreements with institutions other than Unidata. For the CMO experiment, RUC and Eta model data are requested from an upstream host and as the data become available on the upstream host, it is delivered to a WHOI workstation running the LDM software.

Additional model data from NCEP are available on the NIC server and can be acquired via the anonymous file transfer program (FTP). The full suite of RUC model products on the native 87 grid are available from this server, including the analysis and 12 hourly forecast files. Similar RUC products are also available on the 211 grid. The files listed in Table 3 can be downloaded from the directory `pub/ruc` on the NIC server, `nic.fb4.noaa.gov`. Currently, only products on the 87 grid are being obtained from the NIC for the CMO experiment, since the 211 grid products are being acquired from the IDD. Output from other models are also available from the NIC server, including the Eta, Nested Grid Model (NGM), Aviation and Medium Range Forecast (MRF) models.

Table 3. RUC model output files available via anonymous FTP from `nic.fb4.noaa.gov` in the `pub/ruc` directory. All files are in GRIB format. The model run hour is denoted as ##, where possible values are 00, 03, 06, 09, 12, 15, 18, 21. XX denotes the forecast hour from 01 to 12 in one hour increments.

	File
87 Grid	
Analysis Field	`ruc.T##Z.grbbanl`
Initialized Field (0 hour forecast)	`ruc.T##Z.grbbf00`
1–12 hour Forecast	`ruc.T##Z.grbbfXX`
211 Grid	
Analysis Field	`ruc.T##Z.grb2anl`
Initialized Field (0 hour forecast)	`ruc.T##Z.grb2f00`
1–12 hour Forecast	`ruc.T##Z.grb2fXX`

Because of the large volume of model data available, only the surface variables for selected forecasts are archived. These variables are explicitly labeled as the surface variables in the Eta

and RUC files distributed via the IDD. Since there are no separate surface variables distributed in the RUC Analysis and RUC Hourly datasets, the variables from the hybrid level closest to the surface (Level 1) in these datasets are treated as the surface variables. The forecast hours selected for archival are presented in Table 4. Once the model data are acquired from either the IDD or the NIC, the surface variables for the selected forecasts are extracted, reformatted from GRIB to NetCDF and archived.

Table 4. Archived forecast hours and filenames for each model. Year of century, month, day and hour are denoted as YY, MM, DD and HH, respectively. Italicized filename dates are the forecast times and non-italicized dates are model run times.

Model	Forecast Selection	Archived Filename	Archive files per model run	Forecast or analysis fields per file
Eta	0, 6, 12, 18 and 24 hour	YYMMDDHHeta.nc	1	5
RUC	0, 3, 6, 9 and 12 hour	YYMMDDHHruc.nc	1	5
RUC Analysis	Each 3 hour analysis	YYMMDDHHrucanl.nc	1	1
RUC Hourly	1, 2, and 3 hour	*YYMMDDHH*rucflux.nc	3	1

Forecast data from each model run of the Eta model are archived as a single NetCDF file. The file contains the model output for each of the forecast hours listed in Table 4 and the NetCDF format is listed in Appendix C. The RUC model data from the IDD are archived in the same manner as the Eta model. The RUC Analysis data from the NIC are generated only once every model run, so the archived file contains only the analysis fields and no forecast fields. The RUC Hourly data from the NIC are archived as a single NetCDF file for each forecast hour. For each RUC model run, three NetCDF archive files of RUC Hourly data are generated for the 1, 2 and 3 hour forecasts.

Acquisition of the models from both the IDD and NIC is entirely dependent on network availability. Data gaps in the time series of archived model products arise from network or power outages. Fortunately, these outages are infrequent and an uninterruptible power supply (UPS) serves the WHOI LDM workstation to protect against local transient power problems. Since the moored array is relatively close to Woods Hole, the most energetic events that may be scientifically significant (e.g., Hurricane Edouard in early September 1996) can knock power out at WHOI. During these events, model acquisition may become impossible. Data archives of the model data from the IDD are available, but these archives are not supported by Unidata and are available only as a courtesy to the IDD community by other users. The archive used for the CMO experiment at the University of Illinois at Urbana-Champaign only keeps the last

36 hours of NCEP and ECMWF model data due to immense storage requirements. Data on the NIC server is, at most, 24 hours old. Because of outages and implementation problems, the data return of model products has been between 83 and 93%.

Section 4: Data Summary

In situ

To evaluate the accuracy of the numerical weather forecasting models, the model products were compared with in situ observations from buoys in the Middle Atlantic Bight (Figure 3). These observations were collected from the CMO central mooring and six NDBC buoys from 1 August 1996 to 31 January, 1997.

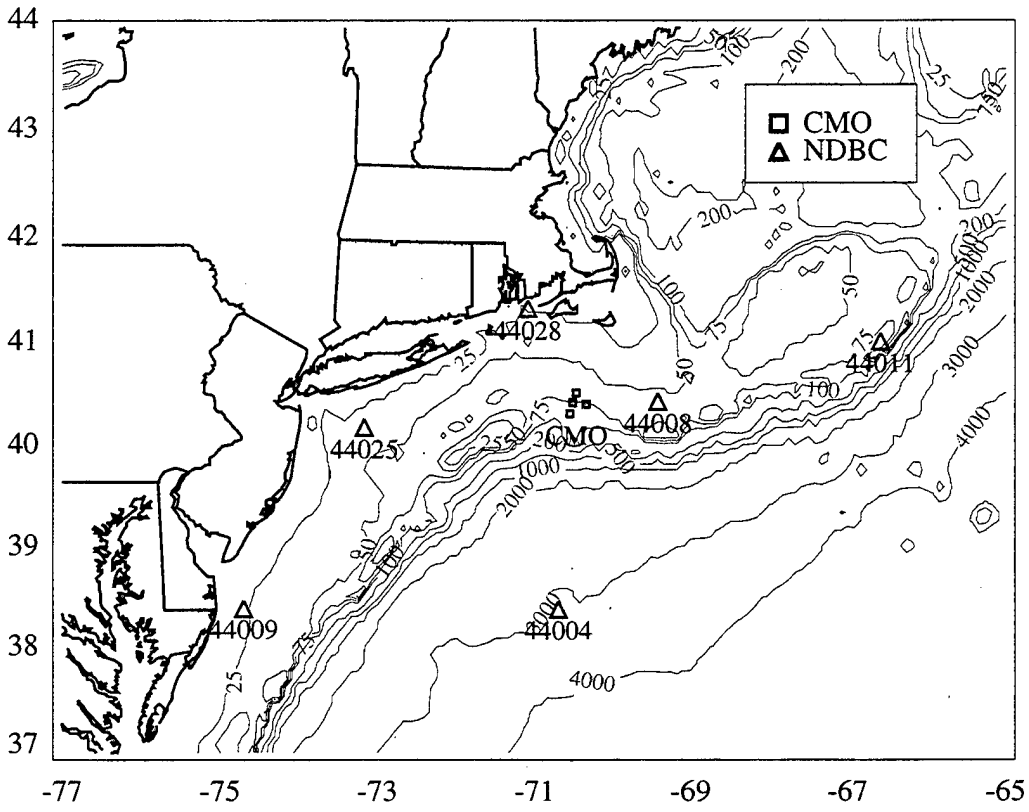

Figure 3. Coastal Mixing and Optics moored array and surrounding National Data Buoy Center buoys.

The CMO central mooring carried two, redundant Vector Averaging Wind Recorder (VAWR) meteorological packages (Weller *et al.*, 1990) which measure wind speed and direction, incoming short-wave and long-wave radiation, air temperature, relative humidity, barometric pressure and sea surface temperature at a 15 minute sampling rate (Figure 4). The sensor specifications for this package are presented in Table 5. The VAWR telemeters the meteorological data to the NOAA-series polar orbiting satellites. The data can then be accessed by CMO investigators via Service Argos and once downloaded, the data are calibrated, quality

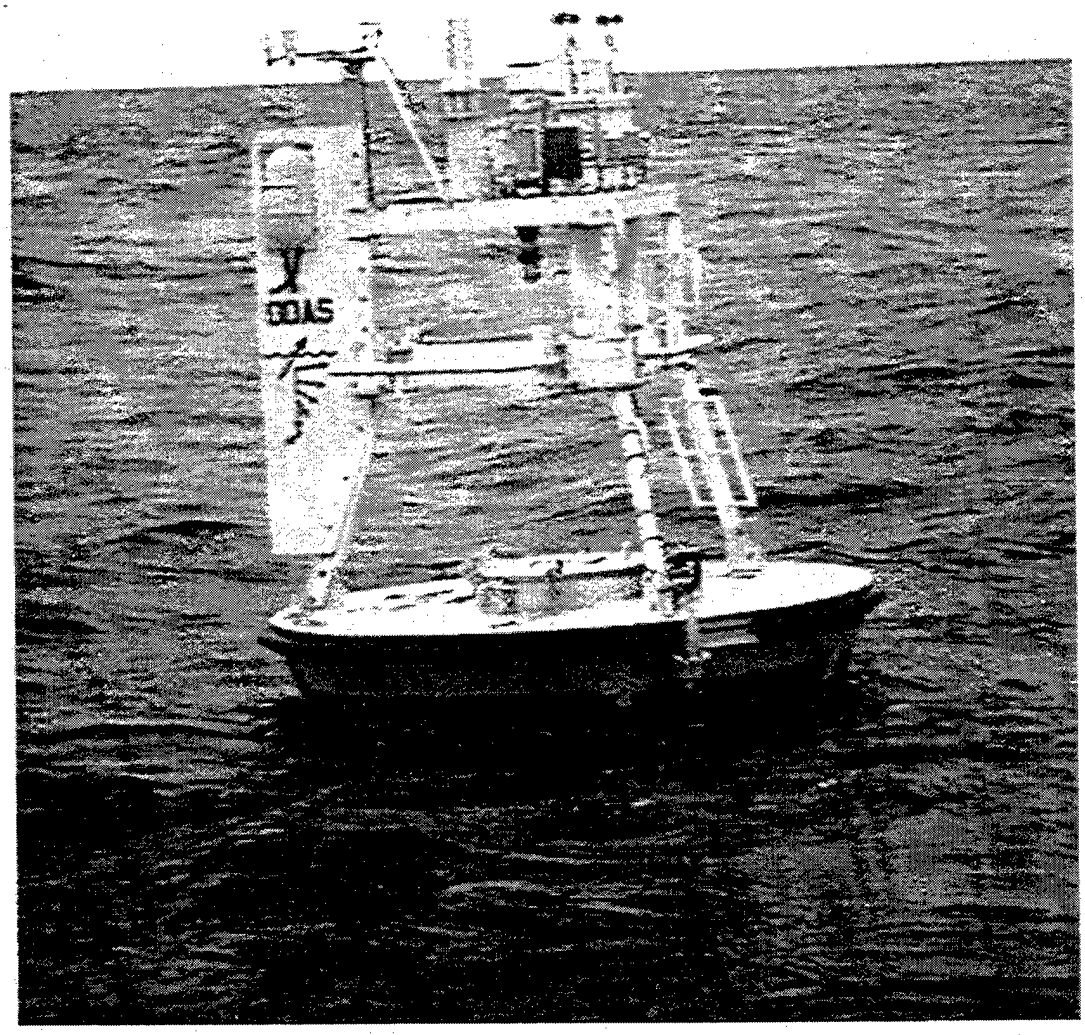

Figure 4. Coastal Mixing and Optics central 3m discus buoy.

controlled and reformatted to NetCDF before analysis. Heat and momentum fluxes were estimated from the telemetered meteorological observations using the TOGA COARE bulk flux algorithm (Fairall *et al.*, 1996) with both the warm layer and cool skin adjustments omitted.

Table 5. VAWR sensor specifications. Wind speed and direction are vector averaged over the sampling interval. Heights are reported as meters above the mean water line.

Parameter	Sampling Interval	Range	Accuracy	Height
Wind speed	15 minute average	0.2–50.0ms^{-1}	±2% above 0.7ms^{-1}	3.30
Wind direction	15 minute average	0–360°	±5.6°	3.02
Air temperature	3.75 minute average	-10–35°C	±0.2°C when wind > 5ms^{-1}	2.63
Sea temperature	3.75 minute average	-5–30°C	±0.005°C	-1.46
Barometric pressure	2.5 second sample	0–1034mbar	±0.2mbar when wind < 20ms^{-1}	2.72
Relative humidity	3.5 second sample	0–100%	±2%	2.68
Short-wave radiation	15 minute average	0–1400Wm^{-2}	±3% of value	3.39
Long-wave radiation	15 minute average	0–700Wm^{-2}	±10%	3.40

Six NDBC buoys deployed in the Middle Atlantic Bight near the CMO mooring were selected for evaluating the model products (Table 6). Each of these buoys carries a DACT sensor payload that measures wind speed and direction, wind gust speed, significant wave height, wave period, air and sea surface temperature and barometric pressure every hour. Sensor specifications for the DACT payload are presented in Table 7 and the buoy hull types are shown in Figure 5. The time series of these measurements is available on the NDBC anonymous FTP server, `seaboard.ndbc.noaa.gov`. Heat fluxes were not computed at the NDBC buoy sites, since no moisture variable (e.g., relative humidity, specific humidity or dewpoint temperature) was measured.

Table 6. Locations, depths and hull types of NDBC buoys. Water depths are in meters.

NDBC Buoy	Latitude	Longitude	Water depth	Hull Type
44004	38° 27' 23" N	70° 41' 23" W	3,163	6m NOMAD
44008	40° 30' 0" N	69° 25' 0" W	62	3m discus
44009	38° 27' 49" N	74° 42' 7" W	28	3m discus
44011	41° 5' 0" N	66° 35' 0" W	88	6m NOMAD
44025	40° 15' 1" N	73° 10' 0" W	40	3m discus
44028	41° 23' 47" N	71° 5' 6" W	22	USCG Large Nav

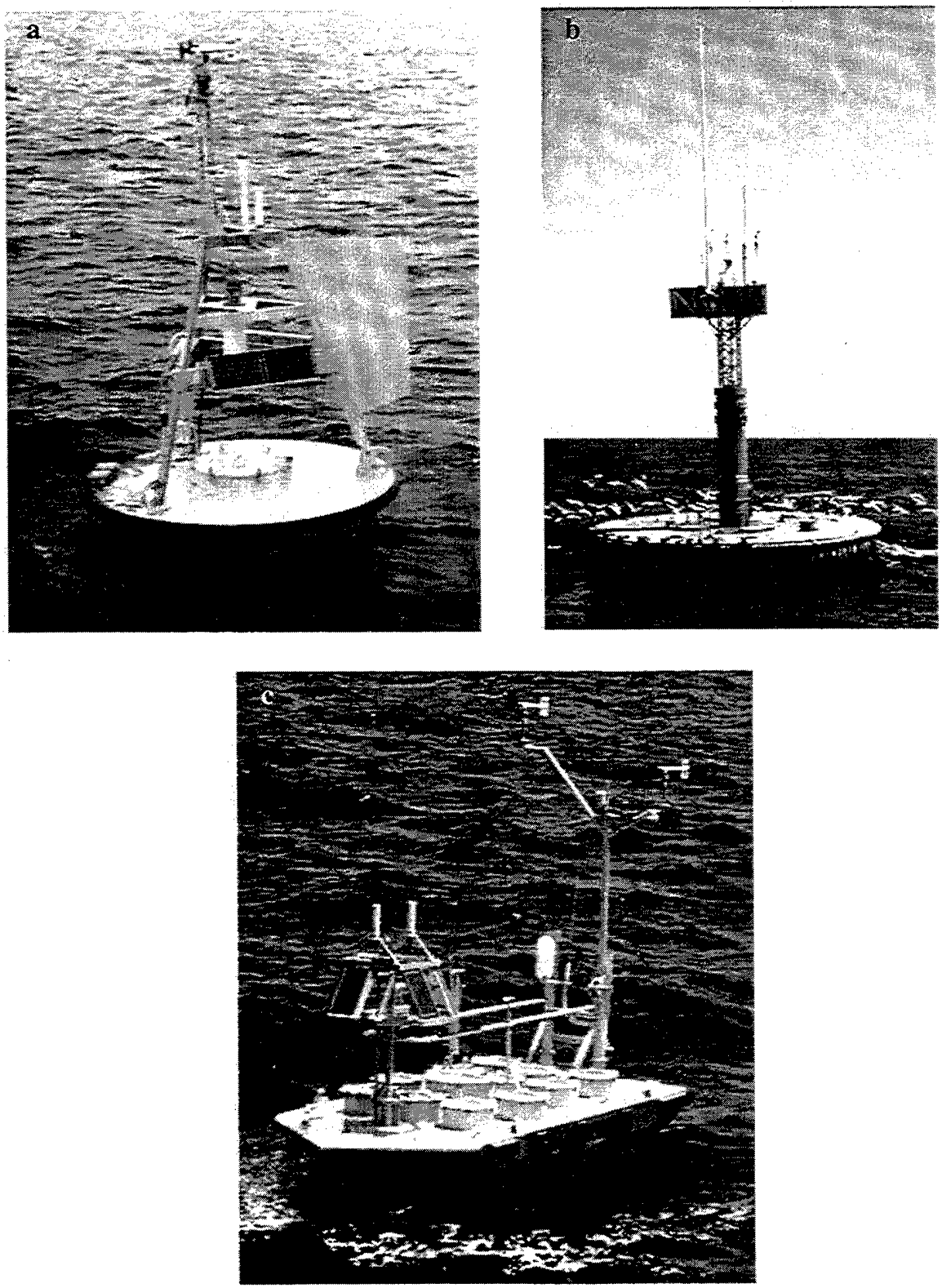

Figure 5. (a) NDBC 3m discus buoy. (b) U.S. Coast Guard large navigational buoy. (c) NDBC 6m NOMAD buoy. Photos courtesy of National Data Buoy Center.

Table 7. NDBC DACT payload sensor specifications. Wind speed is scalar averaged over the sampling interval. Wind direction is calculated as arctan(u/v) where u and v are averaged east and north components, respectively, of a unit vector oriented in the direction of the wind. Heights are in meters relative to the mean water line.

Parameter	Sampling Interval	Range	Accuracy	Height 3m and 6m buoys	Height USCG Large Nav
Wind speed	8 minute average	0.0–61.8ms^{-1}	±1ms^{-1} or ±10%	5.0	13.8
Wind direction	8 minute average	0–355°	±10°	5.0	13.8
Air temperature	8 minute average	-40–50°C	±1°C	5.0	12.3
Sea temperature	8 minute average	-6.7–40.6°C	±1°C	-1.0	-1.5
Barometric pressure	8 minute average	900–1100mbar	±1mbar	0.0	0.0

All in situ data were averaged to 6, 3, 3 and 1 hours to match the time base of the Eta, RUC, RUC Analysis and RUC Hourly datasets, respectively. Averages were centered on the model forecast time.

Model Products

The atmospheric model data were extracted from the archived files at the grid point closest to each of the buoys. For each time series, several processing steps were necessary to obtain the most accurate set of model products at the buoy location. At any point in the time series, data from several forecasts and possibly an initialized field (0 hour forecast) may be available. A simple selection algorithm was implemented to choose data from either an initialized field if available or from the closest forecast time. For example, to find the best RUC data for 1800 hours on a particular day, data may be available from a 12 hour forecast generated at 0600, a 9 hour forecast generated at 0900, a 6 hour forecast generated at 1200, a 3 hour forecast generated at 1500 and an initialized field from the 1800 hour model run. Since the initialized field is assumed to be the most accurate, it would be selected. If the initialized field is not available, the 3 hour forecast would be selected and so on.

After selection, common variables were derived as necessary. In the case of the RUC Analysis and Hourly datasets, moisture and temperature are represented as condensation pressure and potential temperature, respectively, which were converted to relative humidity, specific humidity and air temperature for analysis. Wind vectors also required adjustment, since the components of the wind vectors were oriented toward the +x and +y directions in the model domain, not true east and north. To account for this, wind vectors were rotated by the angles reported in Table 8. Wind directions were computed from the vector components in oceanographic convention, i.e., the direction toward which the wind is blowing.

Table 8. Rotation angles for wind vectors in degrees. All angles rotate east of north.

Buoy	Grid 211	Grid 87
CMO Central	10.2	34.7
NDBC 44004	10.4	34.1
NDBC 44008	11.0	35.7
NDBC 44009	8.5	30.1
NDBC 44011	11.9	38.0
NDBC 44025	9.4	32.3
NDBC 44028	10.3	33.9

The time series of most archived model products spanned 1 August 1996 to 31 January 1997. The entire RUC Analysis dataset, however, and the potential temperature and condensation pressure of the RUC Hourly dataset were not collected for the first two and a half months of the experiment. After preliminary analyses of the acquired model data and many subsequent conversations with Lauren Morone of NCEP, acquisition and archival of these model products was initiated on 25 October 1996.

No attempts were made to account for possible differences in the measurement heights of the in situ observations and the model products. The designated heights of the model products distributed as the surface fields or as the gridded fields closest to the surface are unclear. These products are probably equivalent to 10m winds and 2m air temperature and humidity, however, for the sake of simplicity, the following analyses treat the in situ and model data as measured or forecast at the same height.

Section 5: Evaluation of Model Products

In situ data from the CMO central mooring and the six NDBC buoys were compared to time series of model products at the grid points closest to each of these platforms (Figure 6). Evaluations of wind speed and direction, barometric pressure and air temperature were possible for all platforms while relative and specific humidity, sensible and latent heat fluxes and global radiation could only be evaluated at the CMO central buoy. Sea surface temperature from the RUC Hourly was evaluated at each buoy site. Detailed presentations of the comparisons are included in Appendix A. Summary information is provided below.

The mean and standard deviations of the difference between the model and the in situ observations are presented in Figure 7. Positive differences indicate that the model is higher or larger than the in situ data. The NDBC buoys are grouped as the offshore (44004, 44008 and 44011) and inshore (44009, 44025, 44028) buoys. Positive heat flux and global radiation values indicate ocean heating.

Wind Speed

Analyses of the model wind speeds versus the observed in situ wind speeds are presented in Figures A1 through A28. The mean differences and correlation coefficients between the model and the in situ wind speeds are shown in Table A1 and summarized in Table 9. The mean differences for the Eta model slightly exceed the accuracies of the sensors for the VAWR and NDBC buoys 44004, 44008 and 44009, however the overall mean difference (the average of the mean differences for all of the buoys) is comparatively small. This suggests that despite discrepancies at a few of the buoys, the wind speeds are reasonably accurate over the entire study area. The mean differences shown in Figure 7 also indicate that the Eta wind speeds may be a little too low near the coast and too high farther offshore.

Table 9. Average and range of mean [model - in situ] wind speed differences and range of model versus in situ wind speed correlation coefficients for all buoys.

	Mean Differences ($m\ s^{-1}$)			Correlation Coefficient	
Model	Average	Minimum	Maximum	Minimum	Maximum
Eta	0.13	-1.62	1.35	0.80	0.88
RUC	-0.64	-2.17	0.33	0.74	0.83
RUC Analysis	-1.27	-1.85	-0.73	0.72	0.85
RUC Hourly	-0.78	-1.50	-0.26	0.77	0.85

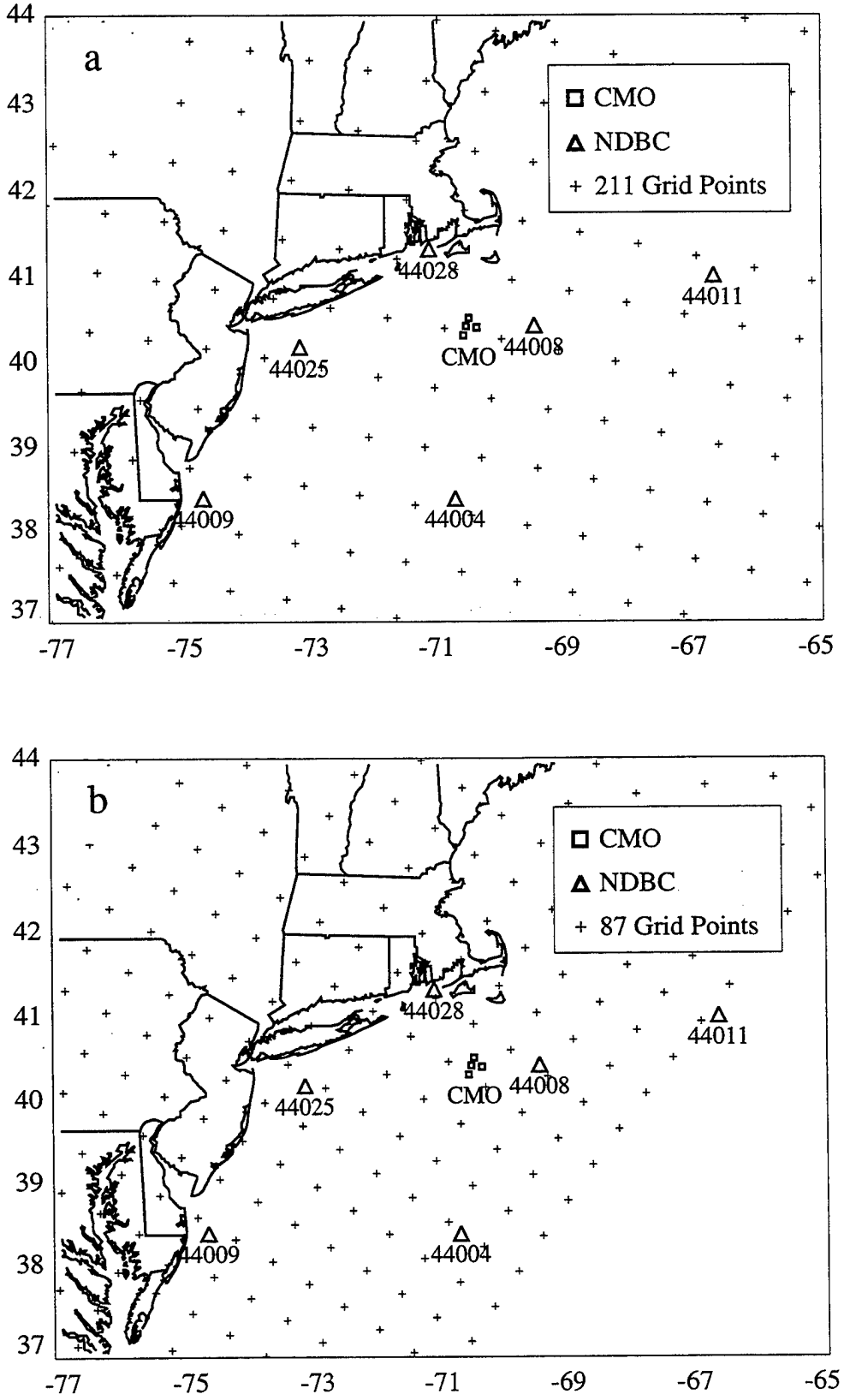

Figure 6. Locations of CMO buoys, NDBC buoys and (a) 211 and (b) 87 grid points.

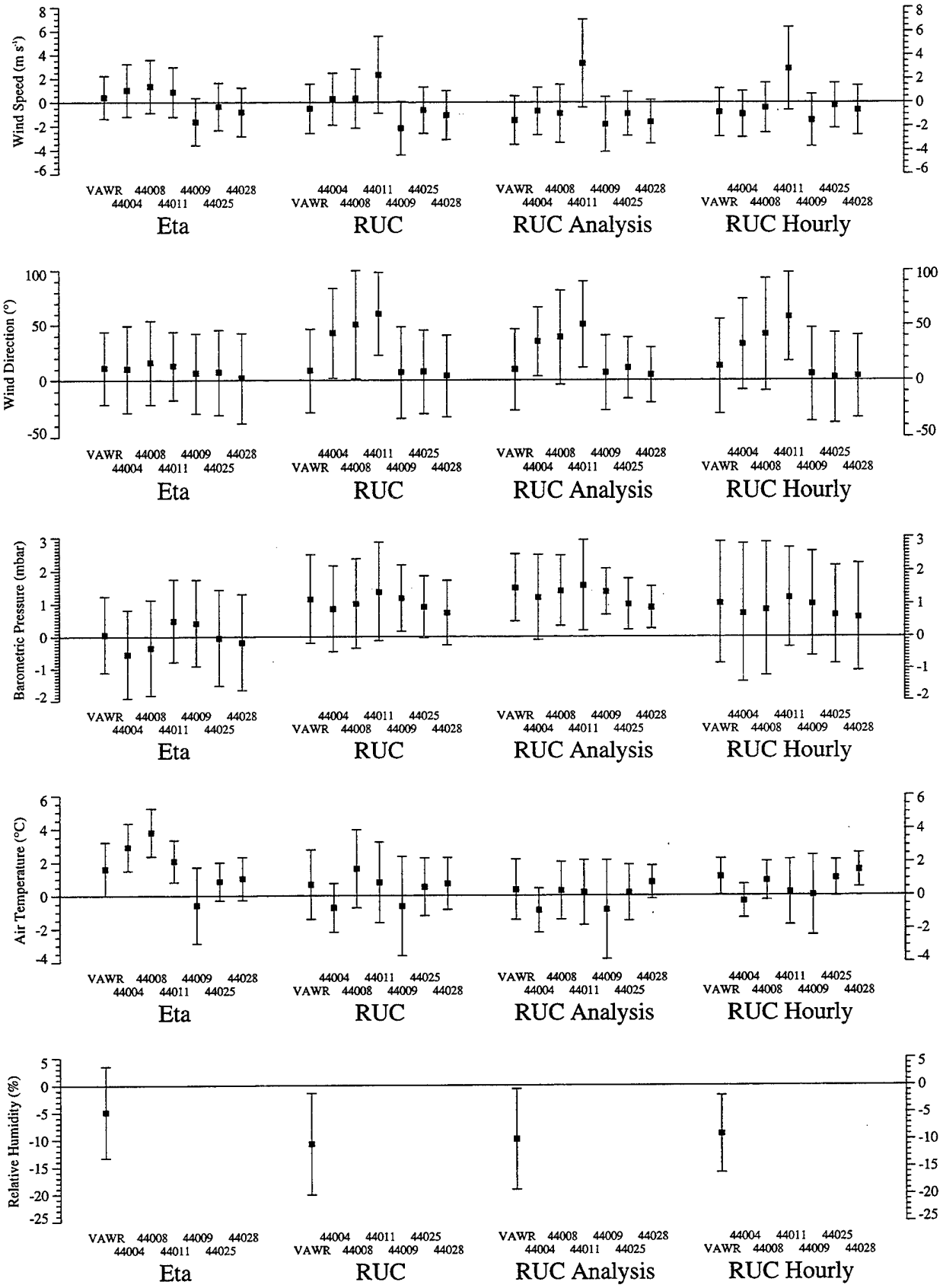

Figure 7. Mean and standard deviation of [model - *in-situ*] differences. Positive differences indicate the model is higher than the buoy.

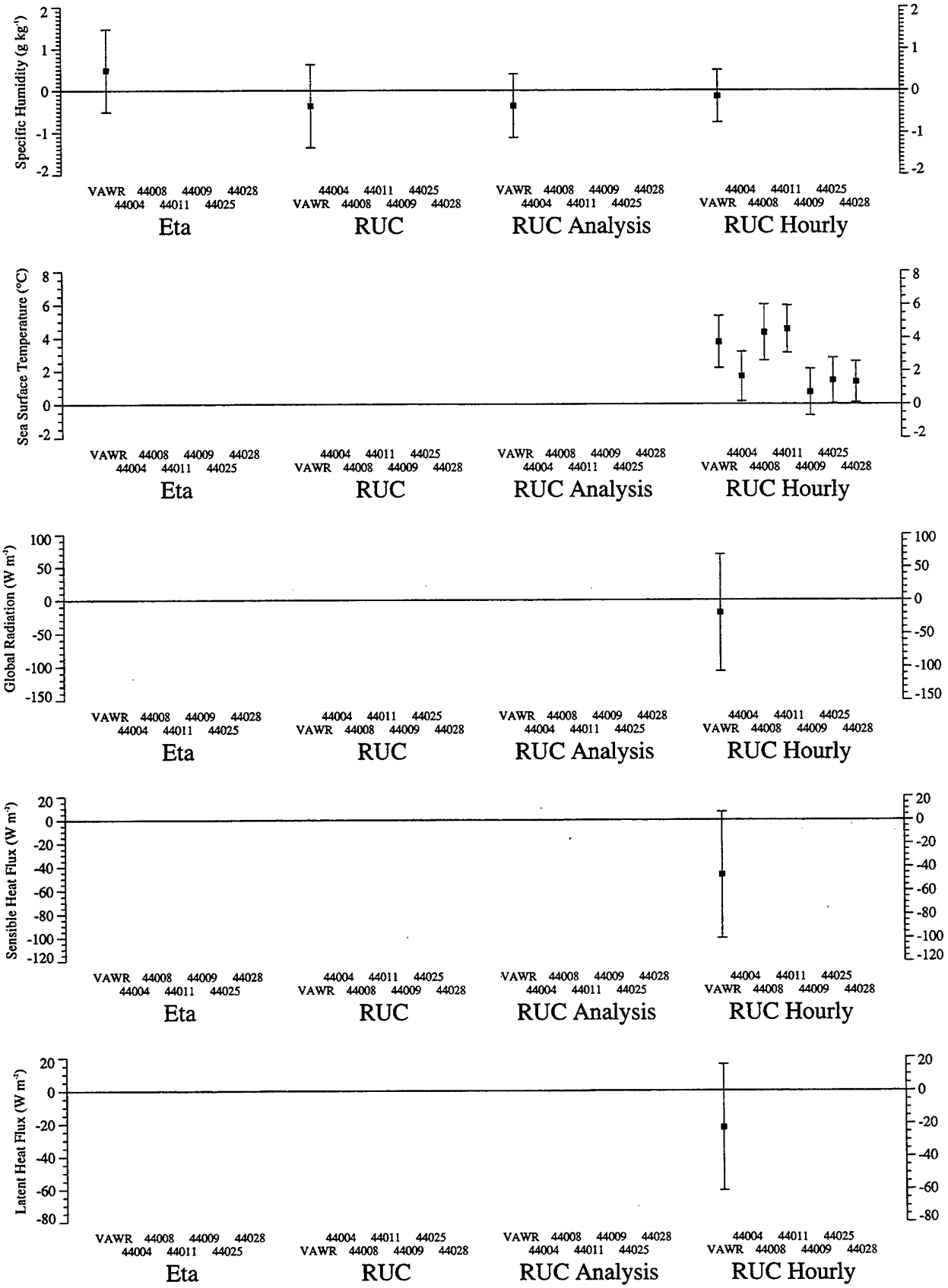

Figure 7 (continued)

The overall means for the RUC, RUC Analysis and RUC Hourly in Table 9 suggest that the wind speeds in the RUC model are low by roughly 0.9m s^{-1}. Although this overall bias is within the accuracy of the NDBC anemometer, the mean differences for the CMO buoy are considerably larger than the accuracy of the VAWR wind measurement. These mean differences, -0.53, -1.50 and -0.84m s^{-1} for the RUC, RUC Analysis and RUC Hourly, respectively, indicate that there is indeed a bias in the RUC model winds.

The comparison data from NDBC buoy 44011 were not included in the summary statistics since this buoy is clearly an outlier. This buoy was compared with a grid point that is at the very edge of the RUC domain (Figure 6b). Because wind speeds along the boundary of the RUC domain are much higher than those of adjacent grid points in the interior (Figure 8), these data were considered unreliable and were omitted from the summary analysis.

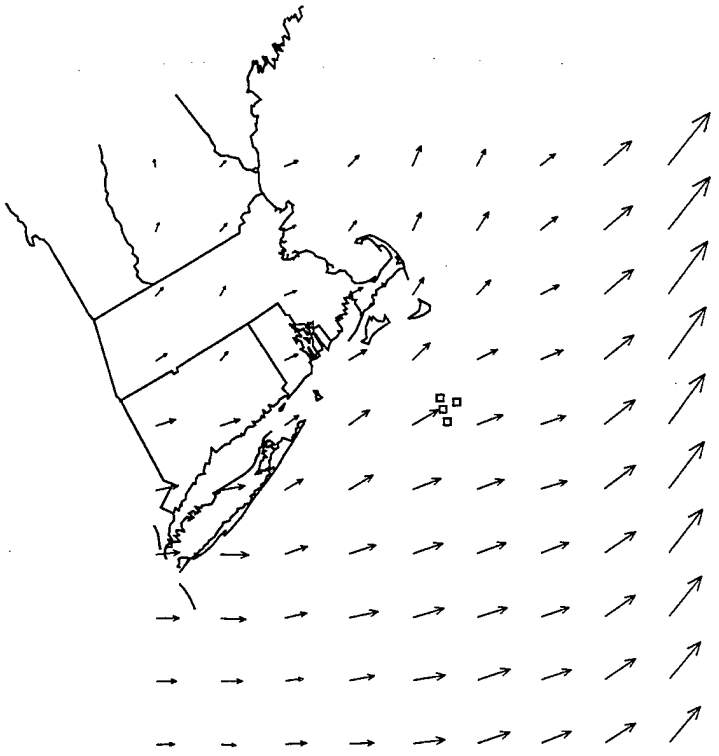

Figure 8. An example of anomalously high wind speeds at the edge of the RUC domain.

Wind Direction

Analyses of the model wind directions versus the observed wind directions are presented in Figures A29 through A56 and Table A2. The mean differences and correlation coefficients from the analyses are summarized in Table 10. Positive differences indicate that the model is rotated east of north (clockwise) relative to the buoy wind direction. The Eta model wind directions at the inshore NDBC buoys (44009, 44025 and 44028) are within the ±10° accuracy of the NDBC anemometer, however the Eta winds at the offshore NDBC buoys show a mean offset of 13.2° east of north relative to the observed wind direction. The Eta model winds at the CMO buoy are rotated well above the accuracy of the VAWR anemometer (±5.6°). These results suggest that the Eta model winds have a mean bias of approximately 10° east of north over the Middle Atlantic Bight.

Table 10. Average and range of mean [model - in situ] wind direction differences and range of model versus in situ wind direction correlation coefficients for all buoys.

	Mean Differences (°)			Correlation Coefficient	
Model	Average	Minimum	Maximum	Minimum	Maximum
Eta	9.6	2.2	16.1	0.93	0.96
RUC	25.9	4.1	60.4	0.90	0.94
RUC Analysis	22.5	4.8	50.7	0.91	0.97
RUC Hourly	22.4	2.5	57.8	0.89	0.94

The mean biases between the observed and RUC, RUC Analysis and RUC Hourly wind directions were 6.4, 7.6 and 4.0° at the inshore NDBC buoys and 51.2, 41.5 and 44.1° at the offshore NDBC buoys, respectively. All but one of the mean differences at the inshore NDBC buoys were within the ±10° accuracy of the NDBC anemometer, indicating good agreement. The mean biases between the RUC, RUC Analysis and RUC Hourly wind directions and those observed at the CMO buoy were 8.8, 9.8 and 12.8°, respectively. Table 11 shows the mean differences between the model and observed wind directions ordered by decreasing distance to the RUC domain boundary. The reported distance is between the RUC grid point closest to the buoy (i.e., the grid point from which the wind directions are selected for analysis) and the nearest boundary grid point. An inshore-offshore gradient in wind direction accuracy is evident, with the lowest biases occurring at the inshore sites and the largest biases (up to 60.4°) occurring at those sites closest to the domain boundary.

Table 11. Mean [model - in situ] wind direction differences in degrees, ordered by distance to the RUC domain boundary.

Buoy	Distance from boundary (km)	RUC	RUC Analysis	RUC Hourly
44009	412.2	7.3	6.9	5.7
44025	358.2	7.9	11.2	2.5
44028	301.4	4.1	4.8	3.8
CMO	240.0	8.8	9.8	12.8
44008	120.1	50.4	38.9	41.7
44004	118.4	42.8	35.0	32.7
44011	0.0	60.4	50.7	57.8

The large biases in wind direction at the offshore sites in the RUC, RUC Analysis and RUC Hourly are a result of the boundary conditions used in the RUC analysis and model. The boundary of the RUC domain (up to 5 grid points from the edge) is relaxed to the output of another NCEP regional model, the Nested Grid Model (NGM). Since the offshore buoys are within this boundary, the corresponding intercomparisons do not necessarily reflect the accuracy of the RUC model itself, but instead, evaluate the use of the NGM as a boundary condition for the RUC (Stan Benjamin, personal communication). Because of the large discrepancies in the model wind field near the RUC domain boundary, these wind directions should be used with considerable caution.

Barometric Pressure

Analyses of the model barometric pressure versus the observed in situ pressure are presented in Figures A57 through A84. The mean differences and correlation coefficients between the model and the in situ pressure are shown in Table A3 and summarized in Table 12. The Eta barometric pressures agree with the in situ observations within the accuracy of both the VAWR (±0.2mbar) and the NDBC sensor (±1mbar), indicating that this model is accurately representing the pressure field. The RUC, RUC Analysis and RUC Hourly datasets have mean differences of 1.0, 1.3 and 0.9mbars, respectively. These statistics suggest that the RUC pressure field is too high by roughly 1mbar, which might explain this model's lower wind speeds.

Table 12. Average and range of mean [model - in situ] barometric pressure differences and range of model versus in situ barometric pressure correlation coefficients for all buoys.

	Mean Differences (mbar)			Correlation Coefficient	
Model	Average	Minimum	Maximum	Minimum	Maximum
Eta	0.0	-0.6	0.5	0.98	0.99
RUC	1.0	0.7	1.4	0.99	0.99
RUC Analysis	1.3	0.9	1.6	0.99	1.00
RUC Hourly	0.9	0.6	1.2	0.97	0.99

Note that the high pressure events starting on 5 October 1996, 15 November 1996 and 27 January 1997 each exceeded the maximum measurement value for the VAWR barometric pressure sensor (Figures A57, A64, A71 and A78). The range of this instrument is 0 to 1034mbar (Table 5). Maximum pressures during these periods at NDBC buoy 44008 were 1037.3, 1037.9 and 1039.2mbar, respectively.

Air Temperature

Analyses of model versus in situ air temperatures are presented in Figures A85 through A112 and Table A4. A summary of the mean differences and correlation coefficients is shown in Table 13. The Eta model air temperatures have an overall mean bias of 1.67°C, however the time series (Figure A85–A91) indicates that larger differences exist between 1 August and 1 November than at any other time. The mean difference between the Eta model and the VAWR before 1 November is 2.52°C and 0.62°C after 1 November. These biases are especially large for the offshore NDBC buoys and the VAWR. A potential source for these differences might be enhanced ocean heat loss due to an incorrect sea surface temperature or inaccurate boundary layer parameterization.

Table 13. Average and range of mean [model - in situ] air temperature differences and range of model versus in situ air temperature correlation coefficients for all buoys.

	Mean Differences (°C)			Correlation Coefficient	
Model	Average	Minimum	Maximum	Minimum	Maximum
Eta	1.67	-0.58	3.80	0.96	0.99
RUC	0.42	-0.73	1.61	0.92	0.98
RUC Analysis	0.00	-0.89	0.80	0.80	0.98
RUC Hourly	0.64	-0.34	1.53	0.87	0.99

The mean differences between the RUC Analysis and the in situ air temperatures are quite small. This would be expected if the NDBC buoy reports are regularly used in the data assimilation of the RUC Analysis. The model air temperatures from the RUC and RUC Hourly are slightly high, however. The mean differences across all the platforms average to 0.42 and 0.64°C for the RUC and RUC Hourly, respectively. Note that the standard deviations of the differences between all the models and NDBC buoy 44009 are high. This variability in the differences is due to the pronounced diurnal cycle in surface air temperature in the models near this buoy. The nearest grid point to this buoy is most likely treated as if it were over land in the models and not over the ocean. Consequently, the strong diurnal signal of daytime heating and nighttime cooling over land is evident in the time series of the model and is absent in the time series of air temperatures at the coastal buoy.

Relative and Specific Humidity

Comparisons of relative humidity differences between the models and in situ observations are presented in Figures A113 through A116 and Table A5. The analyses of model versus in situ specific humidity are presented in Figures A117 through A120 and Table A6. Since only the CMO VAWR measured moisture, only one comparison was possible for each model. The mean differences and correlation coefficients for both relative and specific humidity are shown in Table 14. The evaluation of relative humidity suggests that both models are too dry, however, relative humidity is influenced by temperature. The Eta model has a large bias in air temperature (Table 13) which "balances" the drier relative humidity. This causes a specific humidity which is, on average, slightly more moist than the in situ observations.

Table 14. Mean differences of [model - in situ] relative and specific humidity and model versus in situ relative and specific humidity correlation coefficients for the CMO central buoy.

	Relative Humidity (%)		Specific Humidity (g kg^{-1})	
Model	Mean Difference	Correlation Coefficient	Mean Difference	Correlation Coefficient
Eta	-4.9	0.75	0.49	0.97
RUC	-10.8	0.80	-0.37	0.97
RUC Analysis	-9.9	0.83	-0.36	0.95
RUC Hourly	-9.0	0.87	-0.14	0.96

The RUC Analysis air temperatures were reasonably accurate while those of the RUC and RUC Hourly were slightly high. These temperature differences are not large enough to have a

significant influence on the specific humidity, however. The RUC model remains too dry in specific humidity, although only slightly so in the case of the RUC Hourly.

It is important to note that these conclusions are based on only one set of in situ observations. The analyses of the wind field, barometric pressure and air temperature benefited considerably from the inclusion of the NDBC buoy data. Since this was not possible in the evaluation of humidity, caution must be used in interpreting these results.

Sea Surface Temperature

Analyses of sea surface temperature are presented in Figures A121 through A127 and Table A7. The mean differences between the RUC Hourly and in situ sea surface temperatures ranged from 0.71 to 4.51°C and the overall average difference was 2.52°C. Correlation coefficients ranged from 0.93 to 0.98. The surface temperature over the ocean in the RUC Hourly dataset is a monthly climatological mean and is clearly a step function (Figures A121–A127). Mean differences were lowest for the inshore NDBC buoys, however the model surface temperatures for these buoys were still, on average, 1.14°C too warm. These differences could potentially have a significant impact on the estimation of latent and sensible heat fluxes and outgoing long-wave radiation.

Heat Fluxes

Comparisons of the estimated heat flux components (sensible and latent heat flux and global radiation) from the RUC Hourly dataset and the CMO buoy are presented in Figures A128 through A130 and Table A8. Positive heat fluxes indicate ocean heating.

Global radiation is the sum of the net short-wave and net long-wave radiation components and mean differences between the RUC Hourly and the CMO estimates for this variable averaged -18.9W m^{-2}. This indicates that the model prescribes too much ocean heat loss. The correlation coefficient was 0.91. Since net short-wave falls to zero at night, biases in net long-wave can be evaluated by examining only nighttime global radiation. Mean differences between the model and the in situ estimates of global radiation at night (i.e., net long-wave radiation) were -47.1W m^{-2} (standard deviation of 28.9W m^{-2}), indicating that the model was prescribing much larger oceanic heat loss than was observed. This bias may be due to either higher than observed outgoing long-wave radiation caused by higher sea surface temperatures or lower incoming long-wave radiation caused by lower boundary layer humidity or lower

cloud cover. The RUC Hourly sea surface temperatures are indeed too high, however this accounts for an average of only -19.7W m^{-2} (standard deviation of 8.8W m^{-2}), less than half of the mean -47.1W m^{-2} difference[1]. This suggests that not only is outgoing long-wave too high due to the model sea surface temperature being too warm, but incoming long-wave radiation is too low. This seems plausible, since the surface humidity in the RUC Hourly dataset is too dry (see above).

Since cloud cover can influence incoming long-wave radiation, daytime global radiation was examined to see if incoming short-wave radiation was too high, an indication that cloud cover is too low. To investigate this, an offset of 47.1W m^{-2} was applied to the global radiation as an average bias in the net long-wave radiation. Any errors in the global radiation after applying the net long-wave bias are then assumed to be in the incoming short-wave. Daytime mean differences in the adjusted global radiation were 68.2W m^{-2}, indicating that the model's incoming short-wave radiation was indeed too large. This suggests that the model cloud cover over the CMO buoy might be too low. An alternative explanation for the model's larger incoming short-wave radiation, however, is the selection of an atmospheric transmissivity in the model that is too large.

Mean differences between the RUC Hourly and the CMO sensible and latent heat flux estimates were -46.8W m^{-2} and -22.5W m^{-2}, respectively, indicating that the model overestimates the ocean heat loss. The estimation of the sensible heat flux is sensitive to the air-sea temperature difference while the estimation of the latent heat flux is sensitive to the air-sea humidity gradient. Both are sensitive to the parameterization of the boundary layer in the aerodynamic bulk formulae. To examine the effect of errors in the air-sea temperature and humidity gradients and the sensitivity of the fluxes to the parameterization of the boundary layer, the model fluxes were re-computed with the TOGA COARE flux algorithm (i.e., the same algorithm used to compute the buoy fluxes) using the model observables as the input variables. The model fluxes, buoy fluxes and the re-computed fluxes are shown in Figure 9.

The differences between the model and re-computed fluxes demonstrate that the parameterization of the boundary layer is clearly different between the model and the TOGA COARE algorithm. The mean difference between the re-computed model sensible heat flux and that of the CMO buoy is -14.1W m^{-2} (standard deviation of 20.6W m^{-2}), indicating good

[1] The outgoing long-wave is computed as $\varepsilon\sigma T^4$, where ε is the emissivity of the sea surface, σ is the Stefan-Boltzmann constant and T is the sea surface temperature in °K. An emissivity of 0.97 was used for this analysis.

agreement between the two. The re-computed latent heat fluxes, however, are less accurate than the model's original latent heat fluxes. The mean difference between the re-computed and CMO buoy latent heat fluxes is -36.2W m^{-2} (standard deviation of 44.0W m^{-2}).

Note that in Figure 9b, the model latent heat flux never exceeds zero, meaning that there is never condensation on the sea surface. Excluding times when the CMO latent heat fluxes become positive, the mean difference between the model and CMO buoy latent heat fluxes is -13.6W m^{-2} (standard deviation of 36.8W m^{-2}). This suggests that the model latent heat fluxes are in good agreement with the estimated latent heat fluxes from the CMO buoy.

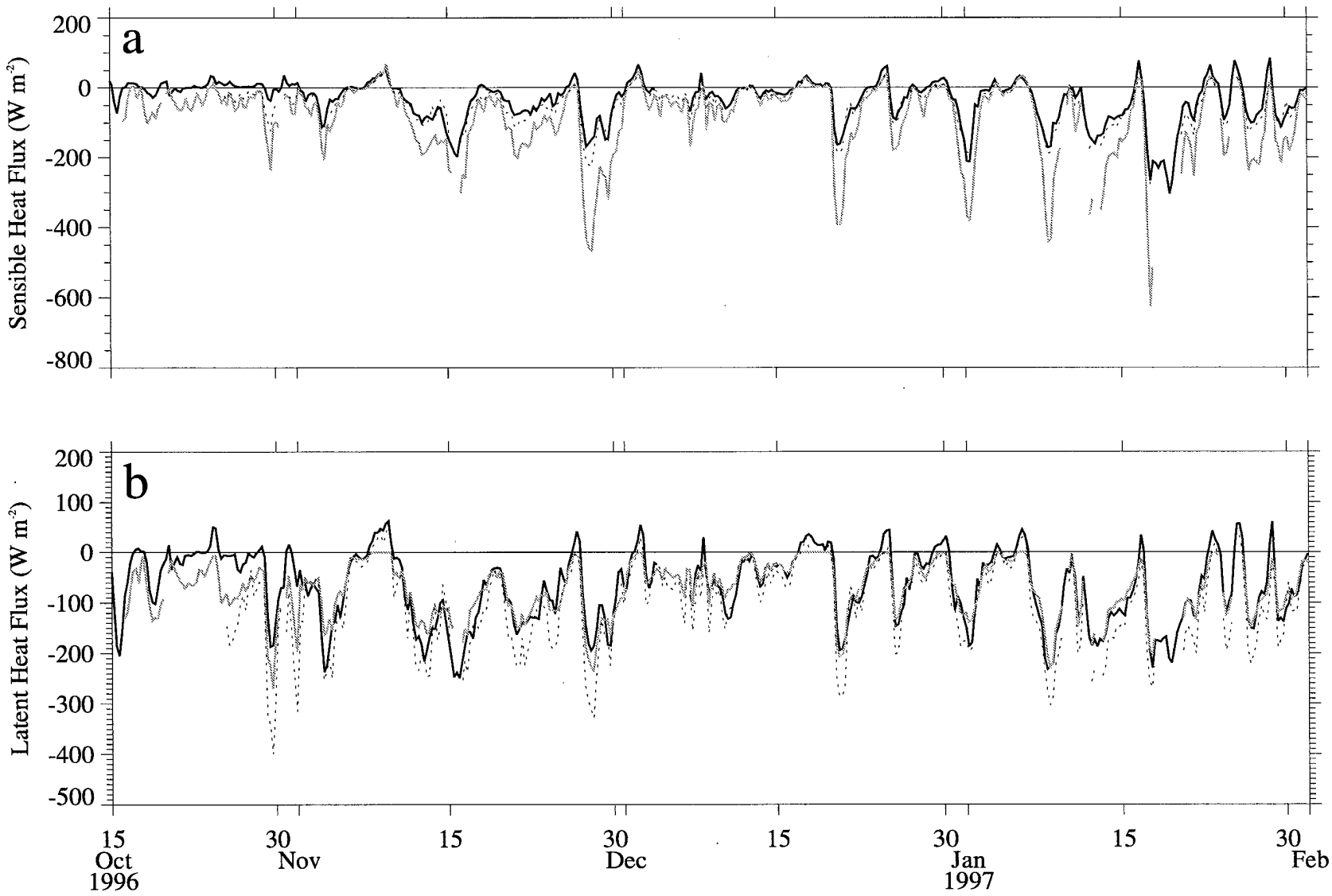

Figure 9. (a) Sensible and (b) latent heat fluxes for CMO buoy (solid black), RUC Hourly (solid gray) and from TOGA COARE flux algorithm using RUC Hourly observables as input (dotted black). Time series are 6 hour averaged.

Literature Cited

Fairall, C.W., E.F. Bradley, D.P. Rogers, J.B. Edson and G.S. Young, 1996. Bulk parameterization of air-sea fluxes for TOGA COARE. *Journal of Geophysical Research.* **101**, 3747–3764.

Weller, R.A., D.L. Rudnick, R.E. Payne, J.P. Dean, N.J. Pennington and R.P. Trask, 1990. Measuring near-surface meteorology over the ocean from an array of surface moorings in the subtropical convergence zone. *Journal of Atmospheric and Oceanic Technology.* **7**, 85–103.

Acknowledgments

The success of the moored array is due to the efforts of the Woods Hole Oceanographic Institution's Upper Ocean Processes (UOP) group, particularly Nancy Brink, Nancy Galbraith, Steve Lentz, Craig Marquette, Will Ostrom, Dick Payne, Al Plueddemann, Rick Trask, Jonathan Ware and Bryan Way. At Unidata, Linda Miller and Sandra Nilsson guided us through the site licensing process and Steve Chiswell provided valuable advice on the implementation of various Unidata products. David Wojtowicz at the University of Illinois at Urbana-Champaign graciously provided access to their IDD recovery data. The staff of the National Data Buoy Center are gratefully acknowledged for their efforts in data collection, quality control and distribution. The NDBC web site is an exemplary data server which greatly facilitates the acquisition and understanding of NDBC's buoy data. Lauren Morone of the National Centers for Environmental Prediction provided guidance on the acquisition and use of RUC model data from the NOAA Information Center's data server. Stan Benjamin pointed us toward useful references and helped further our understanding of the model products. The Coastal Mixing and Optics moored array experiment was supported by the Office of Naval Research under contract N00014-95-1-0339.

Appendix A: Model versus In situ Comparisons

In the following tables and figures, positive differences indicate the model is higher or larger than the in situ observations. The figures include a time series of the model and in situ variables, a scatterplot, a histogram of the differences and a statistics box. The statistics box displays the sample size, statistics of the [model - in situ] difference (median, mean, standard deviation and standard error), the correlation coefficient and two linear regressions. The first linear regression is denoted by a superscript 1 and is a simple linear regression. The second is forced through the origin and is denoted by a superscript 2. The sample size, statistics of the difference and correlation coefficient are summarized for all the variables in Tables A1 through A8.

Table A1. Statistical summary of model vs in situ comparisons of wind speed. Units for the mean, standard deviation, standard error and median are m s^{-1}. The comparison sample size is N and the correlation coefficient is r.

Model	Buoy	N	Mean	Std. Dev.	Std. Err.	Median	r
Eta	CMO	706	0.42	1.80	0.07	0.28	0.88
	44004	739	1.02	2.21	0.08	1.02	0.85
	44008	736	1.35	2.24	0.08	1.18	0.82
	44009	759	-1.62	1.98	0.07	-1.57	0.80
	44011	774	0.88	2.10	0.08	0.69	0.87
	44025	774	-0.35	1.99	0.07	-0.41	0.82
	44028	771	-0.81	2.03	0.07	-0.86	0.82
RUC	CMO	1367	-0.53	2.07	0.06	-0.51	0.82
	44004	1435	0.29	2.18	0.06	0.25	0.83
	44008	1430	0.33	2.48	0.07	0.27	0.74
	44009	1474	-2.17	2.24	0.06	-2.12	0.75
	44011	1503	2.32	3.25	0.08	1.81	0.76
	44025	1507	-0.66	1.95	0.05	-0.61	0.83
	44028	1499	-1.09	2.05	0.05	-1.04	0.83
RUC Analysis	CMO	725	-1.50	2.05	0.08	-1.47	0.80
	44004	663	-0.73	2.00	0.08	-0.91	0.83
	44008	658	-0.95	2.45	0.10	-1.18	0.72
	44009	702	-1.85	2.30	0.09	-1.89	0.77
	44011	725	3.29	3.72	0.14	2.45	0.73
	44025	728	-0.96	1.84	0.07	-0.84	0.84
	44028	728	-1.64	1.84	0.07	-1.57	0.85
RUC Hourly	CMO	4097	-0.84	2.02	0.03	-0.77	0.82
	44004	4145	-1.00	1.94	0.03	-1.01	0.83
	44008	4063	-0.45	2.09	0.03	-0.42	0.80
	44009	4302	-1.50	2.19	0.03	-1.43	0.77
	44011	4293	2.85	3.50	0.05	2.25	0.75
	44025	4330	-0.26	1.89	0.03	-0.28	0.85
	44028	4286	-0.65	2.08	0.03	-0.57	0.82

Table A2. Statistical summary of model vs in situ comparisons of wind direction. Units for the mean, standard deviation, standard error and median are degrees. The comparison sample size is N and the correlation coefficient is r.

Model	Buoy	N	Mean	Std. Dev.	Std. Err.	Median	r
Eta	CMO	706	11.3	32.6	1.2	11.3	0.96
	44004	739	10.3	38.9	1.4	9.3	0.94
	44008	736	16.1	37.7	1.4	15.8	0.94
	44009	759	6.5	35.8	1.3	7.5	0.94
	44011	774	13.1	30.7	1.1	14.1	0.96
	44025	774	7.3	38.1	1.4	9.7	0.93
	44028	771	2.2	40.4	1.5	5.9	0.93
RUC	CMO	1367	8.8	37.3	1.0	9.3	0.94
	44004	1435	42.8	41.0	1.1	45.5	0.93
	44008	1430	50.4	49.4	1.3	51.3	0.90
	44009	1474	7.3	41.1	1.1	6.9	0.92
	44011	1503	60.4	37.9	1.0	61.5	0.93
	44025	1507	7.9	37.5	1.0	11.2	0.93
	44028	1499	4.1	36.6	0.9	7.0	0.94
RUC Analysis	CMO	725	9.8	36.5	1.4	10.2	0.93
	44004	663	35.0	31.4	1.2	36.4	0.95
	44008	658	38.9	42.7	1.7	38.5	0.91
	44009	702	6.9	33.6	1.3	6.1	0.94
	44011	725	50.7	39.3	1.5	51.7	0.93
	44025	728	11.2	27.5	1.0	13.1	0.96
	44028	728	4.8	24.7	0.9	6.3	0.97
RUC Hourly	CMO	4097	12.8	42.5	0.7	14.2	0.91
	44004	4144	32.7	41.1	0.6	35.1	0.93
	44008	4063	41.7	51.0	0.8	42.7	0.89
	44009	4302	5.7	41.9	0.6	4.2	0.92
	44011	4288	57.8	40.4	0.6	59.7	0.92
	44025	4330	2.5	40.4	0.6	6.9	0.92
	44028	4282	3.8	37.0	0.6	5.5	0.94

Table A3. Statistical summary of model vs in situ comparisons of barometric pressure. Units for the mean, standard deviation, standard error and median are millibars. The comparison sample size is N and the correlation coefficient is r.

Model	Buoy	N	Mean	Std. Dev.	Std. Err.	Median	r
Eta	CMO	680	0.1	1.2	0.0	-0.1	0.99
	44004	741	-0.6	1.4	0.1	-0.7	0.98
	44008	748	-0.4	1.5	0.1	-0.6	0.98
	44009	749	0.4	1.3	0.0	0.2	0.99
	44011	747	0.5	1.3	0.0	0.4	0.99
	44025	748	0.0	1.5	0.1	-0.2	0.98
	44028	749	-0.2	1.5	0.1	-0.4	0.99
RUC	CMO	1366	1.1	1.3	0.0	1.0	0.99
	44004	1491	0.8	1.3	0.0	0.9	0.99
	44008	1505	1.0	1.4	0.0	1.0	0.99
	44009	1505	1.2	1.0	0.0	1.1	0.99
	44011	1501	1.4	1.5	0.0	1.3	0.99
	44025	1506	0.9	0.9	0.0	0.9	0.99
	44028	1505	0.7	1.0	0.0	0.8	0.99
RUC Analysis	CMO	732	1.5	1.0	0.0	1.5	0.99
	44004	723	1.2	1.3	0.0	1.1	0.99
	44008	735	1.4	1.1	0.0	1.4	0.99
	44009	735	1.4	0.7	0.0	1.3	1.00
	44011	731	1.6	1.4	0.1	1.5	0.99
	44025	735	1.0	0.8	0.0	0.9	1.00
	44028	735	0.9	0.6	0.0	0.9	1.00
RUC Hourly	CMO	4084	1.0	1.9	0.0	1.0	0.98
	44004	4279	0.7	2.1	0.0	0.8	0.97
	44008	4270	0.8	2.0	0.0	0.8	0.98
	44009	4368	1.0	1.6	0.0	1.0	0.99
	44011	4284	1.2	1.5	0.0	1.0	0.99
	44025	4317	0.7	1.5	0.0	0.7	0.99
	44028	4331	0.6	1.6	0.0	0.6	0.99

Table A4. Statistical summary of model vs in situ comparisons of air temperature. Units for the mean, standard deviation, standard error and median are °C. The comparison sample size is N and the correlation coefficient is r.

Model	Buoy	N	Mean	Std. Dev.	Std. Err.	Median	r
Eta	CMO	691	1.60	1.61	0.06	1.54	0.98
	44004	751	2.92	1.42	0.05	2.89	0.98
	44008	758	3.80	1.44	0.05	3.64	0.97
	44009	588	-0.58	2.29	0.09	-0.24	0.96
	44011	758	2.08	1.26	0.05	2.04	0.98
	44025	758	0.85	1.14	0.04	0.77	0.99
	44028	341	1.02	1.29	0.07	0.99	0.98
RUC	CMO	1367	0.66	2.09	0.06	0.75	0.97
	44004	1493	-0.73	1.46	0.04	-0.68	0.98
	44008	1506	1.61	2.34	0.06	1.42	0.96
	44009	1168	-0.64	2.98	0.09	-0.45	0.92
	44011	1503	0.79	2.42	0.06	0.62	0.97
	44025	1507	0.52	1.74	0.04	0.62	0.98
	44028	643	0.72	1.57	0.06	0.75	0.97
RUC Analysis	CMO	725	0.36	1.82	0.07	0.57	0.94
	44004	717	-0.89	1.33	0.05	-0.85	0.97
	44008	728	0.28	1.74	0.06	0.32	0.95
	44009	410	-0.85	2.98	0.15	-0.39	0.80
	44011	726	0.18	1.95	0.07	-0.10	0.96
	44025	728	0.16	1.69	0.06	0.36	0.95
	44028	66	0.80	1.00	0.12	0.69	0.98
RUC Hourly	CMO	2182	1.12	1.09	0.02	1.16	0.97
	44004	2088	-0.34	1.01	0.02	-0.27	0.98
	44008	2102	0.89	1.16	0.03	0.83	0.97
	44009	1222	0.02	2.40	0.07	0.26	0.87
	44011	2121	0.20	1.97	0.04	-0.11	0.96
	44025	2147	1.04	1.09	0.02	1.01	0.97
	44028	204	1.53	1.02	0.07	1.70	0.99

Table A5. Statistical summary of model vs in situ comparisons of relative humidity. Units for the mean, standard deviation, standard error and median are percent. The comparison sample size is N and the correlation coefficient is r.

Model	Buoy	N	Mean	Std. Dev.	Std. Err.	Median	r
Eta	CMO	709	-4.9	8.4	0.3	-4.8	0.75
RUC	CMO	1367	-10.8	9.3	0.3	-9.9	0.80
RUC Analysis	CMO	725	-9.9	9.2	0.3	-9.5	0.83
RUC Hourly	CMO	2182	-9.0	7.1	0.2	-8.8	0.87

Table A6. Statistical summary of model vs in situ comparisons of specific humidity. Units for the mean, standard deviation, standard error and median are g kg^{-1}. The comparison sample size is N and the correlation coefficient is r.

Model	Buoy	N	Mean	Std. Dev.	Std. Err.	Median	r
Eta	CMO	674	0.49	0.99	0.04	0.34	0.97
RUC	CMO	1366	-0.37	0.99	0.03	-0.49	0.97
RUC Analysis	CMO	725	-0.36	0.76	0.03	-0.49	0.95
RUC Hourly	CMO	2182	-0.14	0.62	0.01	-0.20	0.96

Table A7. Statistical summary of RUC Hourly vs in situ comparisons of sea surface temperature. Units for the mean, standard deviation, standard error and median are °C. The comparison sample size is N and the correlation coefficient is r.

Model	Buoy	N	Mean	Std. Dev.	Std. Err.	Median	r
RUC Hourly	CMO	4083	3.73	1.58	0.02	3.33	0.95
	44004	4280	1.65	1.50	0.02	1.55	0.93
	44008	4269	4.31	1.69	0.03	4.45	0.96
	44009	4367	0.71	1.40	0.02	0.75	0.98
	44011	4275	4.51	1.43	0.02	4.45	0.95
	44025	4316	1.40	1.39	0.02	1.25	0.97
	44028	4328	1.32	1.23	0.02	1.35	0.97

Table A8. Statistical summary of RUC Hourly model vs in situ comparisons of heat fluxes. Units for the mean, standard deviation, standard error and median are W m^{-2}. The comparison sample size is N and the correlation coefficient is r.

Variable	Buoy	N	Mean	Std. Dev.	Std. Err.	Median	r
Global Radiation	CMO	4038	-18.9	88.1	1.4	-40.5	0.91
Sensible Heat Flux	CMO	4038	-46.8	53.7	0.8	-28.3	0.91
Latent Heat Flux	CMO	4038	-22.5	38.4	0.6	-19.6	0.81

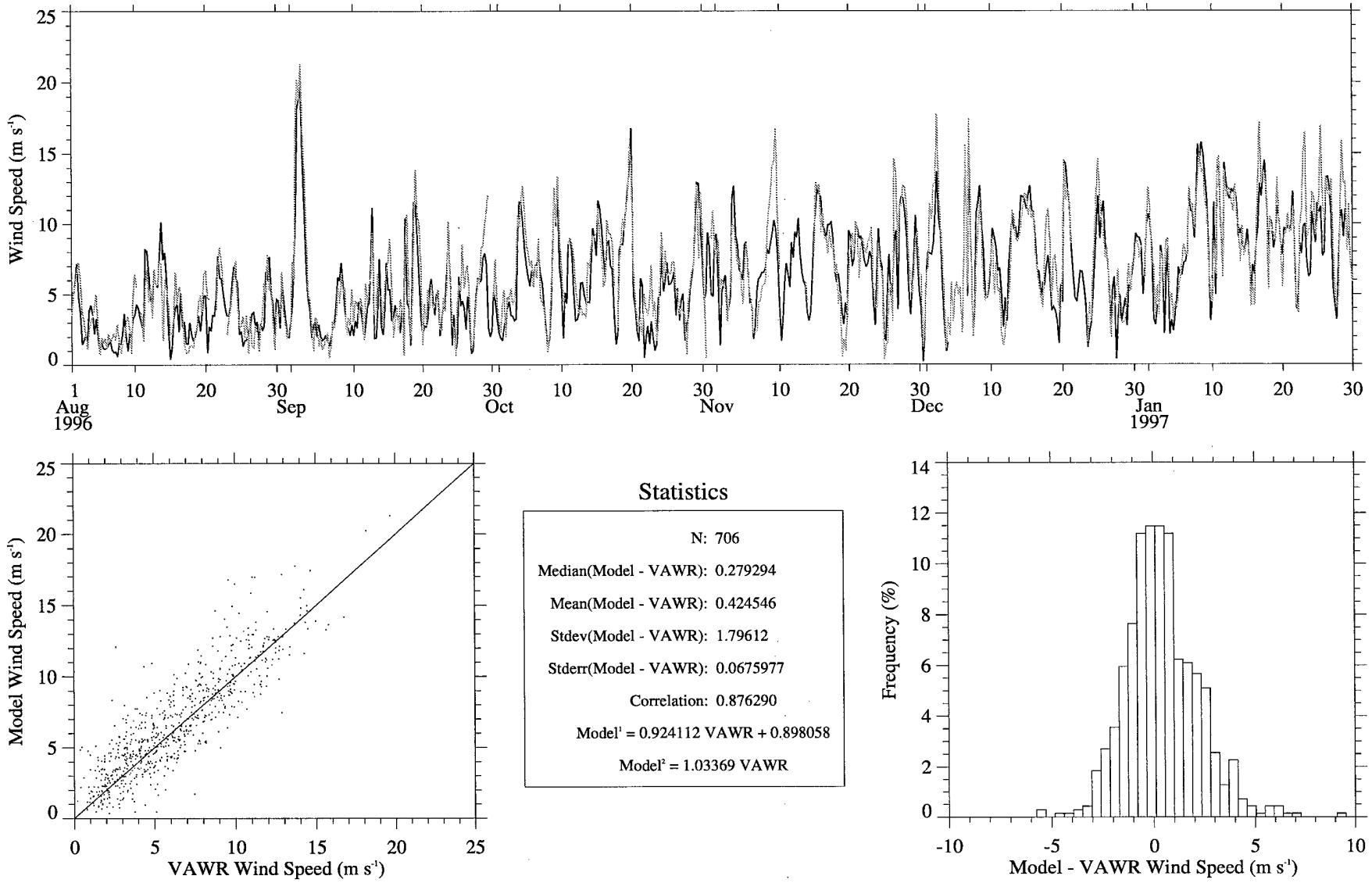

Figure A1. Eta (gray) vs. CMO VAWR 0704 (black) wind speed.

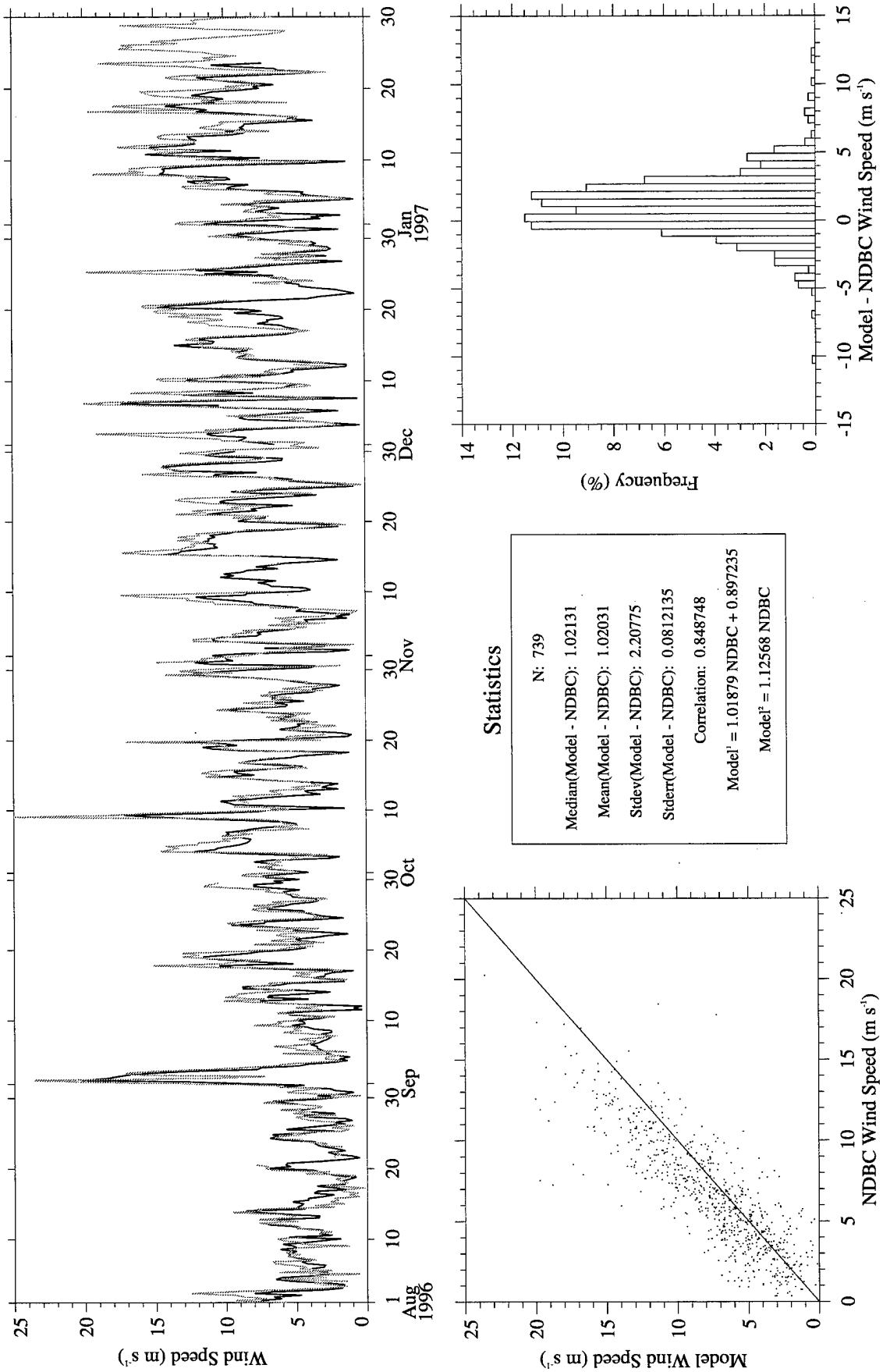

Figure A2. Eta (gray) vs. NDBC Buoy 44004 (black) wind speed.

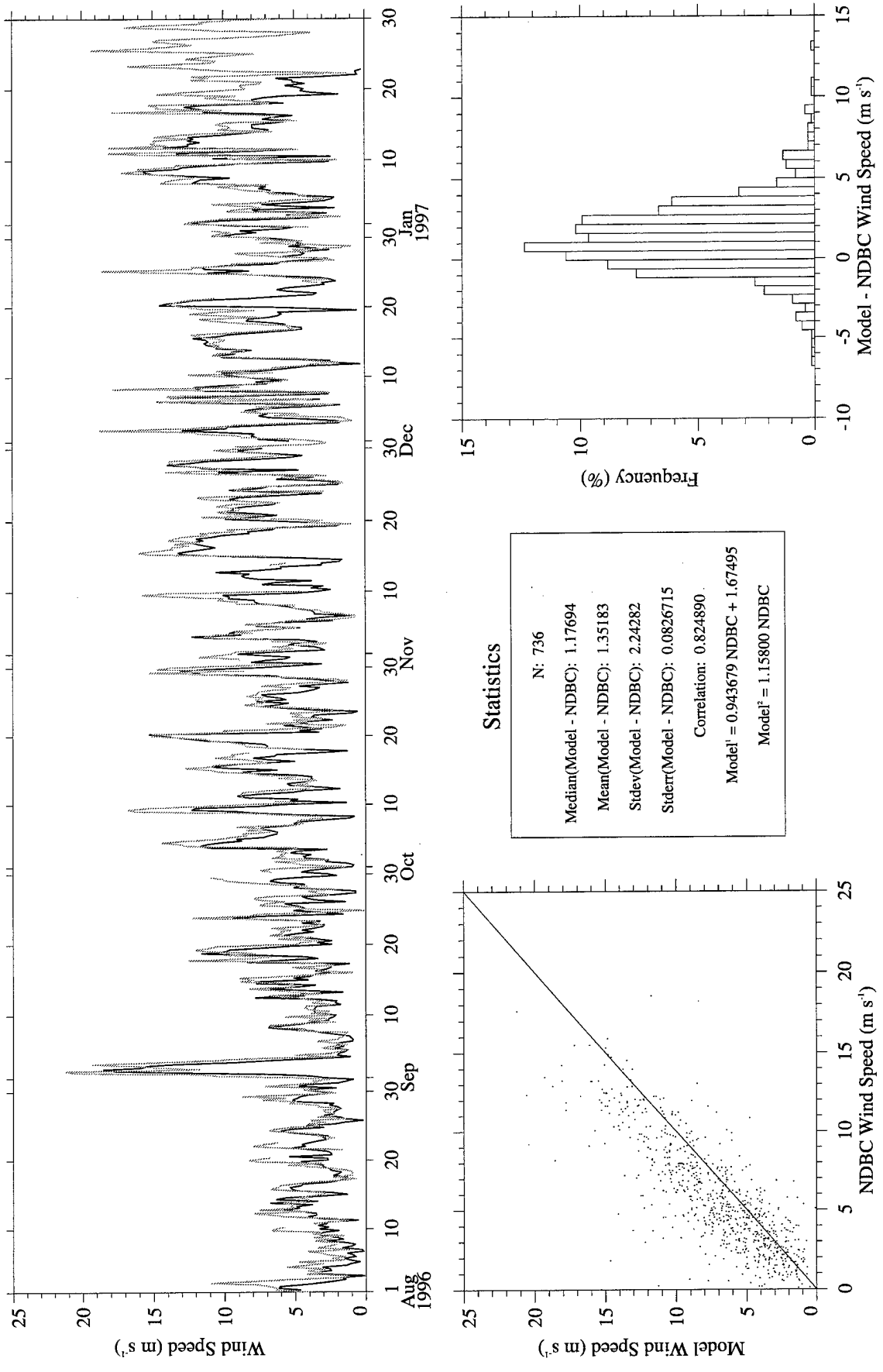

Figure A3. Eta (gray) vs. NDBC Buoy 44008 (black) wind speed.

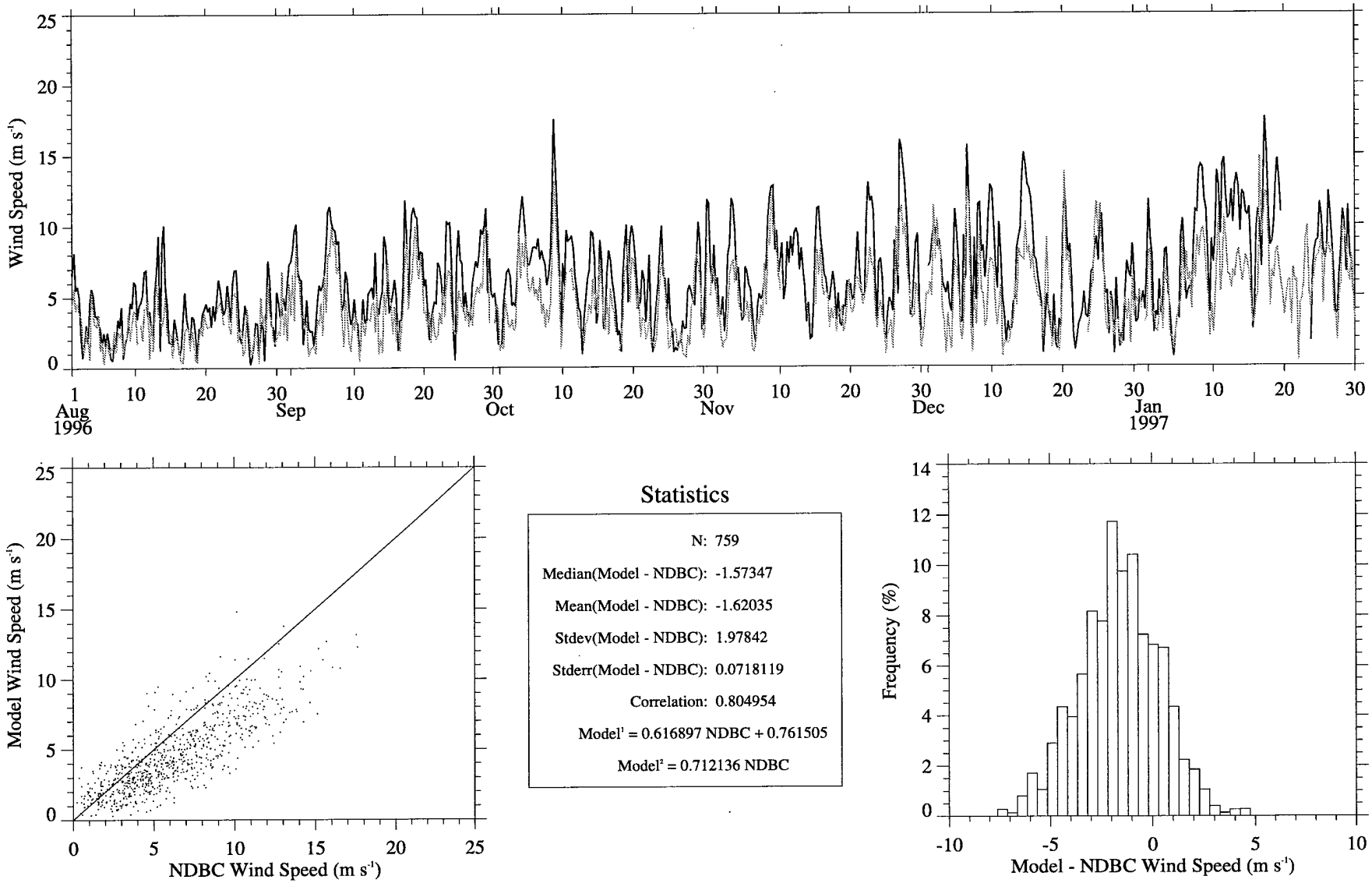

Figure A4. Eta (gray) vs. NDBC Buoy 44009 (black) wind speed.

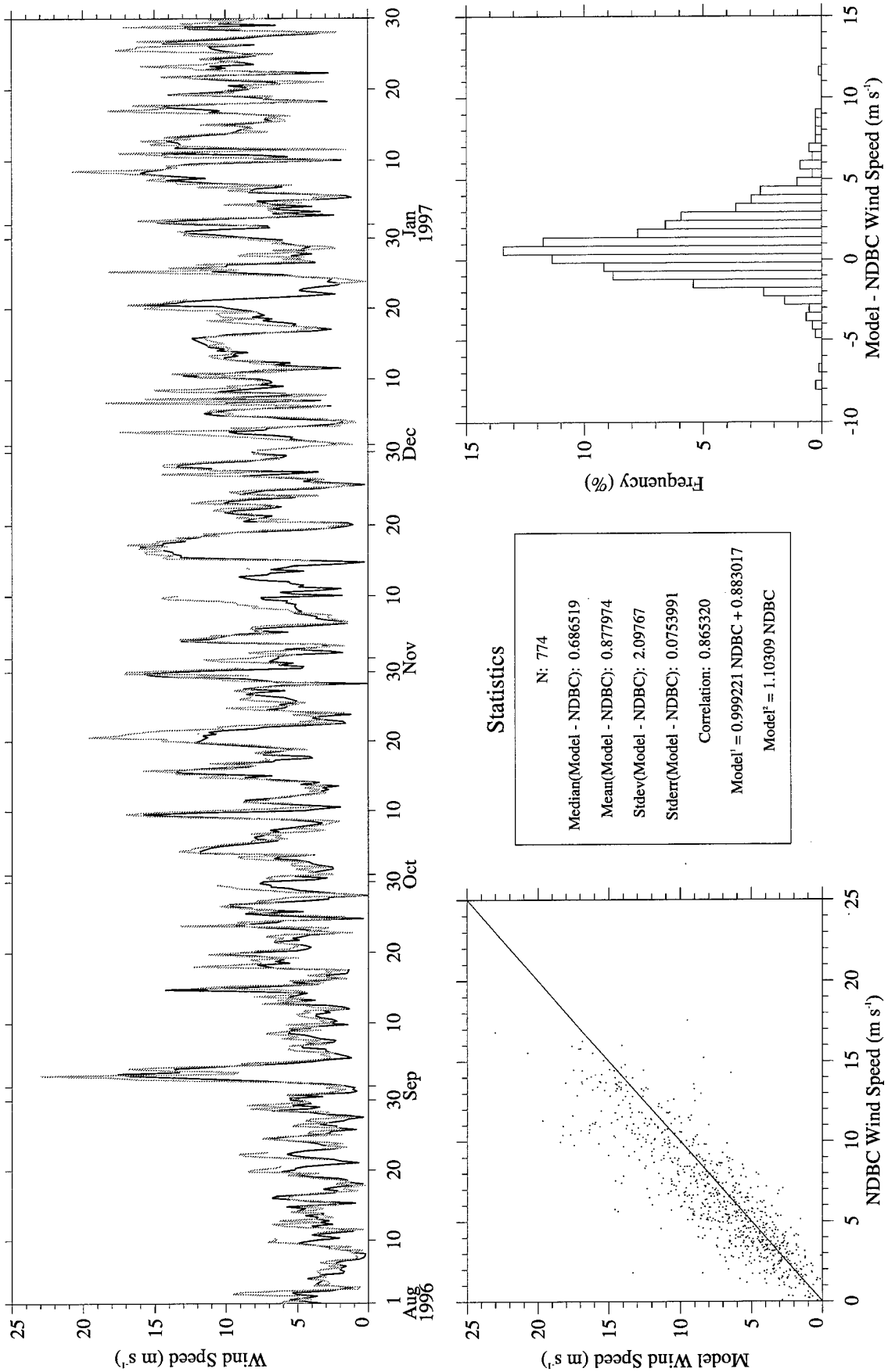

Figure A5. Eta (gray) vs. NDBC Buoy 44011 (black) wind speed.

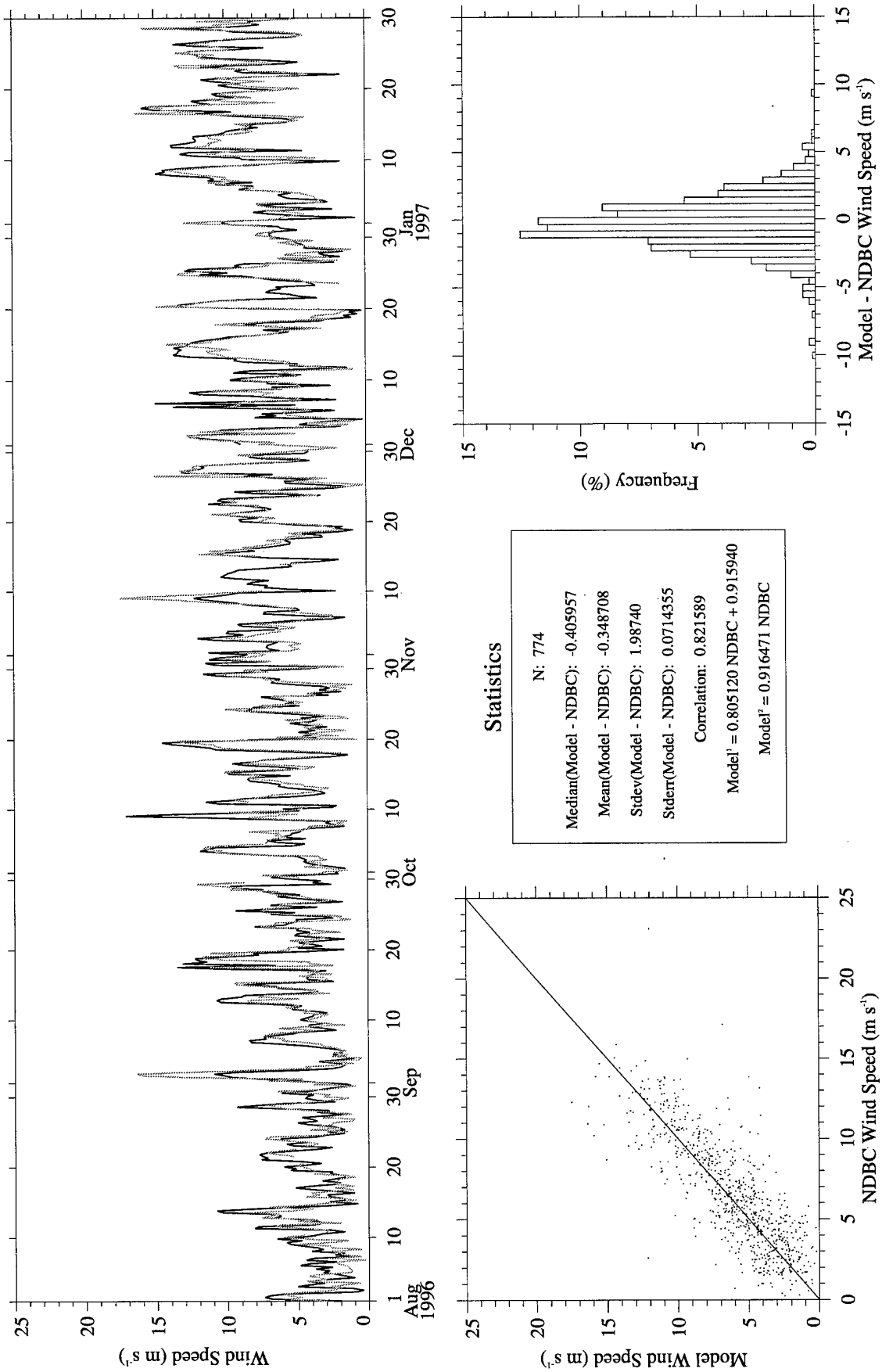

Figure A6. Eta (gray) vs. NDBC Buoy 44025 (black) wind speed.

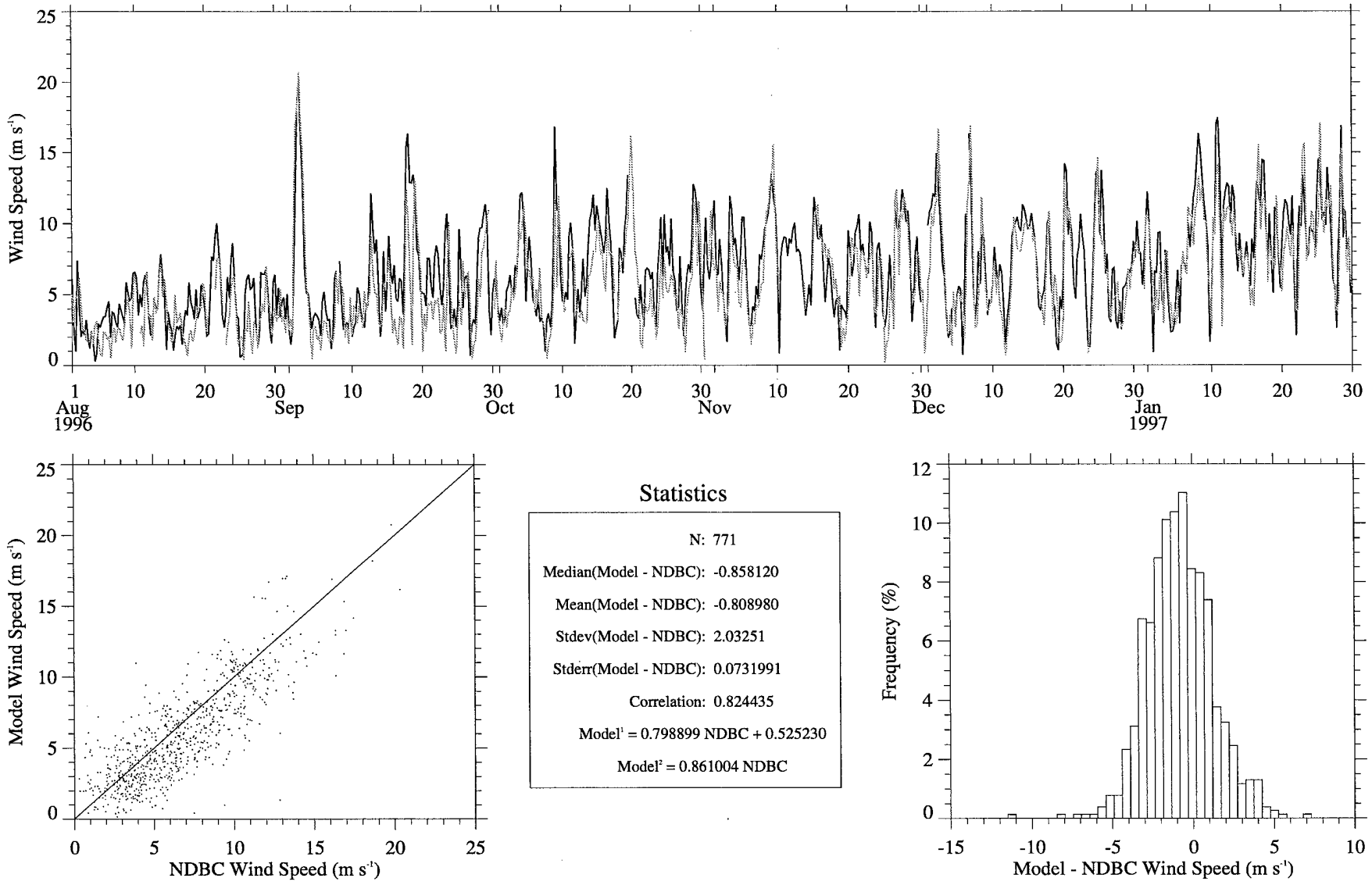

Figure A7. Eta (gray) vs. NDBC Buoy 44028 (black) wind speed.

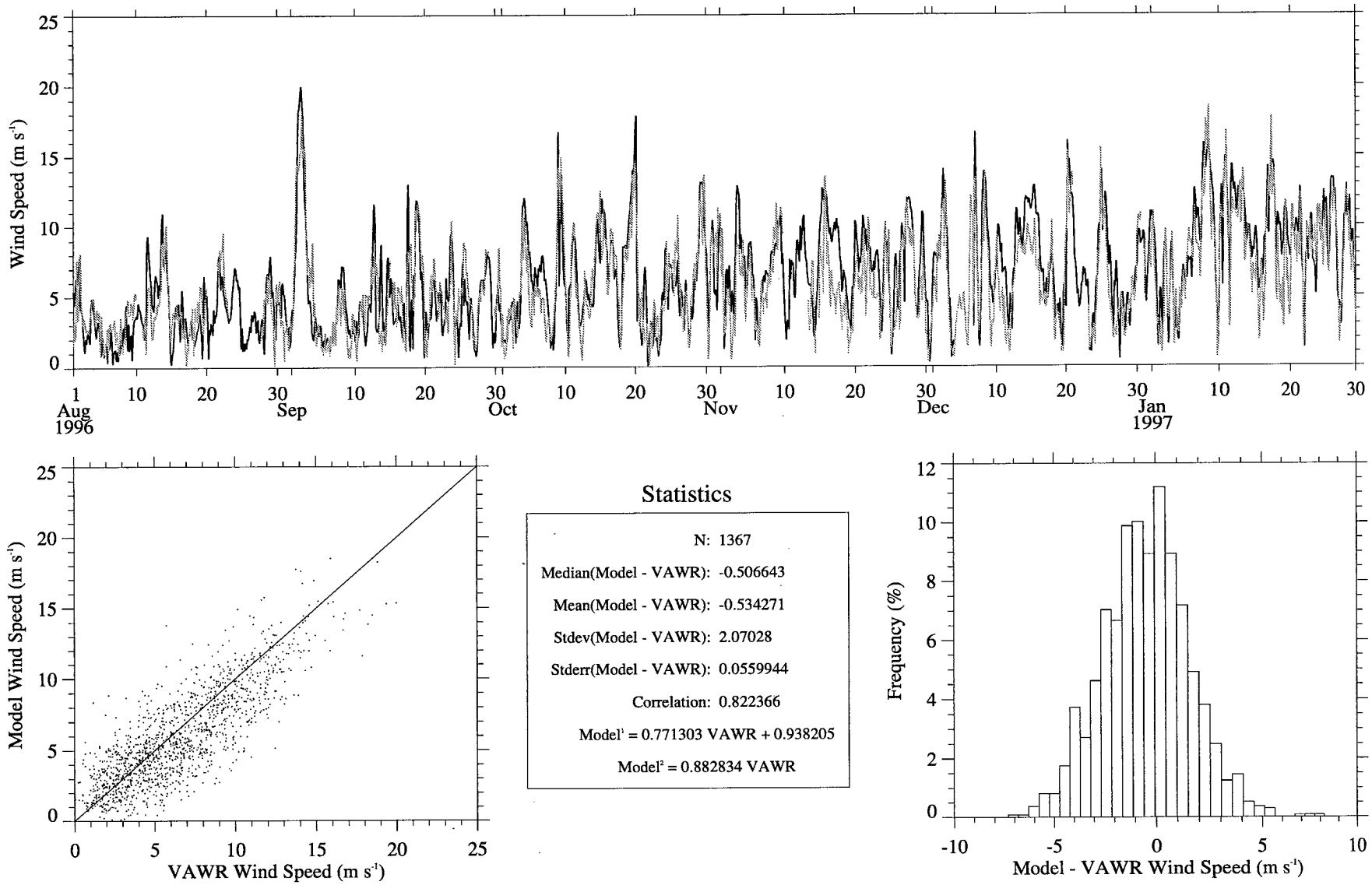

Figure A8. RUC (gray) vs. CMO VAWR 0704 (black) wind speed.

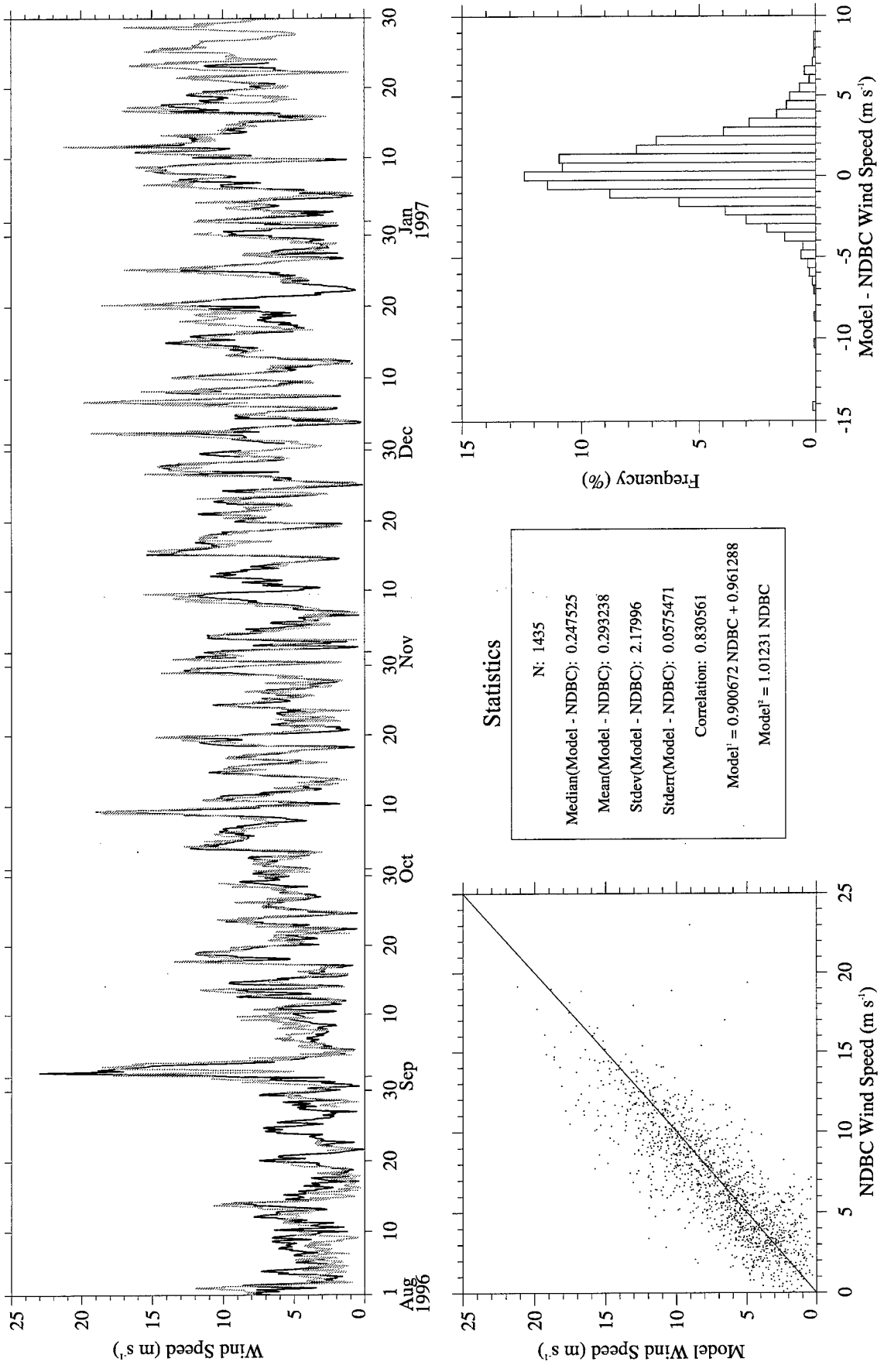

Figure A9. RUC (gray) vs. NDBC Buoy 44004 (black) wind speed.

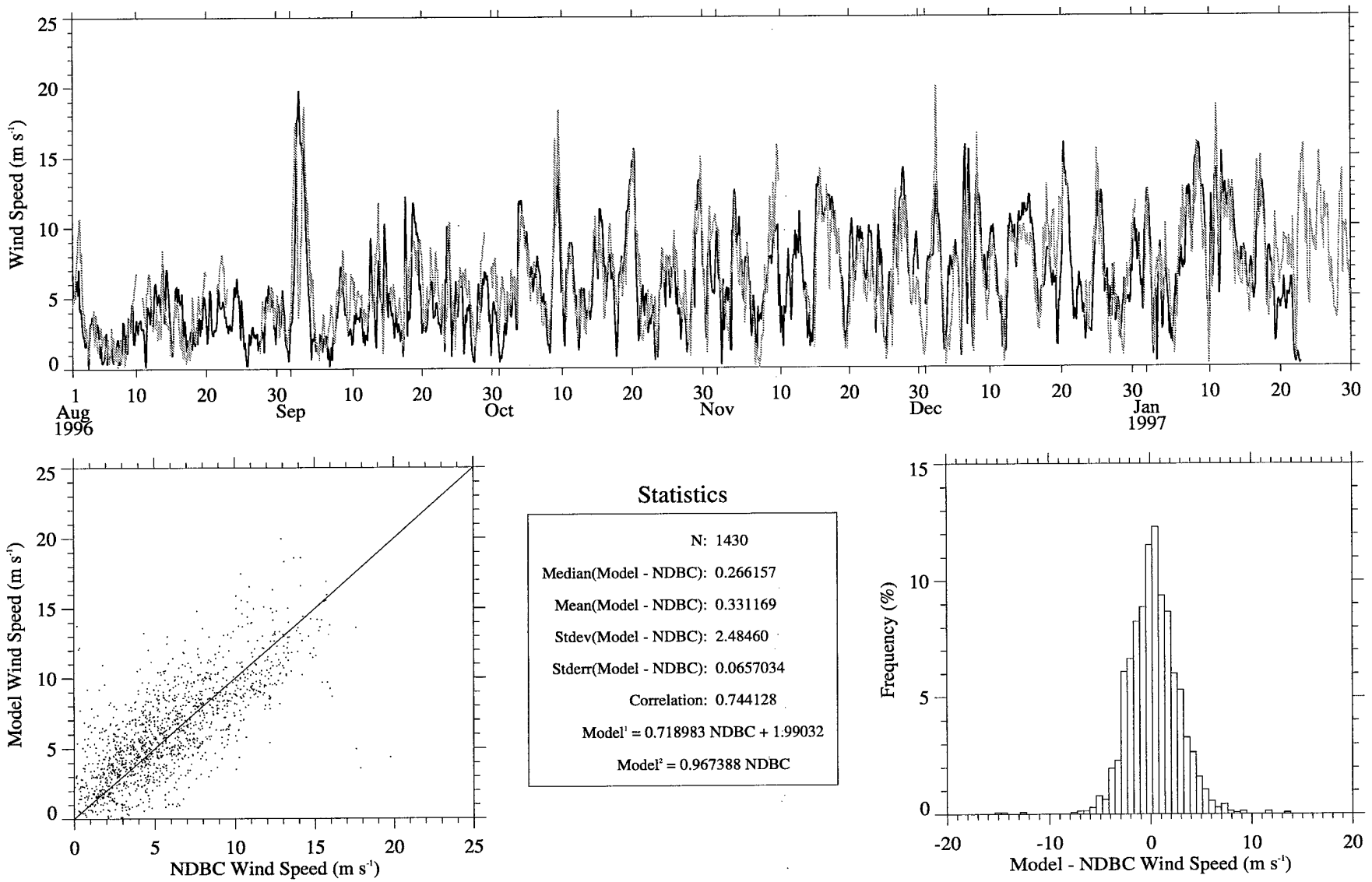

Figure A10. RUC (gray) vs. NDBC Buoy 44008 (black) wind speed.

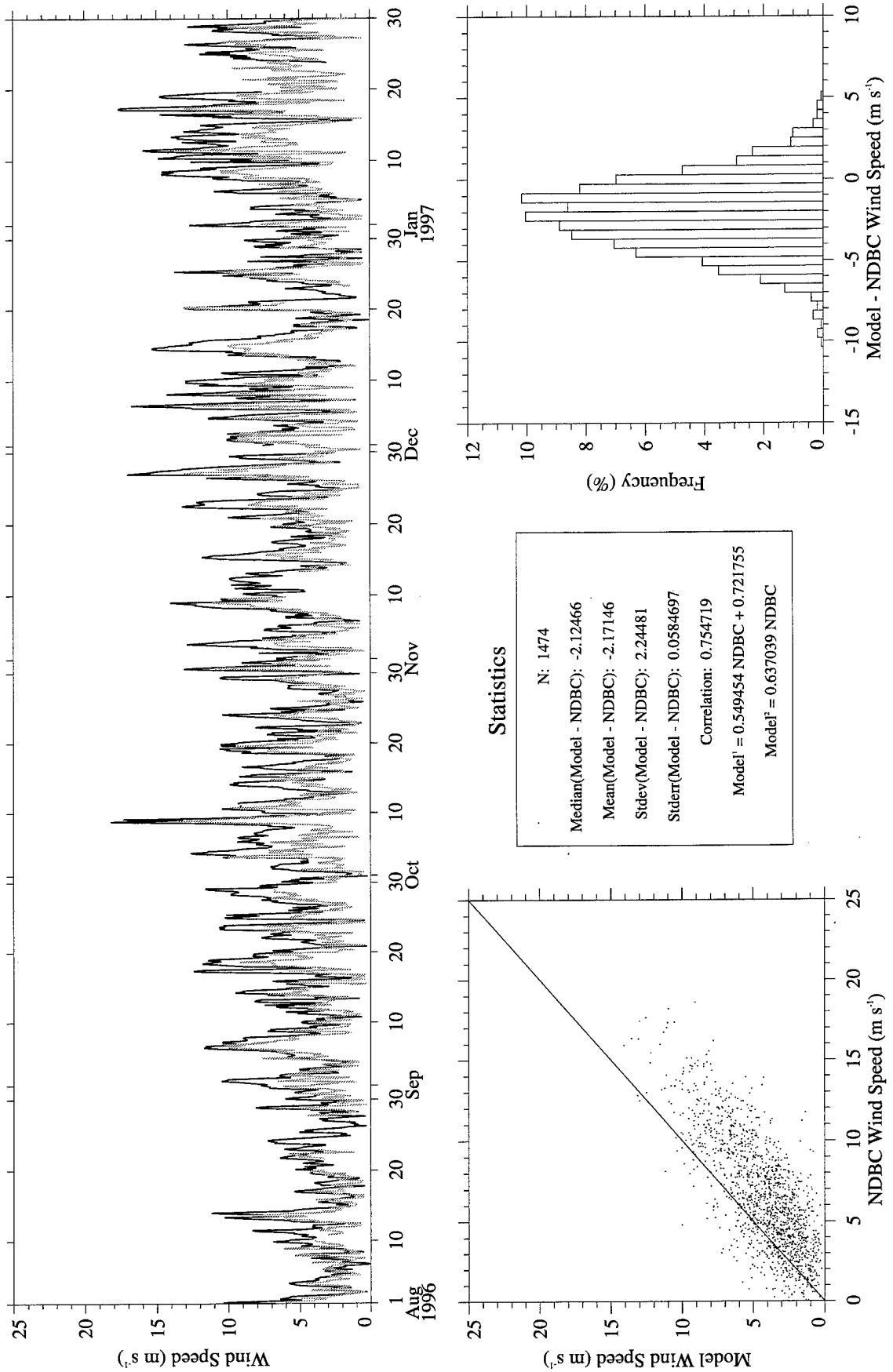

Figure A11. RUC (gray) vs. NDBC Buoy 44009 (black) wind speed.

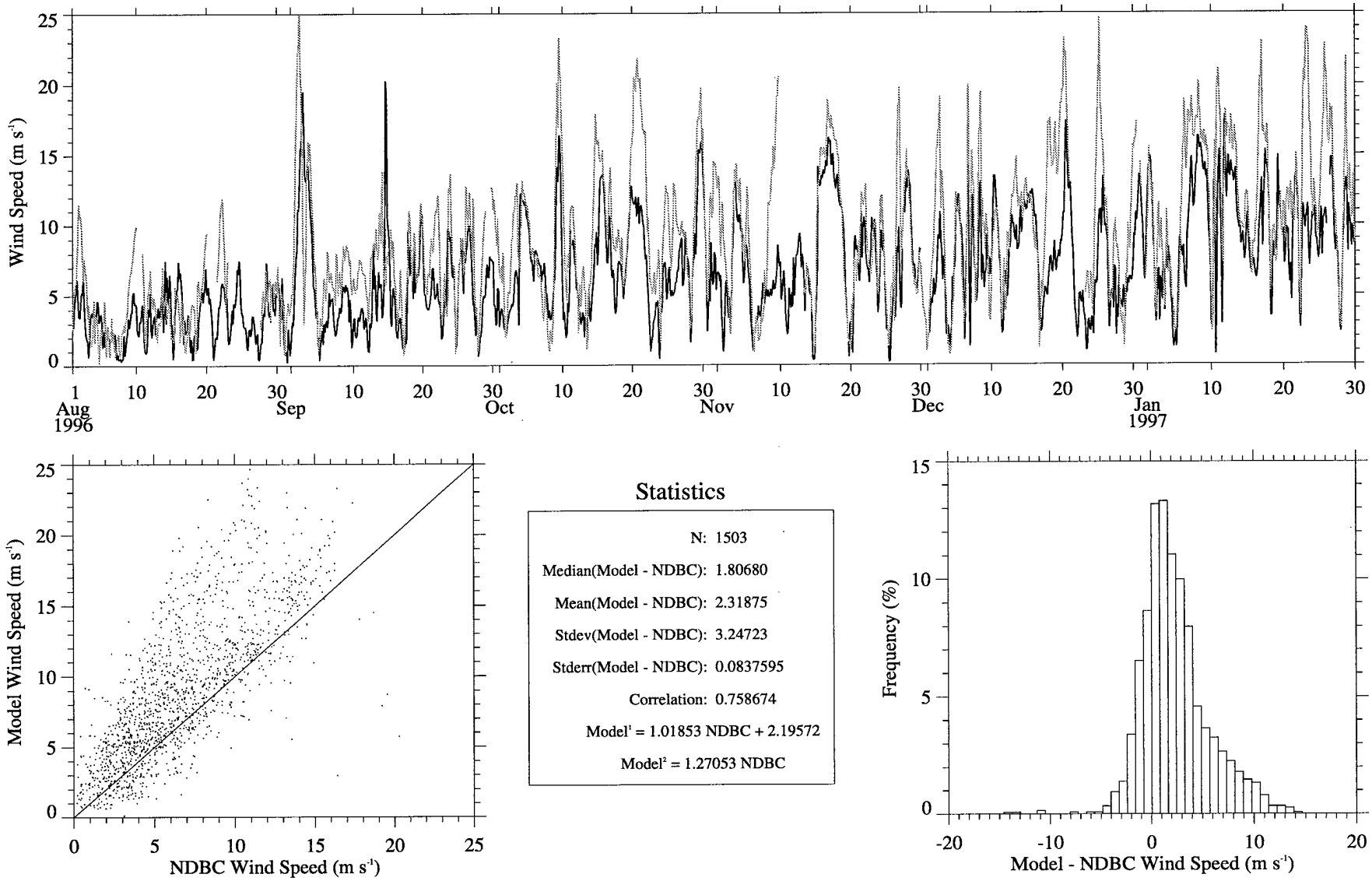

Figure A12. RUC (gray) vs. NDBC Buoy 44011 (black) wind speed.

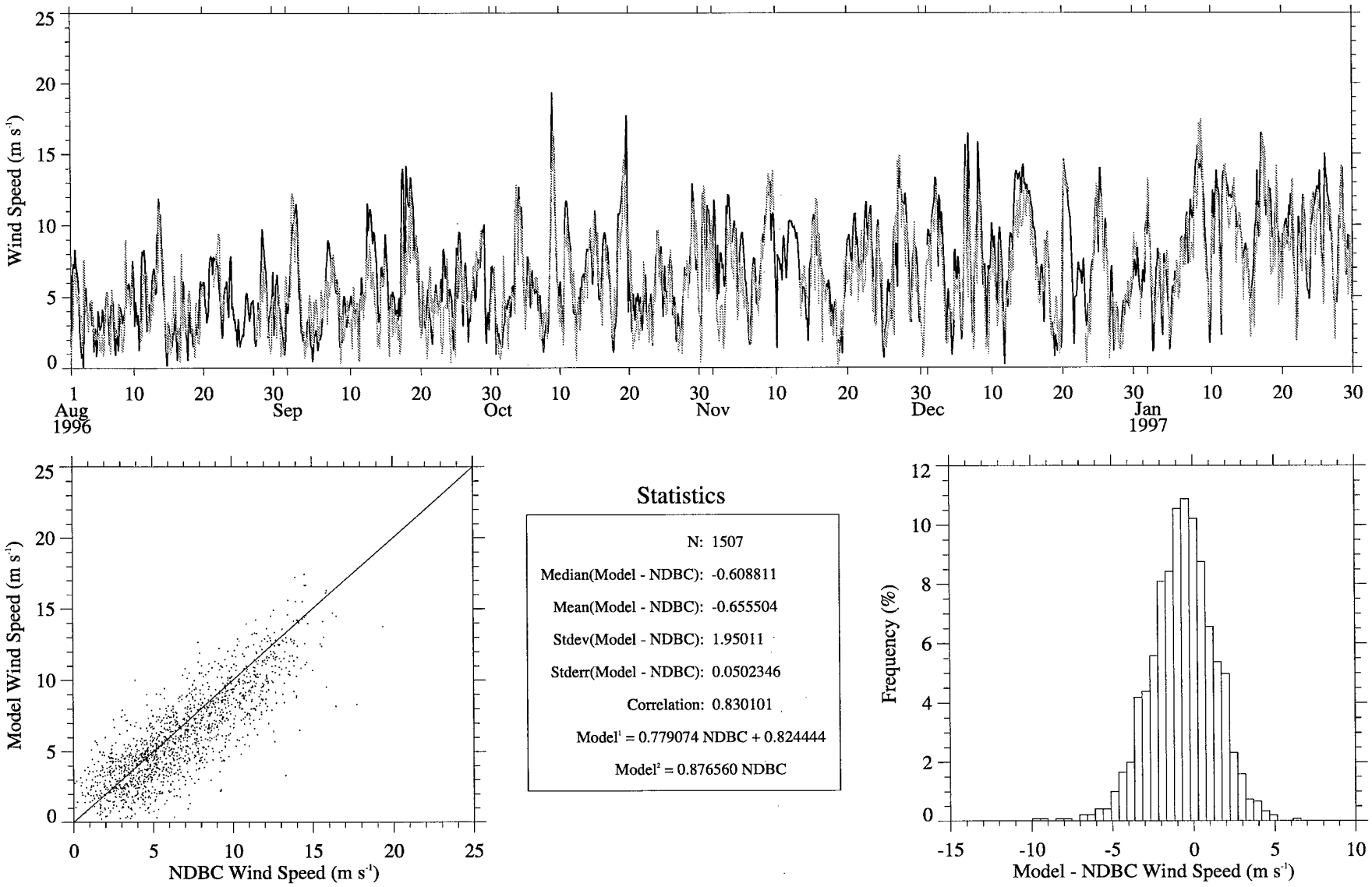

Figure A13. RUC (gray) vs. NDBC Buoy 44025 (black) wind speed.

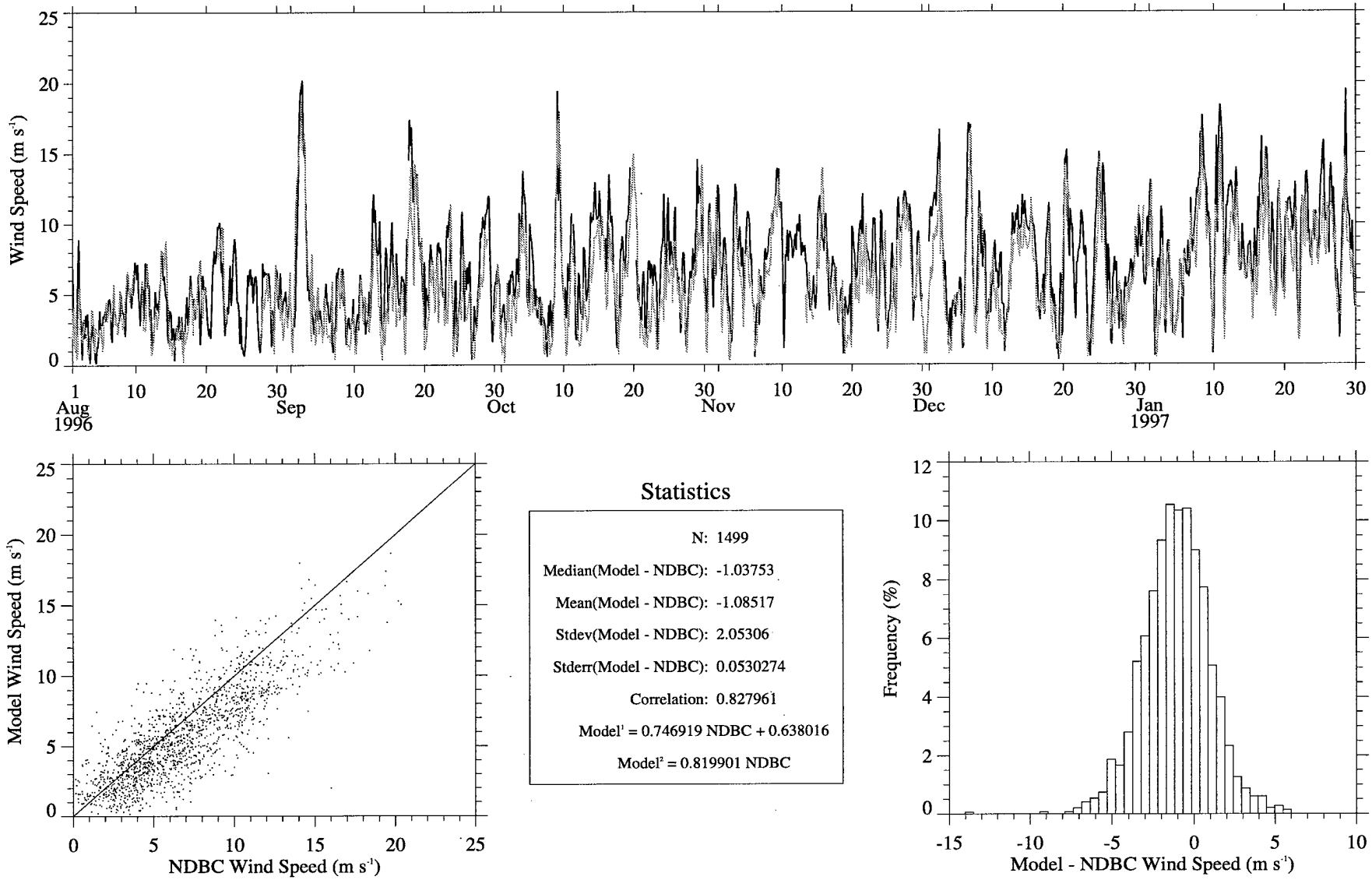

Figure A14. RUC (gray) vs. NDBC Buoy 44028 (black) wind speed.

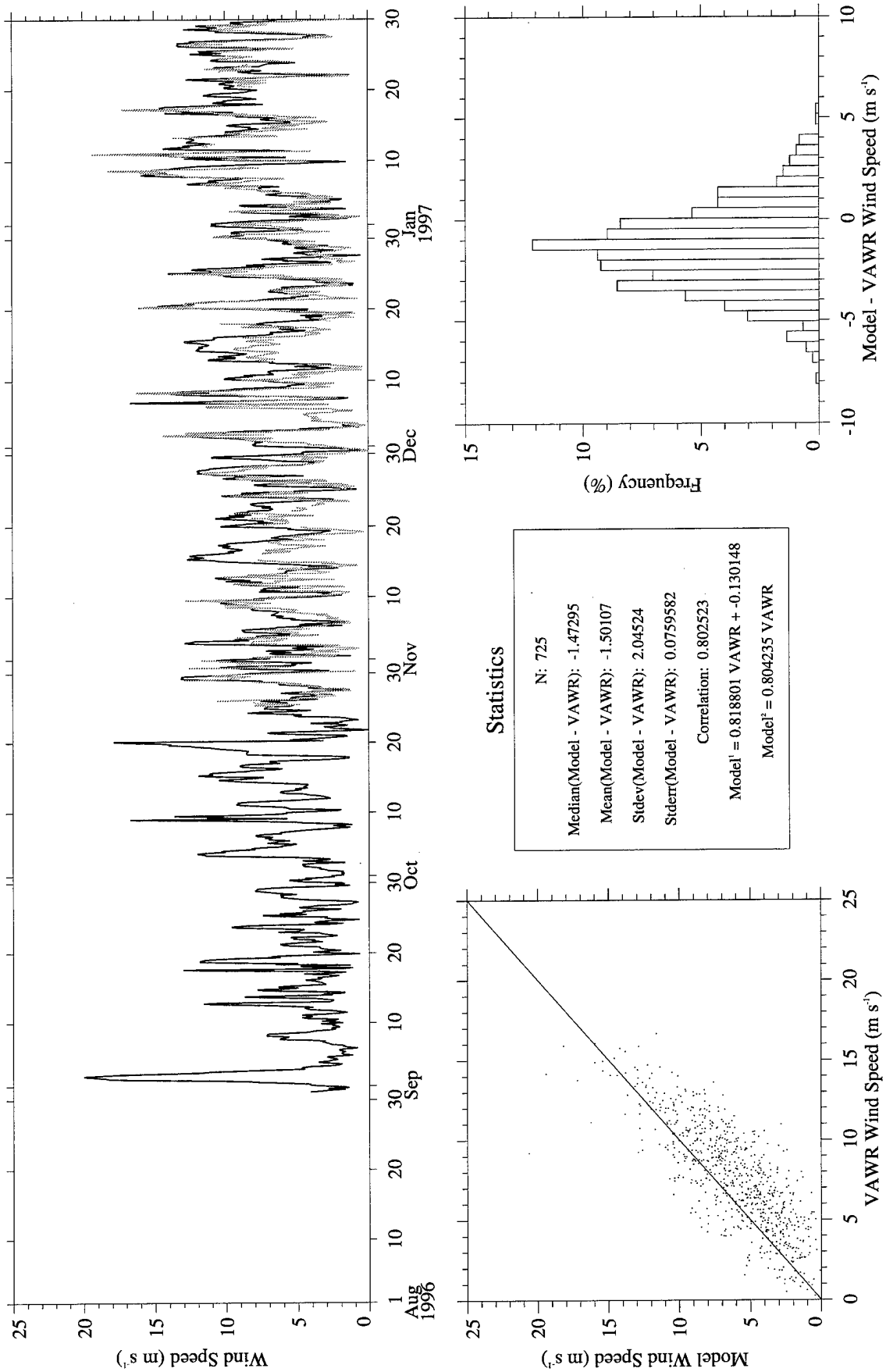

Figure A15. RUC Analysis (gray) vs. CMO VAWR 0704 (black) wind speed.

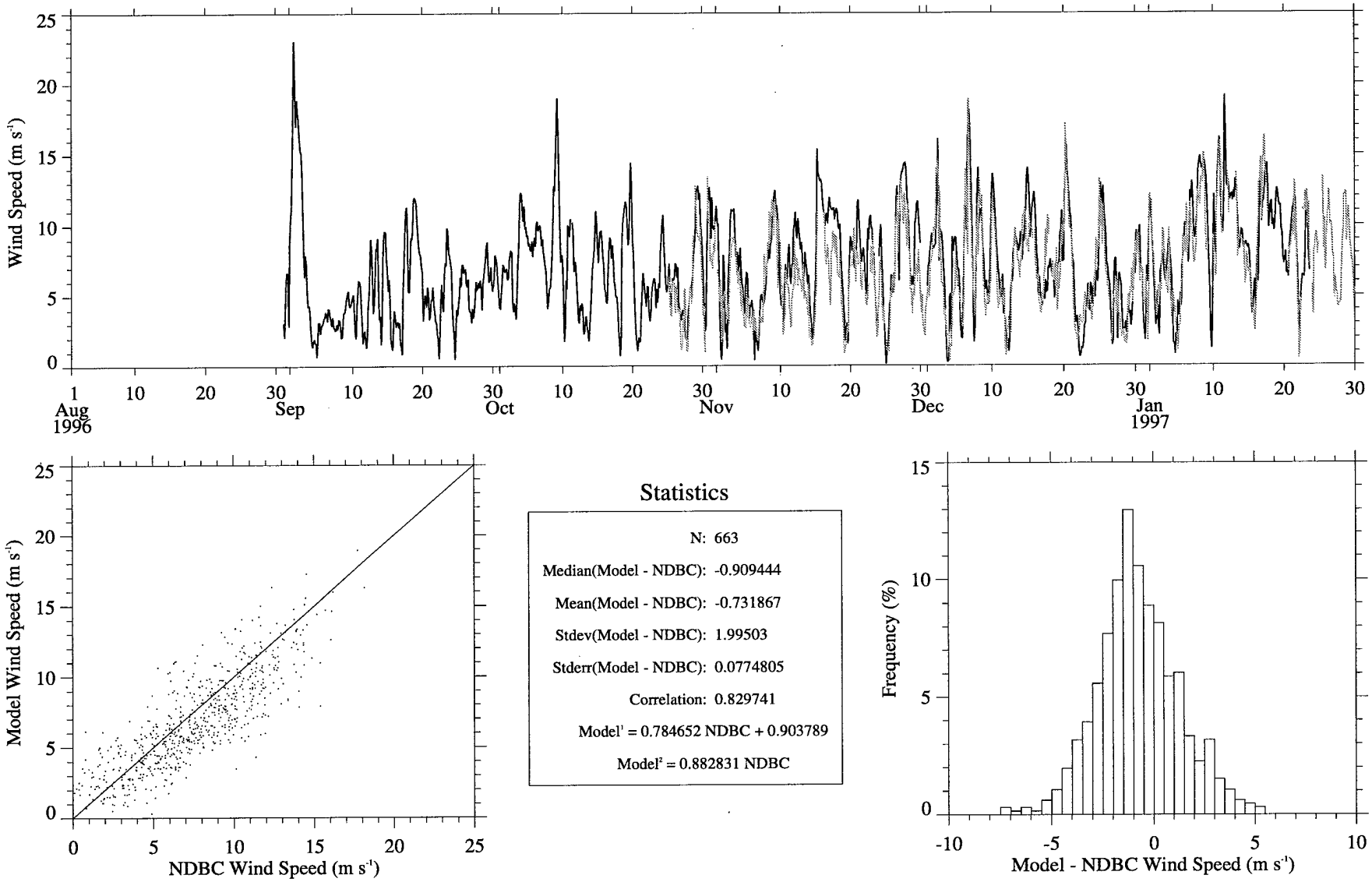

Figure A16. RUC Analysis (gray) vs. NDBC Buoy 44004 (black) wind speed.

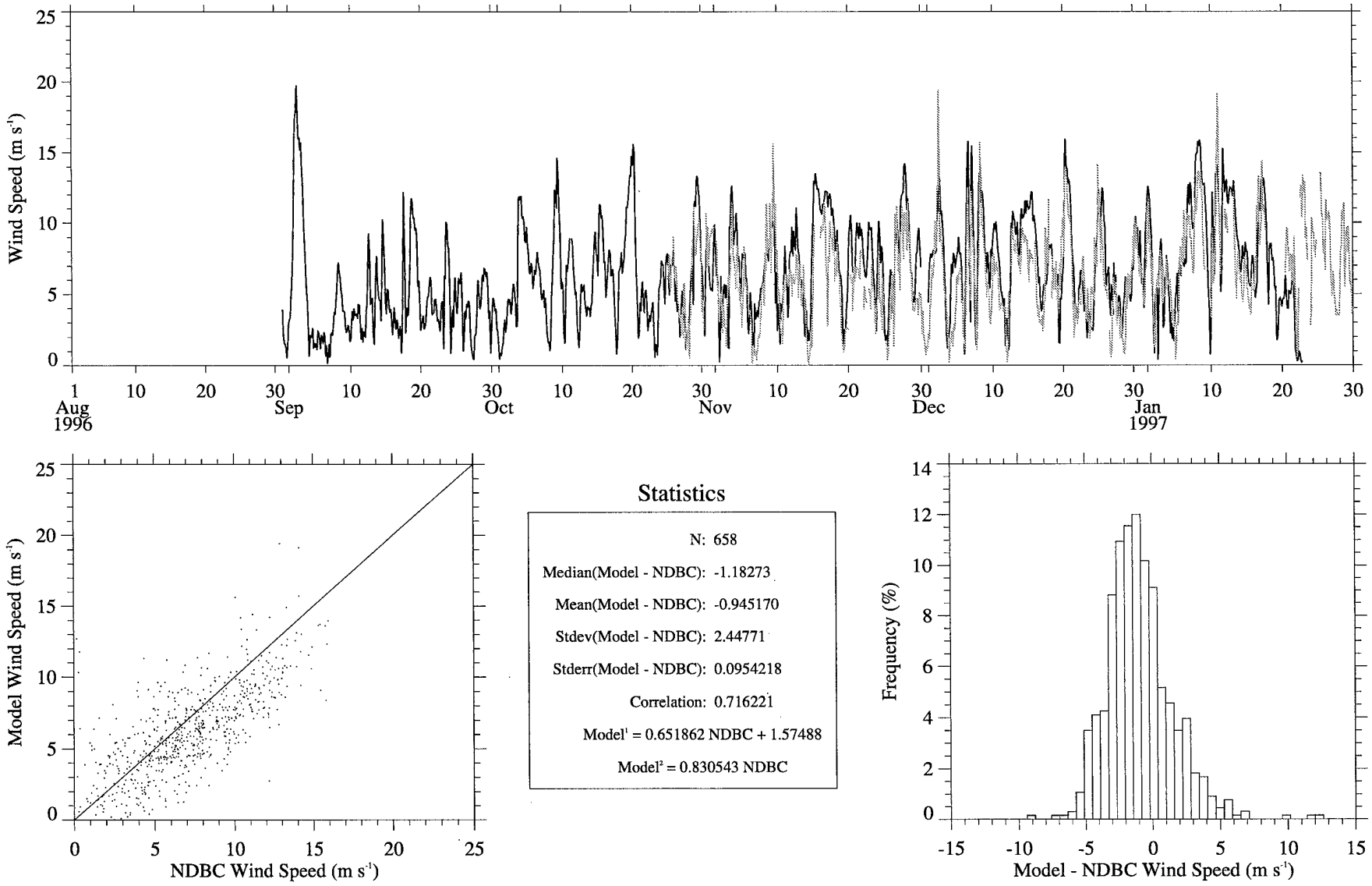

Figure A17. RUC Analysis (gray) vs. NDBC Buoy 44008 (black) wind speed.

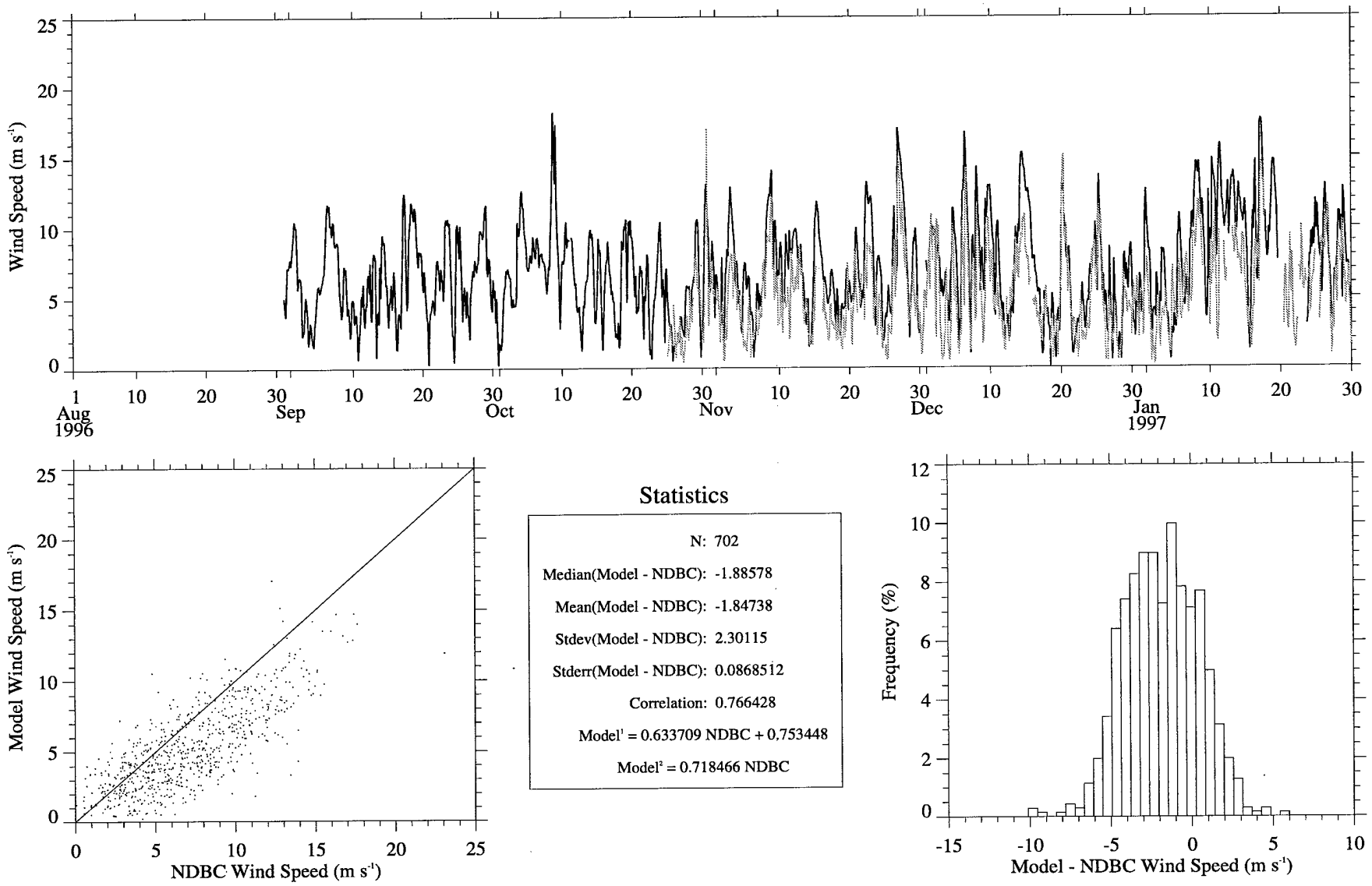

Figure A18. RUC Analysis (gray) vs. NDBC Buoy 44009 (black) wind speed.

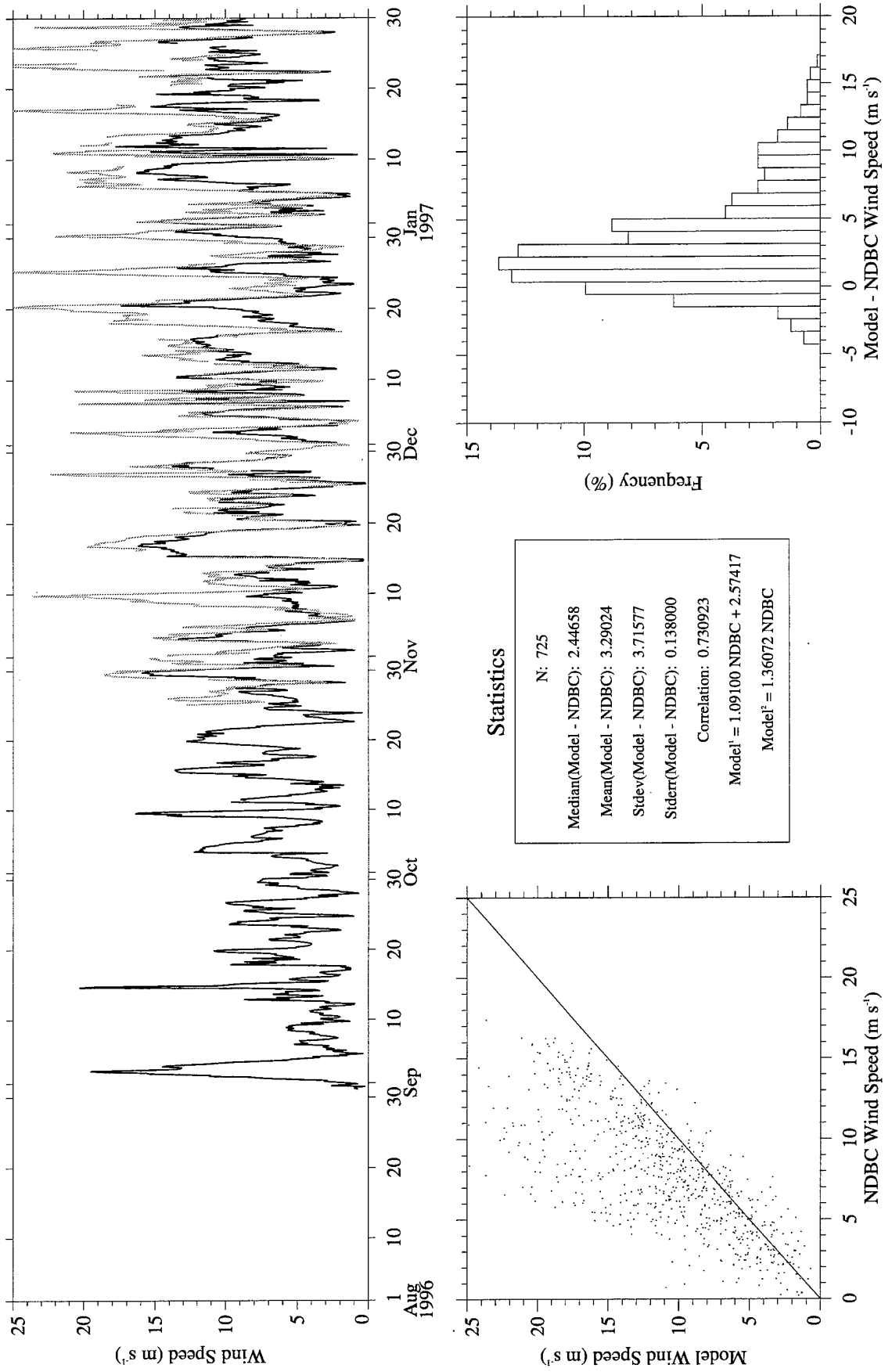

Figure A19. RUC Analysis (gray) vs. NDBC Buoy 44011 (black) wind speed.

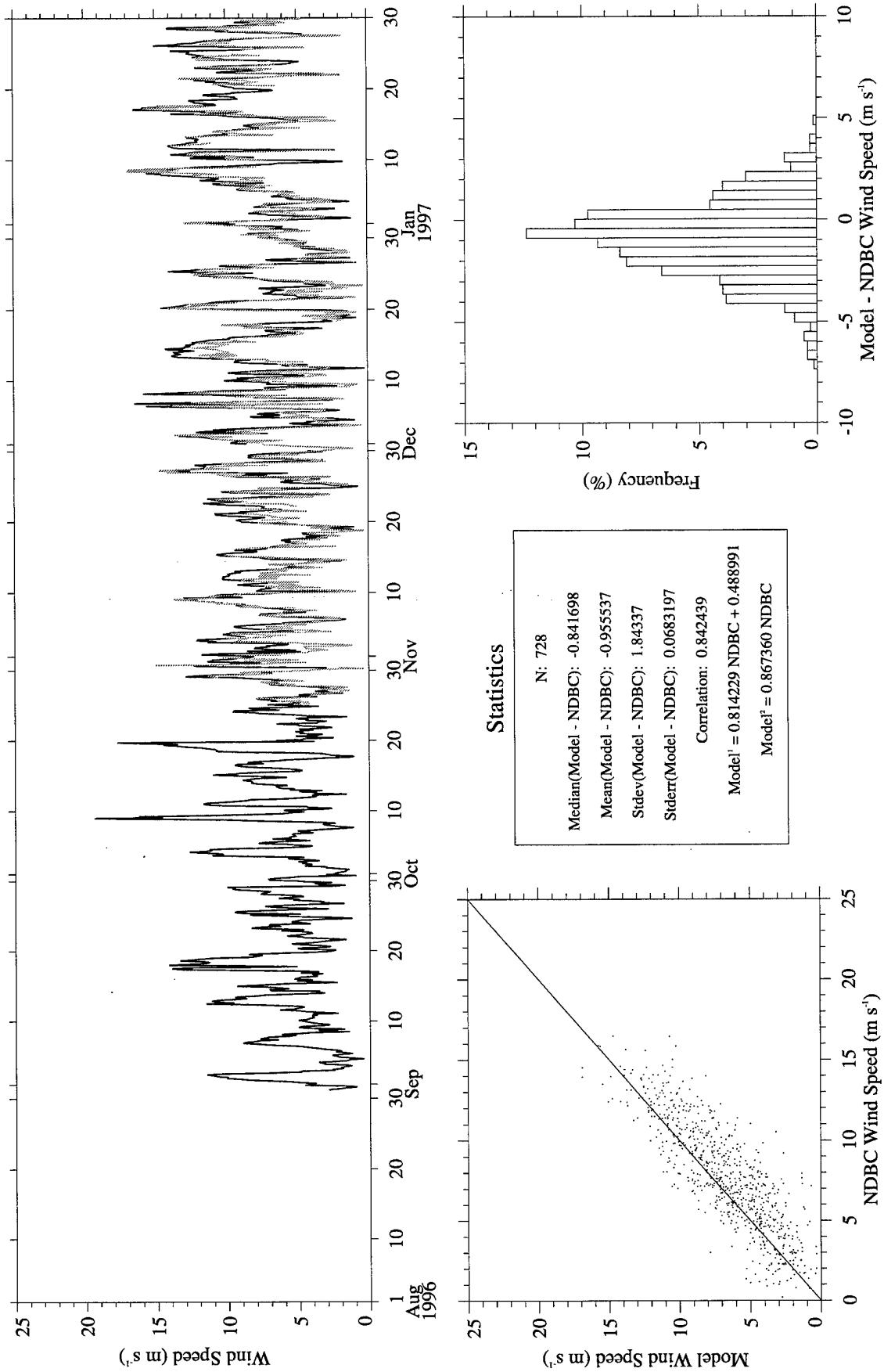

Figure A20. RUC Analysis (gray) vs. NDBC Buoy 44025 (black) wind speed.

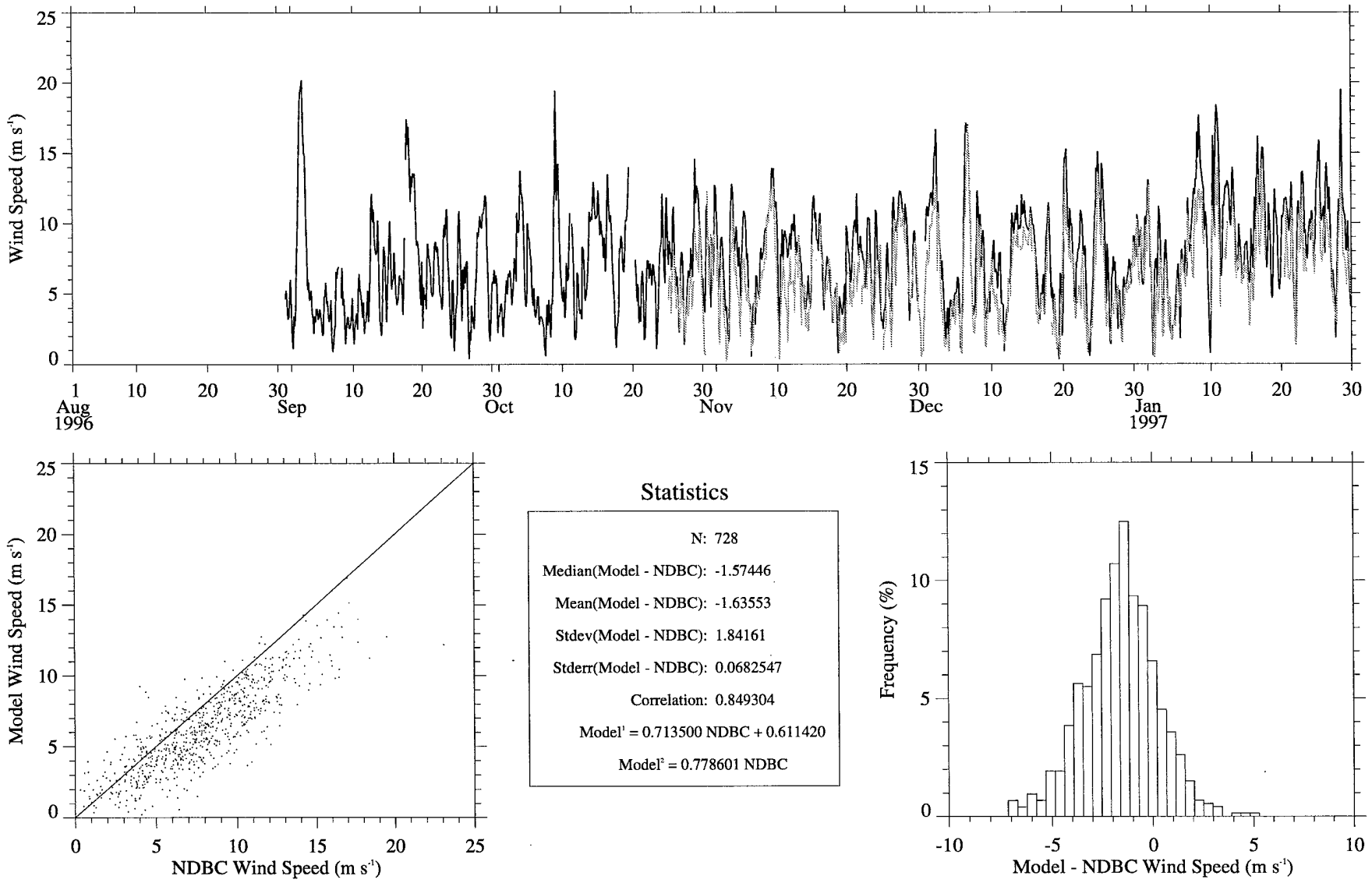

Figure A21. RUC Analysis (gray) vs. NDBC Buoy 44028 (black) wind speed.

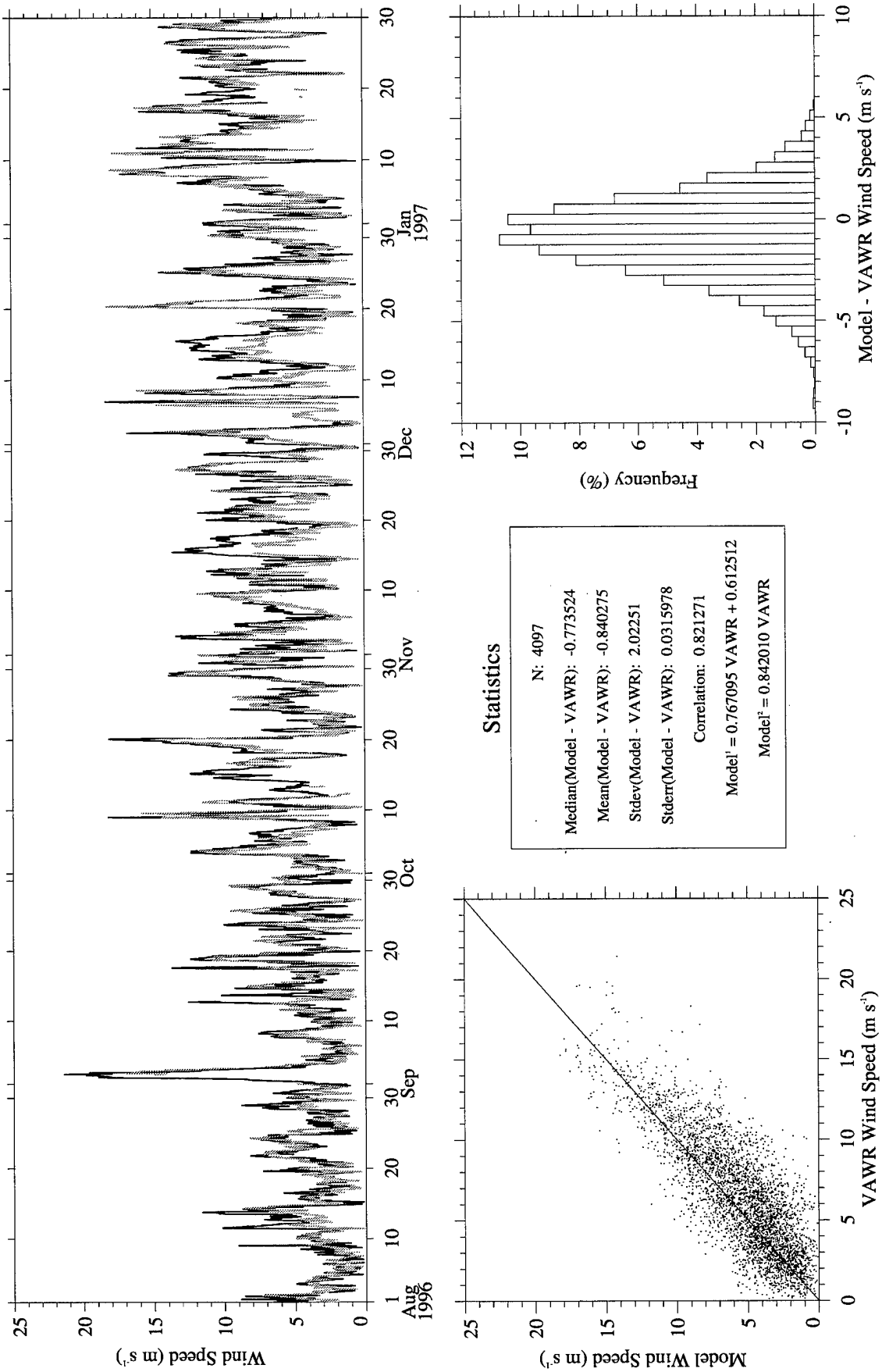

Figure A22. RUC Hourly (gray) vs. CMO VAWR 0704 (black) wind speed.

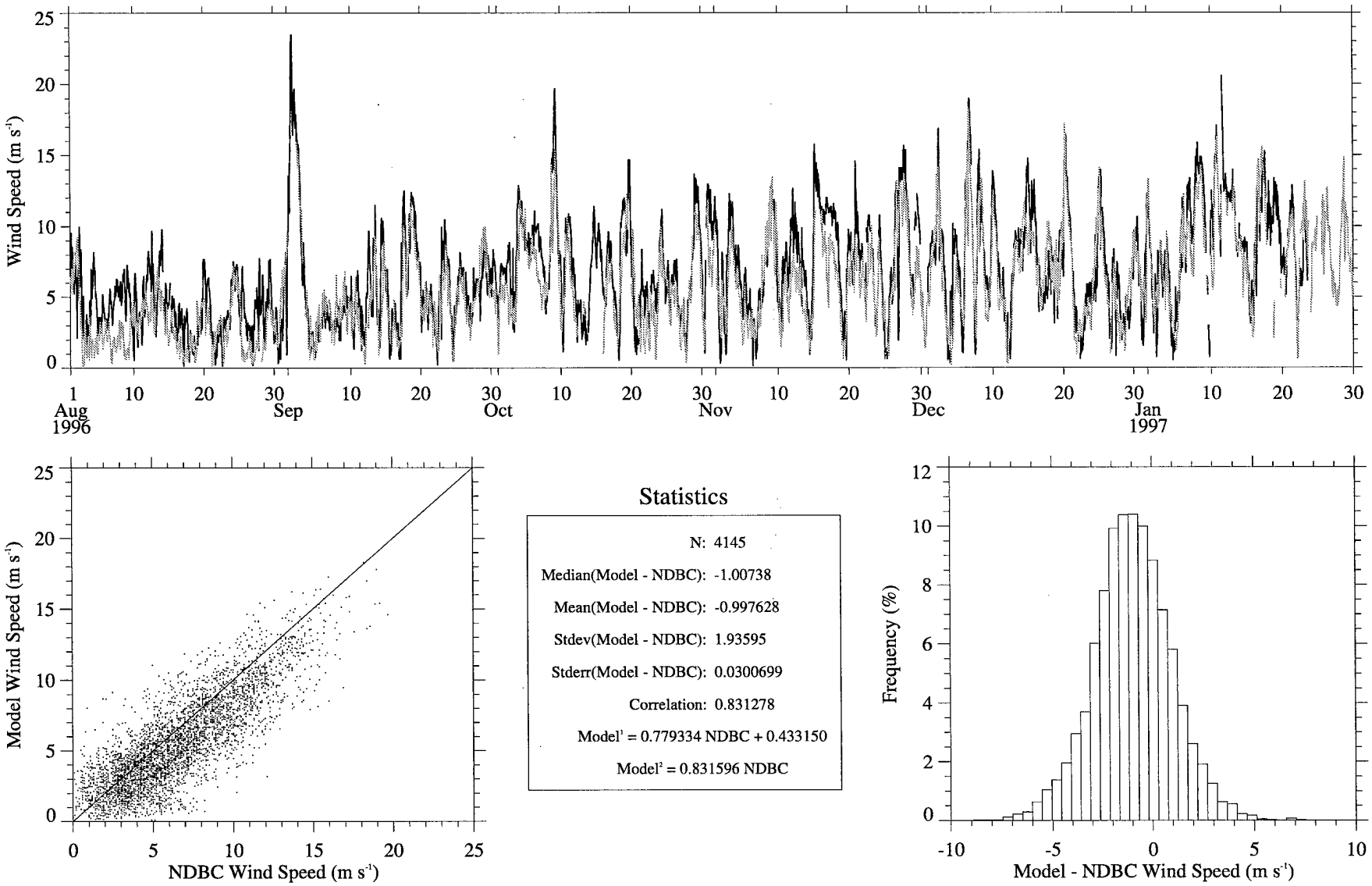

Figure A23. RUC Hourly (gray) vs. NDBC Buoy 44004 (black) wind speed.

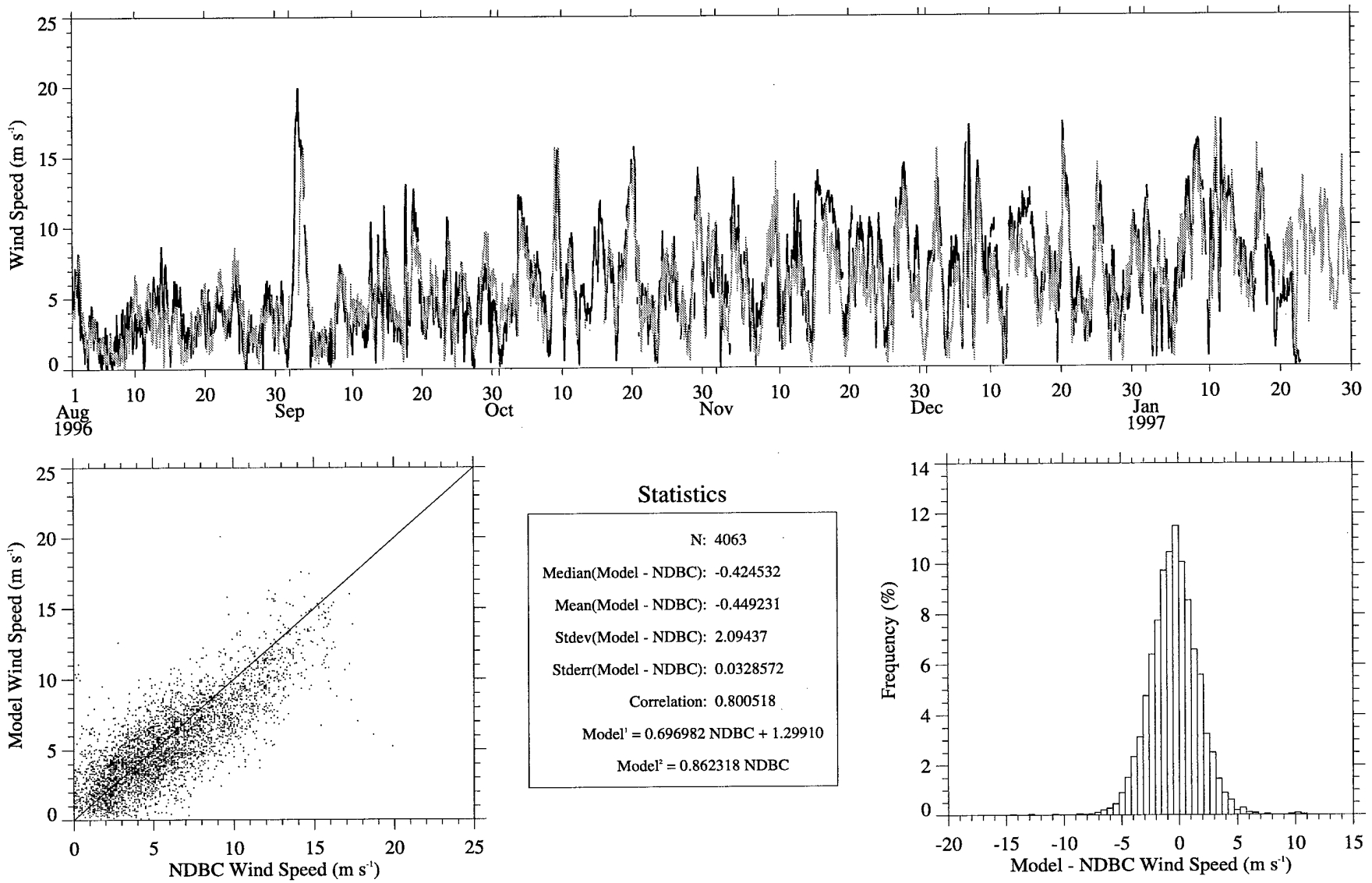

Figure A24. RUC Hourly (gray) vs. NDBC Buoy 44008 (black) wind speed.

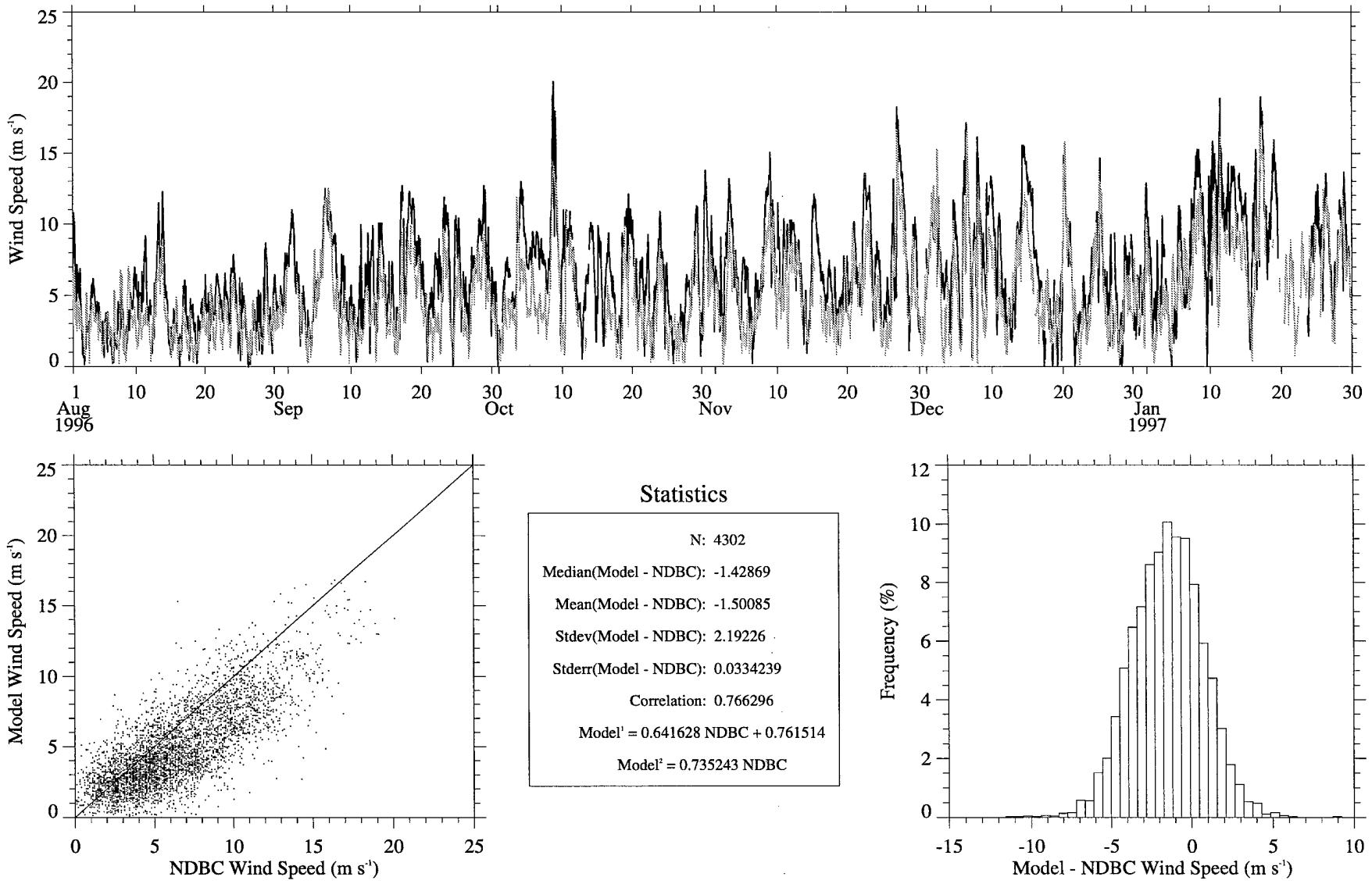

Figure A25. RUC Hourly (gray) vs. NDBC Buoy 44009 (black) wind speed.

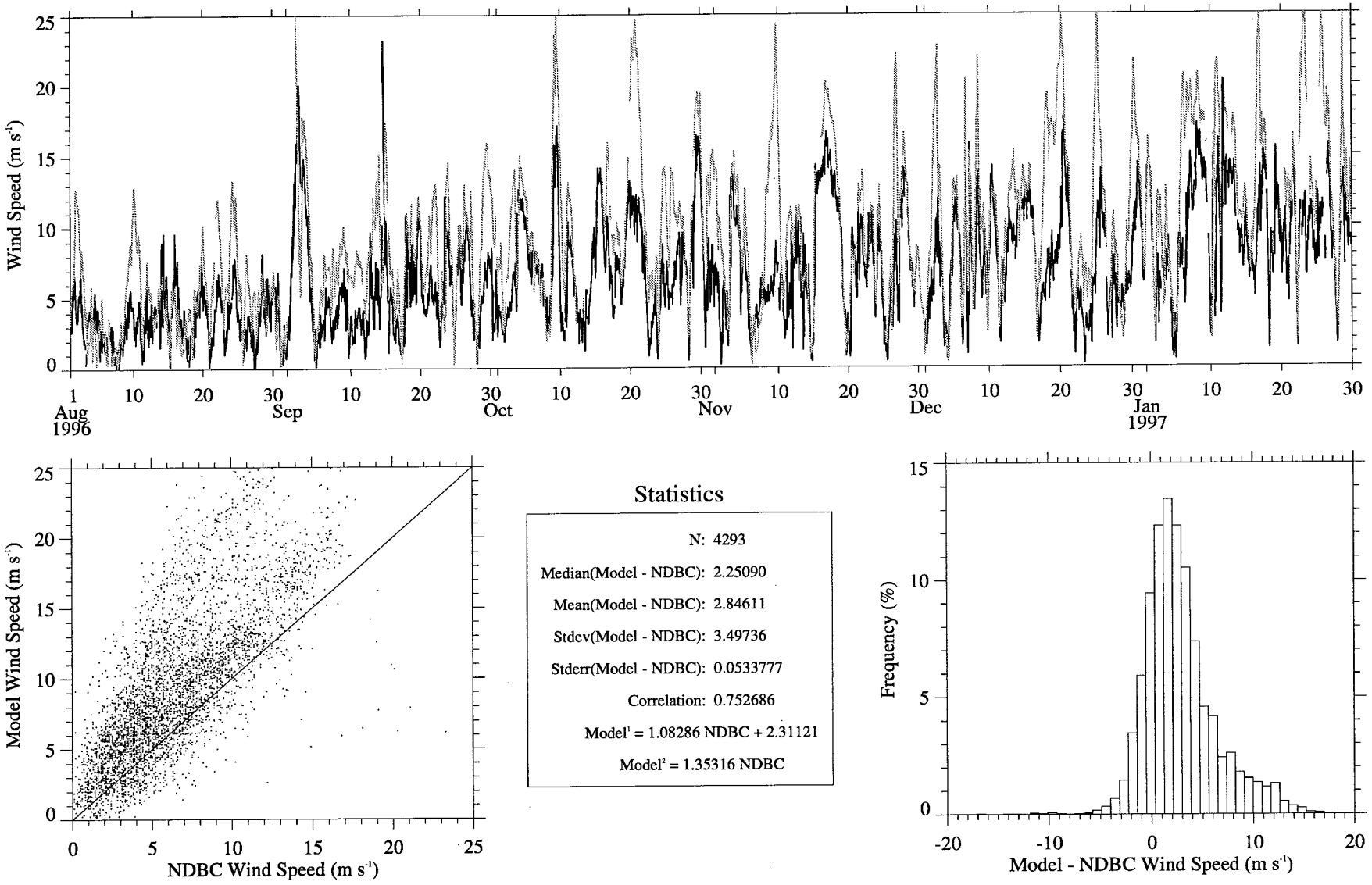

Figure A26. RUC Hourly (gray) vs. NDBC Buoy 44011 (black) wind speed.

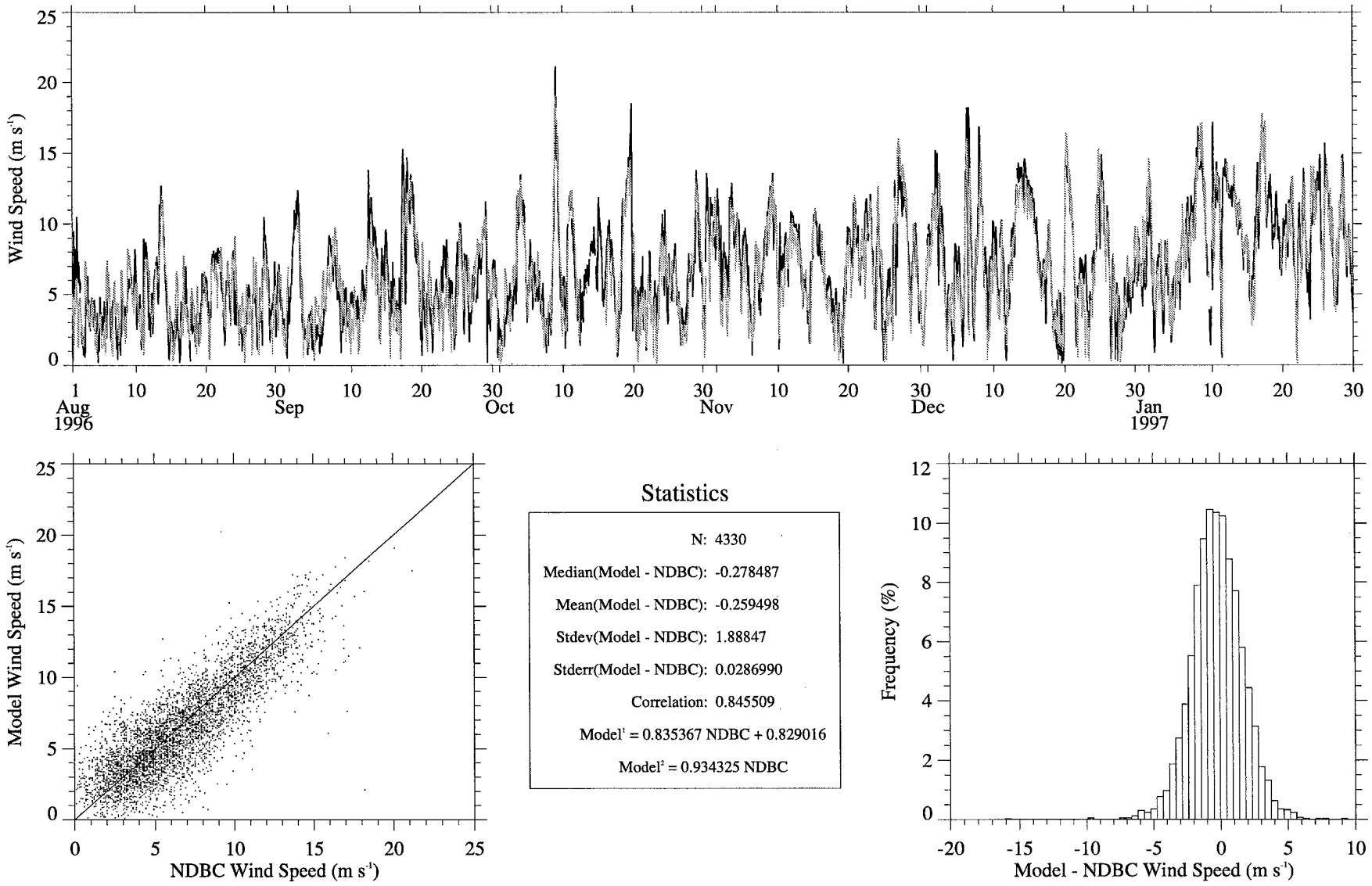

Figure A27. RUC Hourly (gray) vs. NDBC Buoy 44025 (black) wind speed.

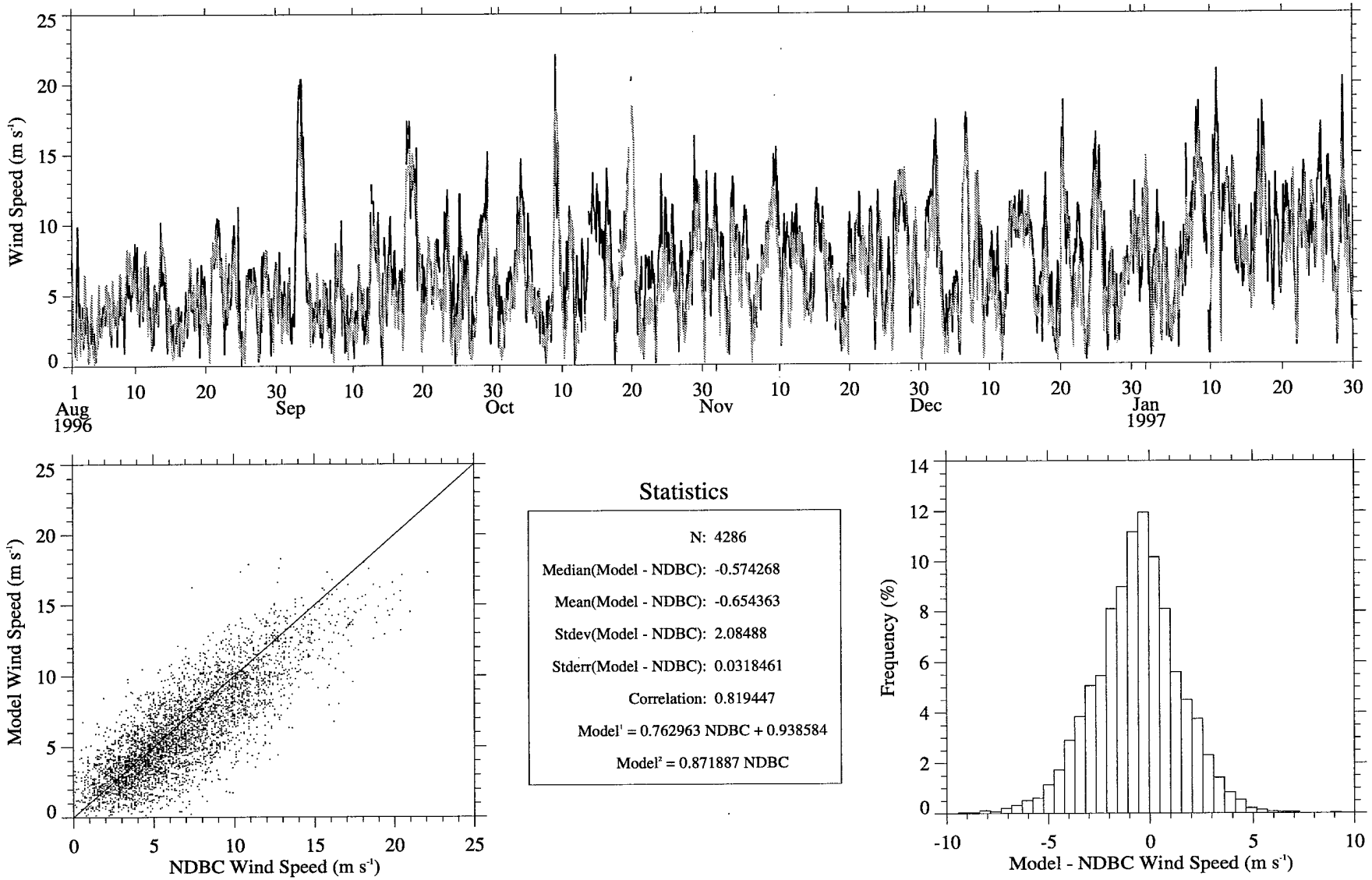

Figure A28. RUC Hourly (gray) vs. NDBC Buoy 44028 (black) wind speed.

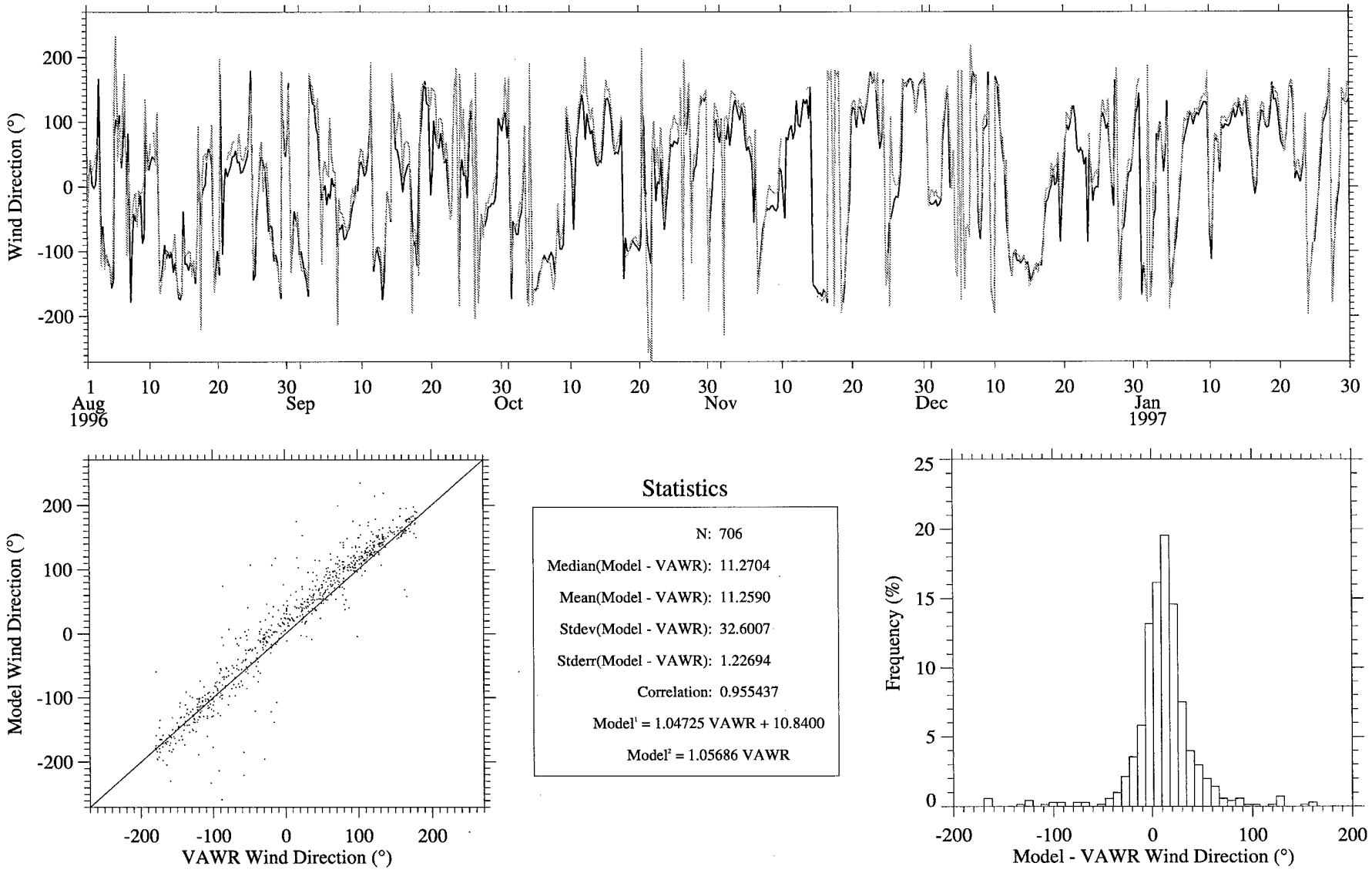

Figure A29. Eta (gray) vs. CMO VAWR 0704 (black) wind direction.

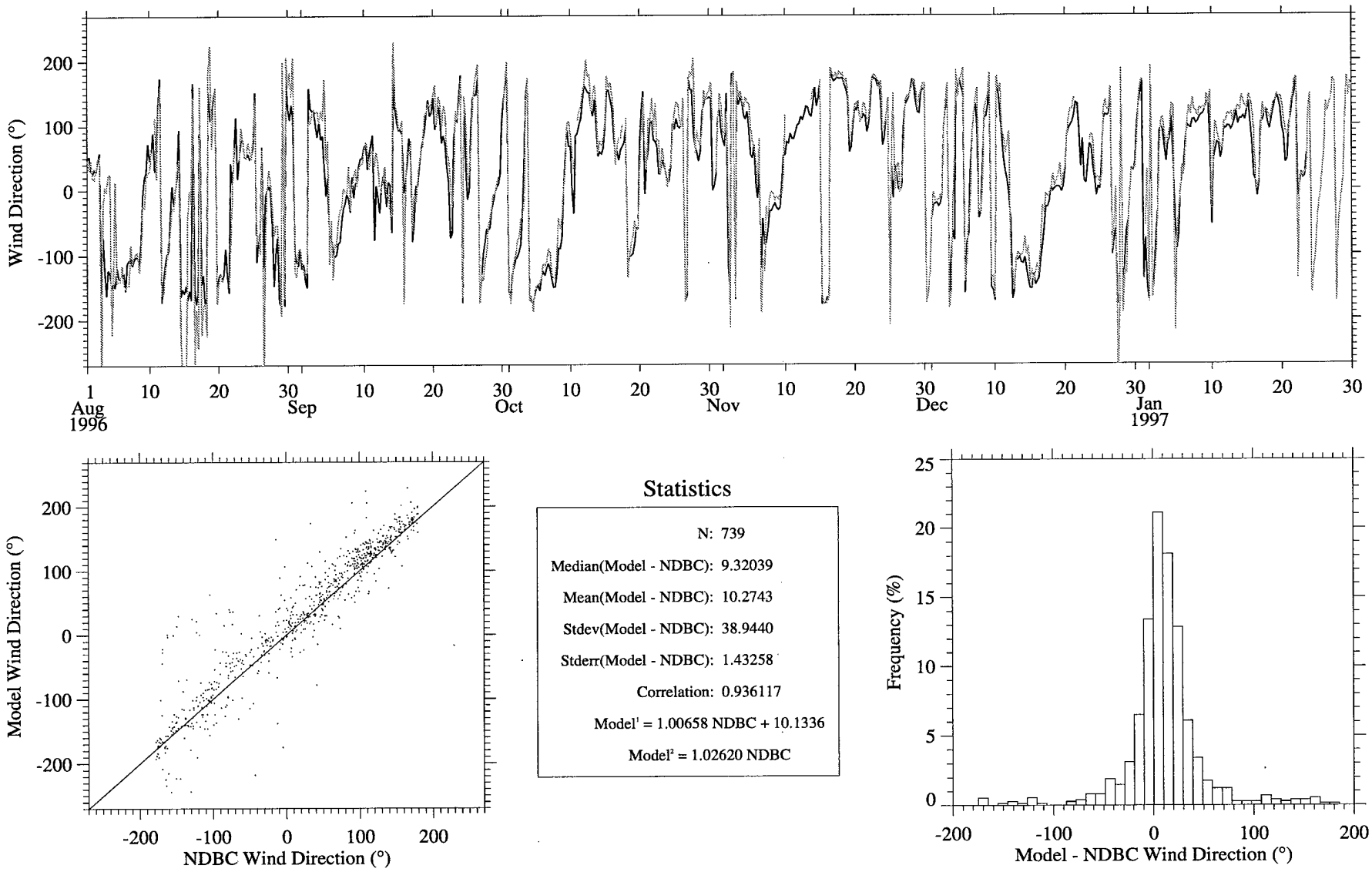

Figure A30. Eta (gray) vs. NDBC Buoy 44004 (black) wind direction.

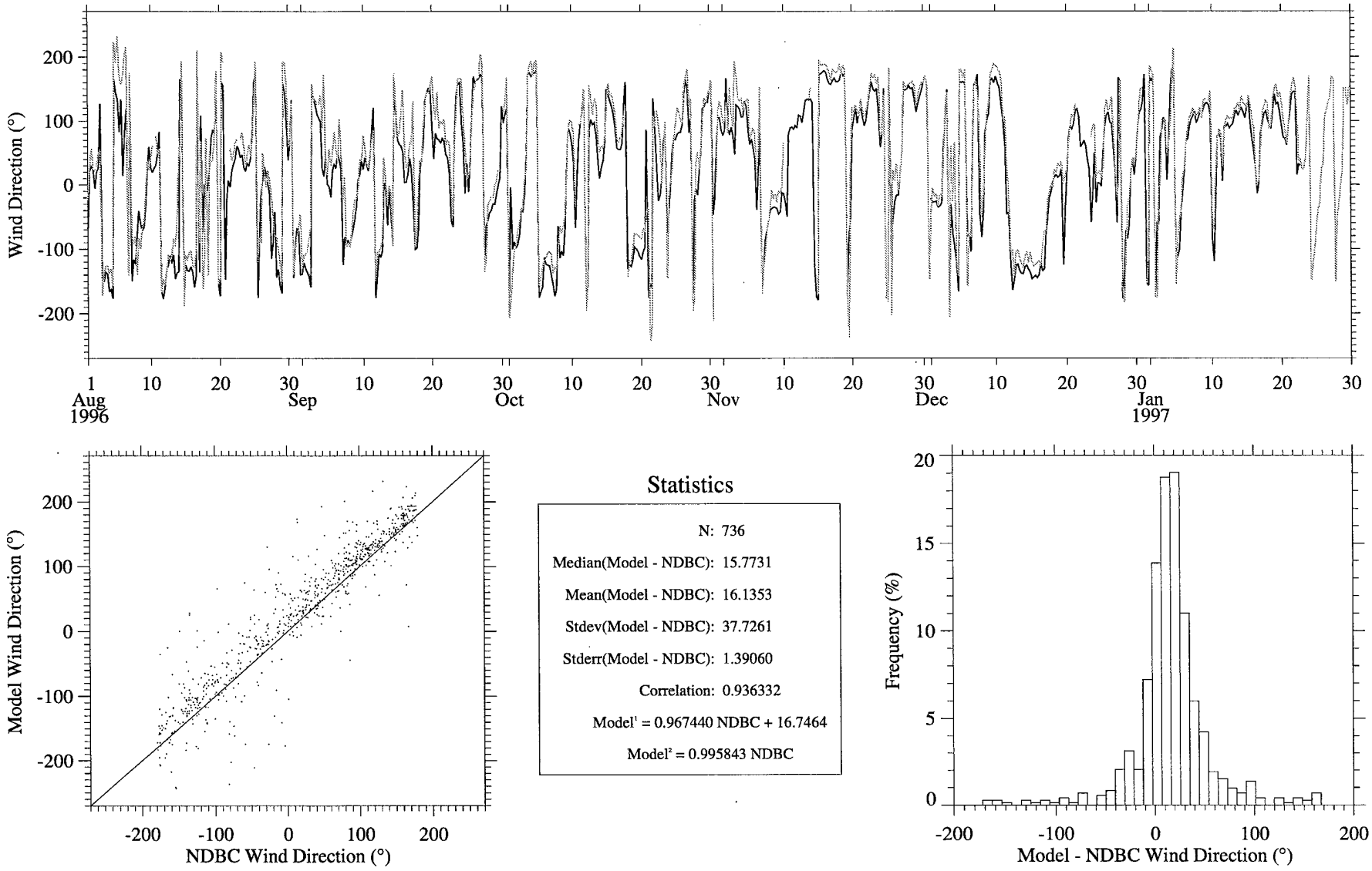

Figure A31. Eta (gray) vs. NDBC Buoy 44008 (black) wind direction.

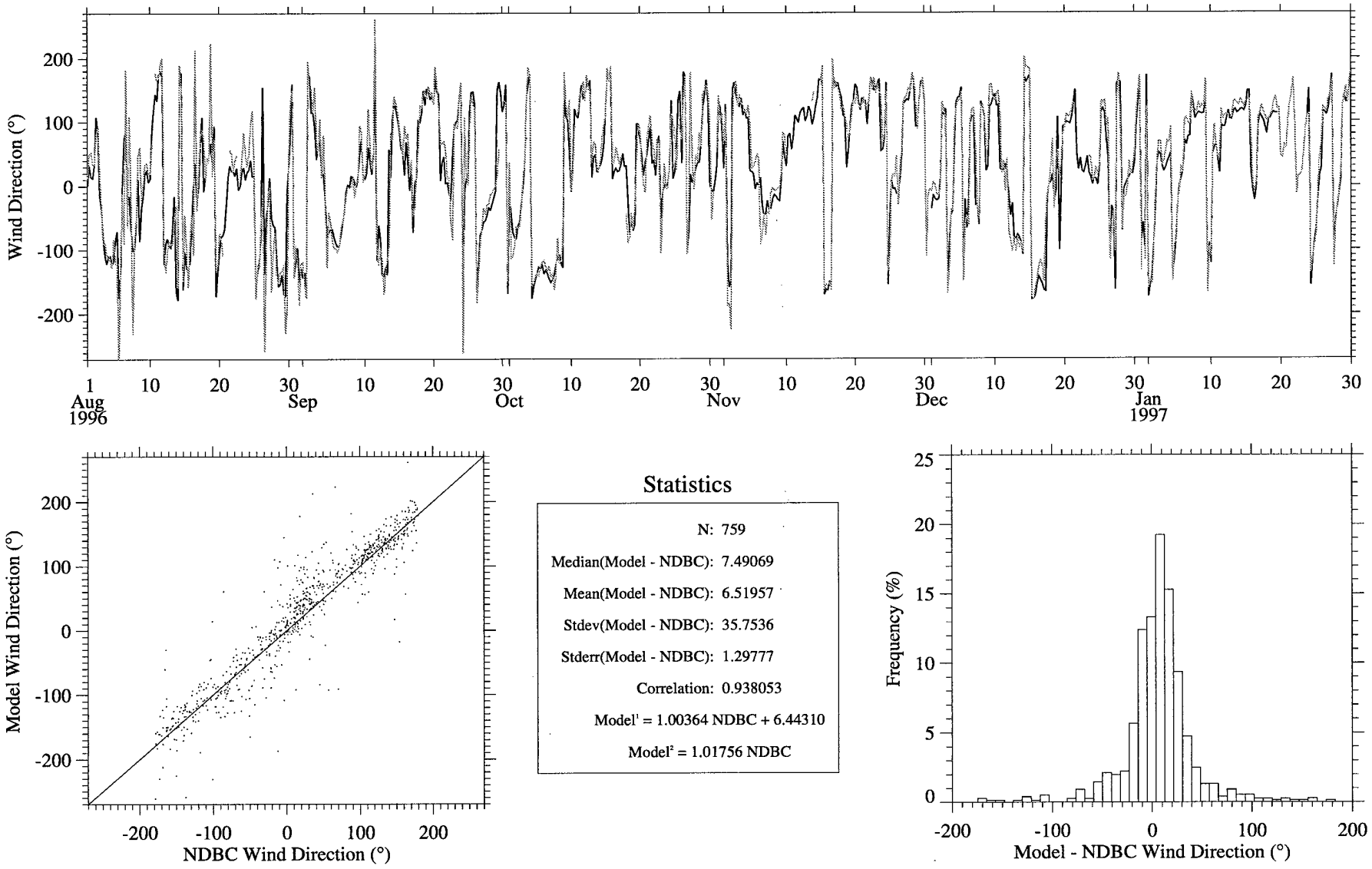

Figure A32. Eta (gray) vs. NDBC Buoy 44009 (black) wind direction.

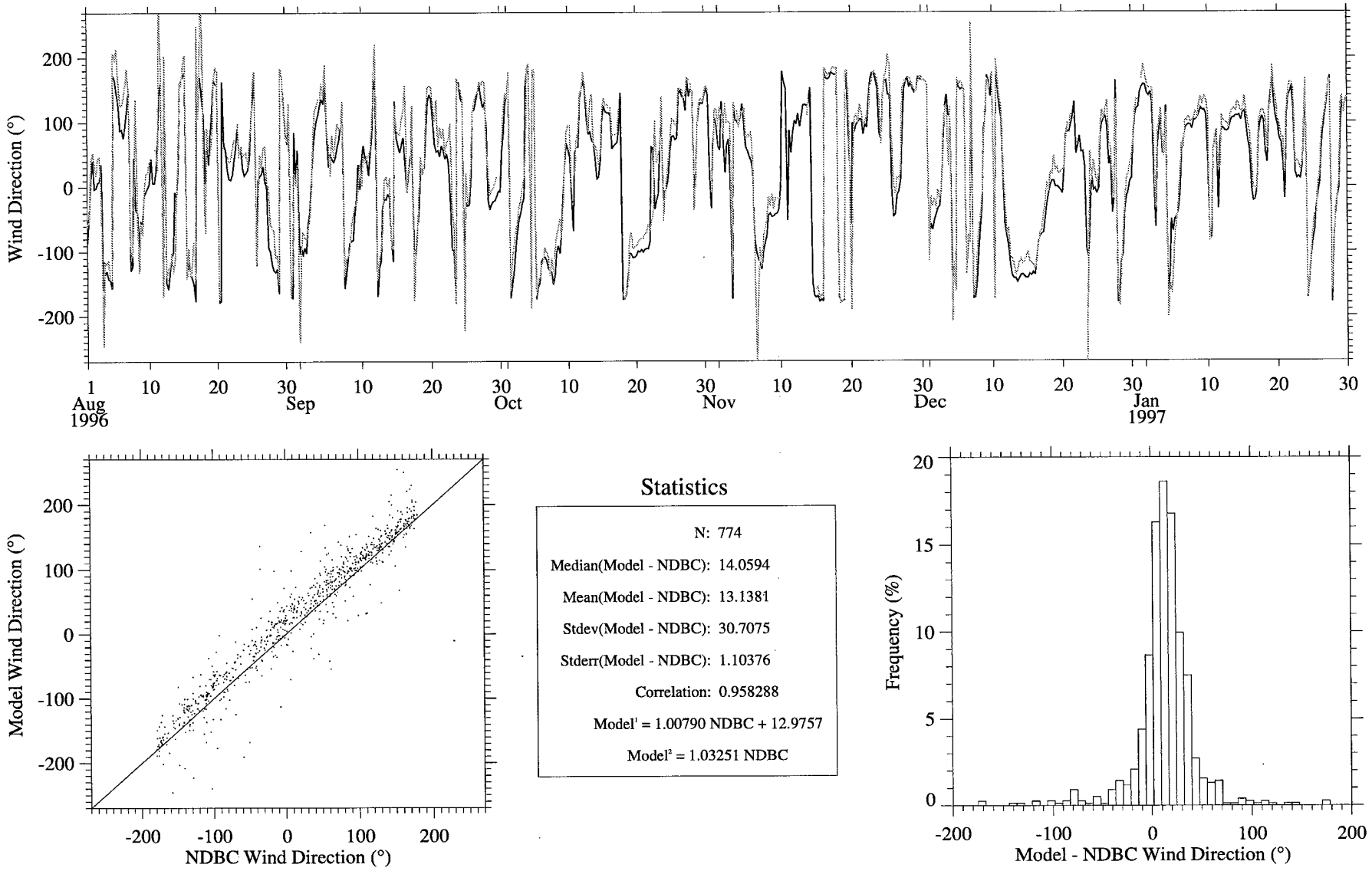

Figure A33. Eta (gray) vs. NDBC Buoy 44011 (black) wind direction.

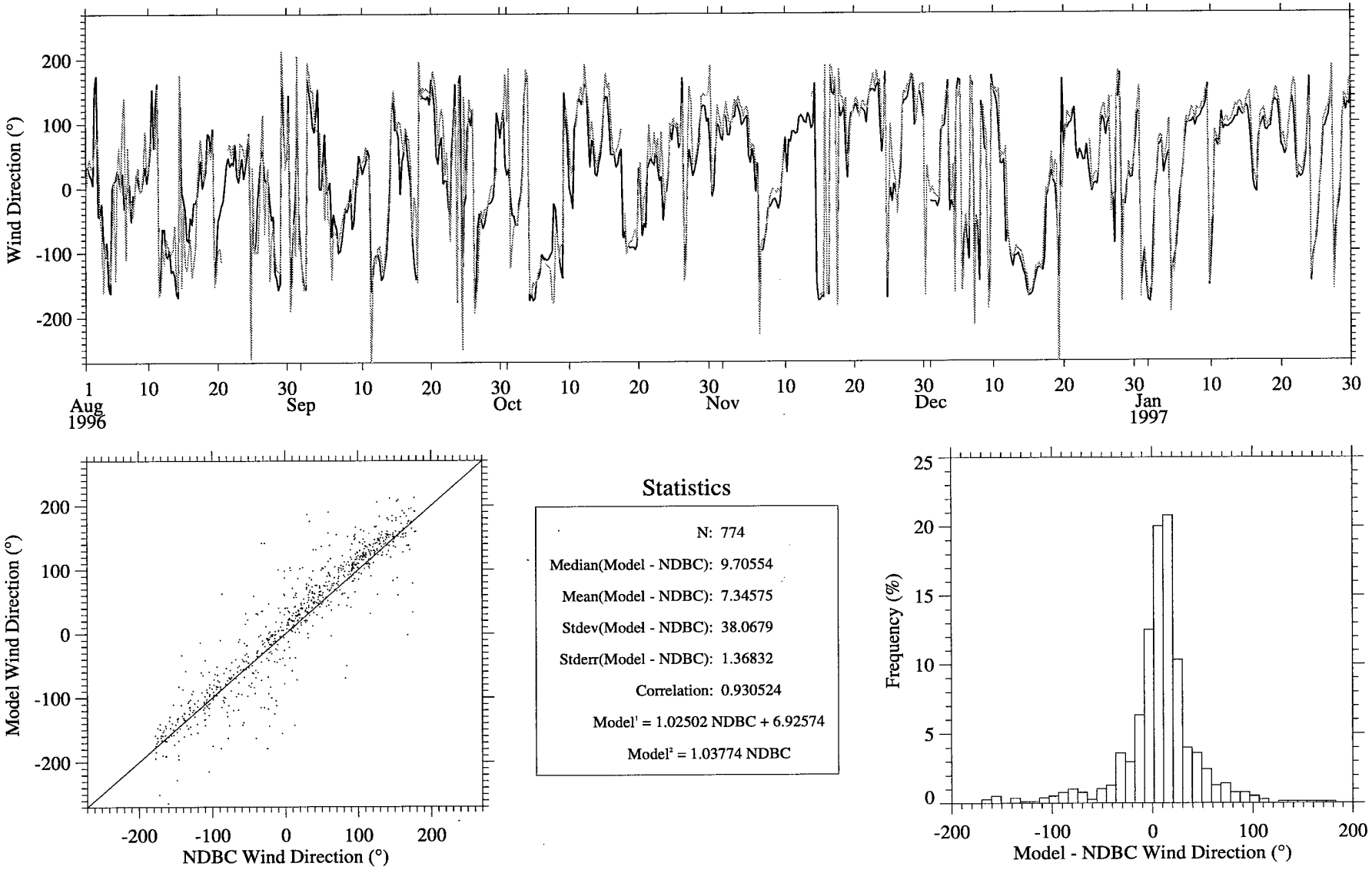

Figure A34. Eta (gray) vs. NDBC Buoy 44025 (black) wind direction.

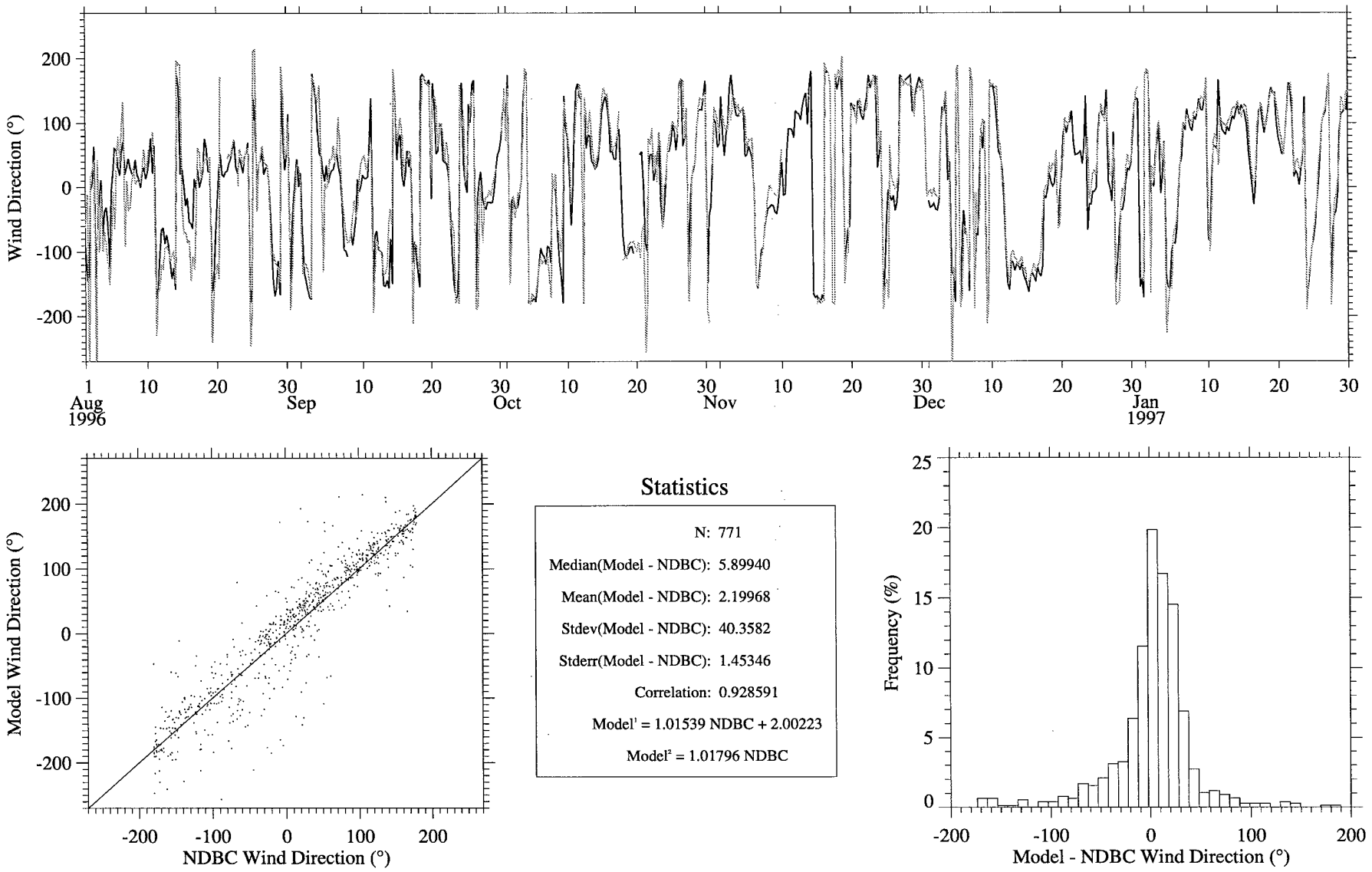

Figure A35. Eta (gray) vs. NDBC Buoy 44028 (black) wind direction.

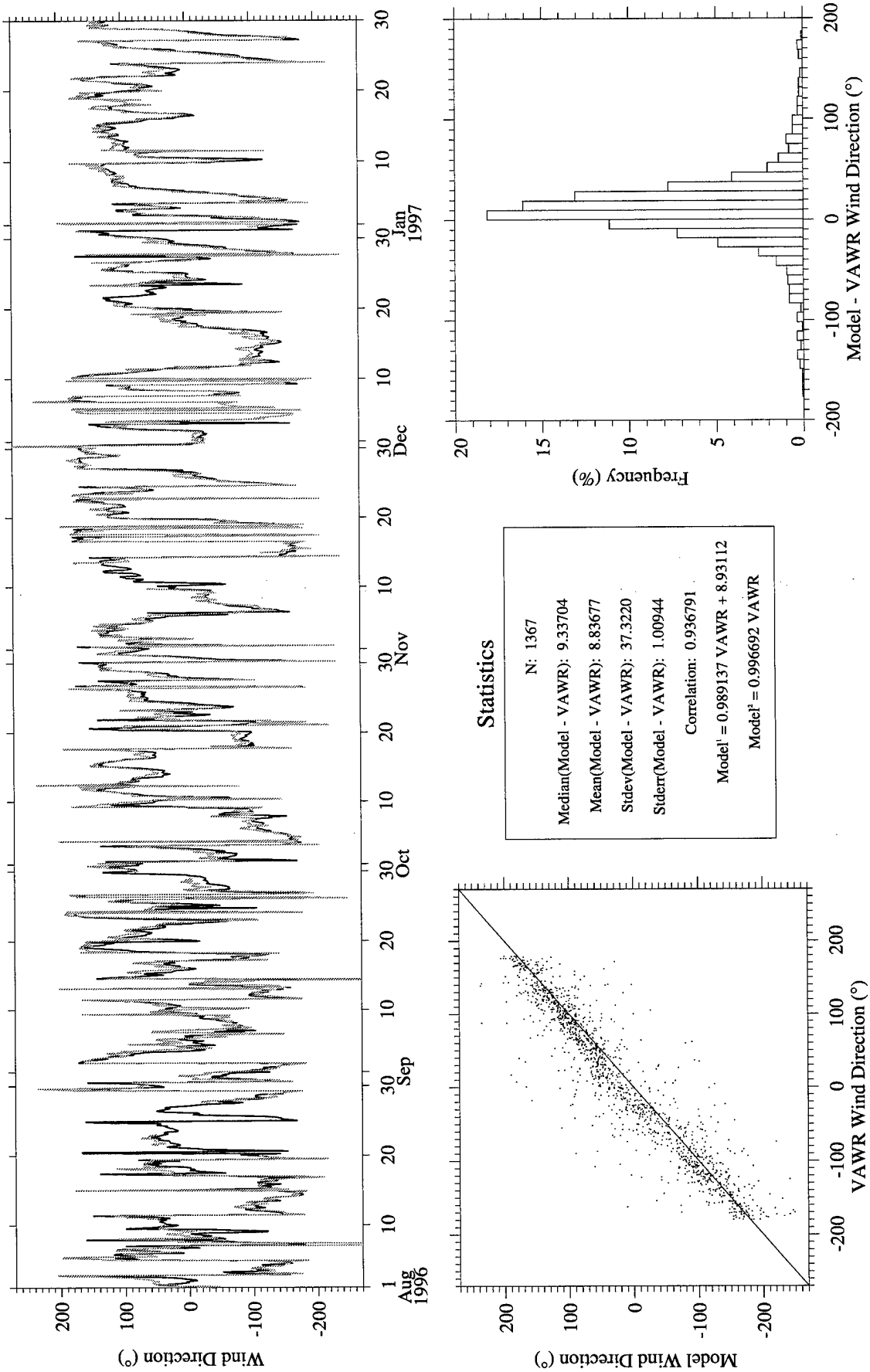

Figure A36. RUC (gray) vs. CMO VAWR 0704 (black) wind direction.

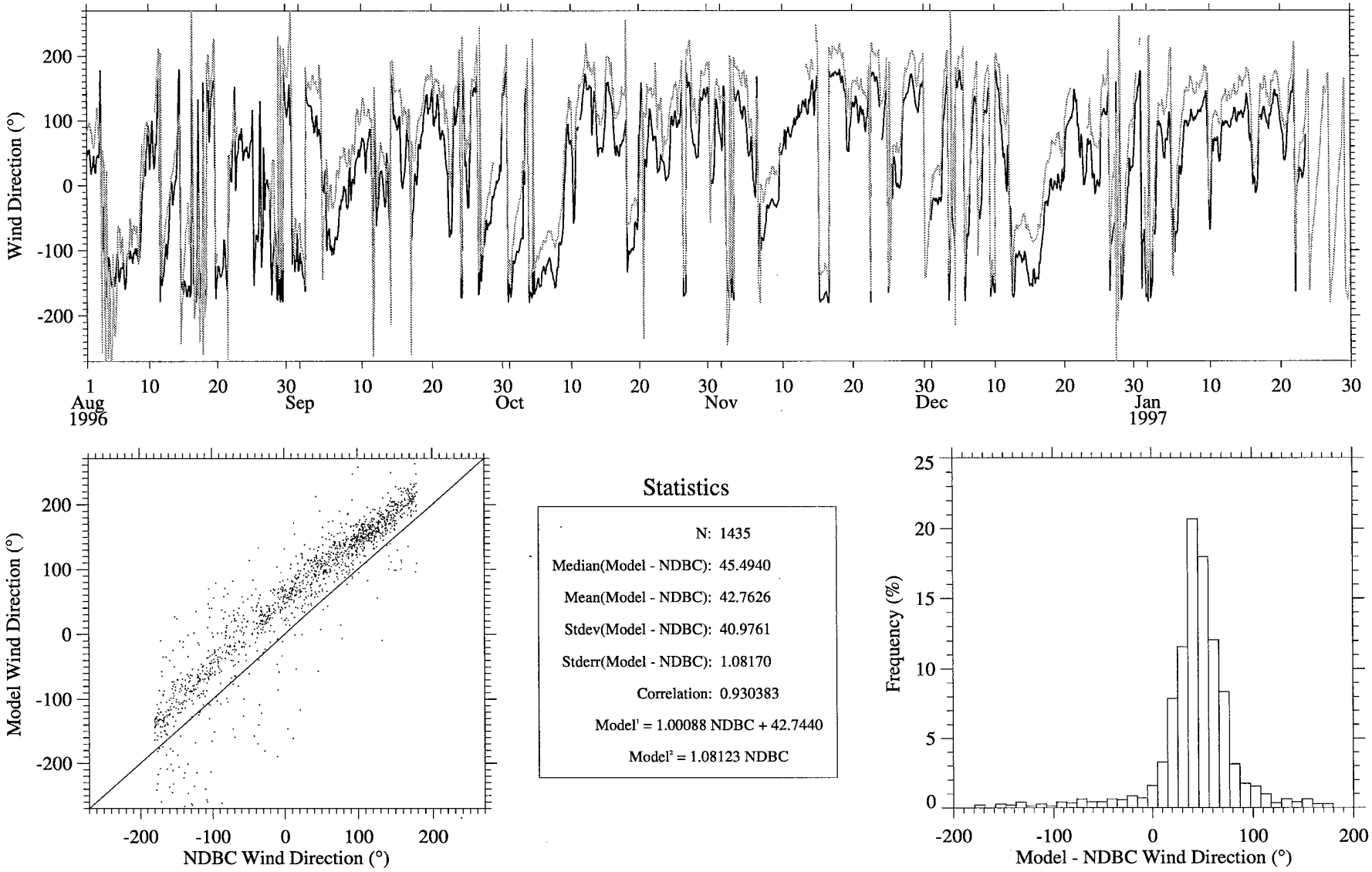

Figure A37. RUC (gray) vs. NDBC Buoy 44004 (black) wind direction.

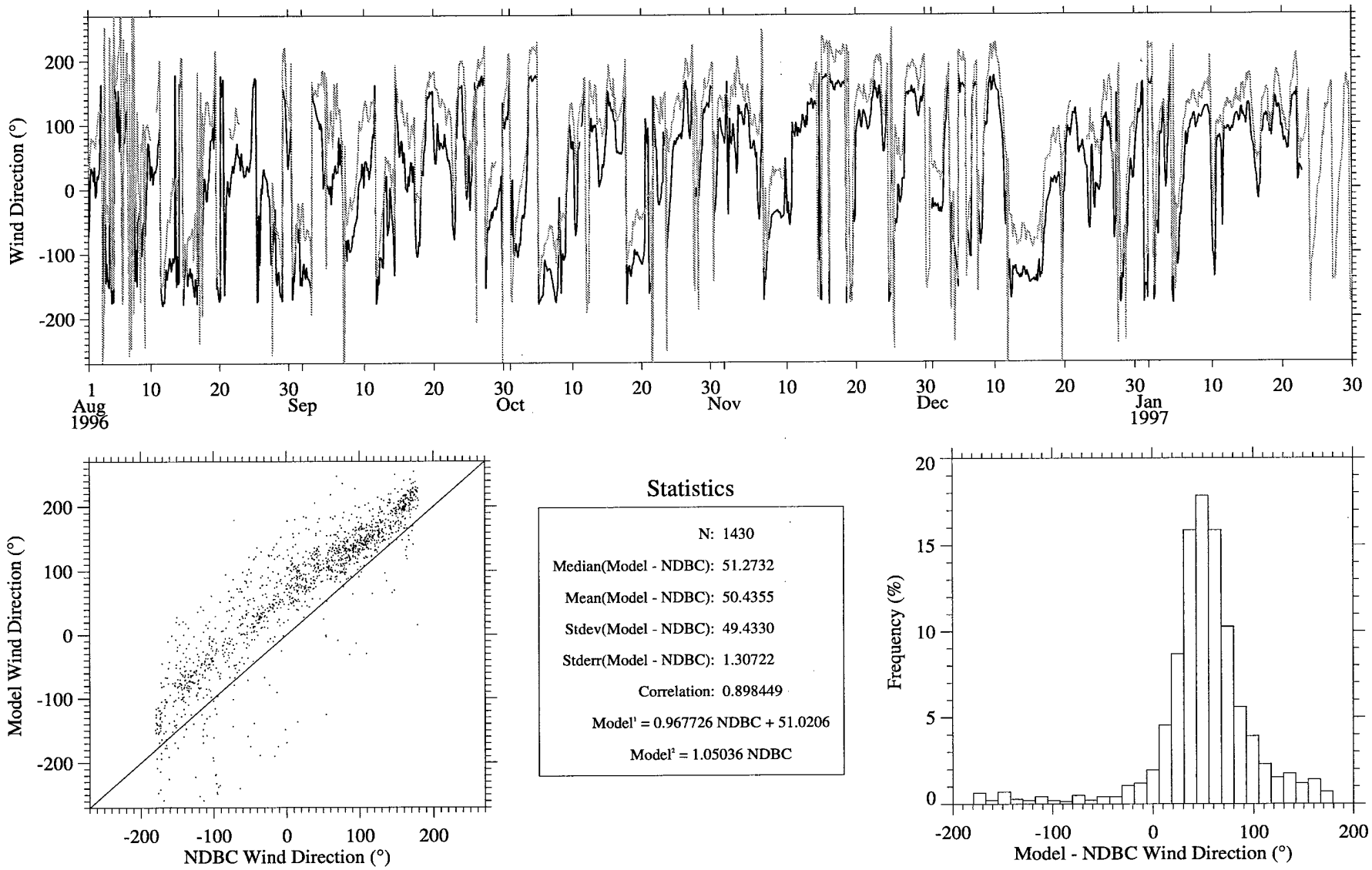

Figure A38. RUC (gray) vs. NDBC Buoy 44008 (black) wind direction.

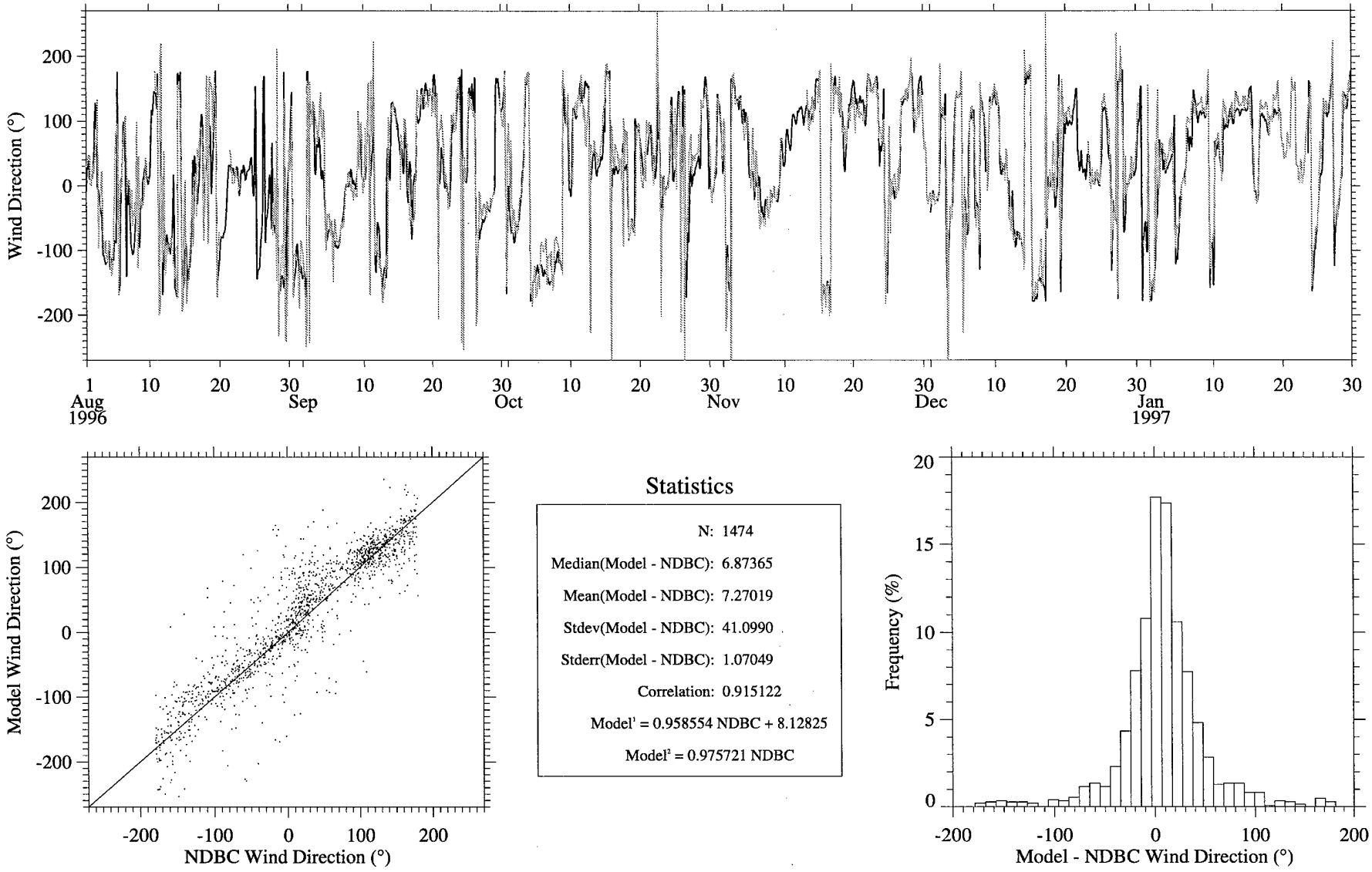

Figure A39. RUC (gray) vs. NDBC Buoy 44009 (black) wind direction.

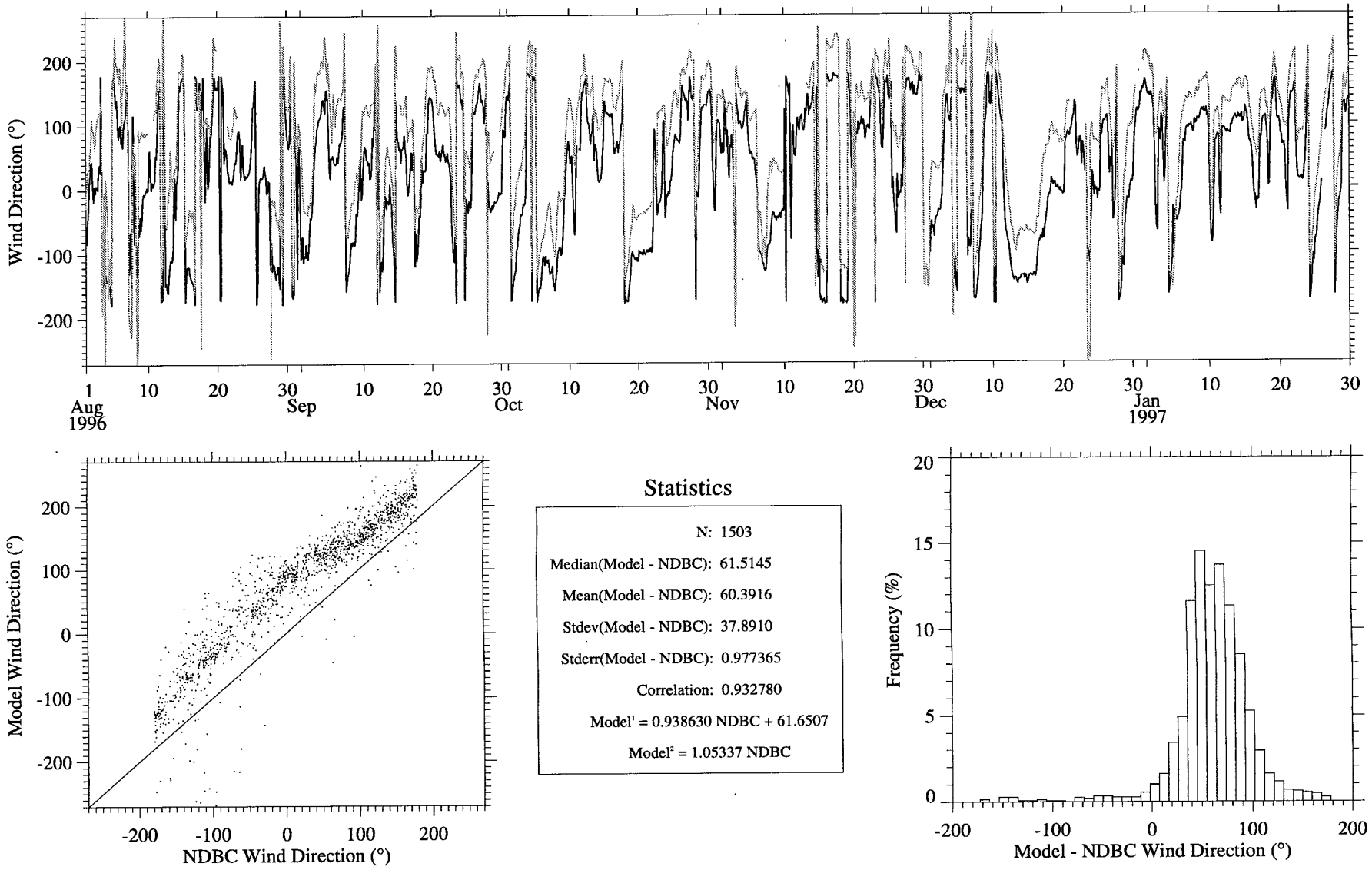

Figure A40. RUC (gray) vs. NDBC Buoy 44011 (black) wind direction.

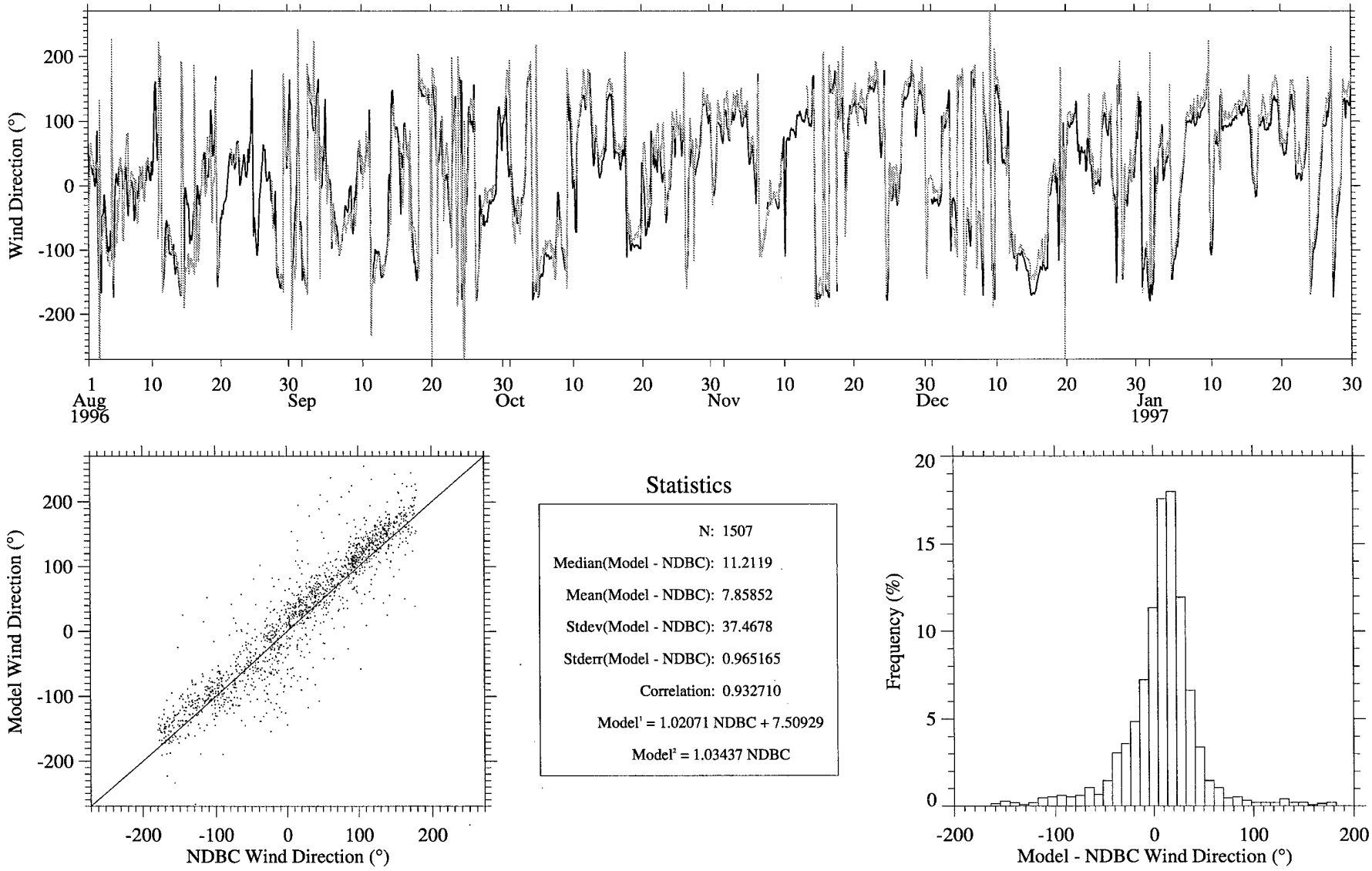

Figure A41. RUC (gray) vs. NDBC Buoy 44025 (black) wind direction.

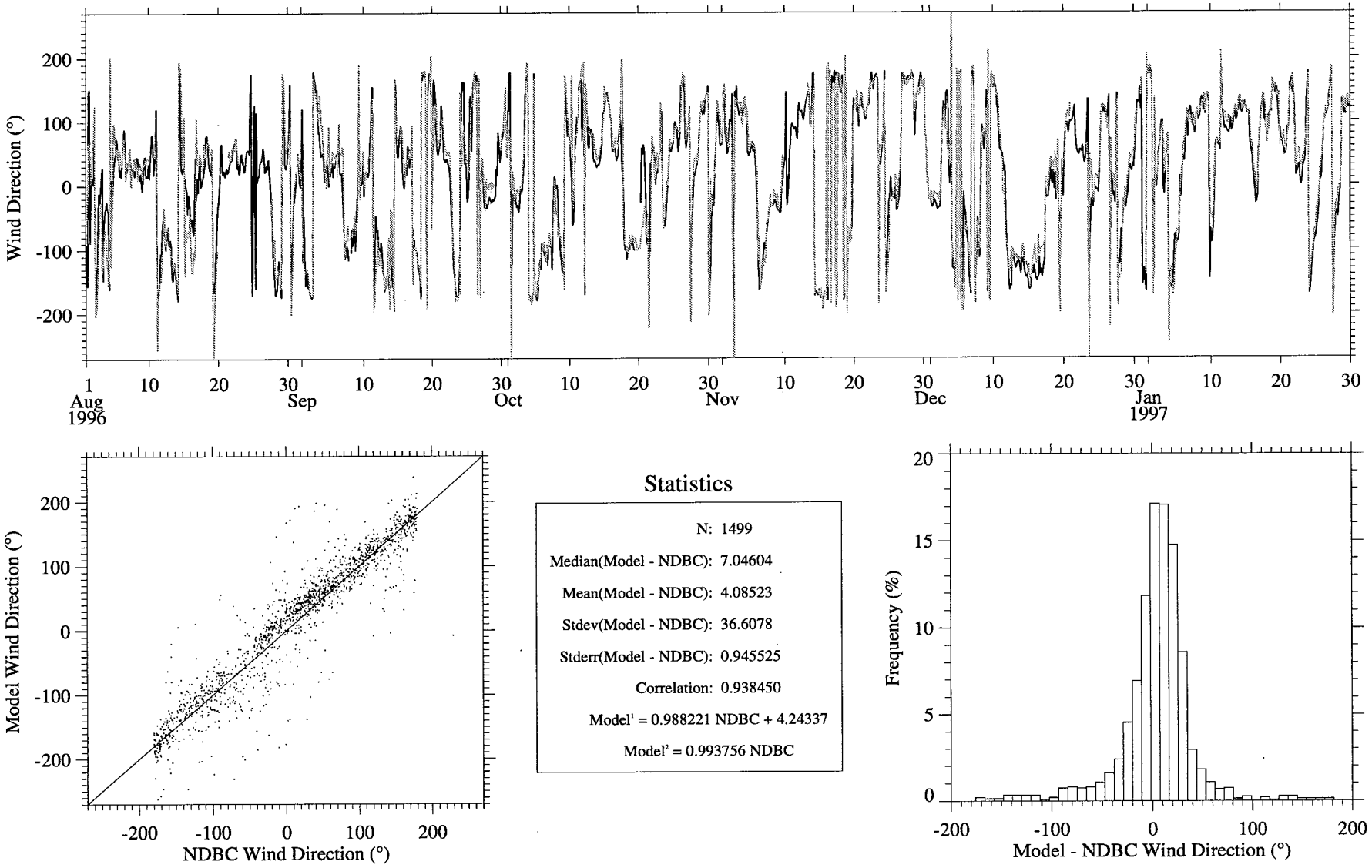

Figure A42. RUC (gray) vs. NDBC Buoy 44028 (black) wind direction.

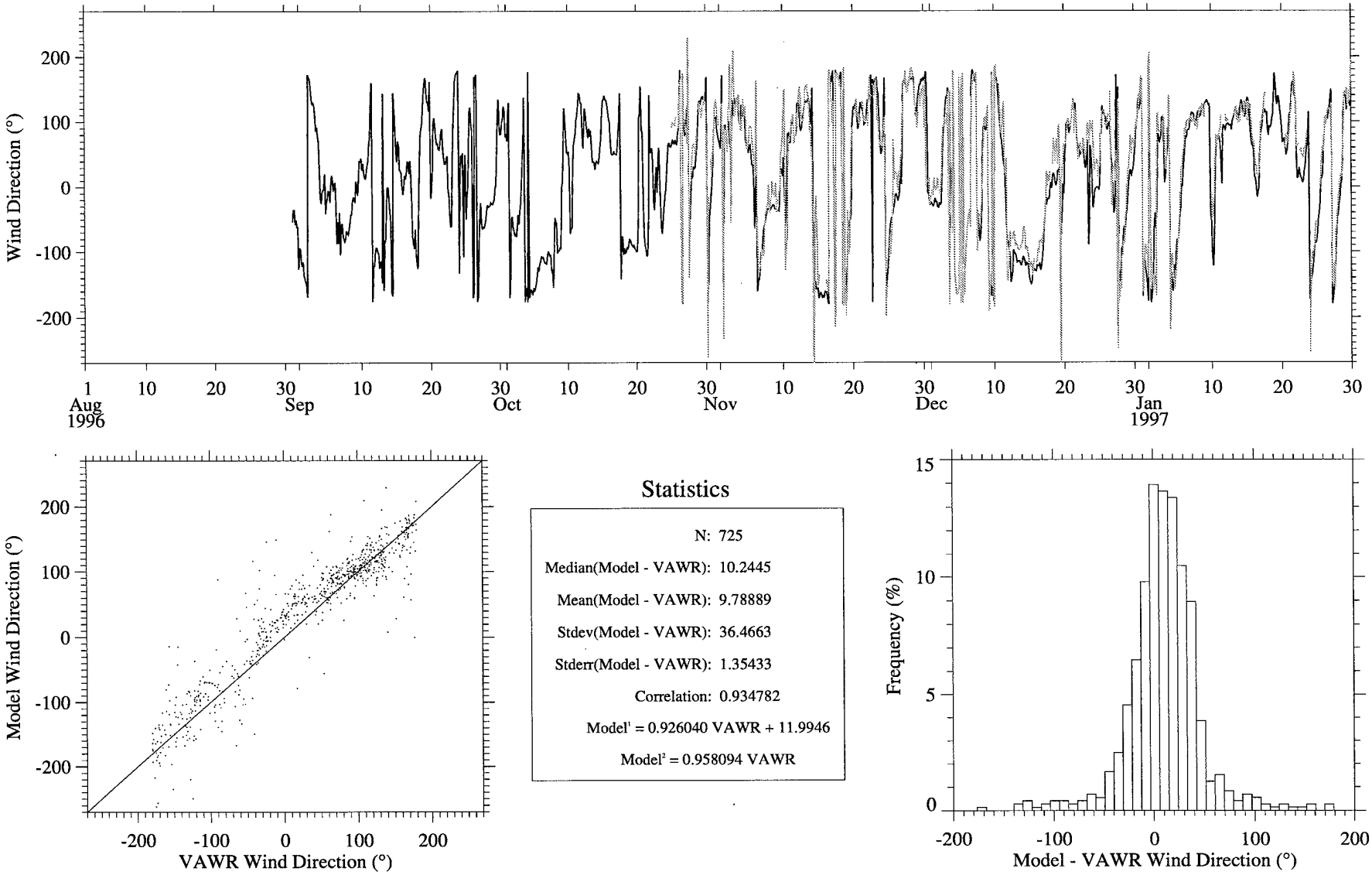

Figure A43. RUC Analysis (gray) vs. CMO VAWR 0704 (black) wind direction.

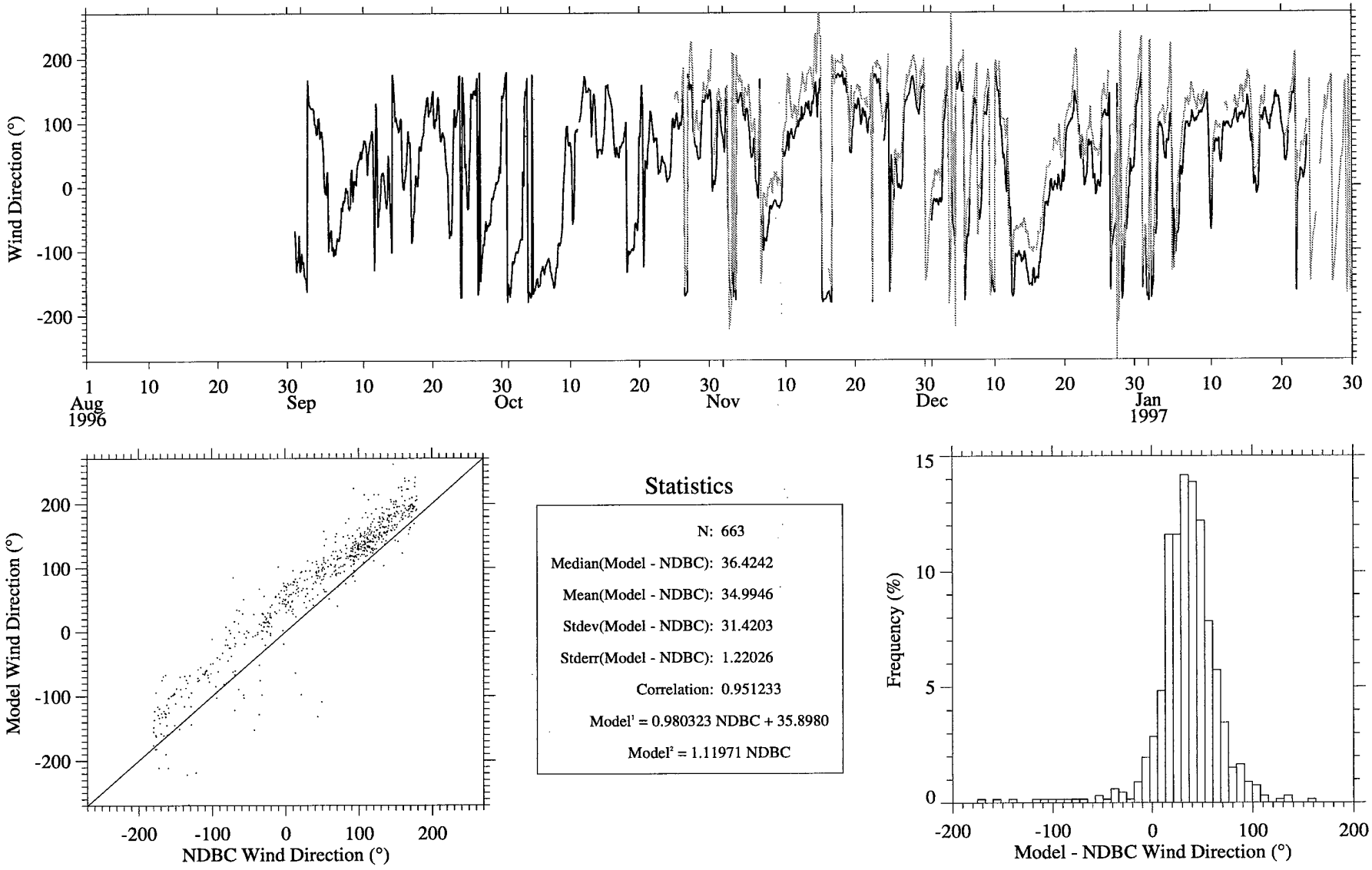

Figure A44. RUC Analysis (gray) vs. NDBC Buoy 44004 (black) wind direction.

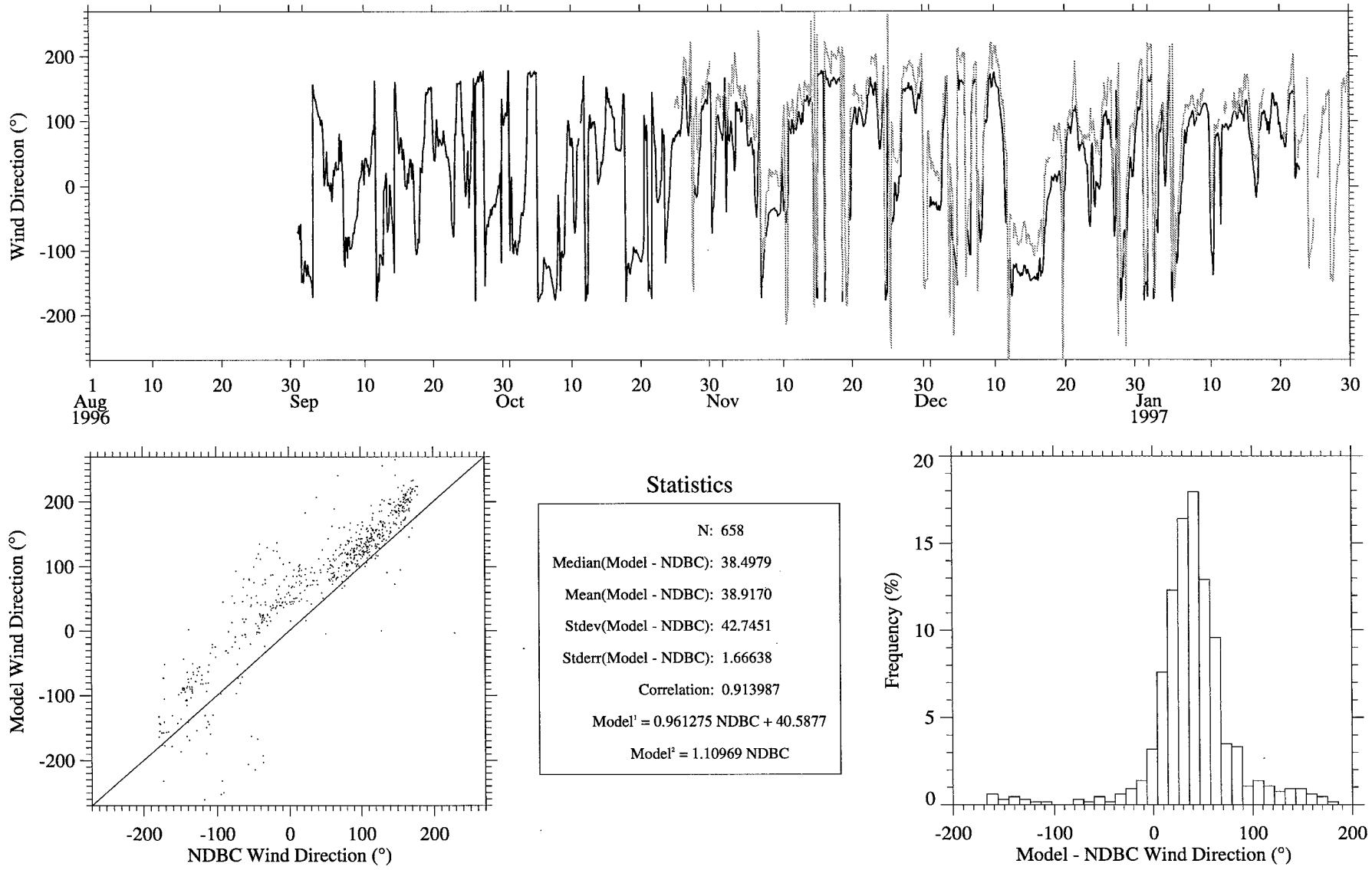

Figure A45. RUC Analysis (gray) vs. NDBC Buoy 44008 (black) wind direction.

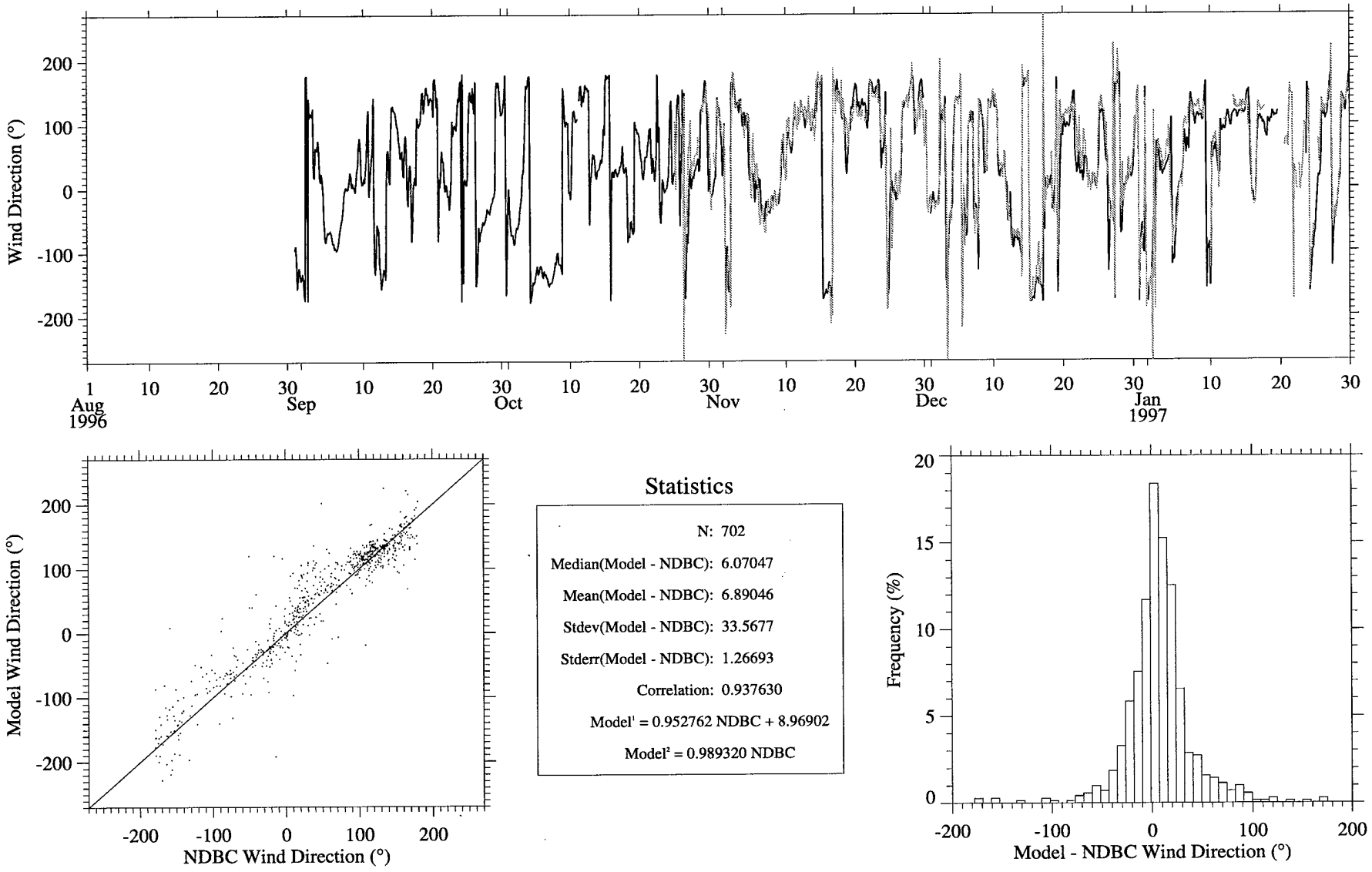

Figure A46. RUC Analysis (gray) vs. NDBC Buoy 44009 (black) wind direction.

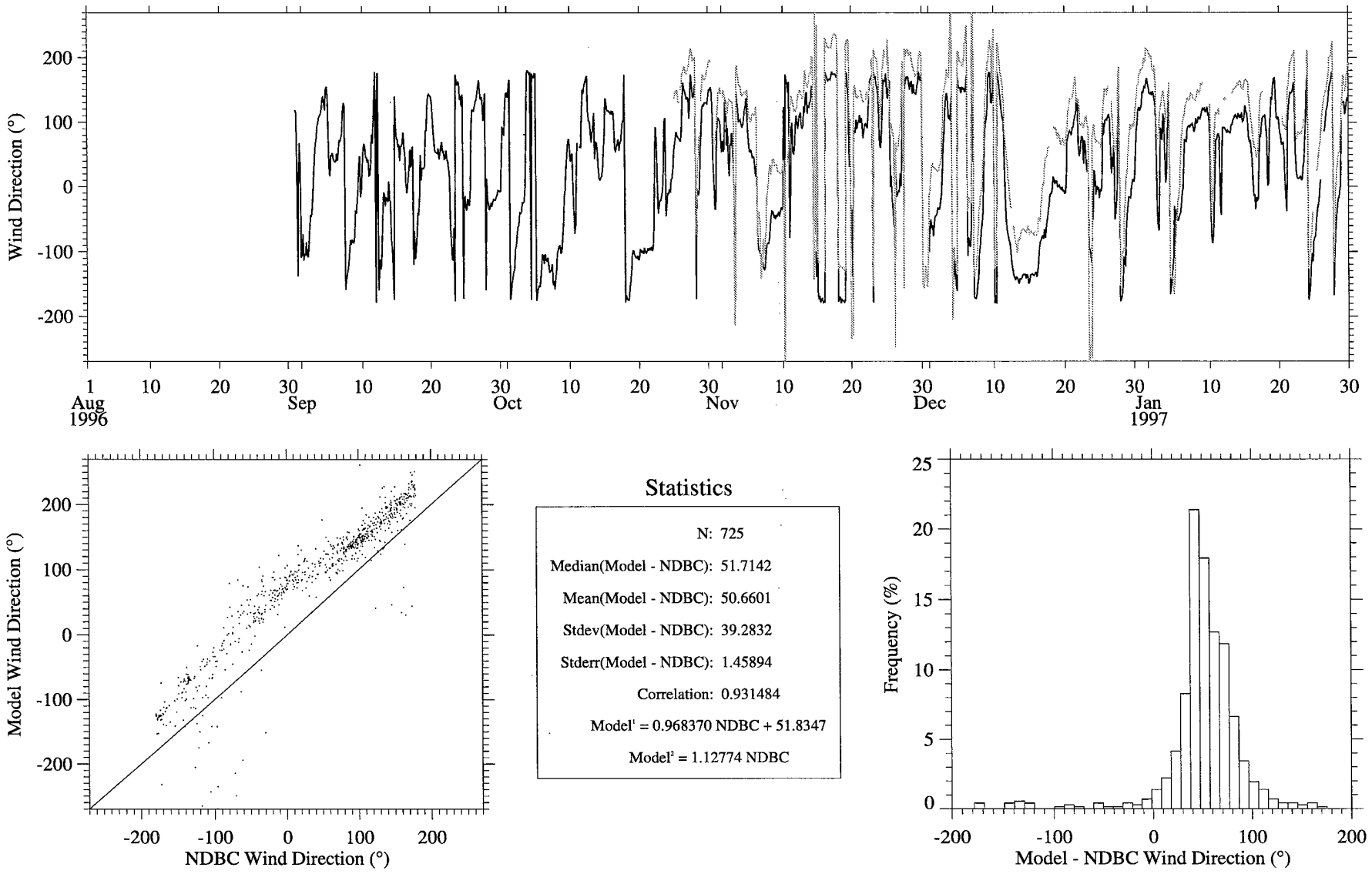

Figure A47. RUC Analysis (gray) vs. NDBC Buoy 44011 (black) wind direction.

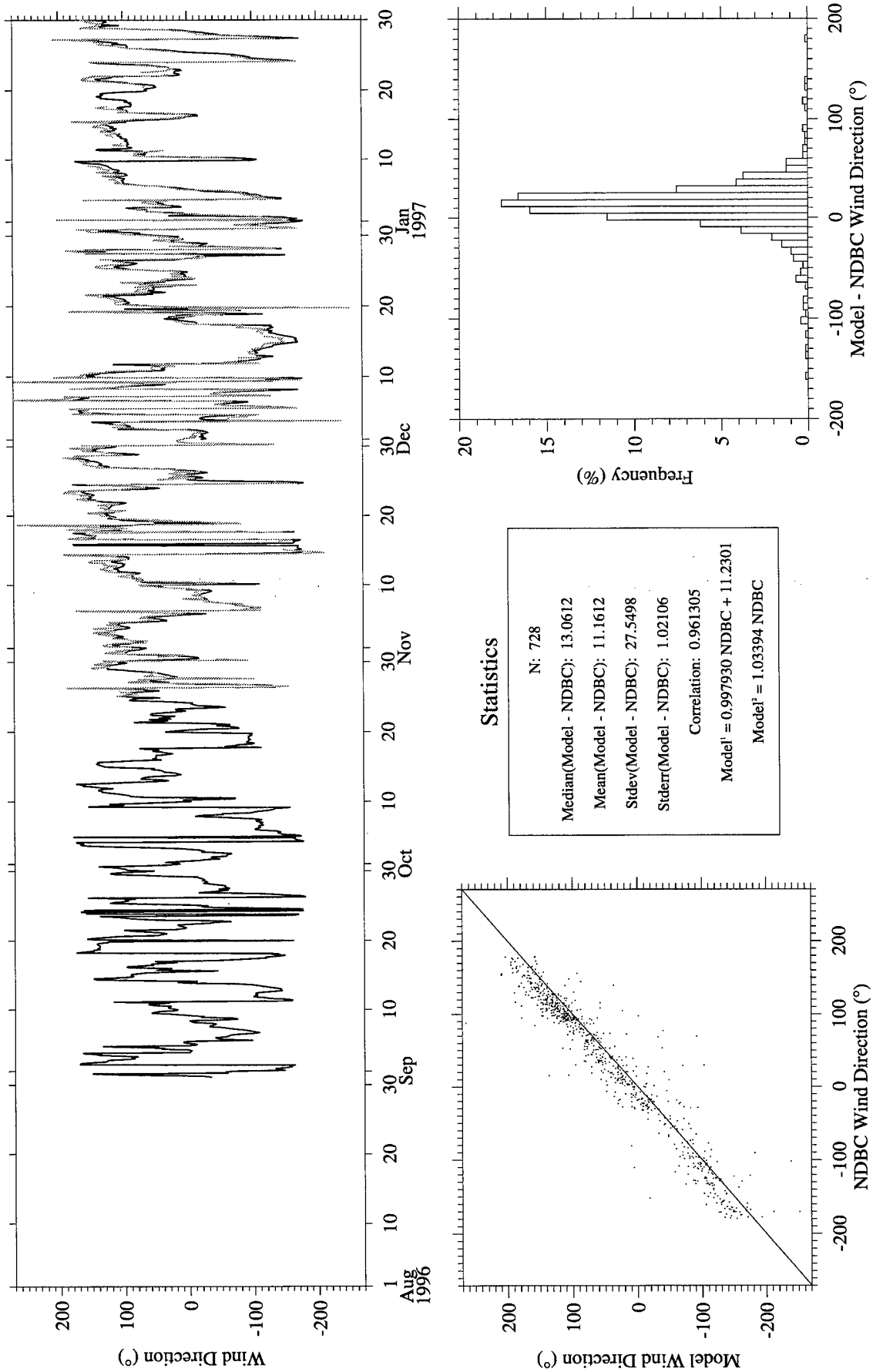

Figure A48. RUC Analysis (gray) vs. NDBC Buoy 44025 (black) wind direction.

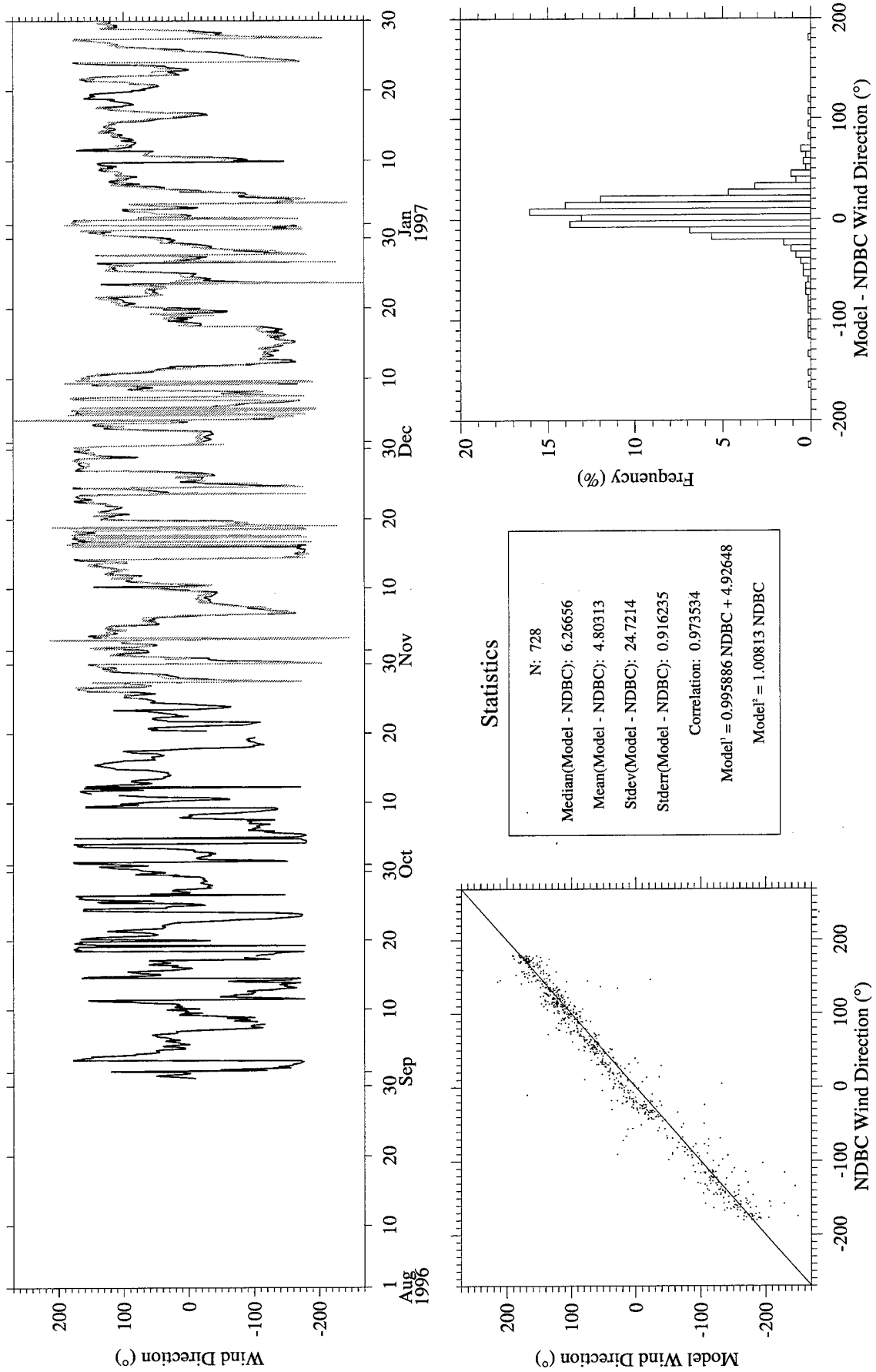

Figure A49. RUC Analysis (gray) vs. NDBC Buoy 44028 (black) wind direction.

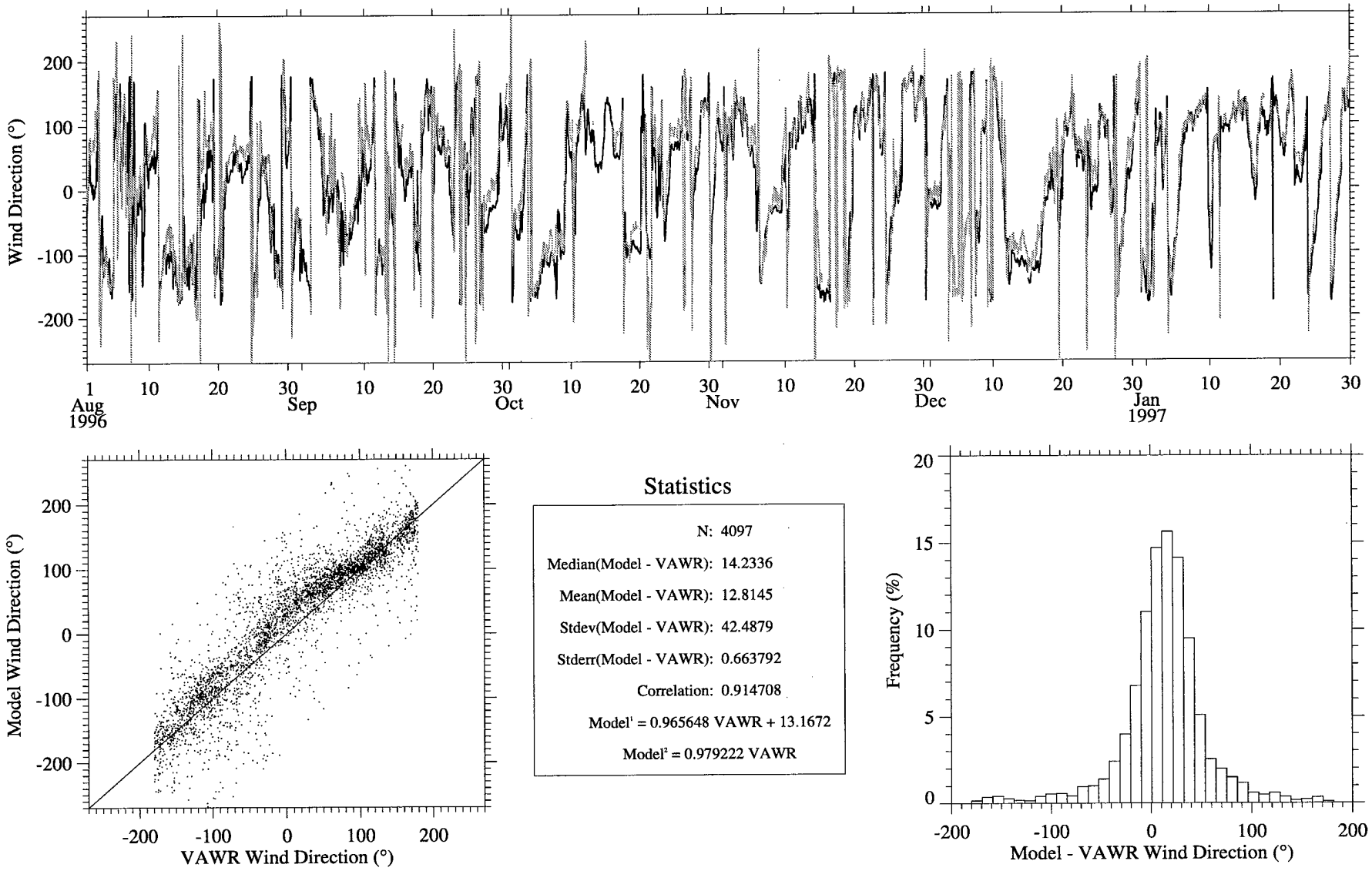

Figure A50. RUC Hourly (gray) vs. CMO VAWR 0704 (black) wind direction.

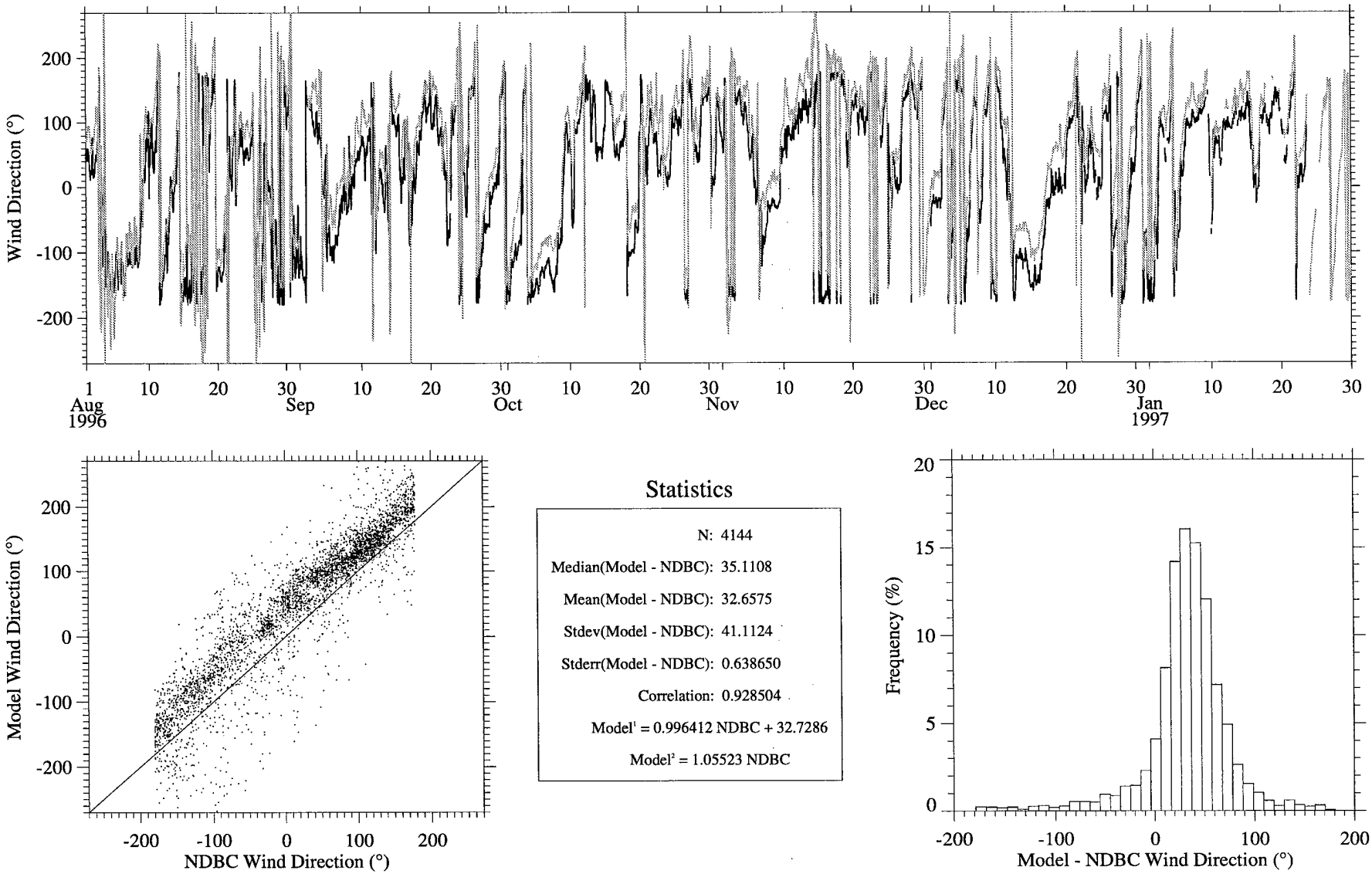

Figure A51. RUC Hourly (gray) vs. NDBC Buoy 44004 (black) wind direction.

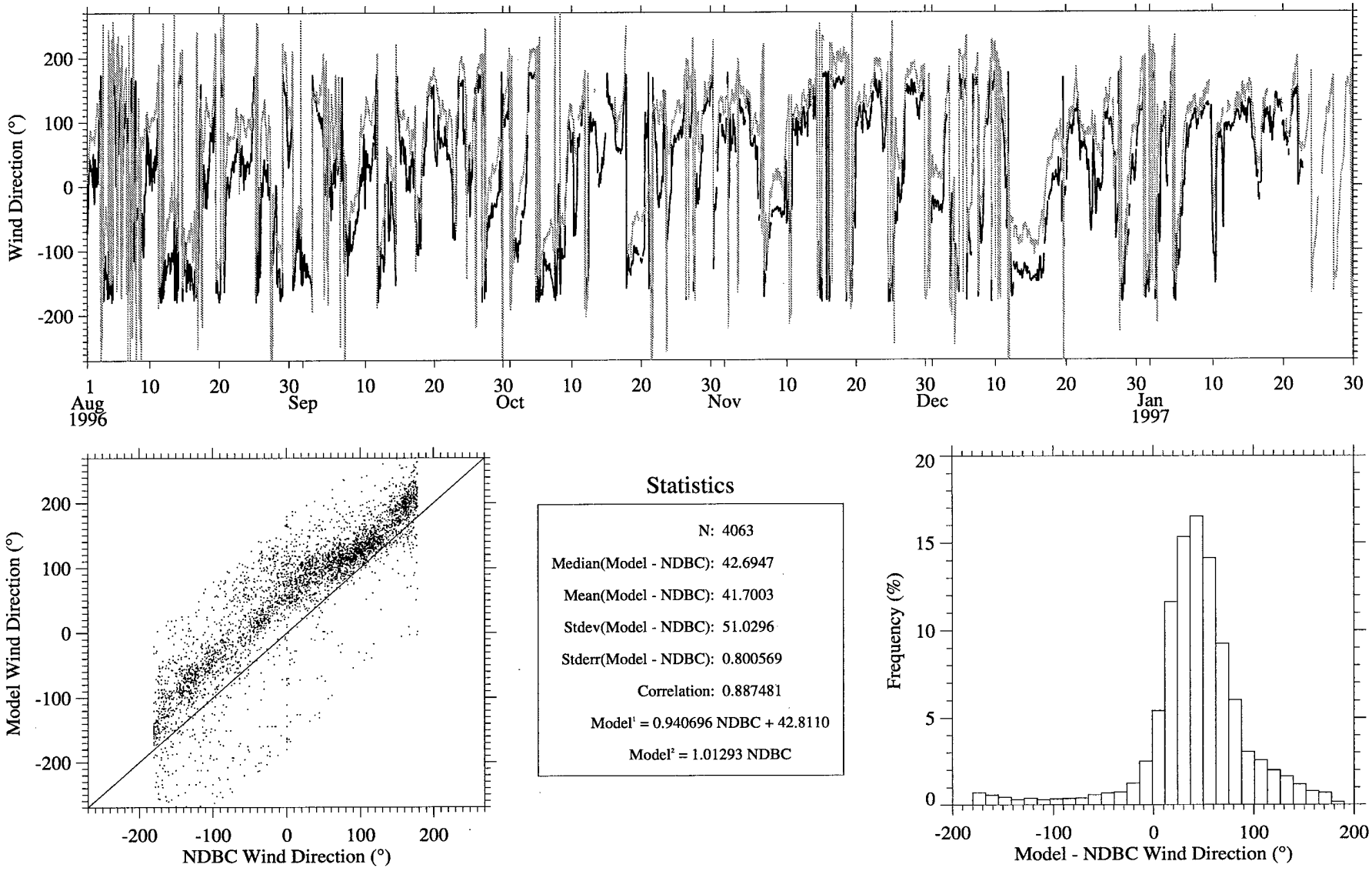

Figure A52. RUC Hourly (gray) vs. NDBC Buoy 44008 (black) wind direction.

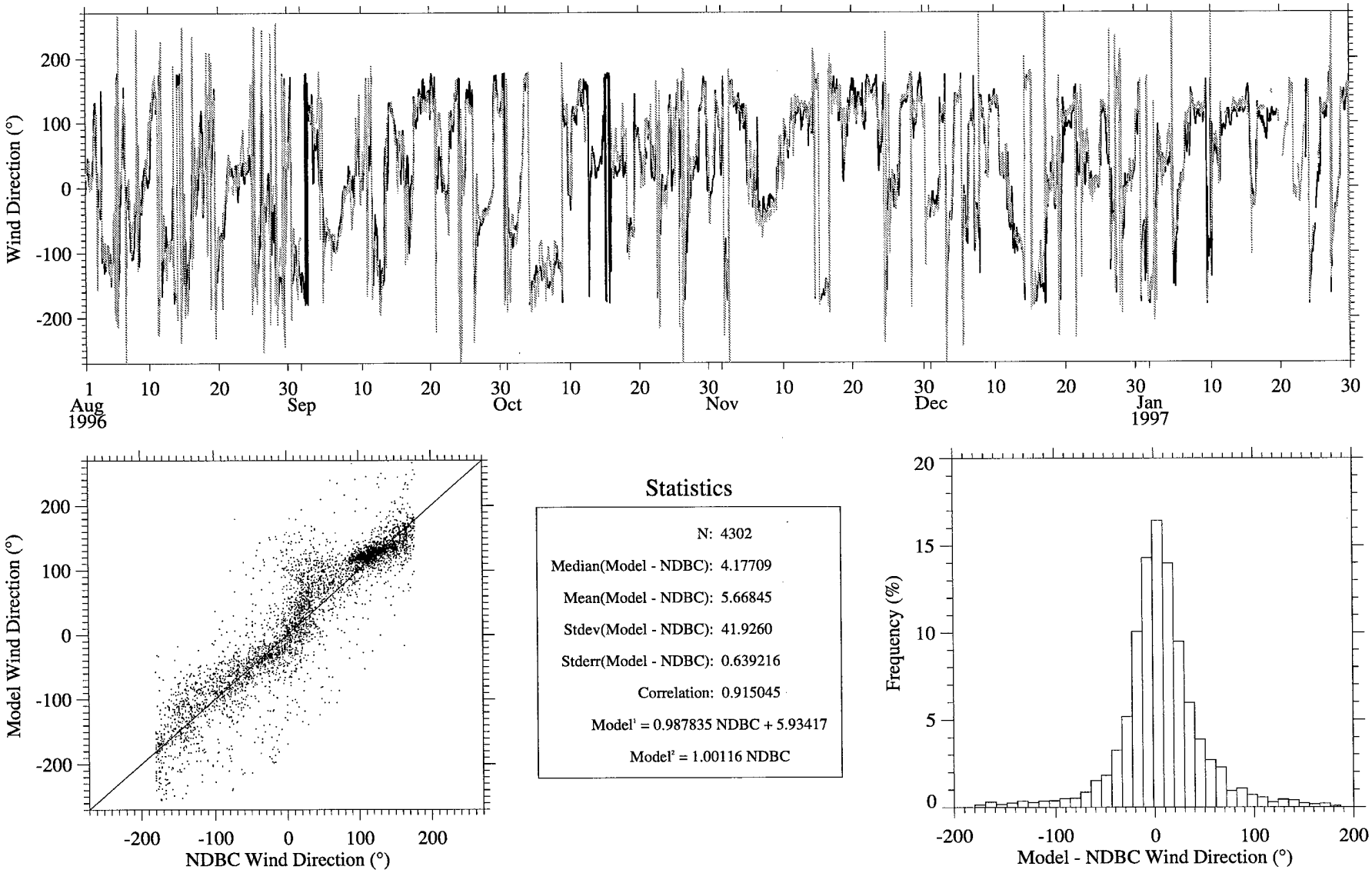

Figure A53. RUC Hourly (gray) vs. NDBC Buoy 44009 (black) wind direction.

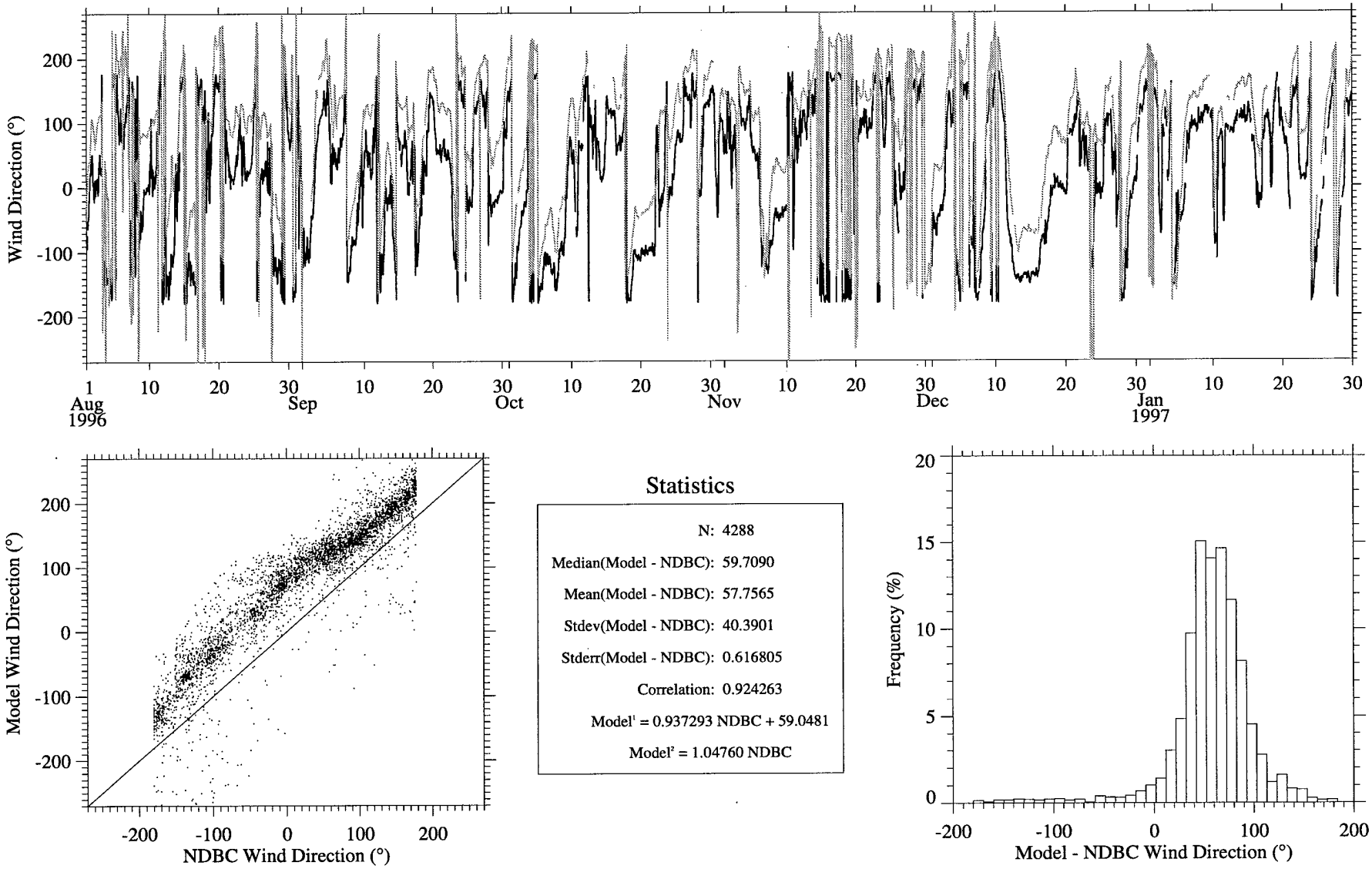

Figure A54. RUC Hourly (gray) vs. NDBC Buoy 44011 (black) wind direction.

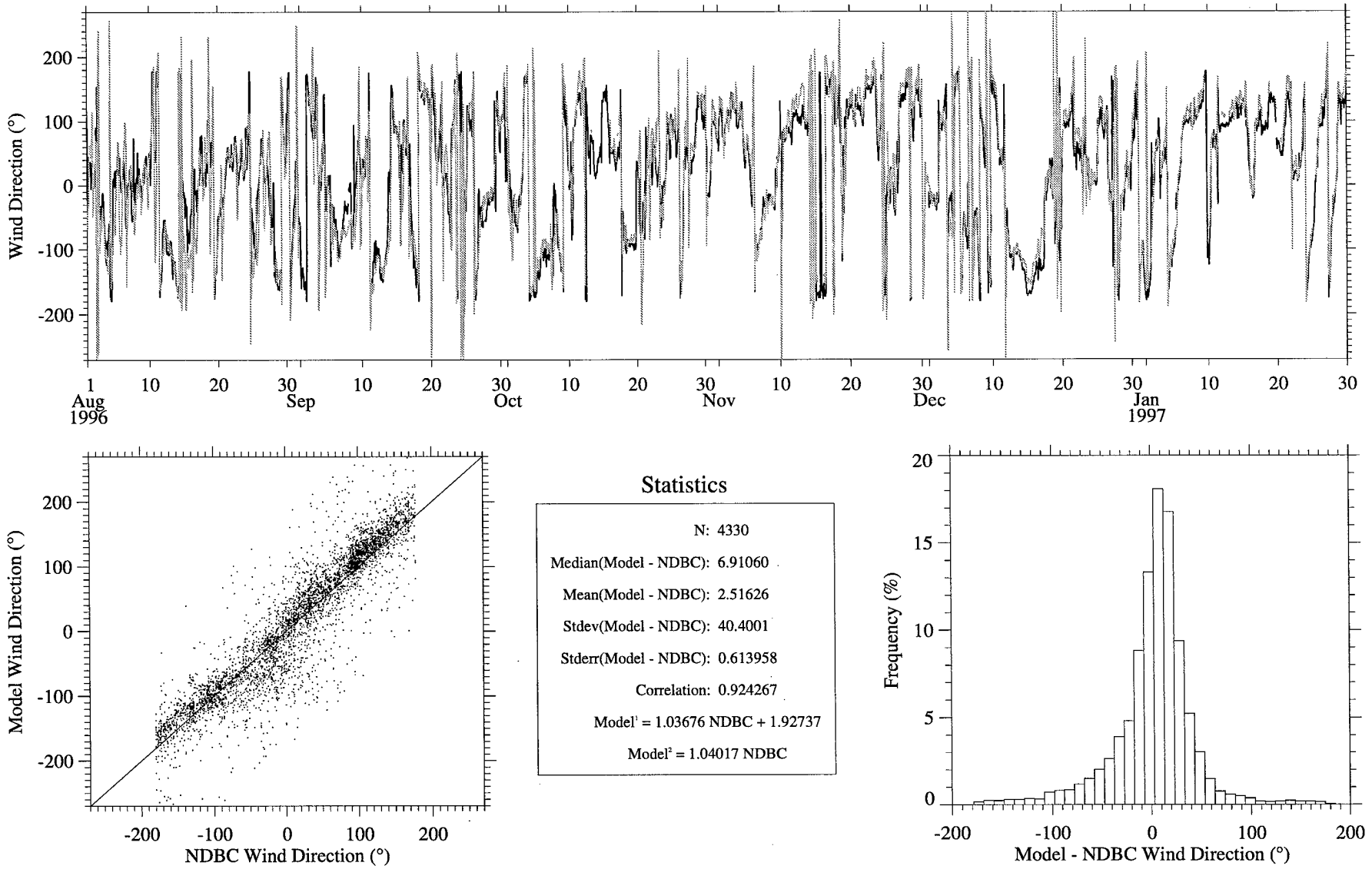

Figure A55. RUC Hourly (gray) vs. NDBC Buoy 44025 (black) wind direction.

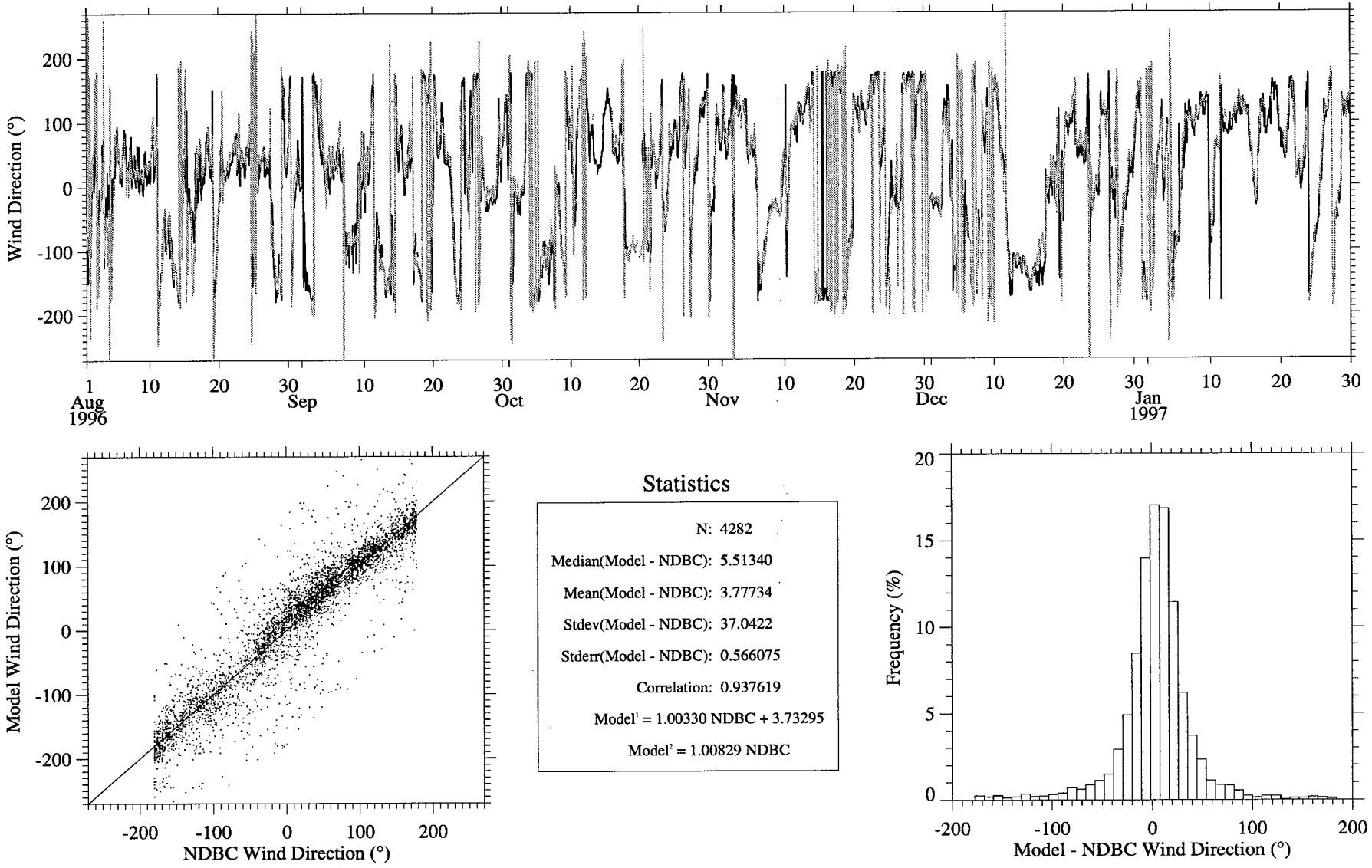

Figure A56. RUC Hourly (gray) vs. NDBC Buoy 44028 (black) wind direction.

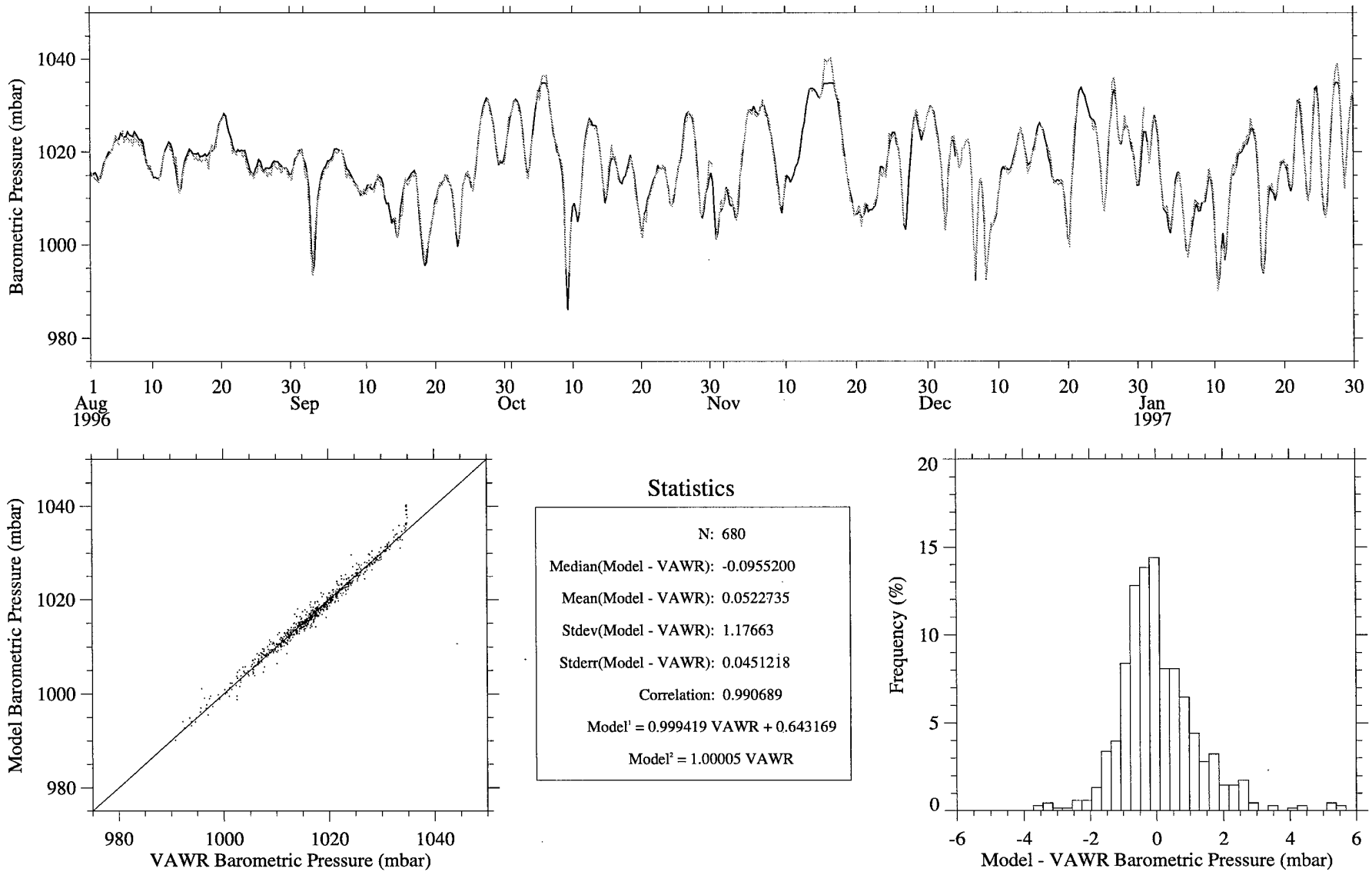

Figure A57. Eta (gray) vs. CMO VAWR 0704 (black) barometric pressure.

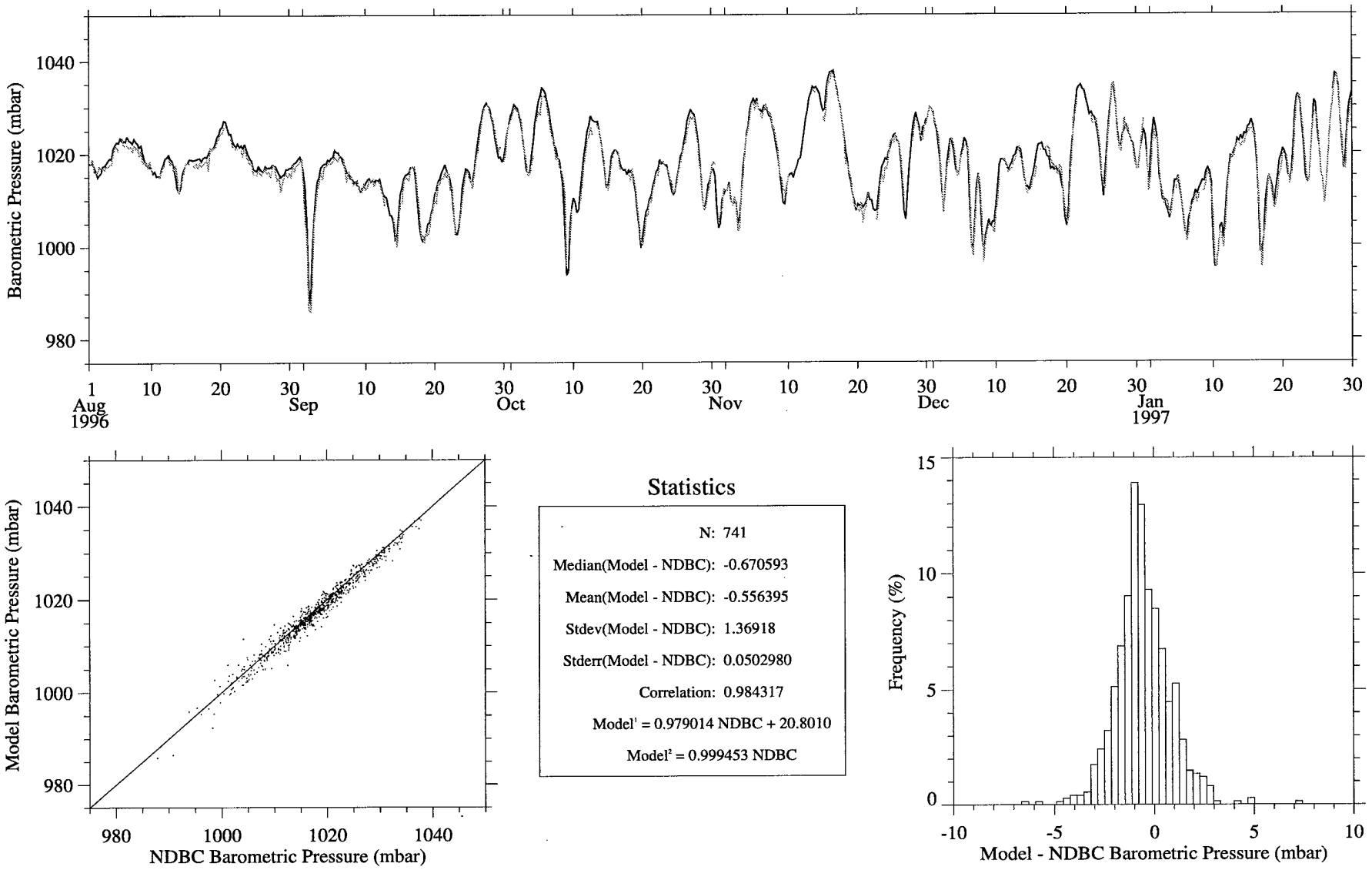

Figure A58. Eta (gray) vs. NDBC Buoy 44004 (black) barometric pressure.

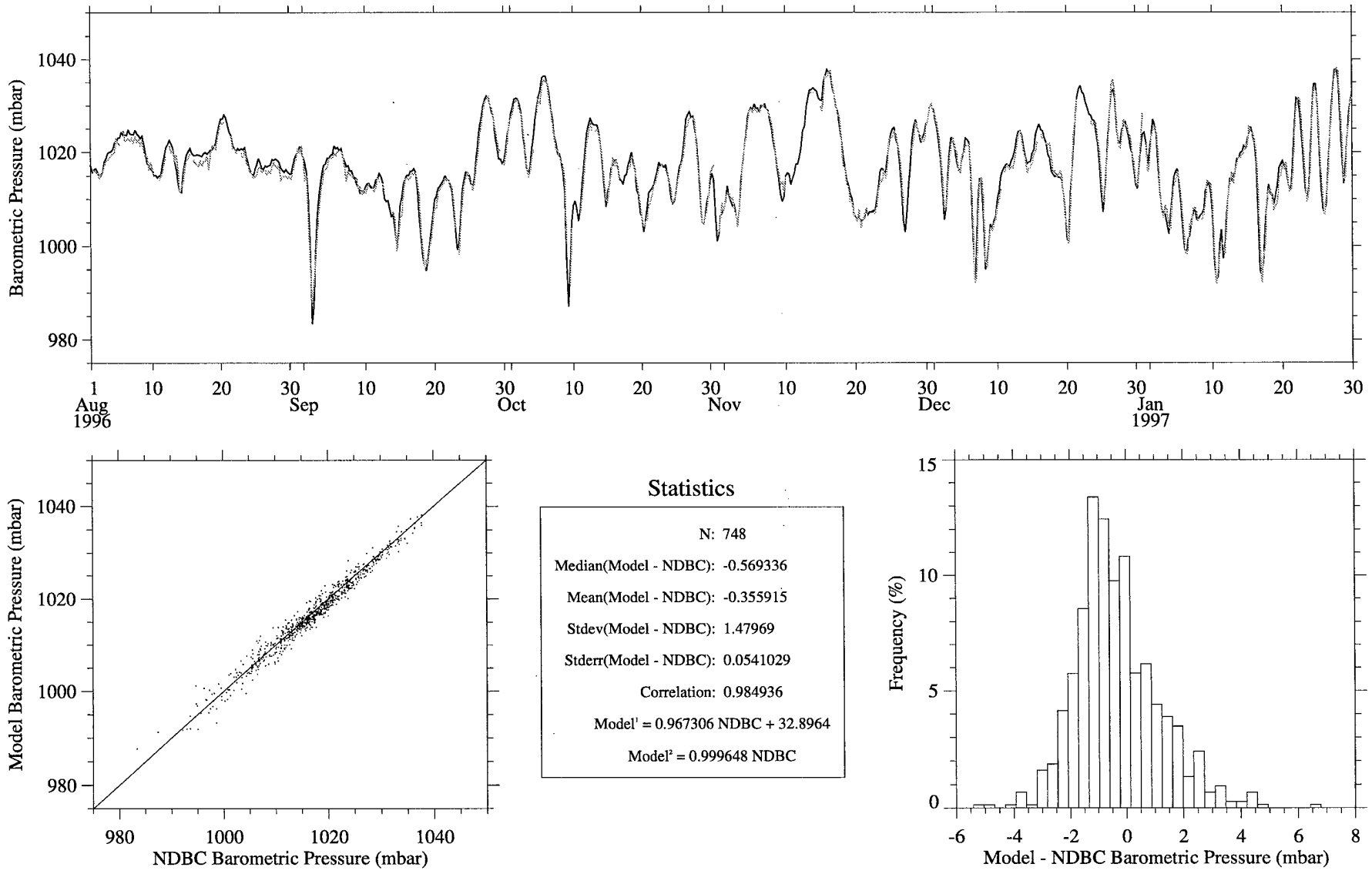

Figure A59. Eta (gray) vs. NDBC Buoy 44008 (black) barometric pressure.

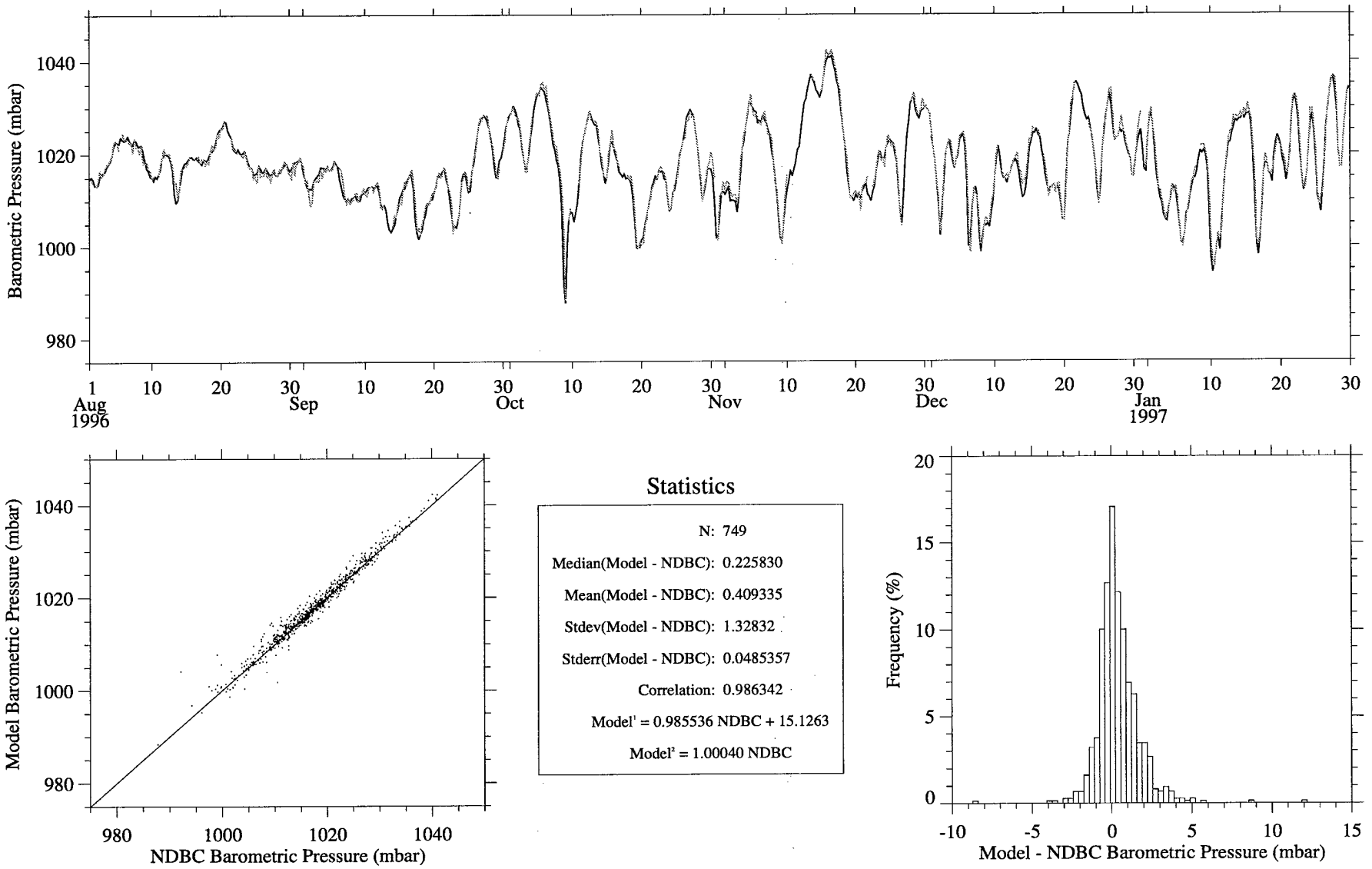

Figure A60. Eta (gray) vs. NDBC Buoy 44009 (black) barometric pressure.

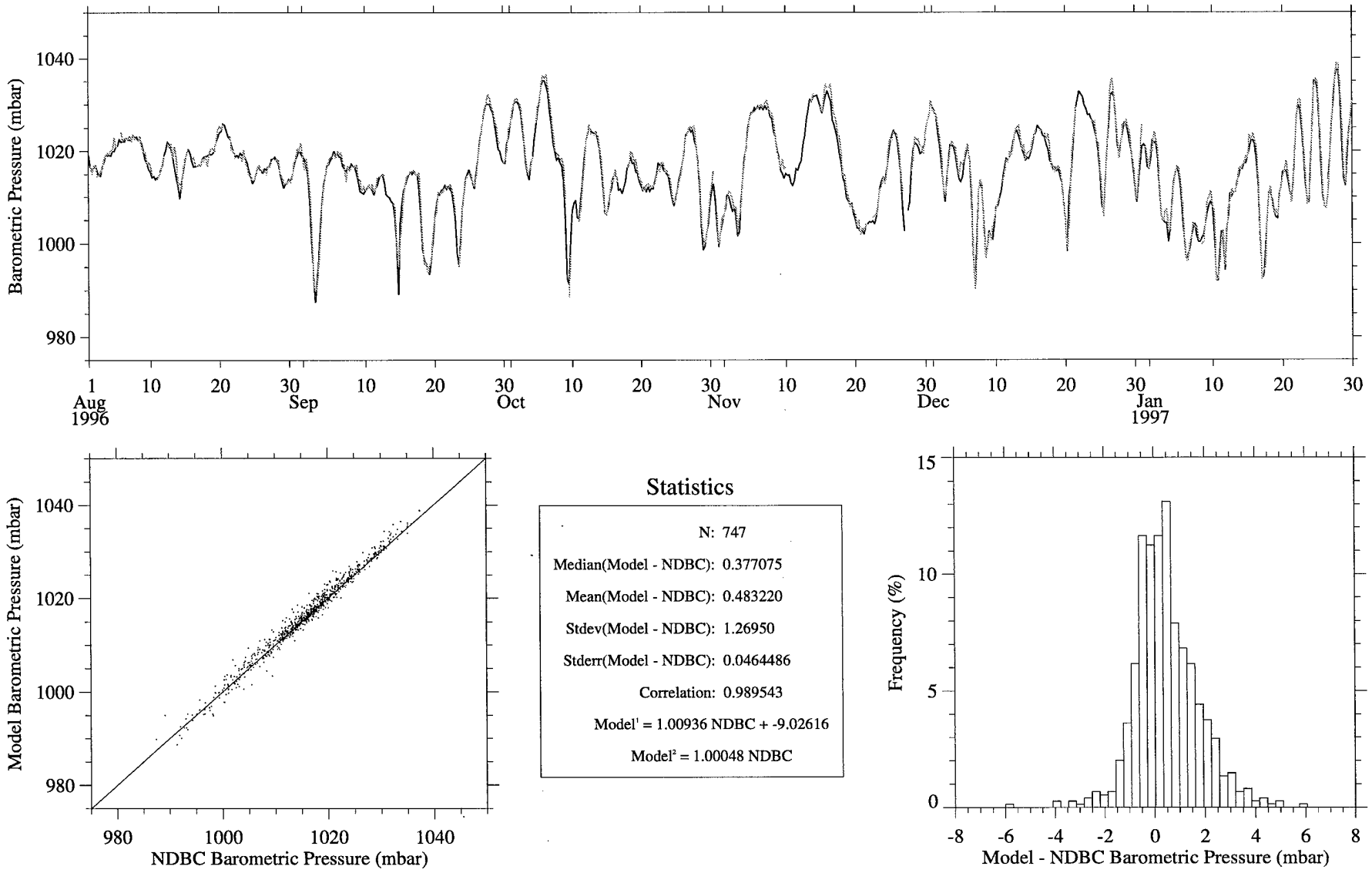

Figure A61. Eta (gray) vs. NDBC Buoy 44011 (black) barometric pressure.

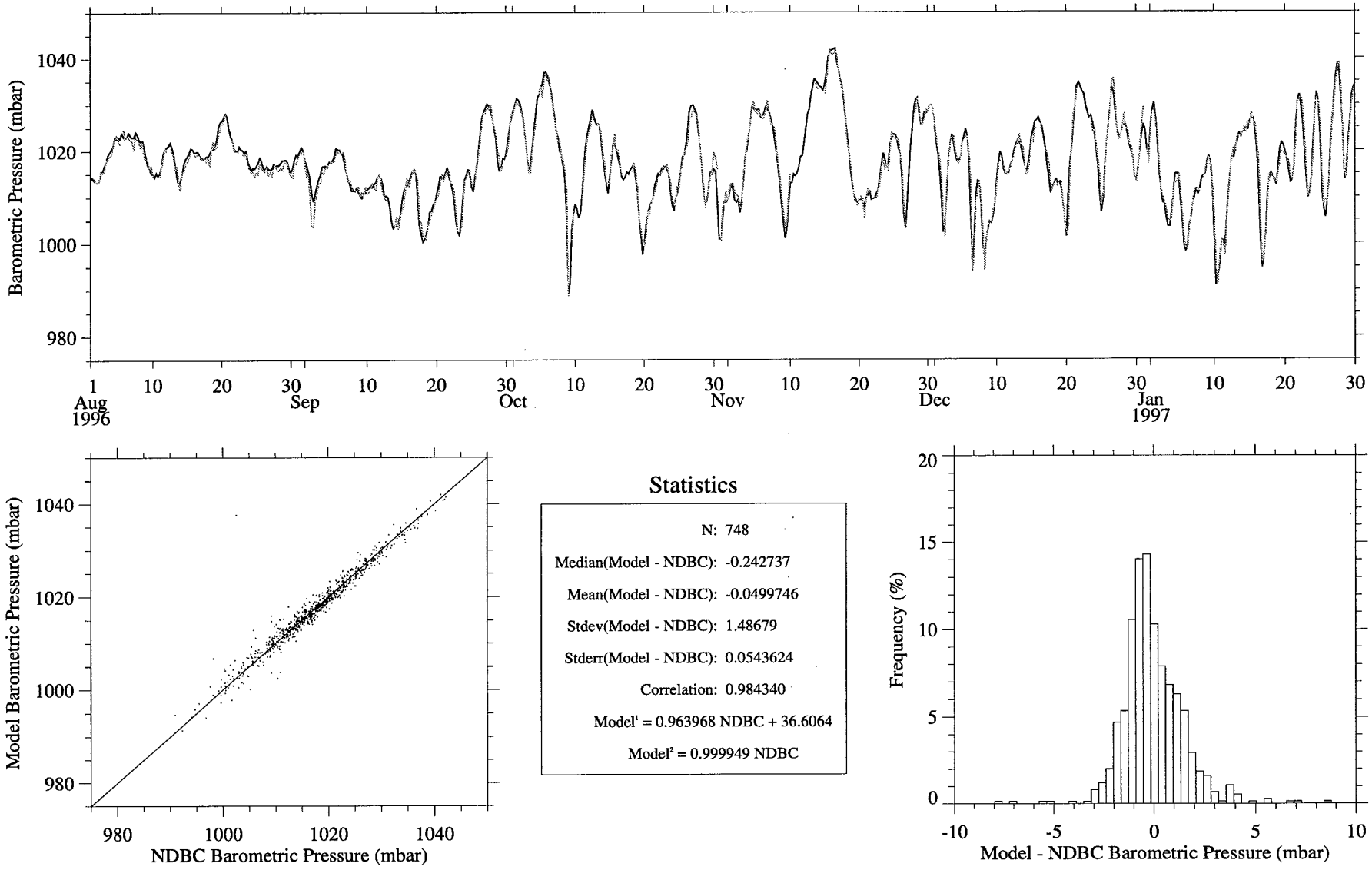

Figure A62. Eta (gray) vs. NDBC Buoy 44025 (black) barometric pressure.

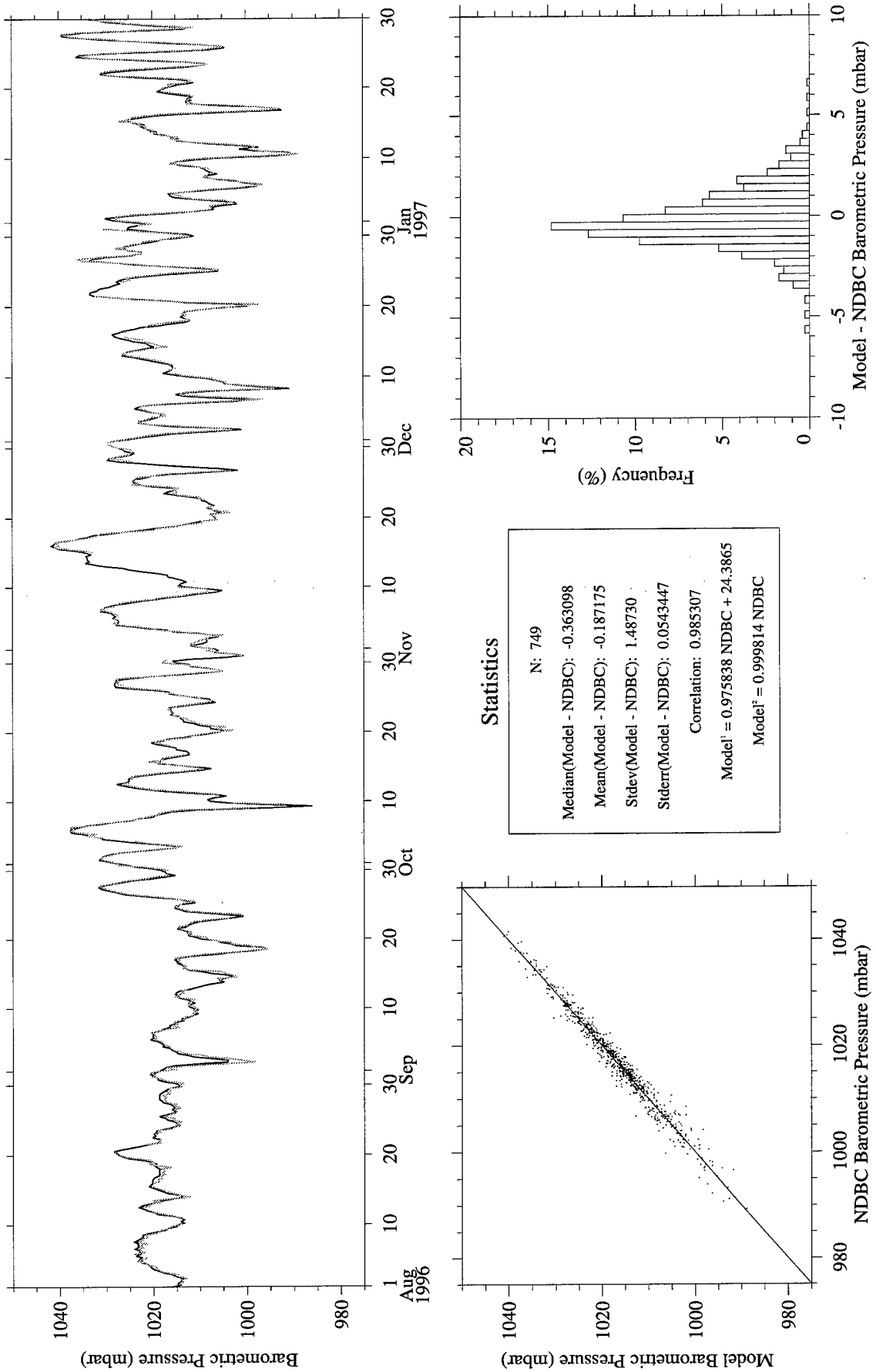

Figure A63. Eta (gray) vs. NDBC Buoy 44028 (black) barometric pressure.

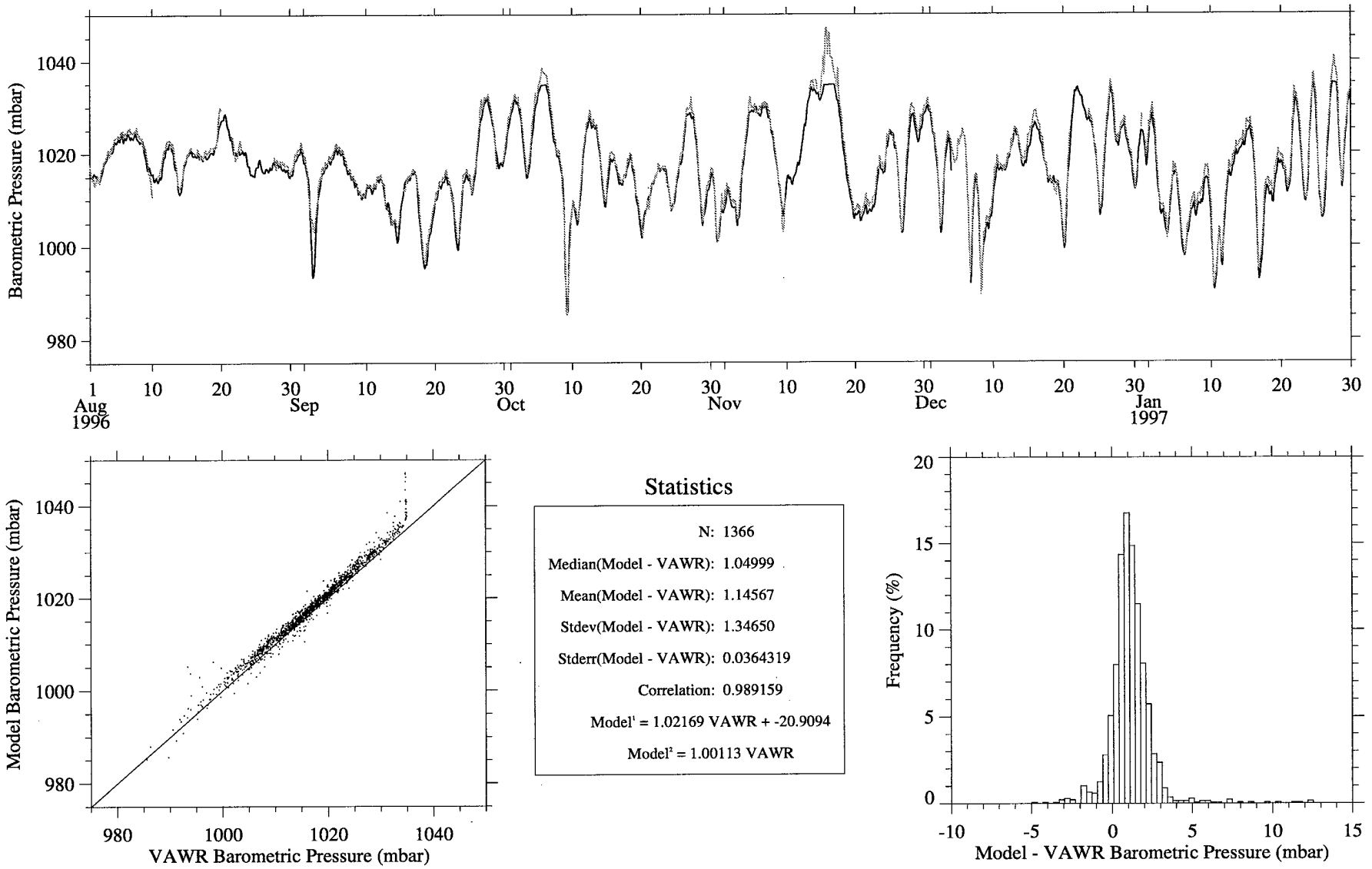

Figure A64. RUC (gray) vs. CMO VAWR 0704 (black) barometric pressure.

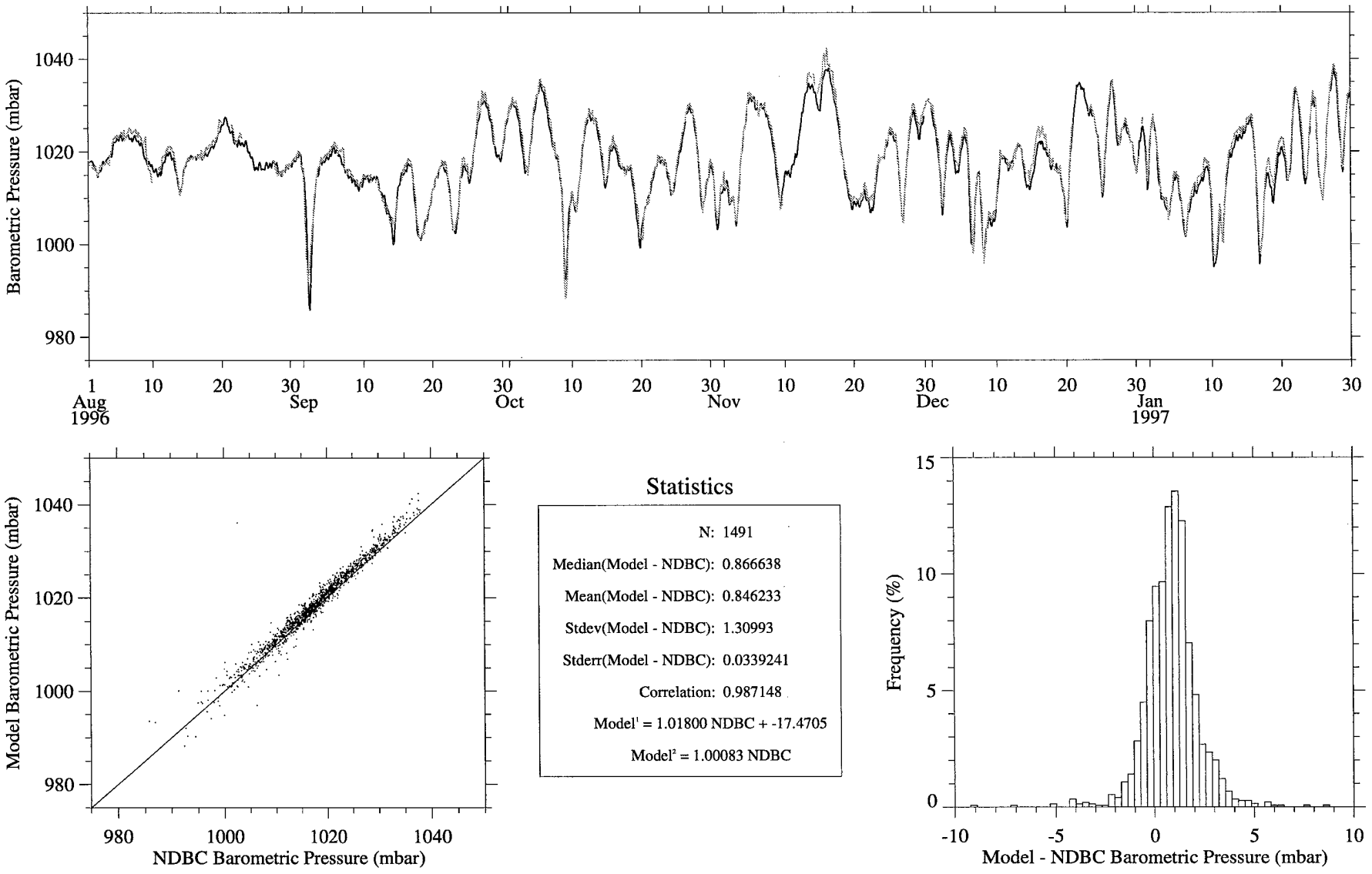

Figure A65. RUC (gray) vs. NDBC Buoy 44004 (black) barometric pressure.

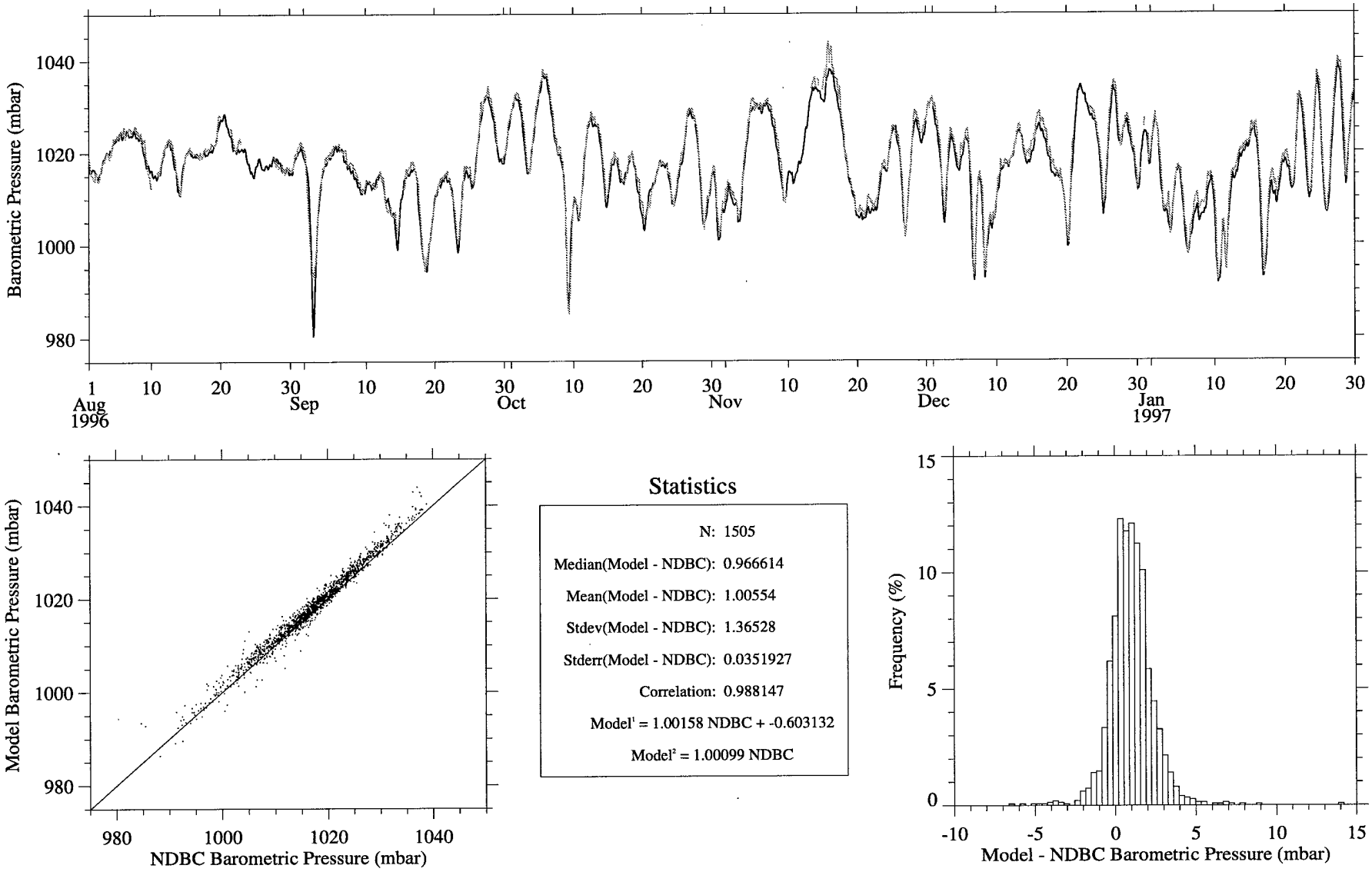

Figure A66. RUC (gray) vs. NDBC Buoy 44008 (black) barometric pressure.

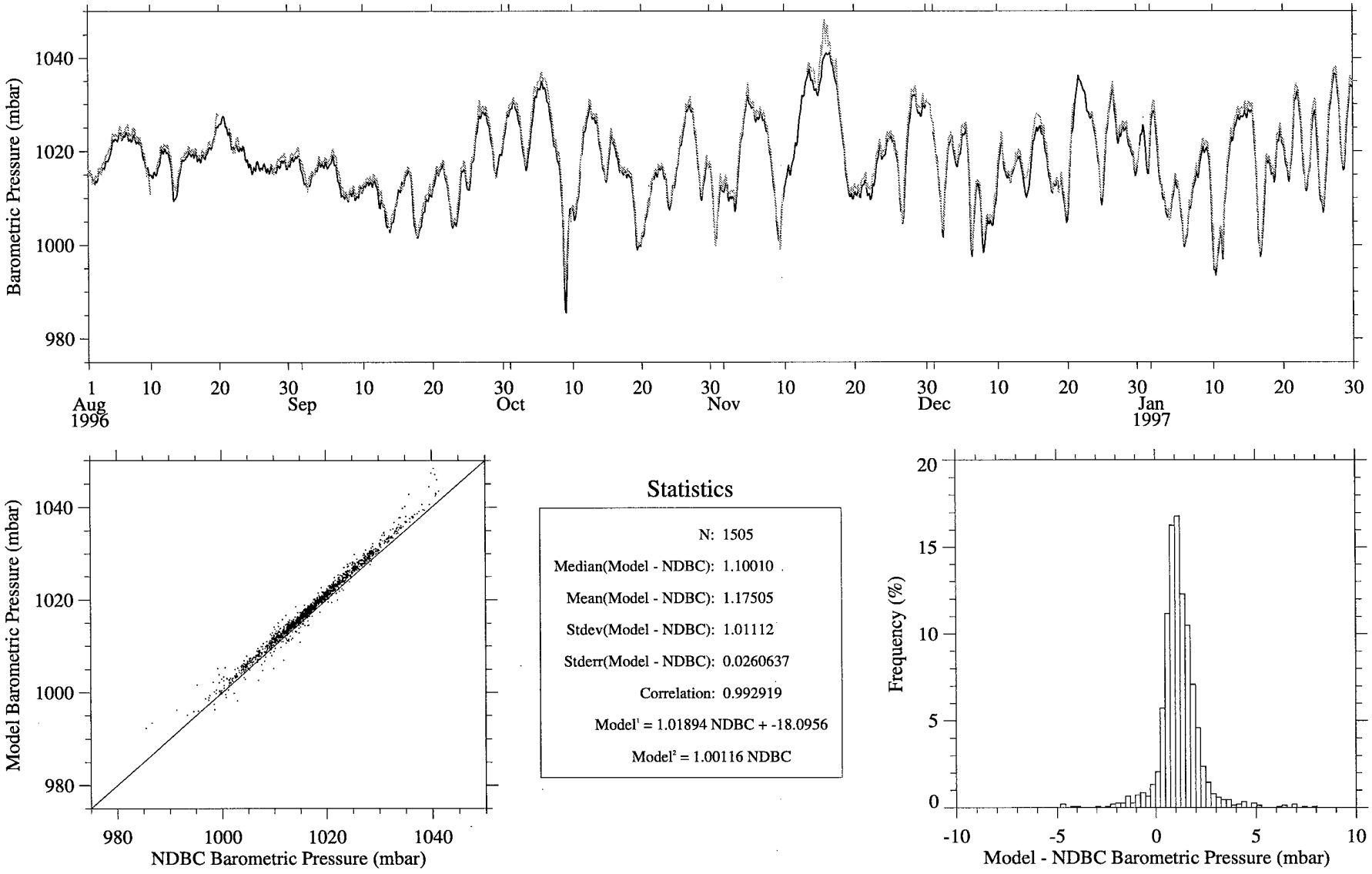

Figure A67. RUC (gray) vs. NDBC Buoy 44009 (black) barometric pressure.

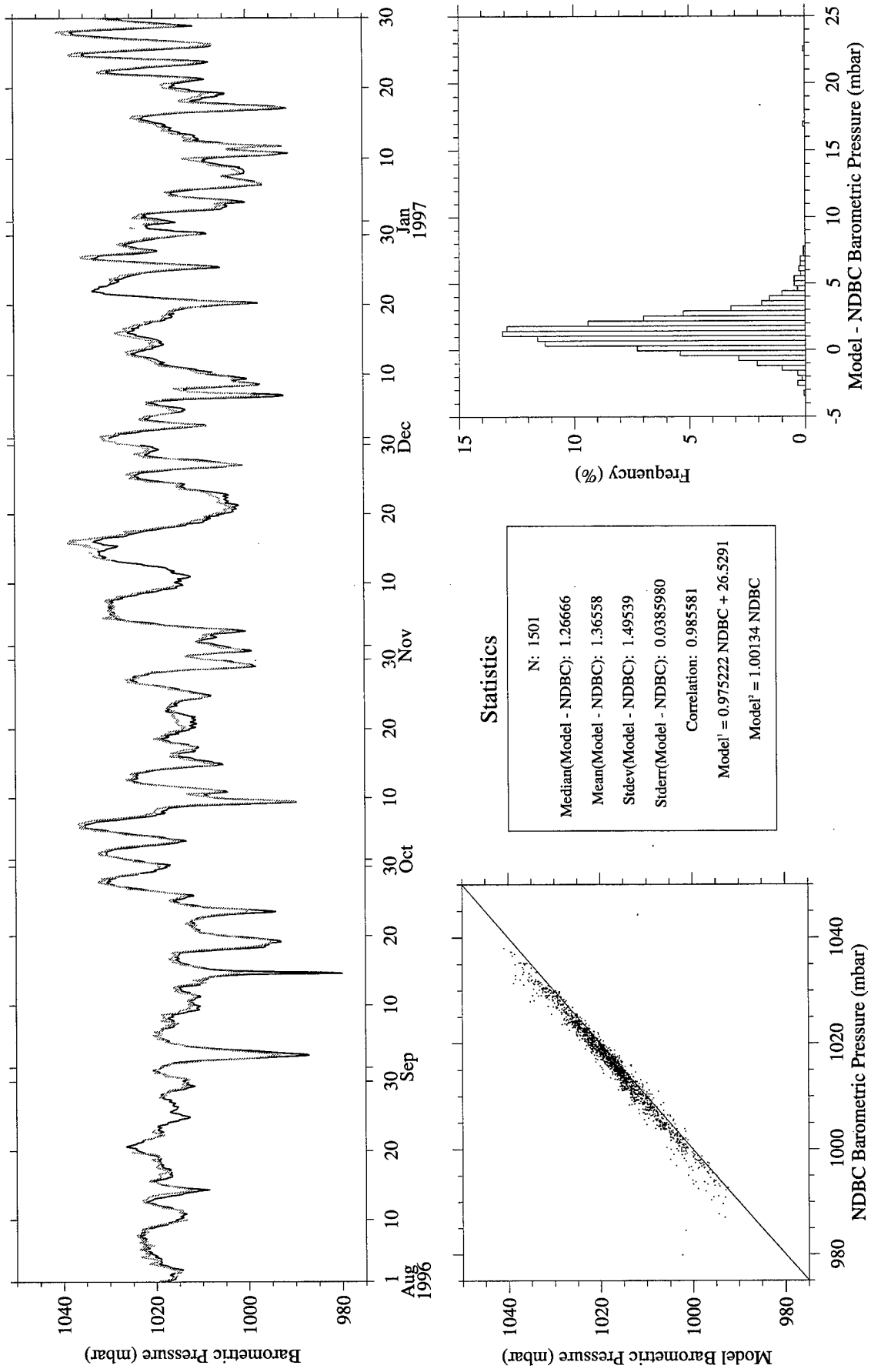

Figure A68. RUC (gray) vs. NDBC Buoy 44011 (black) barometric pressure.

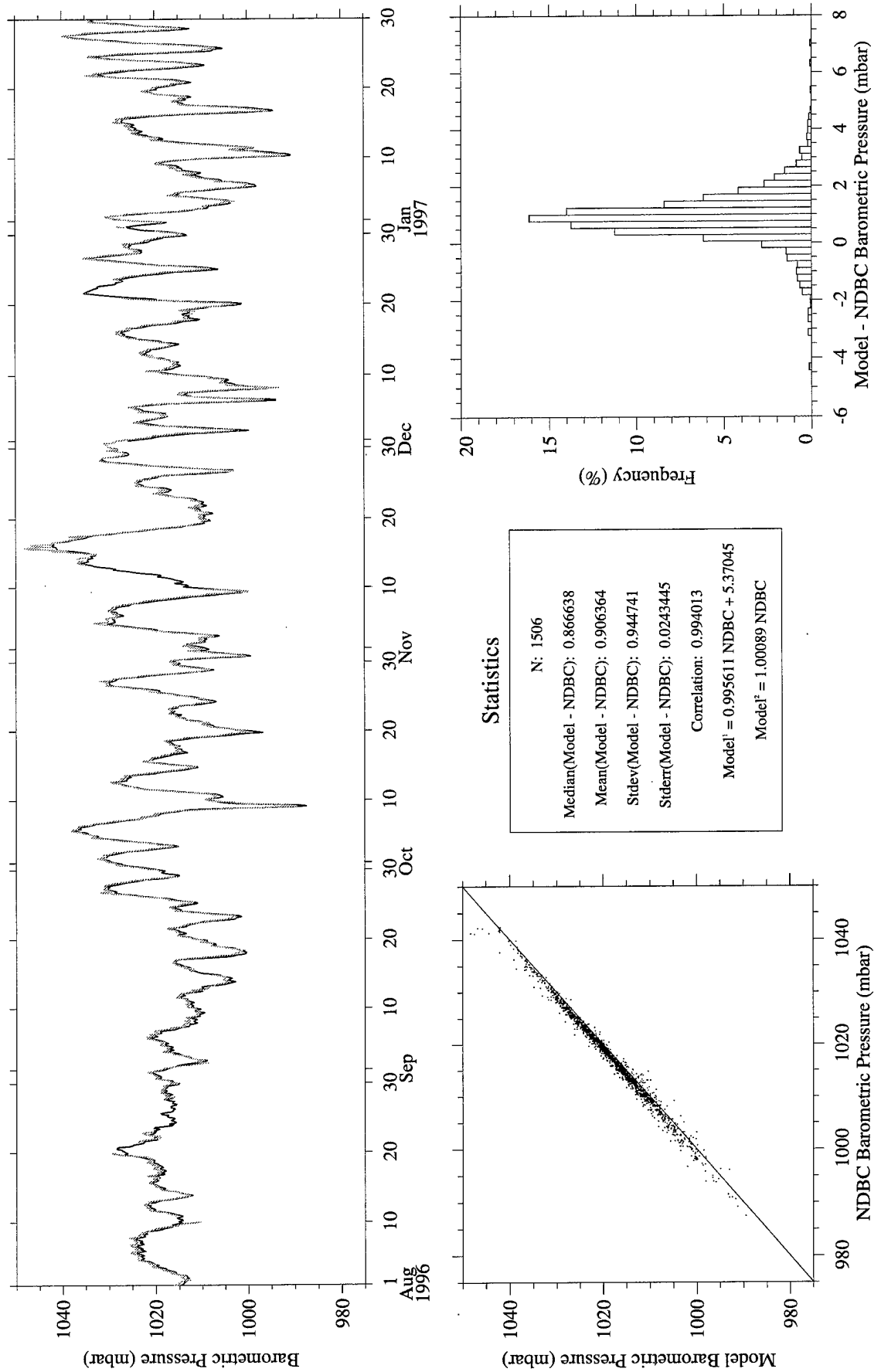

Figure A69. RUC (gray) vs. NDBC Buoy 44025 (black) barometric pressure.

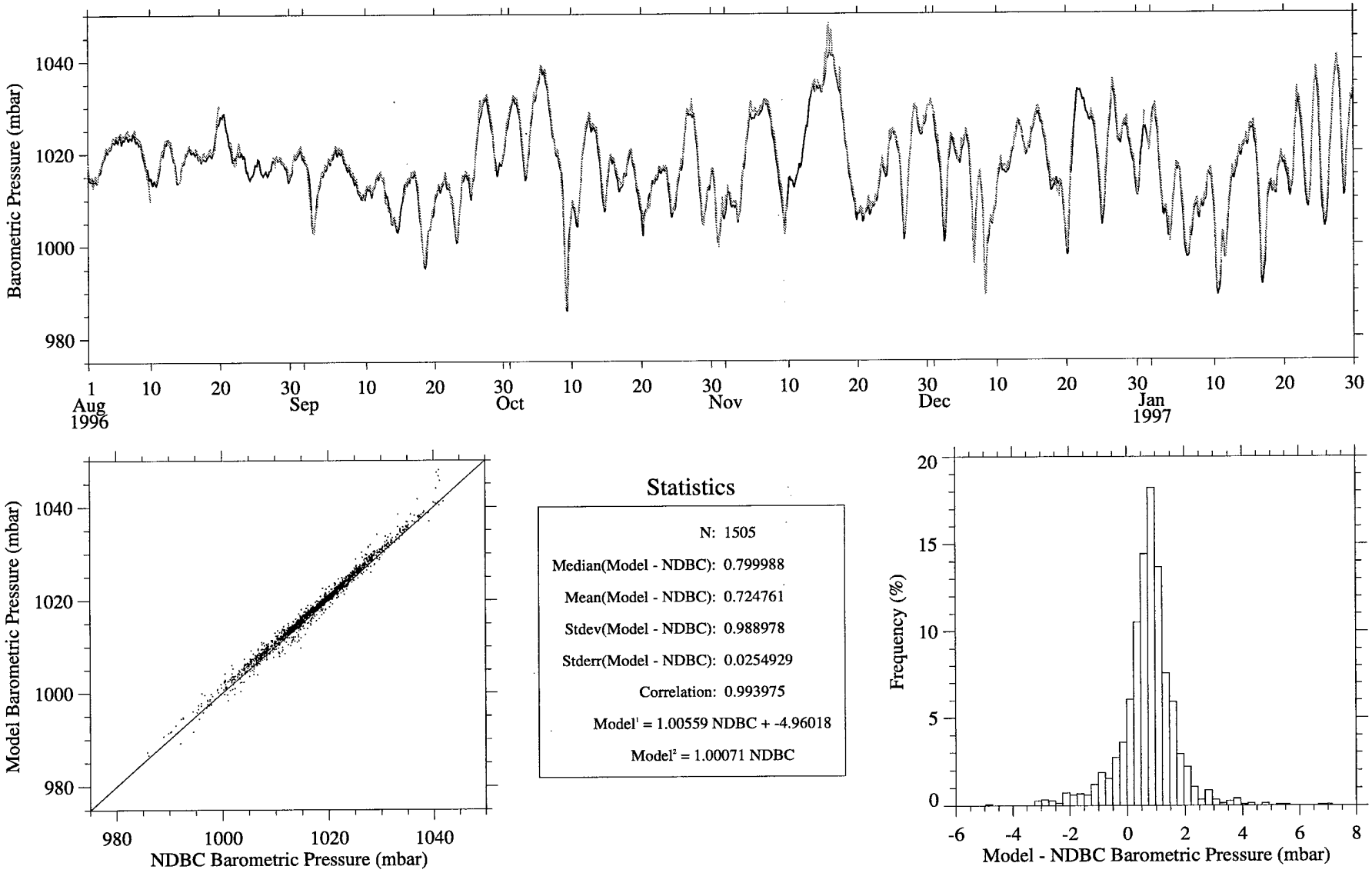

Figure A70. RUC (gray) vs. NDBC Buoy 44028 (black) barometric pressure.

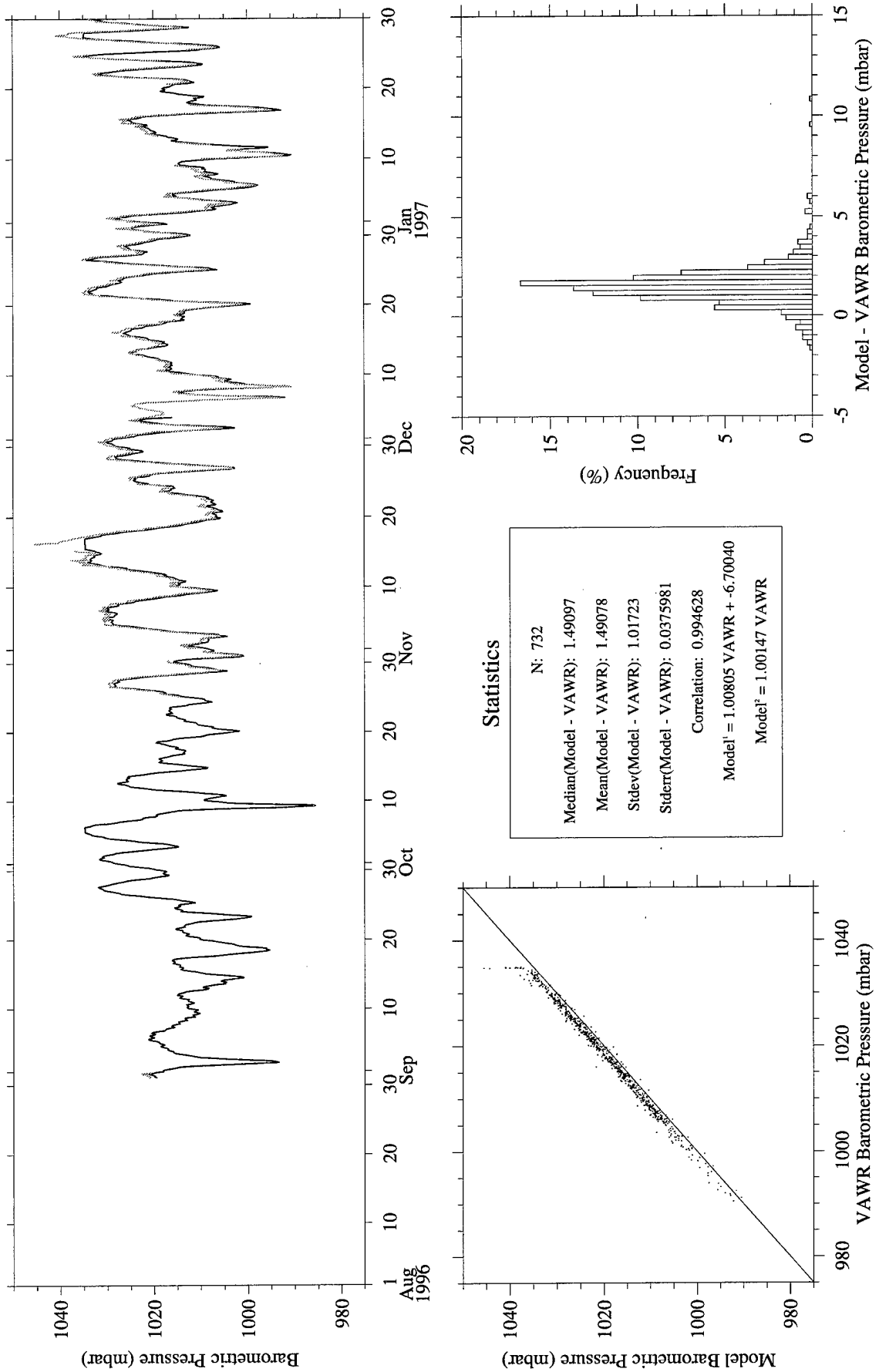

Figure A71. RUC Analysis (gray) vs. CMO VAWR 0704 (black) barometric pressure.

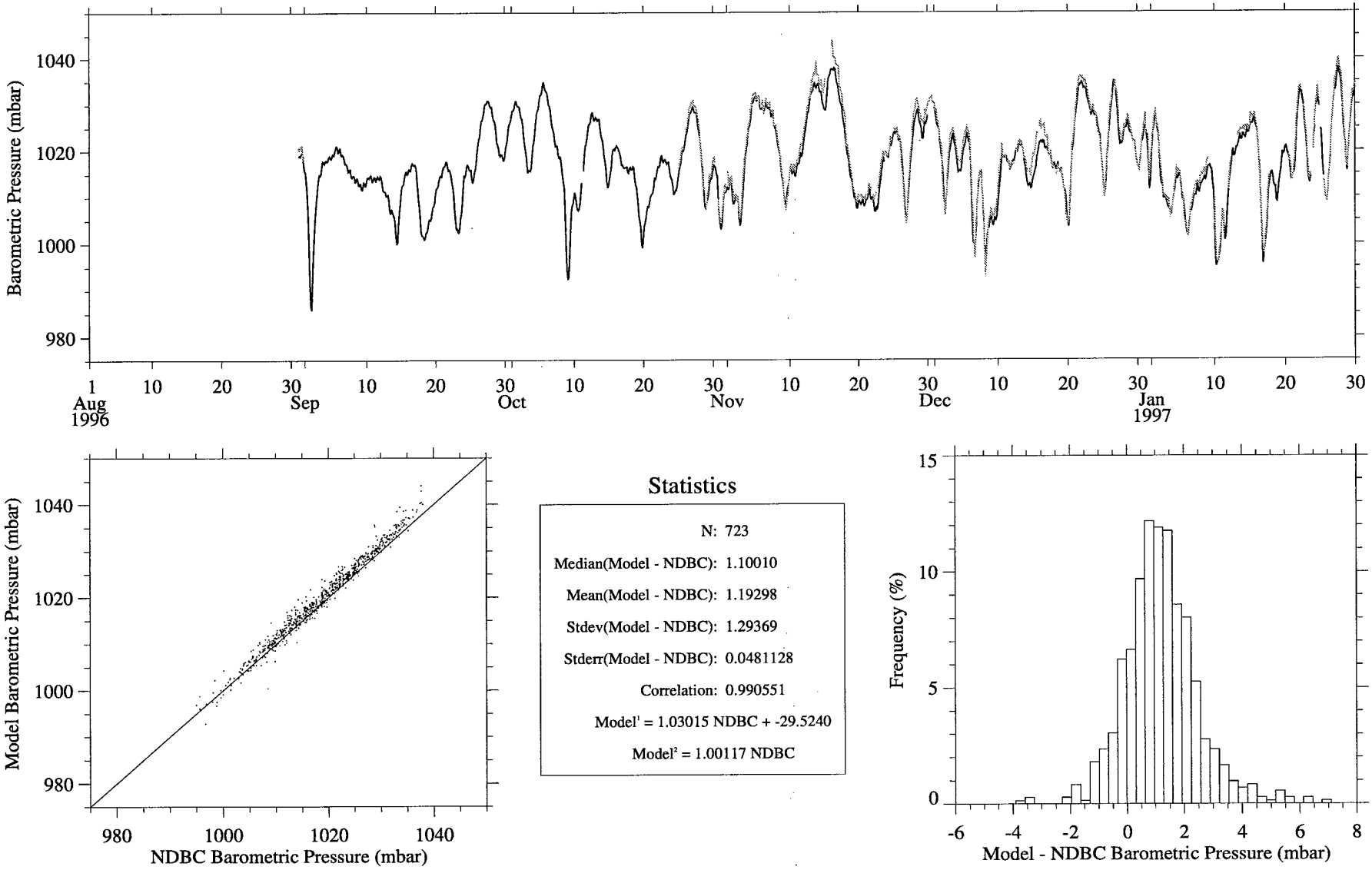

Figure A72. RUC Analysis (gray) vs. NDBC Buoy 44004 (black) barometric pressure.

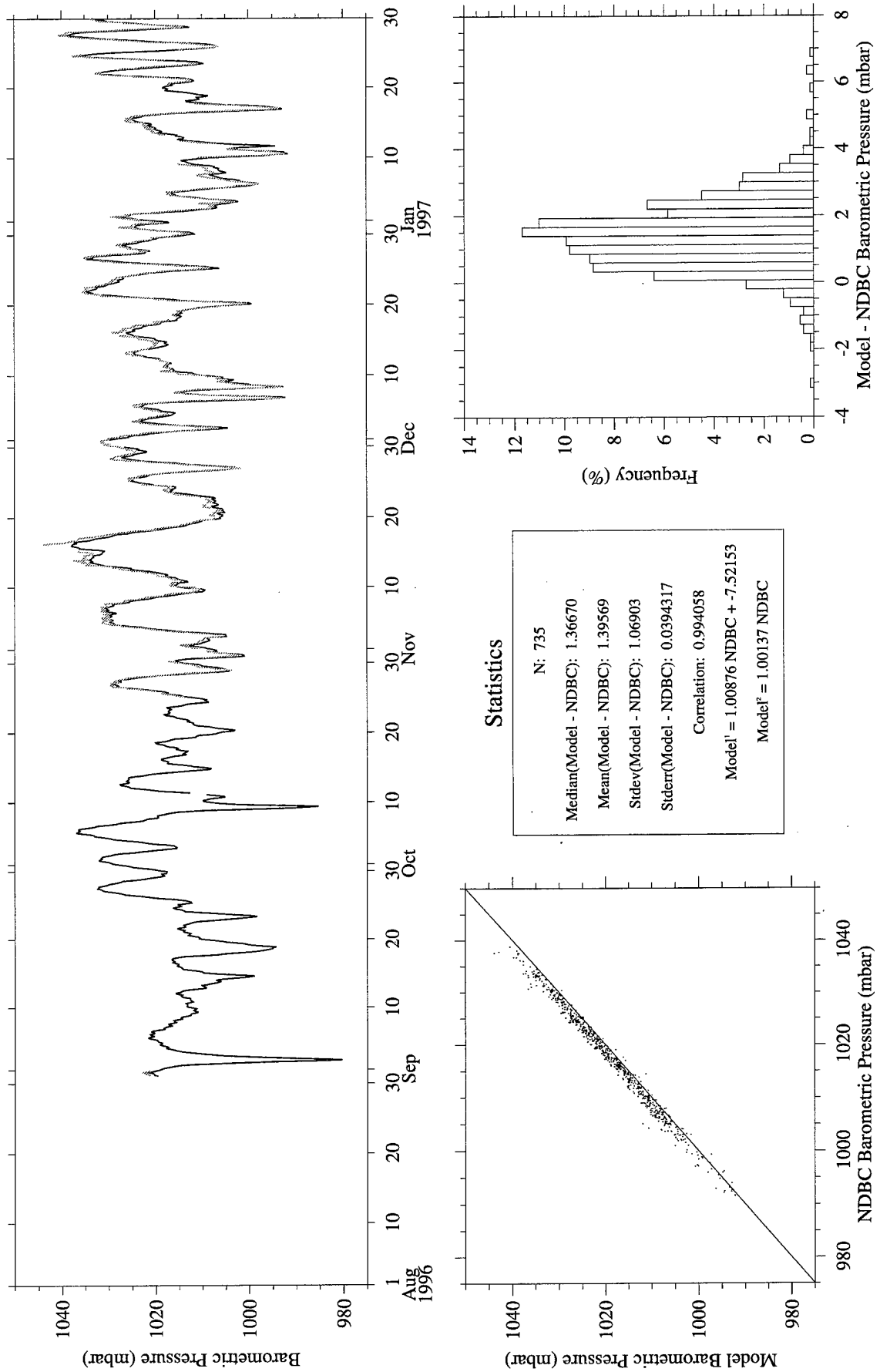

Figure A73. RUC Analysis (gray) vs. NDBC Buoy 44008 (black) barometric pressure.

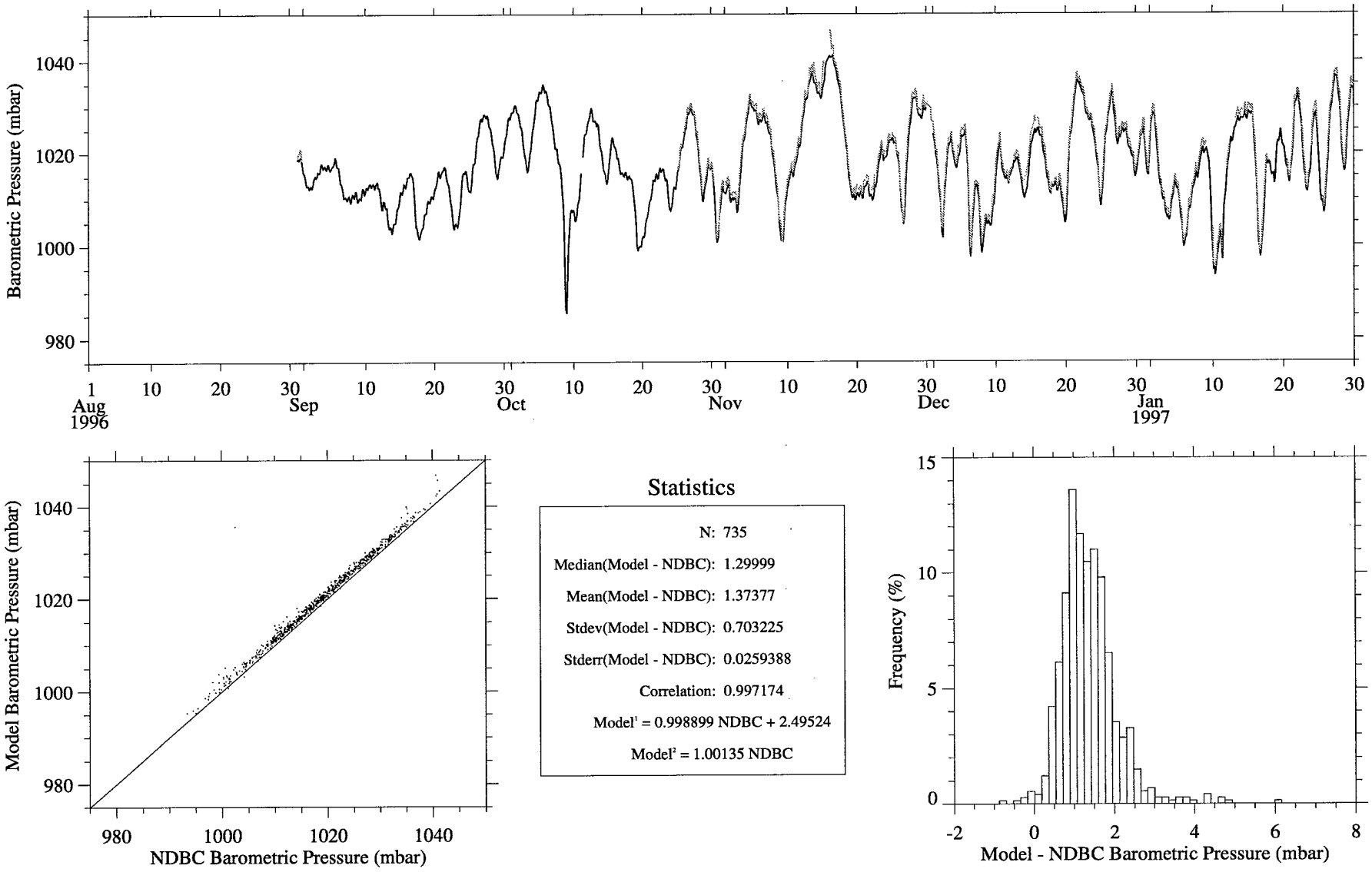

Figure A74. RUC Analysis (gray) vs. NDBC Buoy 44009 (black) barometric pressure.

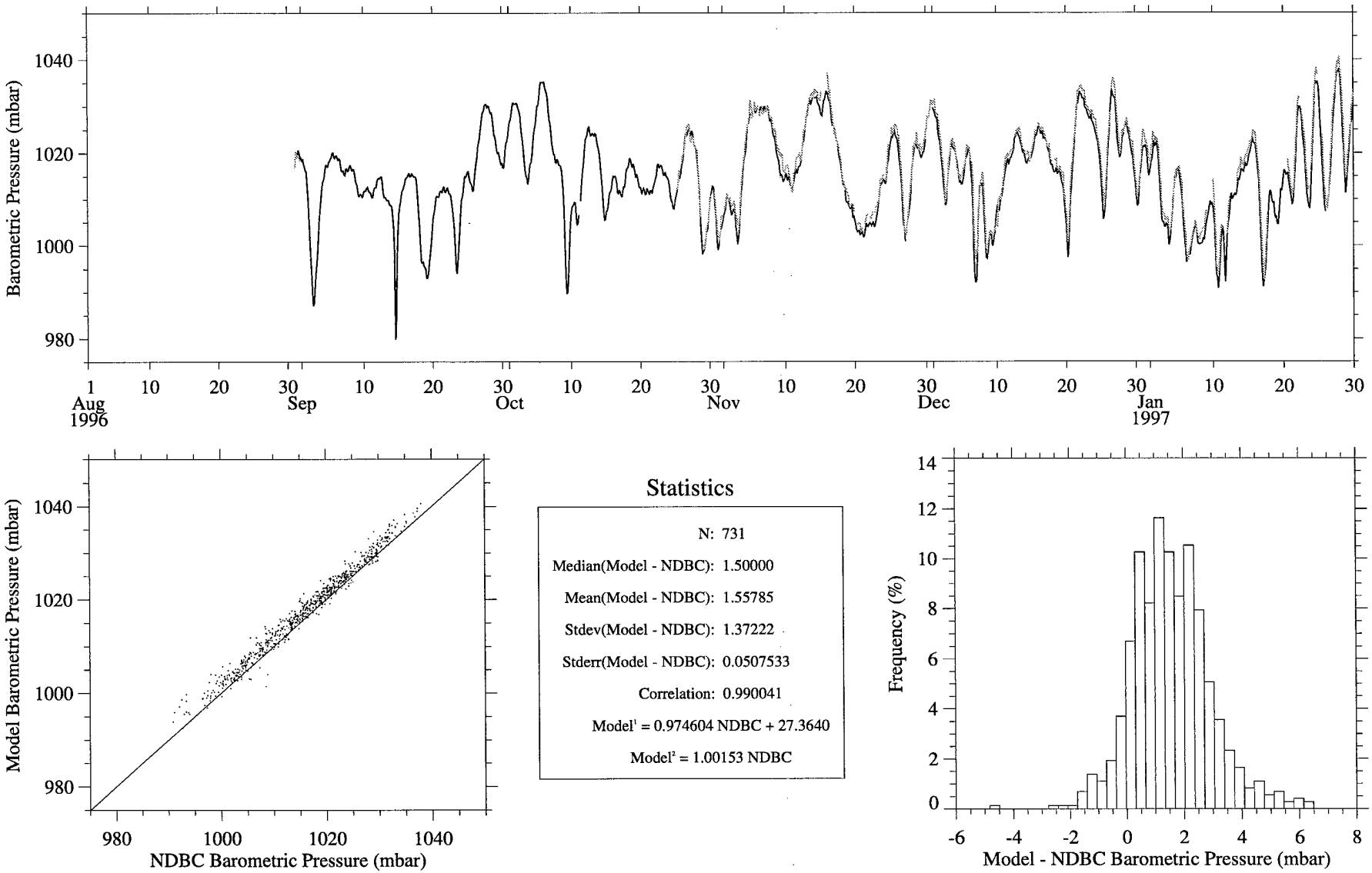

Figure A75. RUC Analysis (gray) vs. NDBC Buoy 44011 (black) barometric pressure.

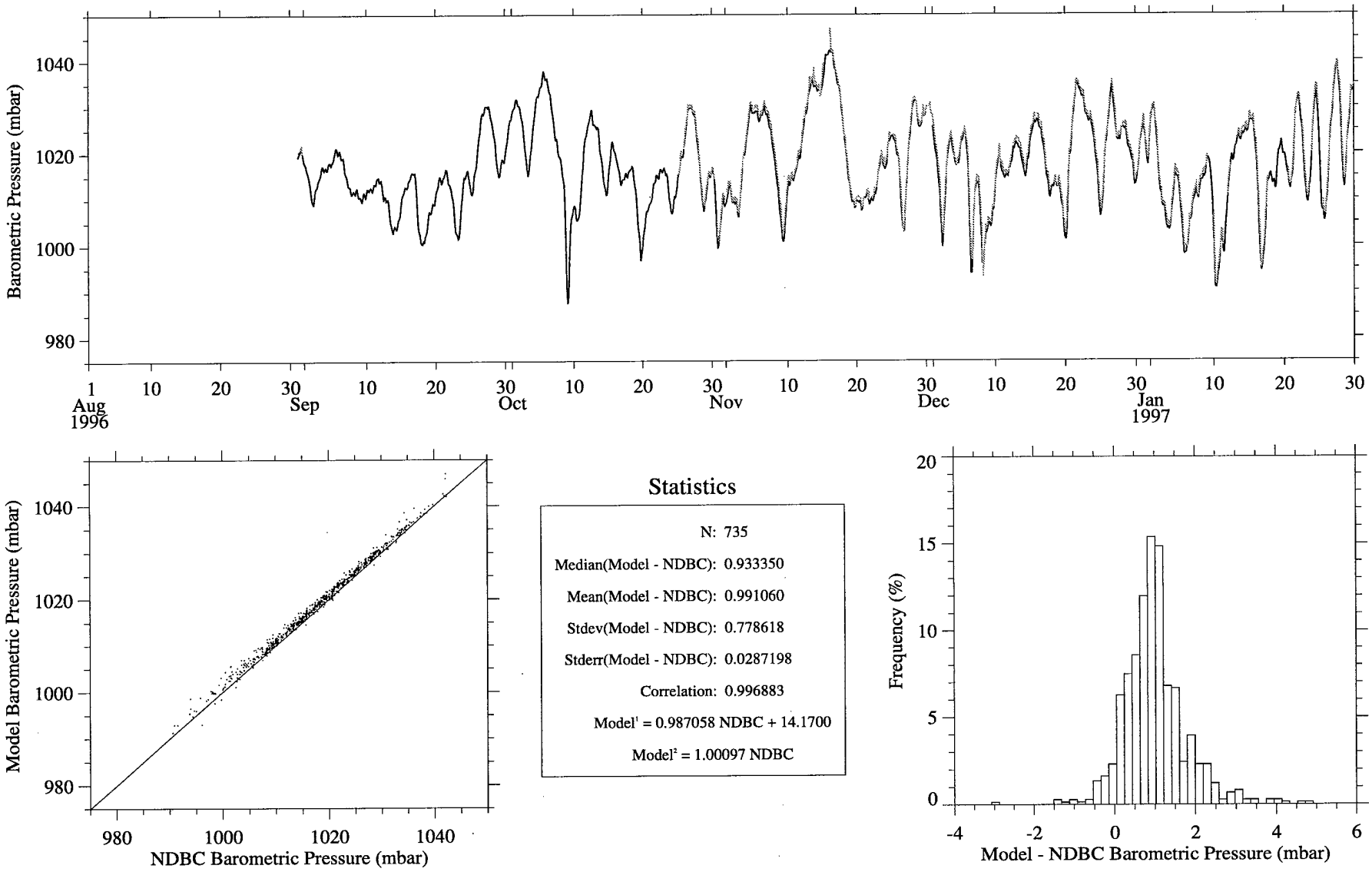

Figure A76. RUC Analysis (gray) vs. NDBC Buoy 44025 (black) barometric pressure.

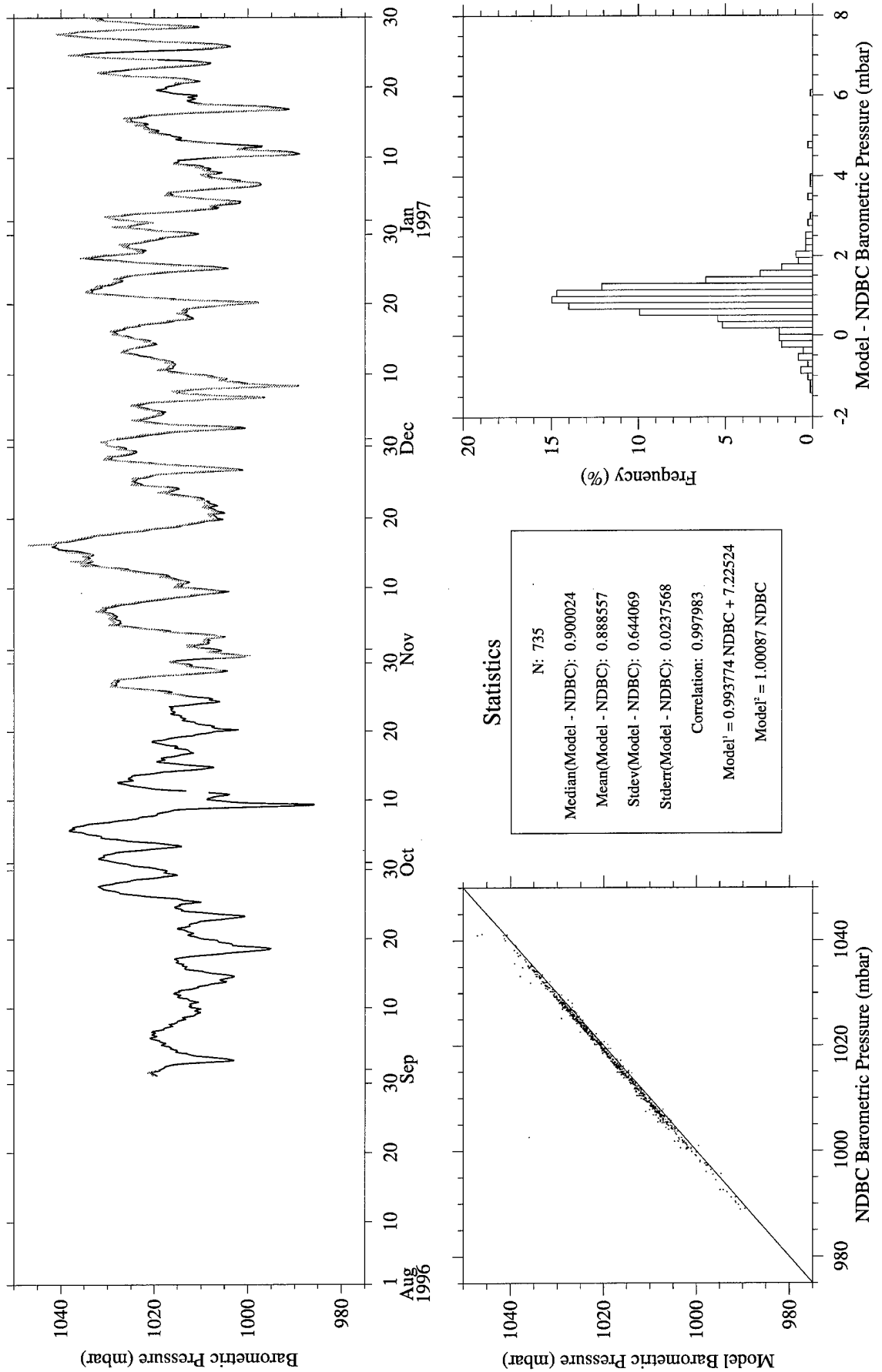

Figure A77. RUC Analysis (gray) vs. NDBC Buoy 44028 (black) barometric pressure.

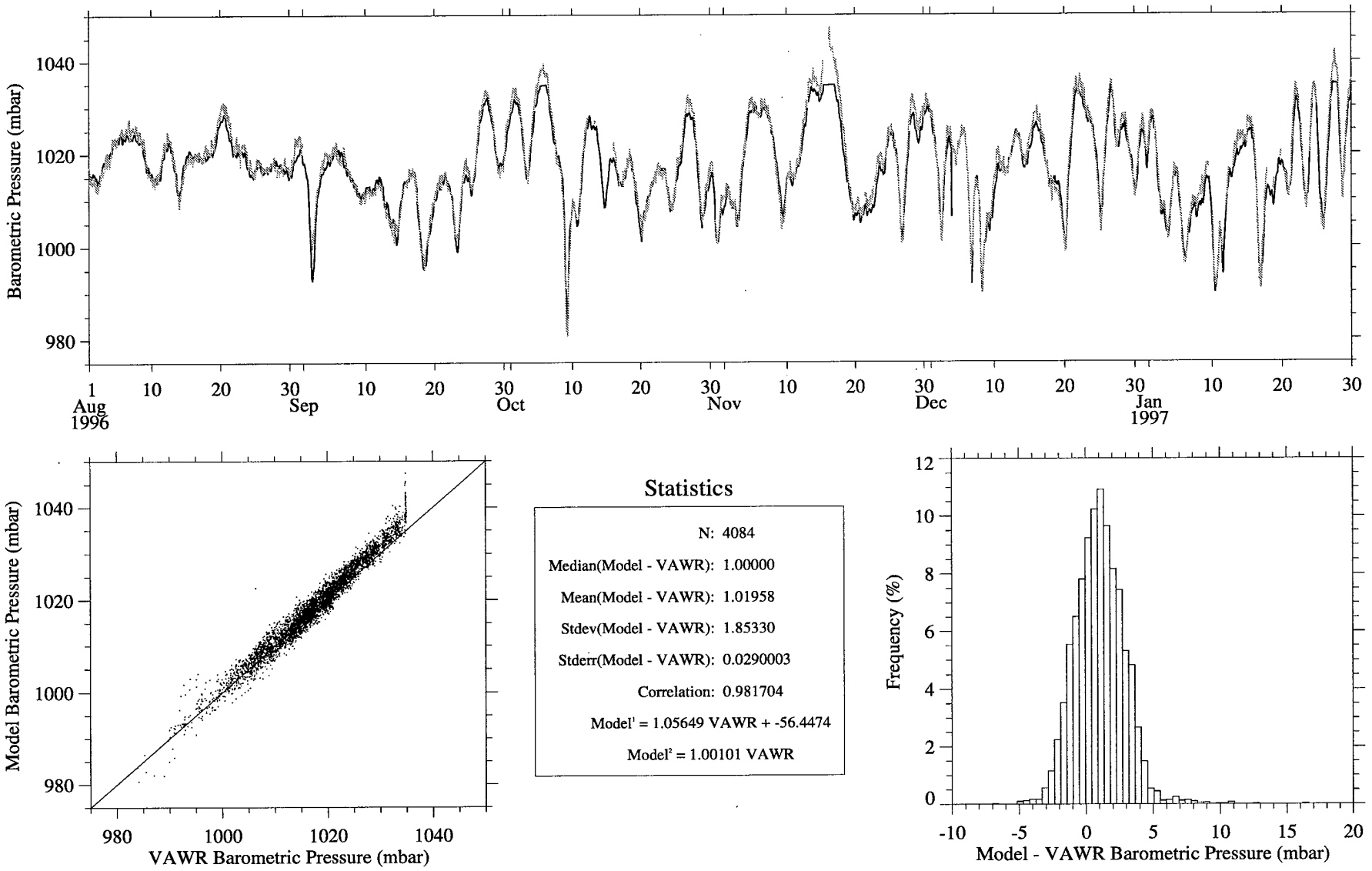

Figure A78. RUC Hourly (gray) vs. CMO VAWR 0704 (black) barometric pressure.

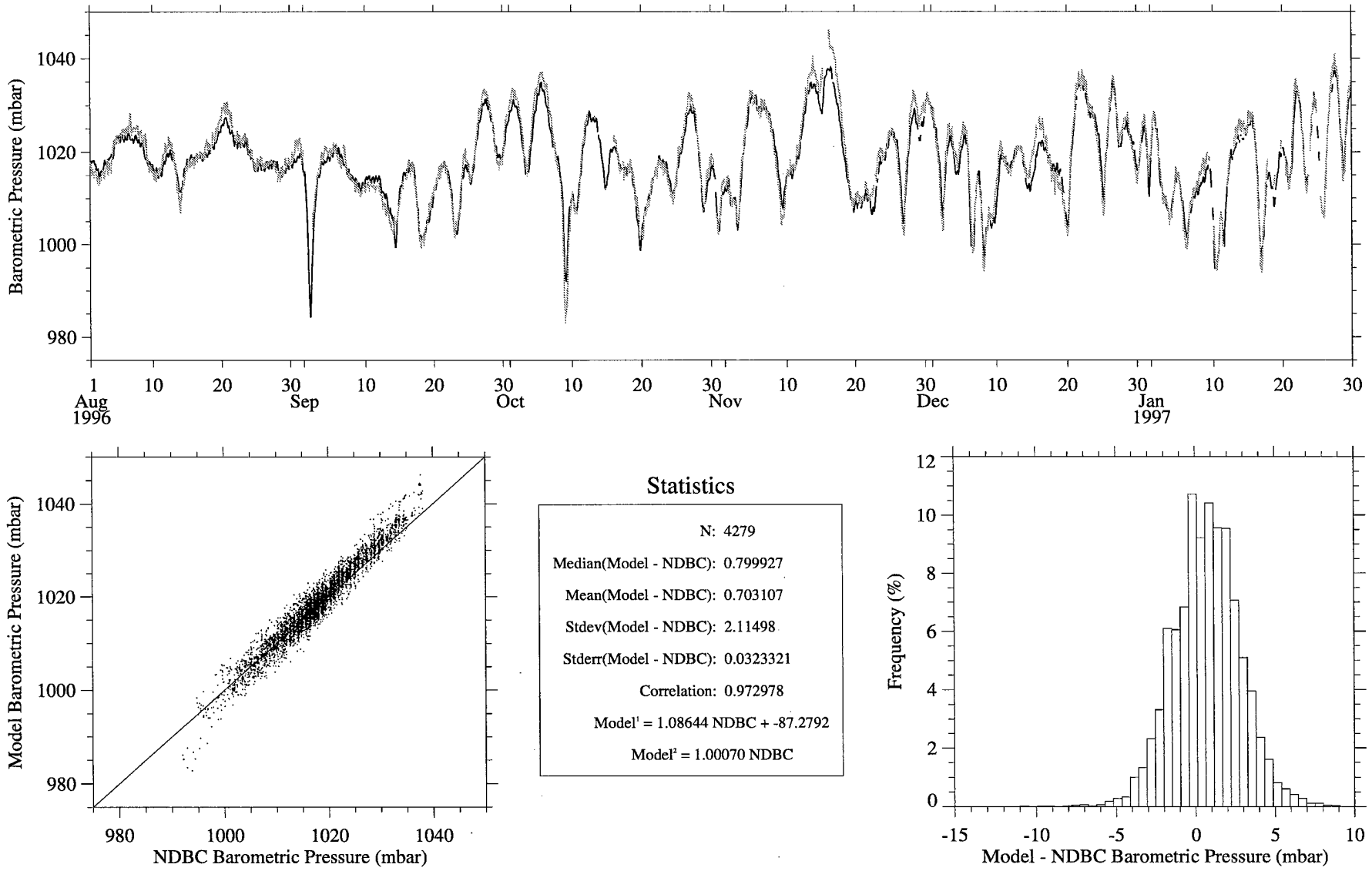

Figure A79. RUC Hourly (gray) vs. NDBC Buoy 44004 (black) barometric pressure.

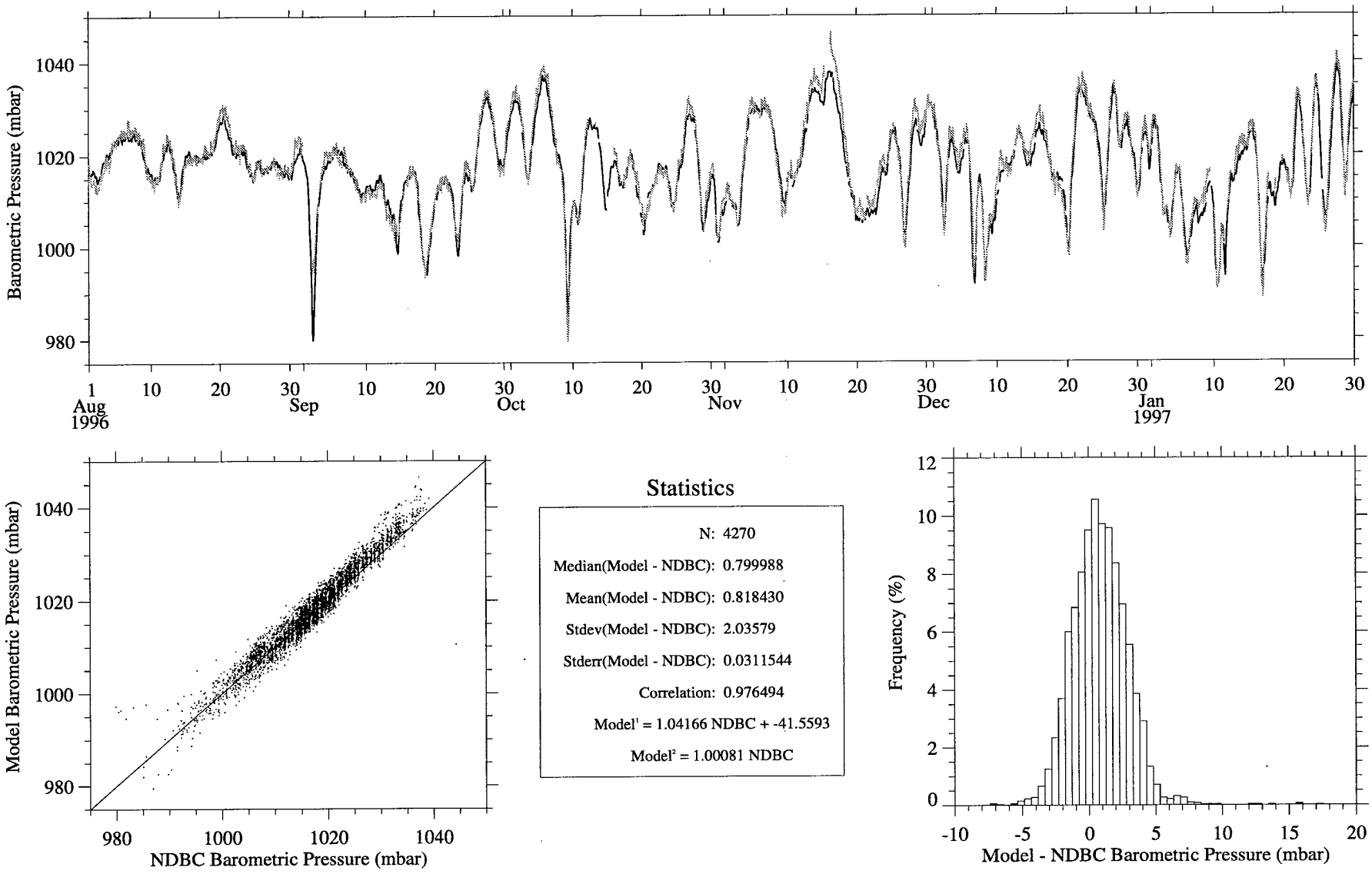

Figure A80. RUC Hourly (gray) vs. NDBC Buoy 44008 (black) barometric pressure.

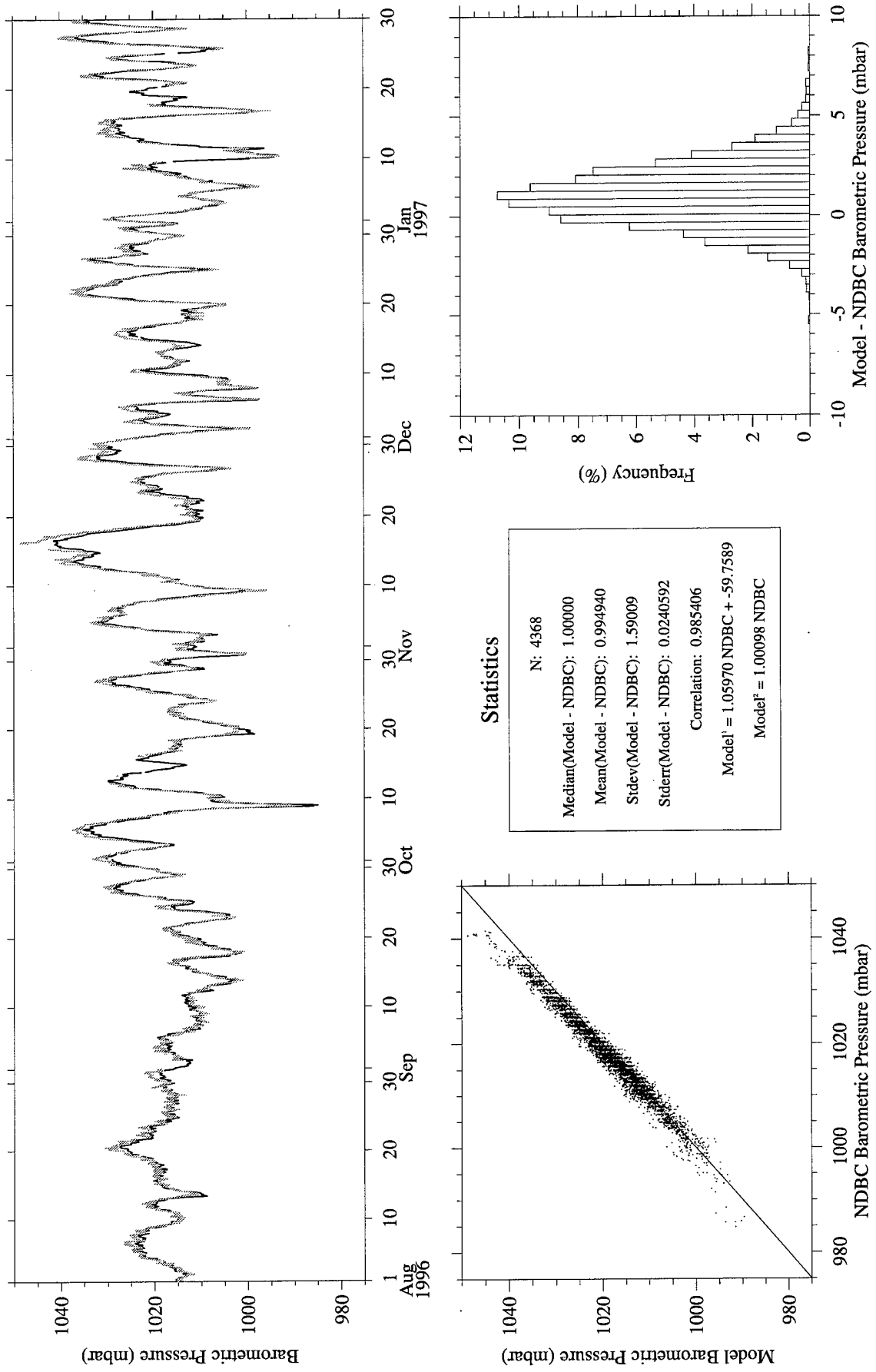

Figure A81. RUC Hourly (gray) vs. NDBC Buoy 44009 (black) barometric pressure.

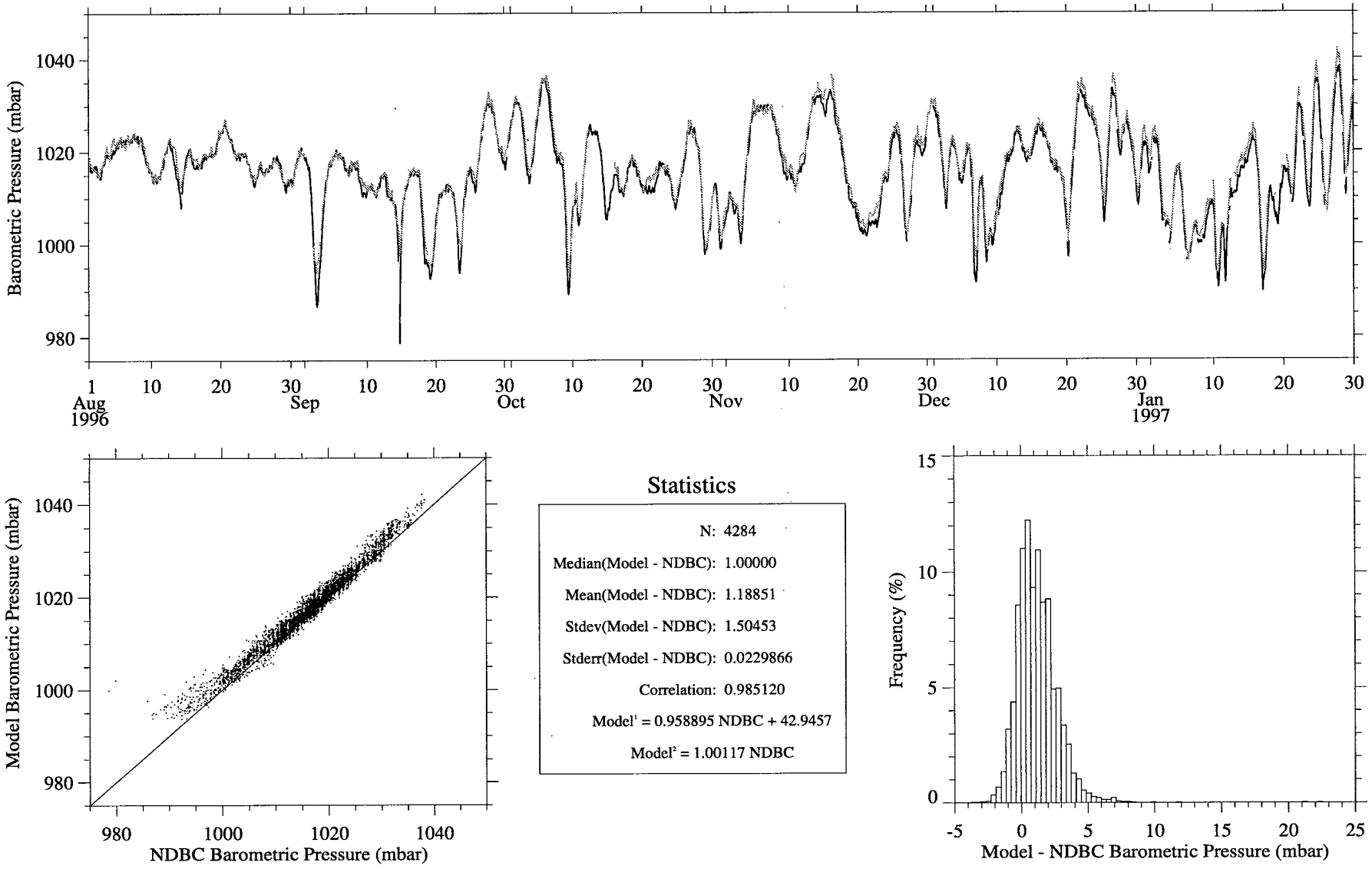

Figure A82. RUC Hourly (gray) vs. NDBC Buoy 44011 (black) barometric pressure.

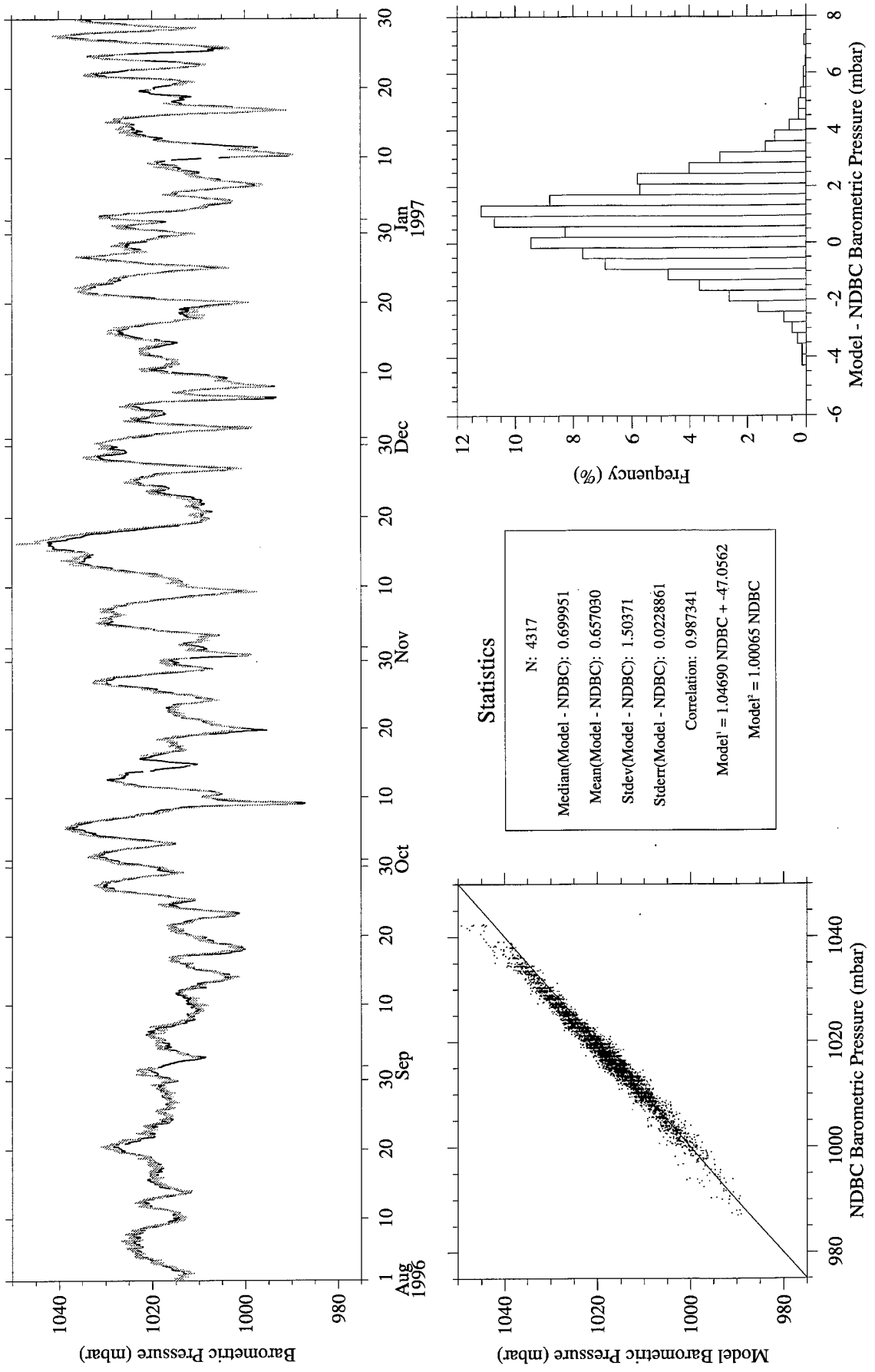

Figure A83. RUC Hourly (gray) vs. NDBC Buoy 44025 (black) barometric pressure.

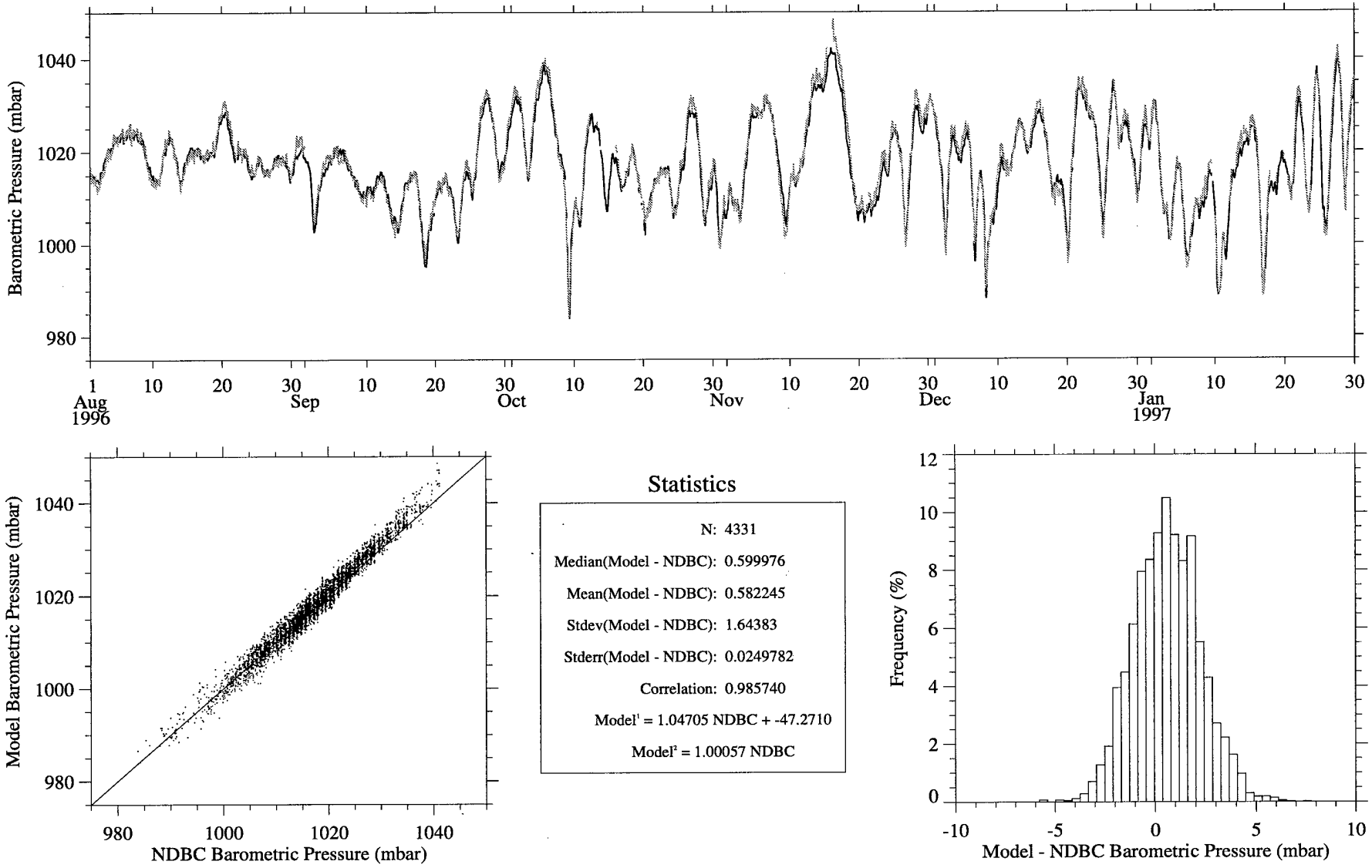

Figure A84. RUC Hourly (gray) vs. NDBC Buoy 44028 (black) barometric pressure.

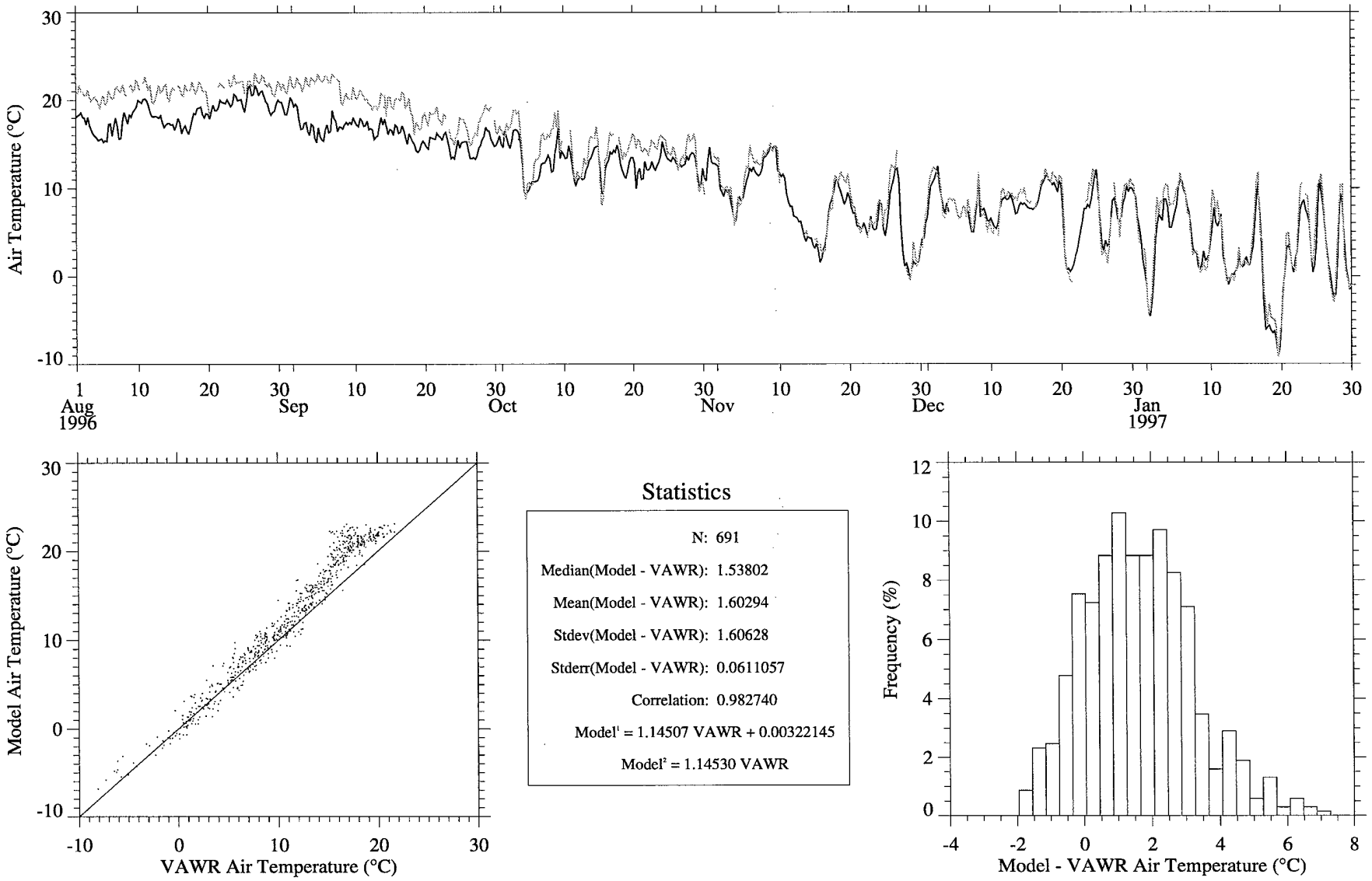

Figure A85. Eta (gray) vs. CMO VAWR 0704 (black) air temperature.

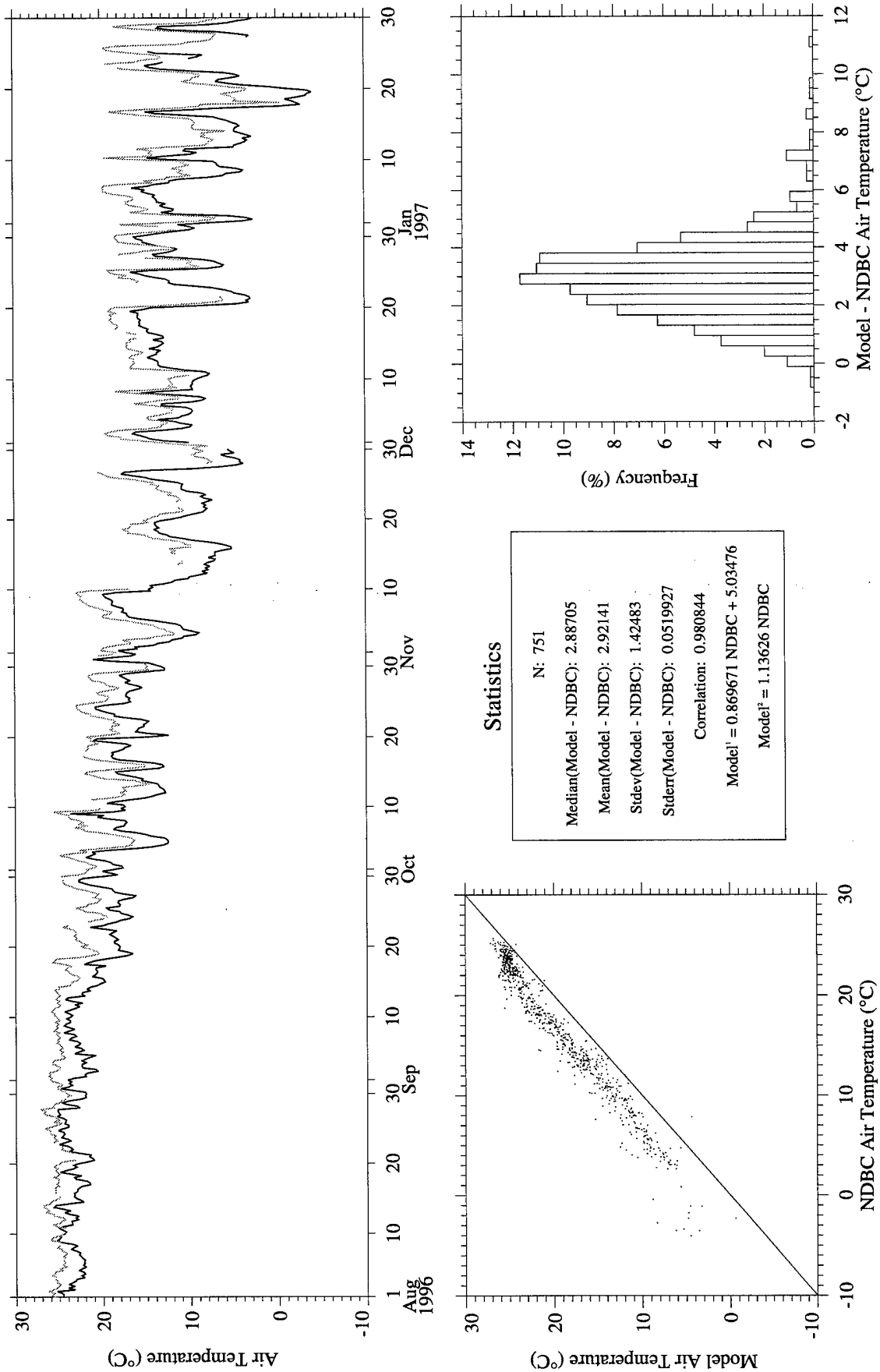

Figure A86. Eta (gray) vs. NDBC Buoy 44004 (black) air temperature.

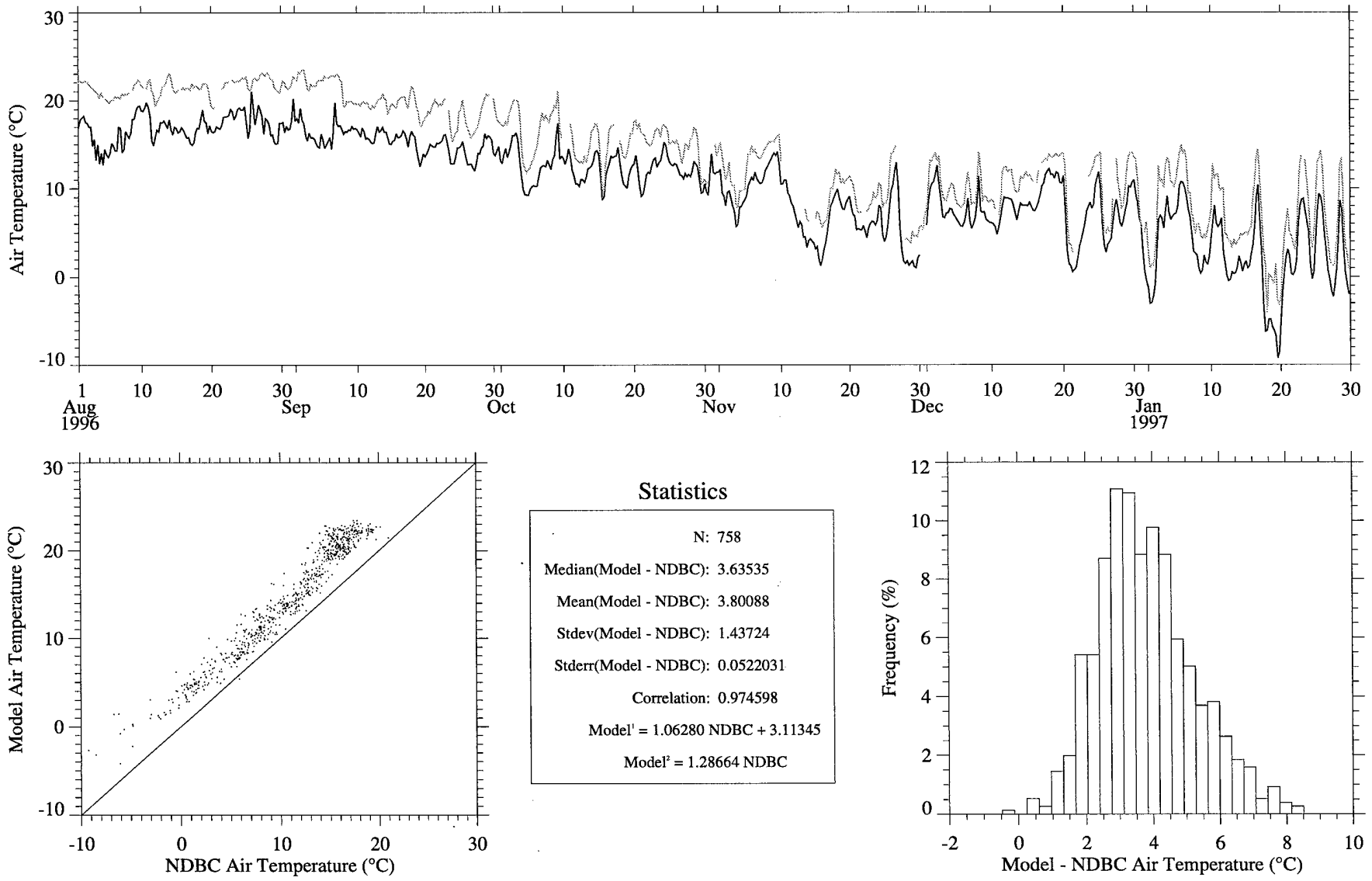

Figure A87. Eta (gray) vs. NDBC Buoy 44008 (black) air temperature.

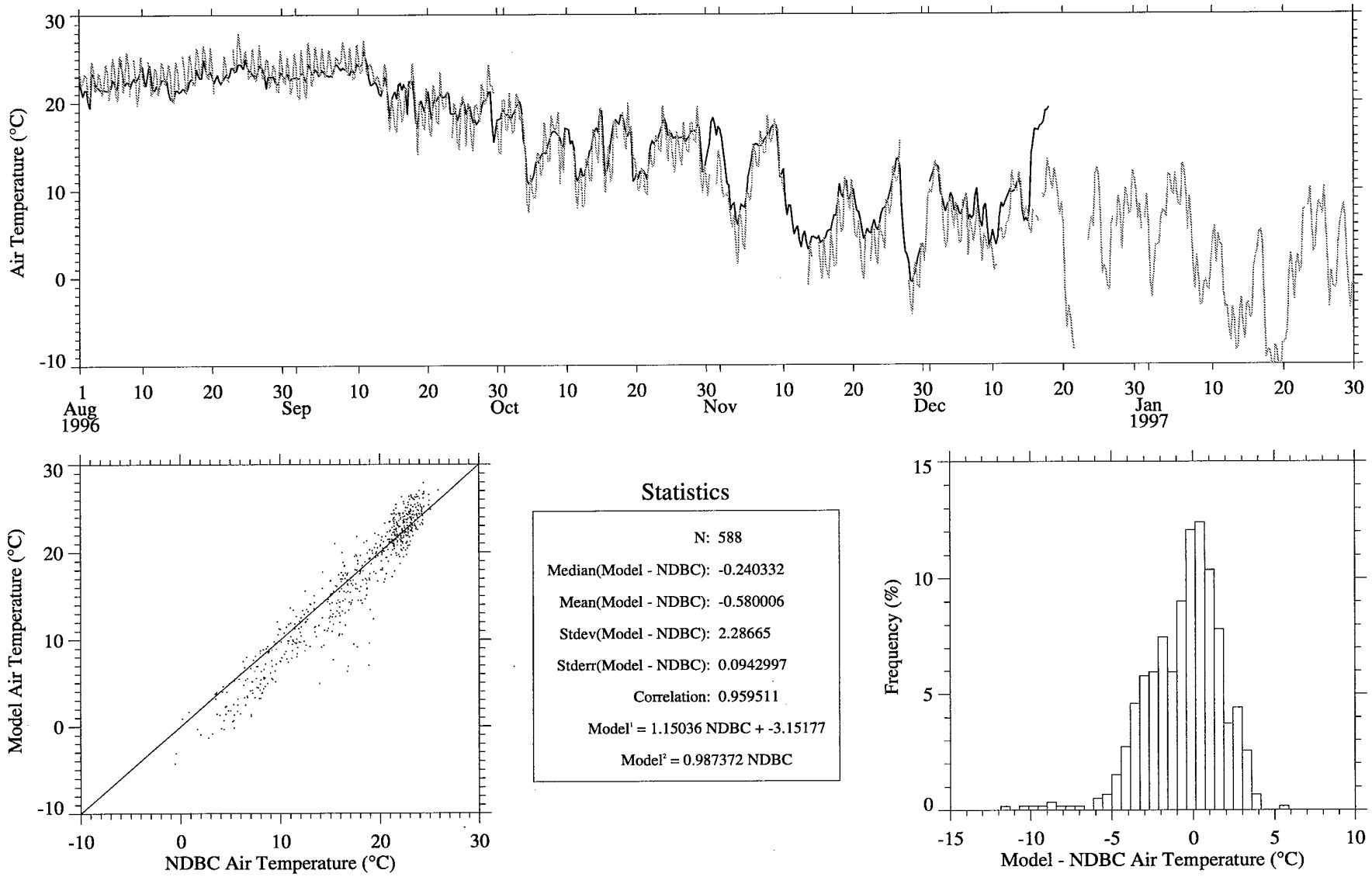

Figure A88. Eta (gray) vs. NDBC Buoy 44009 (black) air temperature.

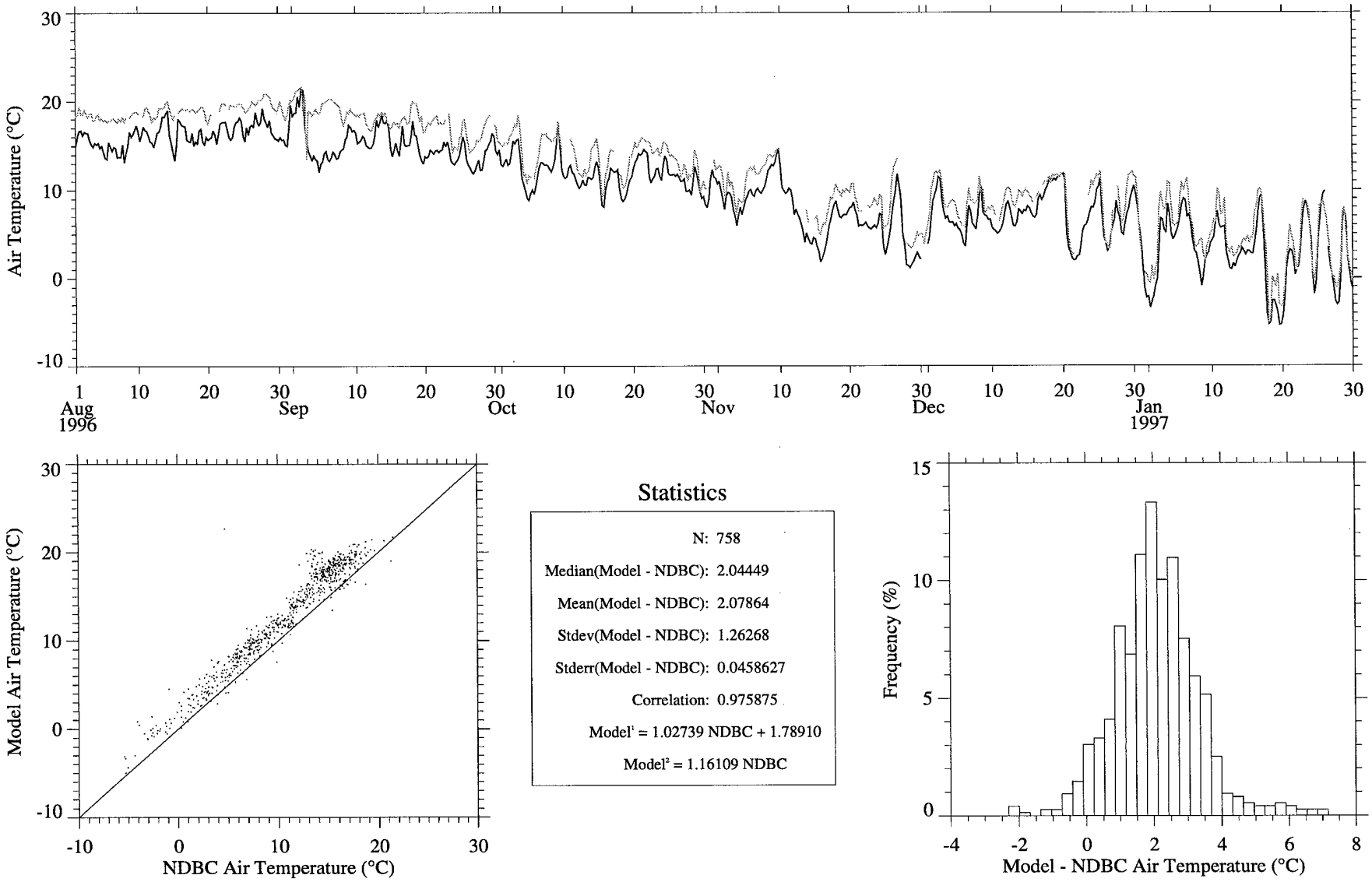

Figure A89. Eta (gray) vs. NDBC Buoy 44011 (black) air temperature.

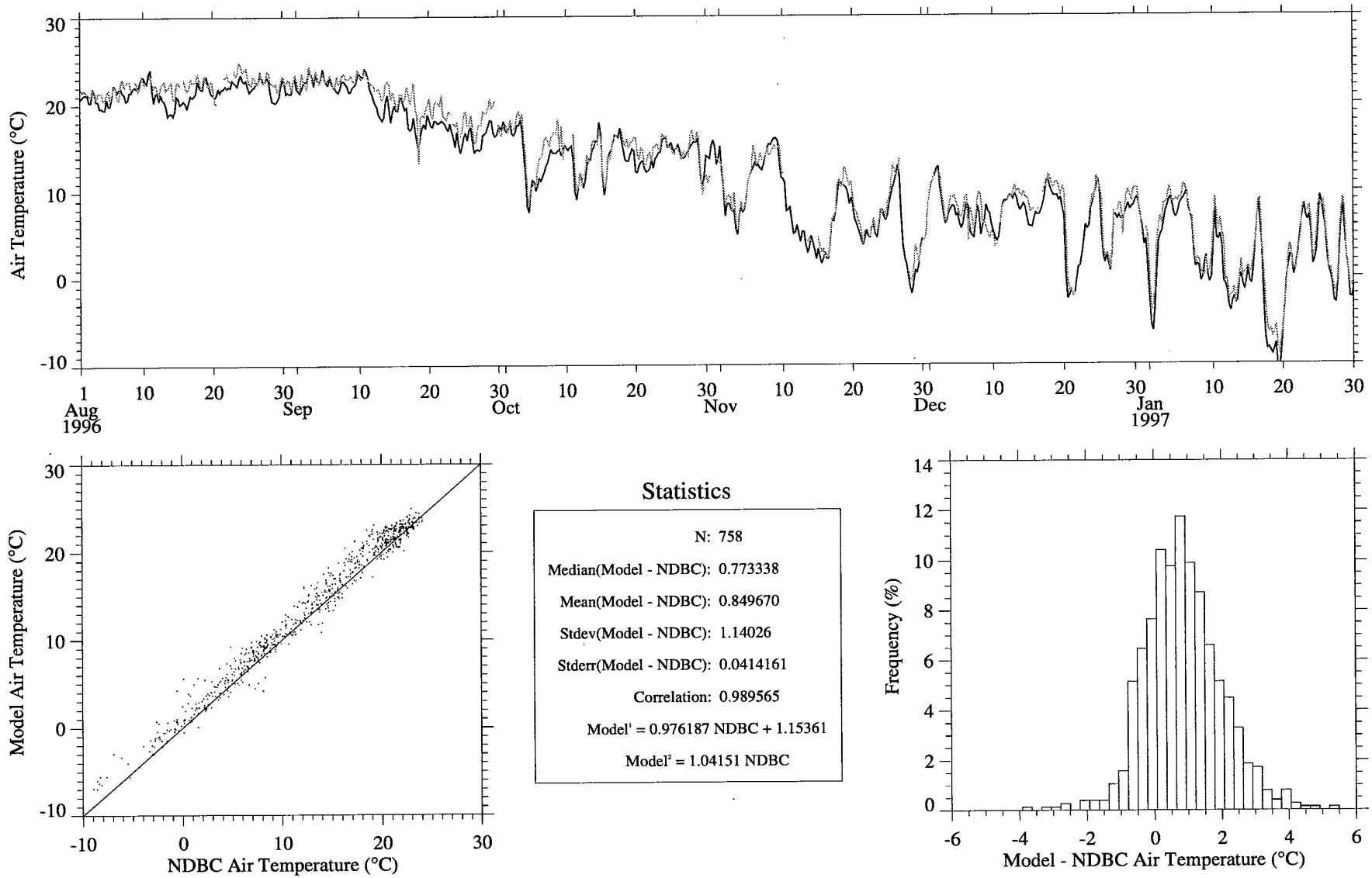

Figure A90. Eta (gray) vs. NDBC Buoy 44025 (black) air temperature.

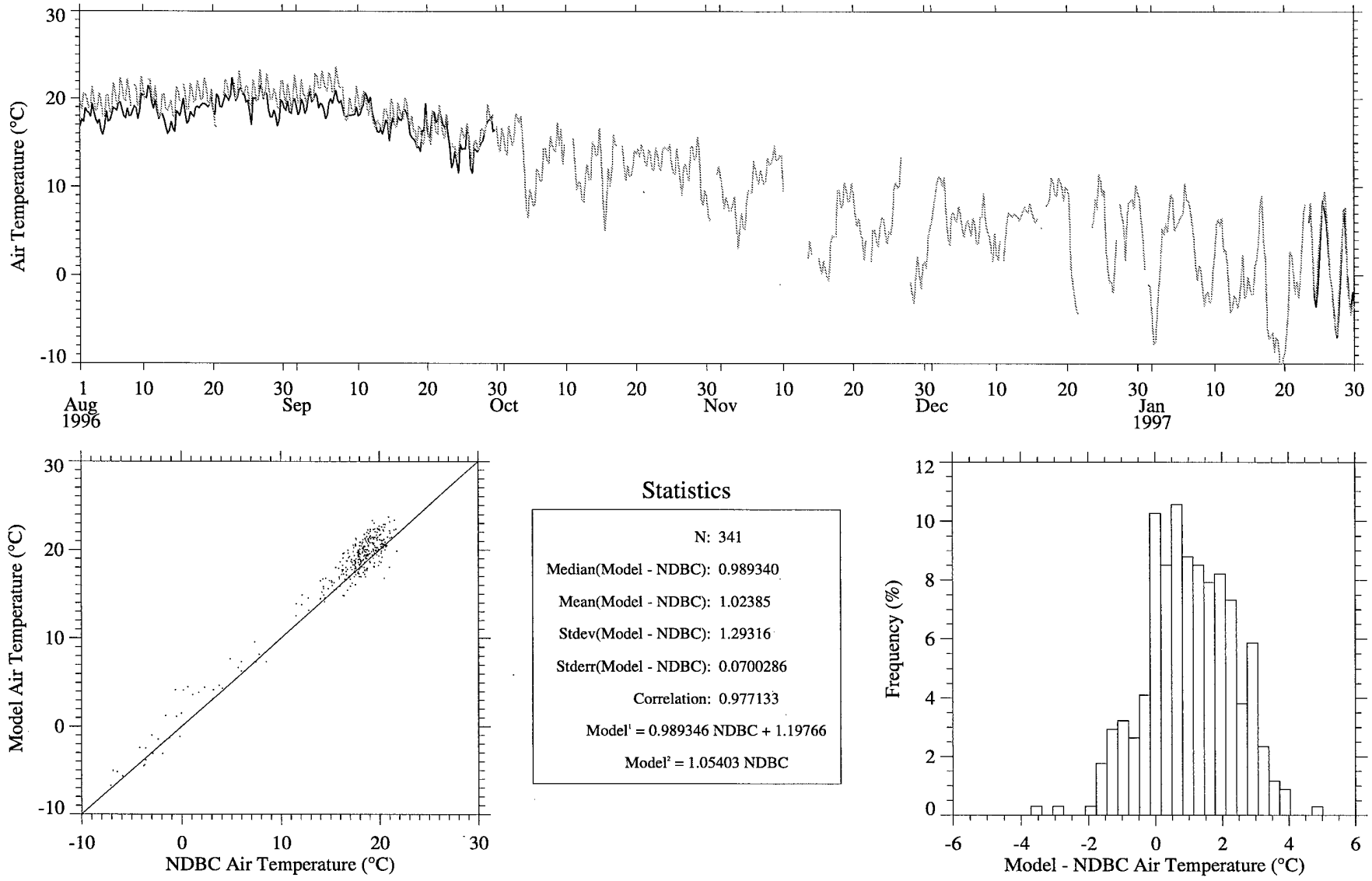

Figure A91. Eta (gray) vs. NDBC Buoy 44028 (black) air temperature.

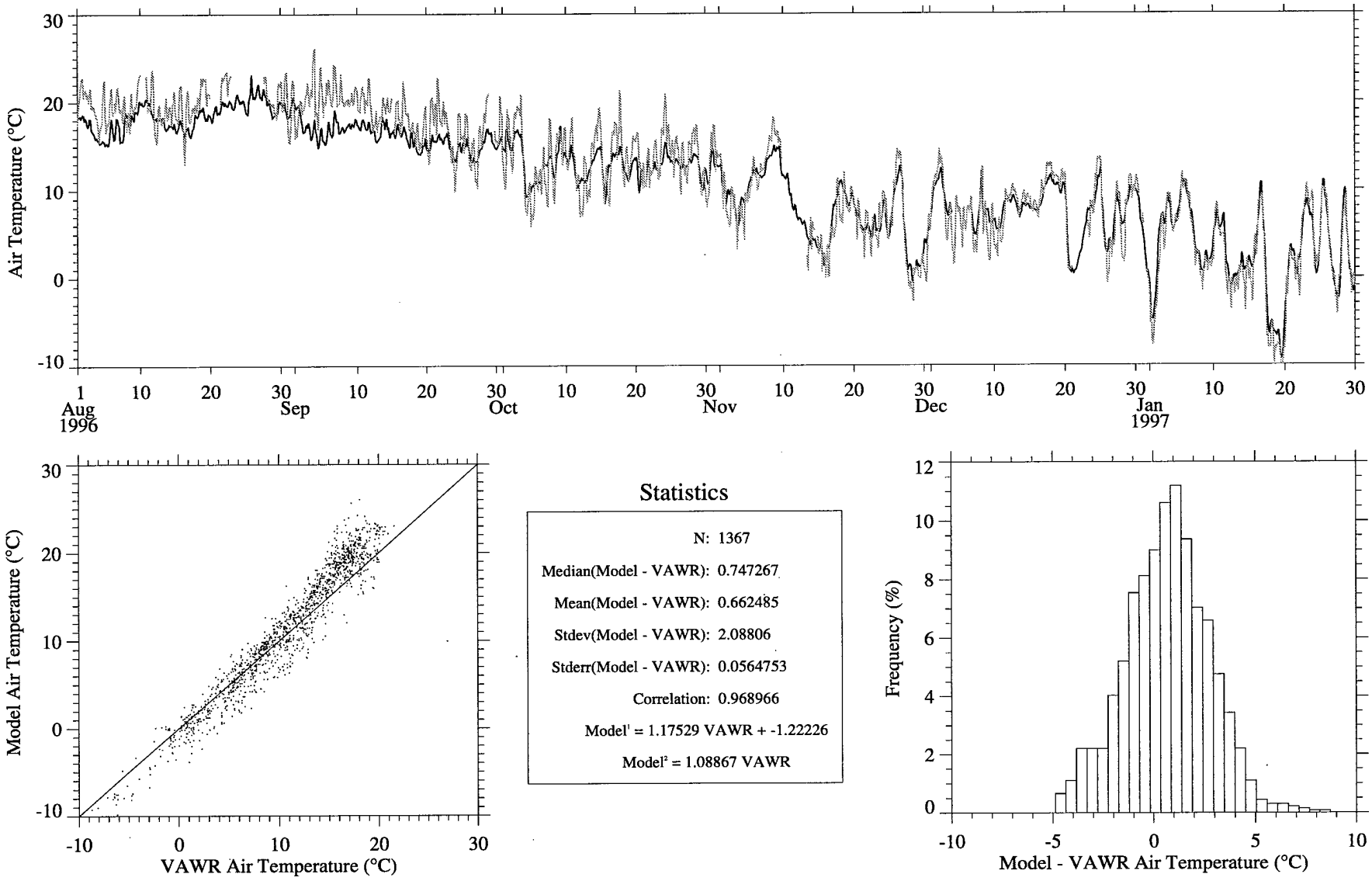

Figure A92. RUC (gray) vs. CMO VAWR 0704 (black) air temperature.

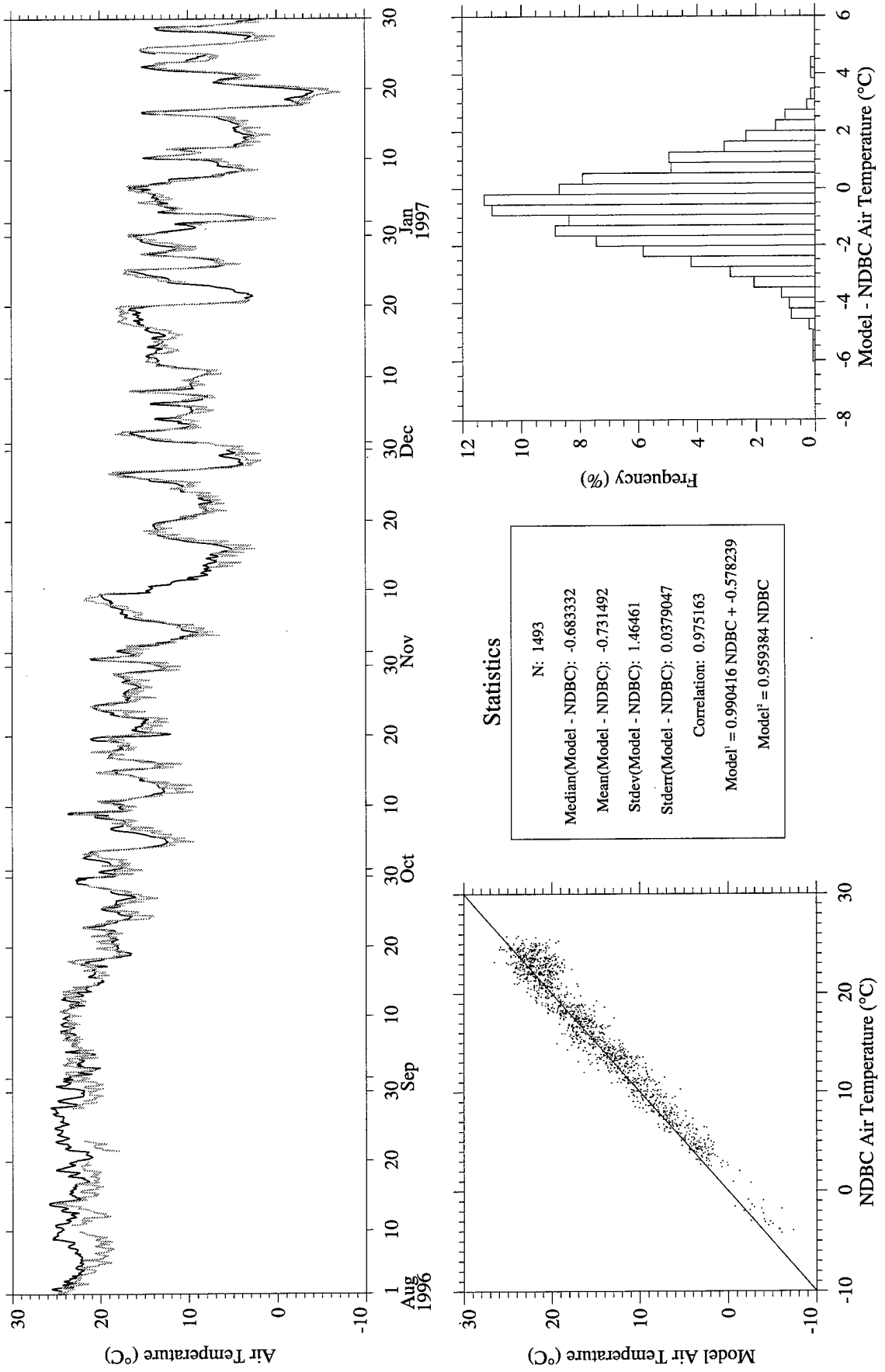

Figure A93. RUC (gray) vs. NDBC Buoy 44004 (black) air temperature.

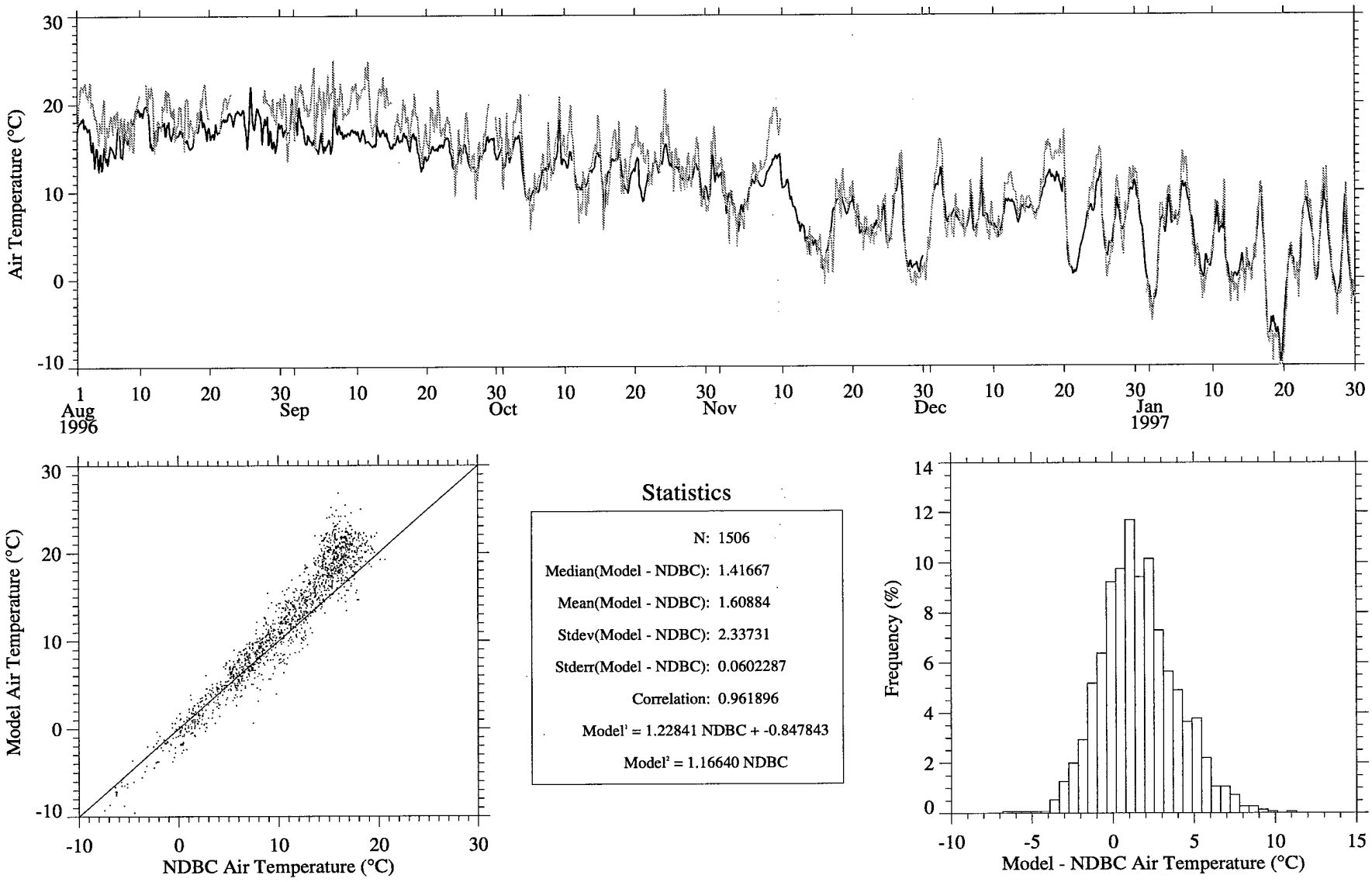

Figure A94. RUC (gray) vs. NDBC Buoy 44008 (black) air temperature.

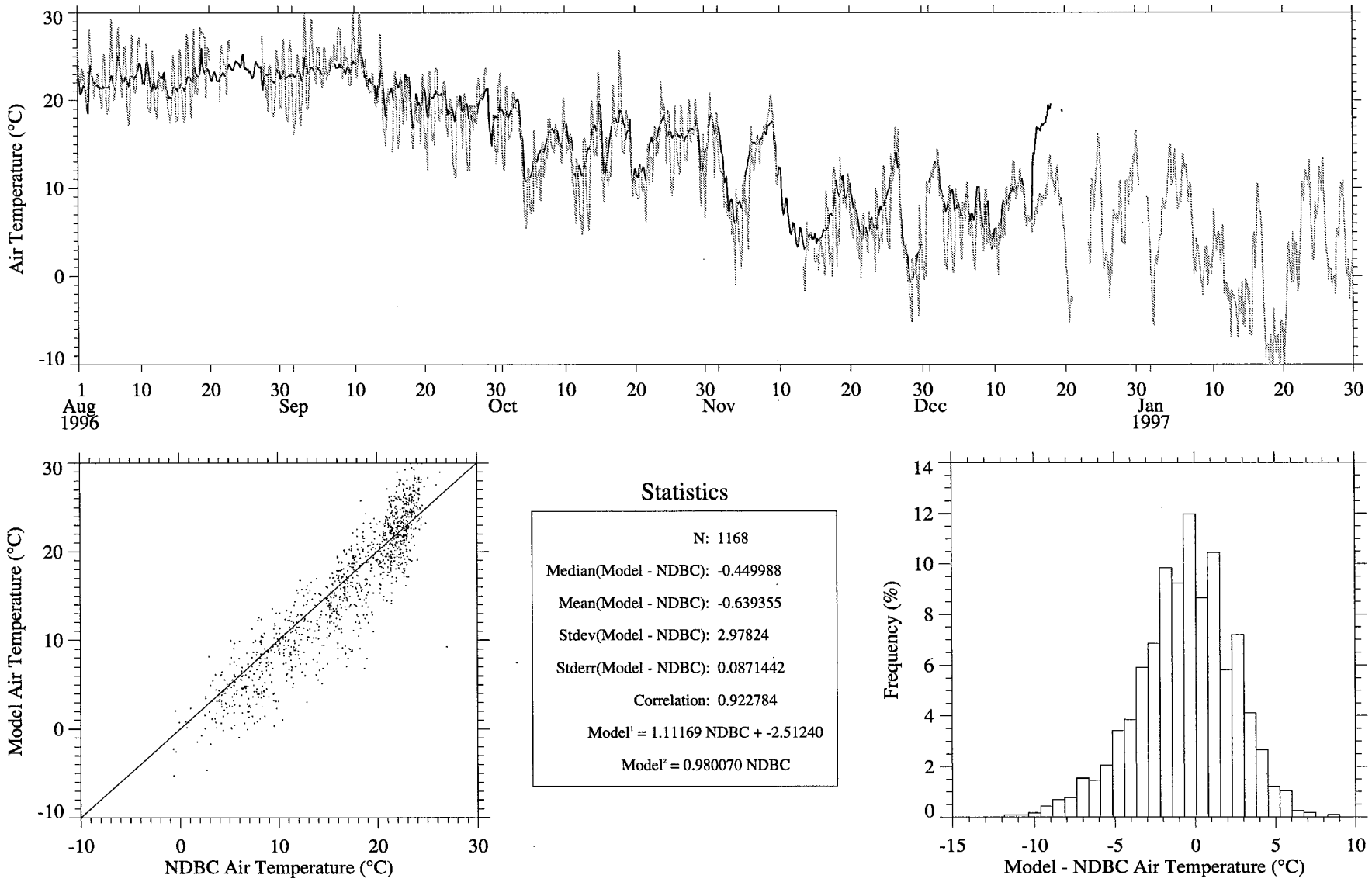

Figure A95. RUC (gray) vs. NDBC Buoy 44009 (black) air temperature.

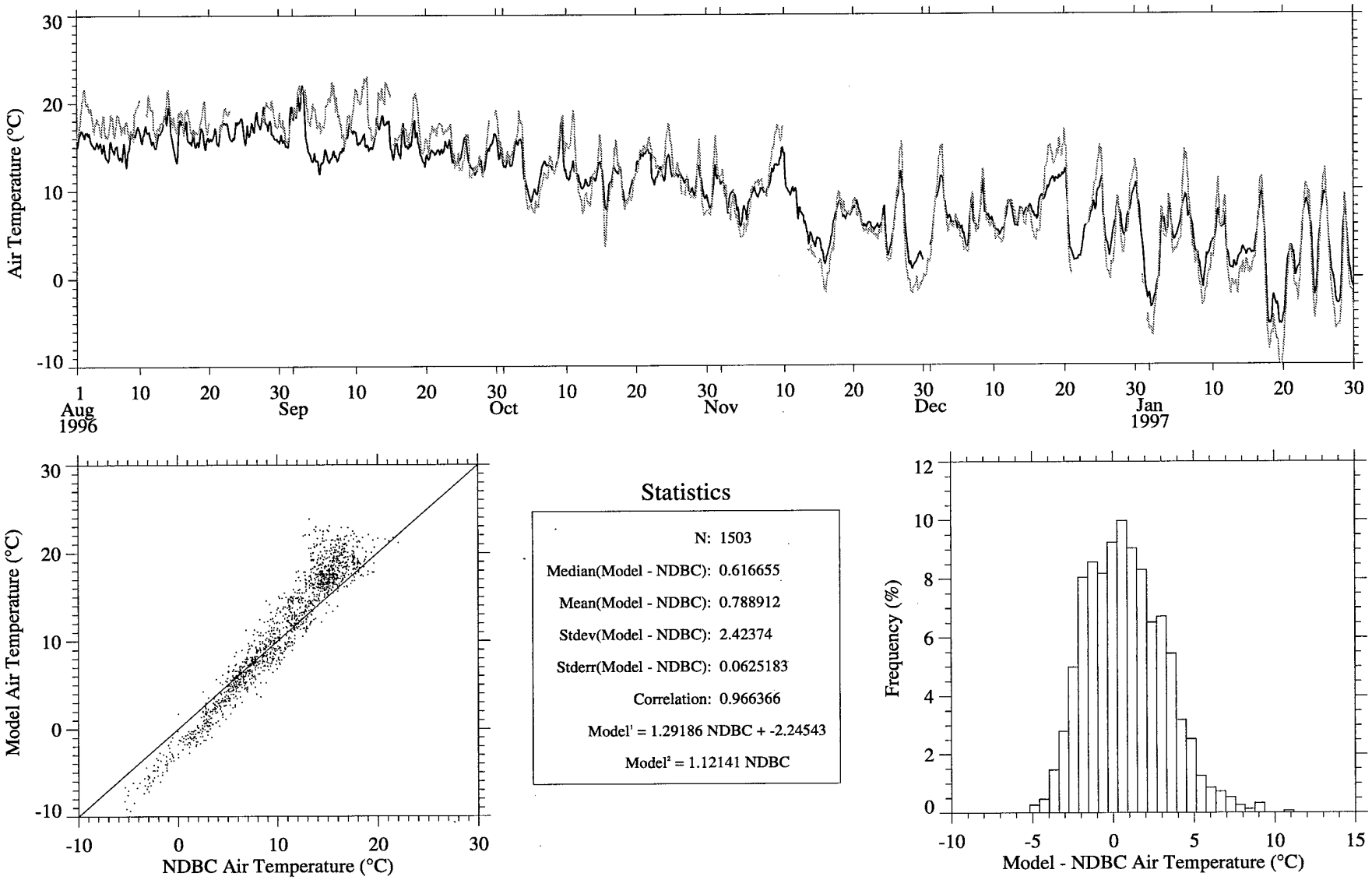

Figure A96. RUC (gray) vs. NDBC Buoy 44011 (black) air temperature.

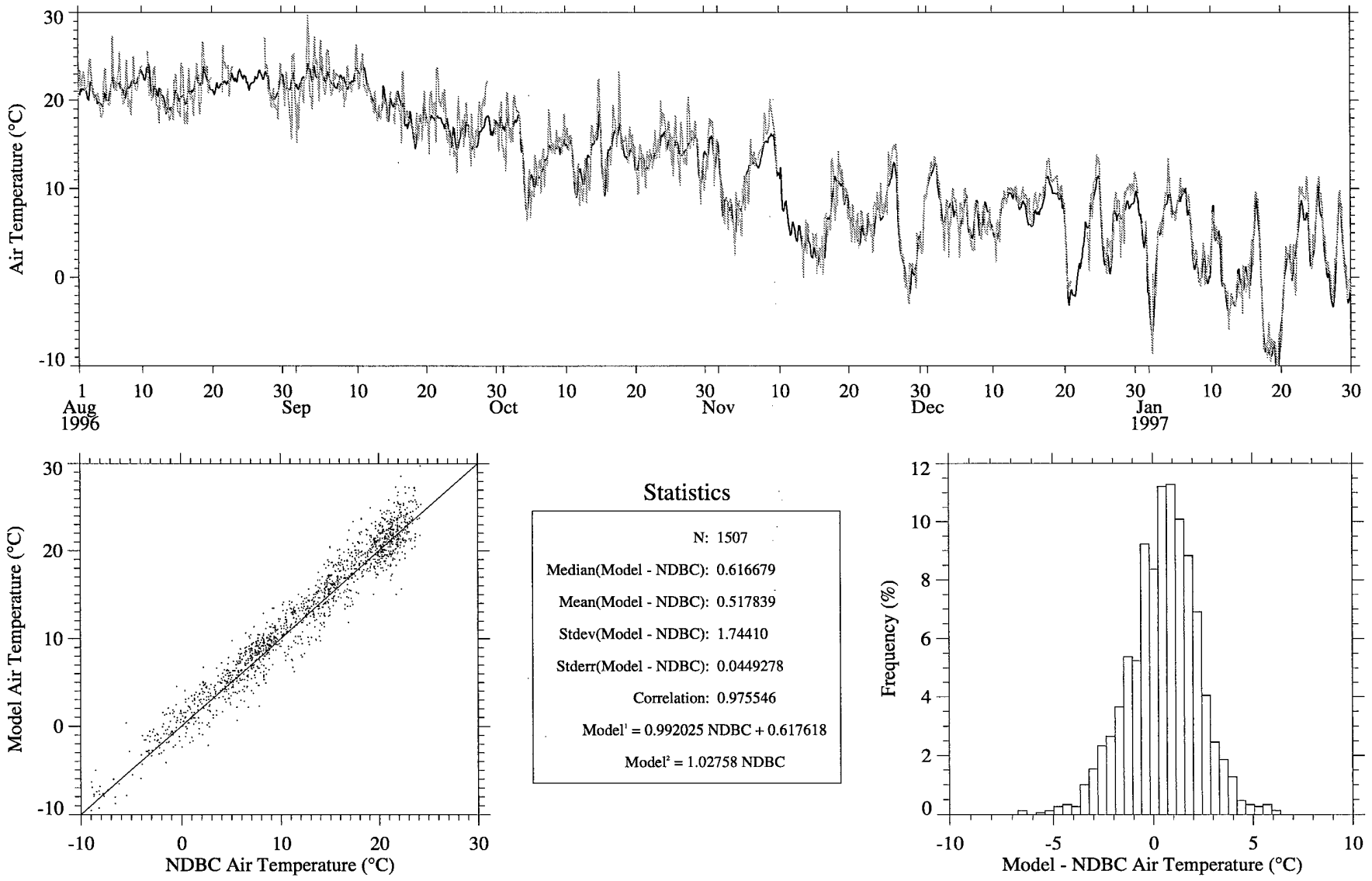

Figure A97. RUC (gray) vs. NDBC Buoy 44025 (black) air temperature.

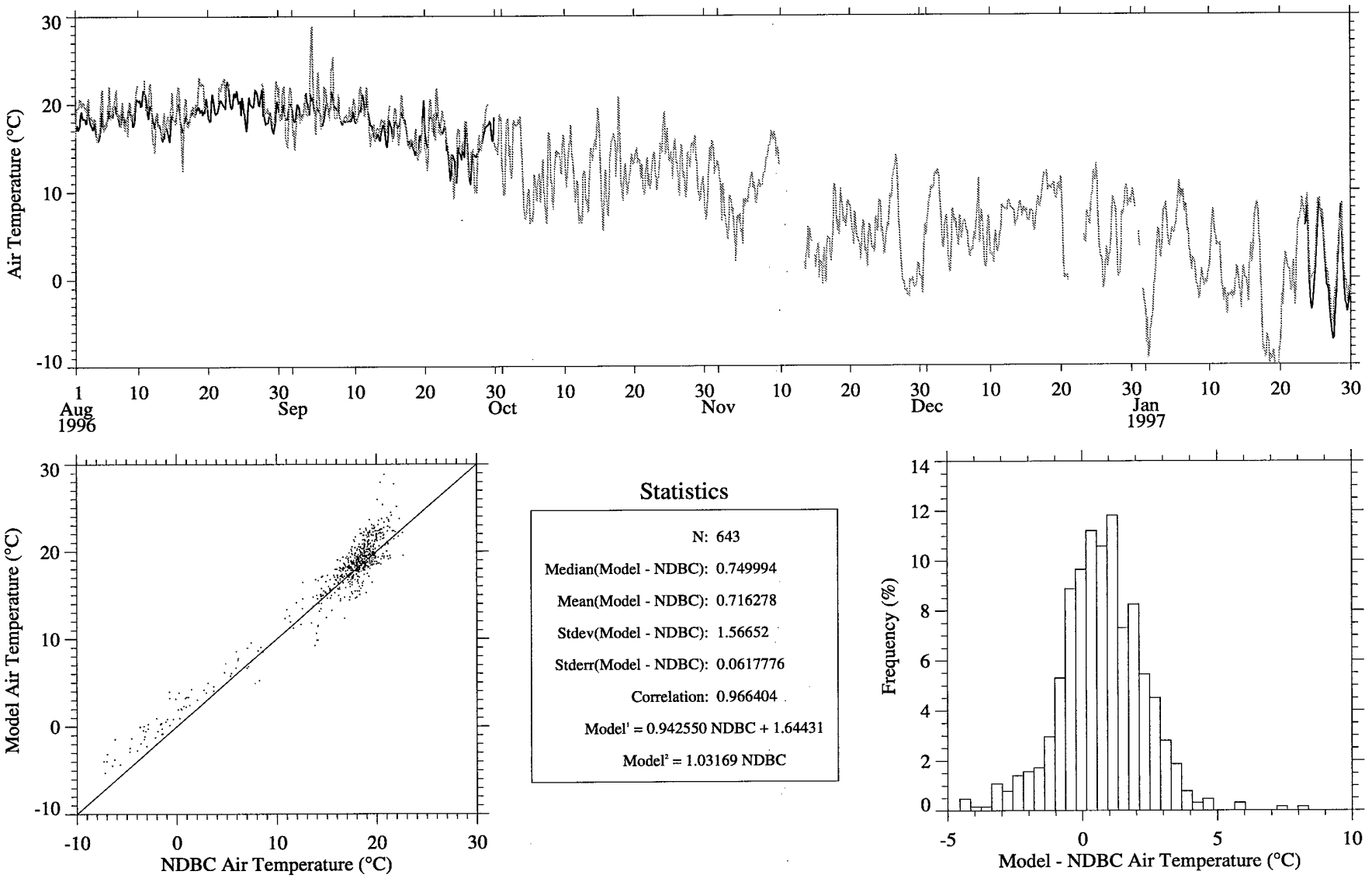

Figure A98. RUC (gray) vs. NDBC Buoy 44028 (black) air temperature.

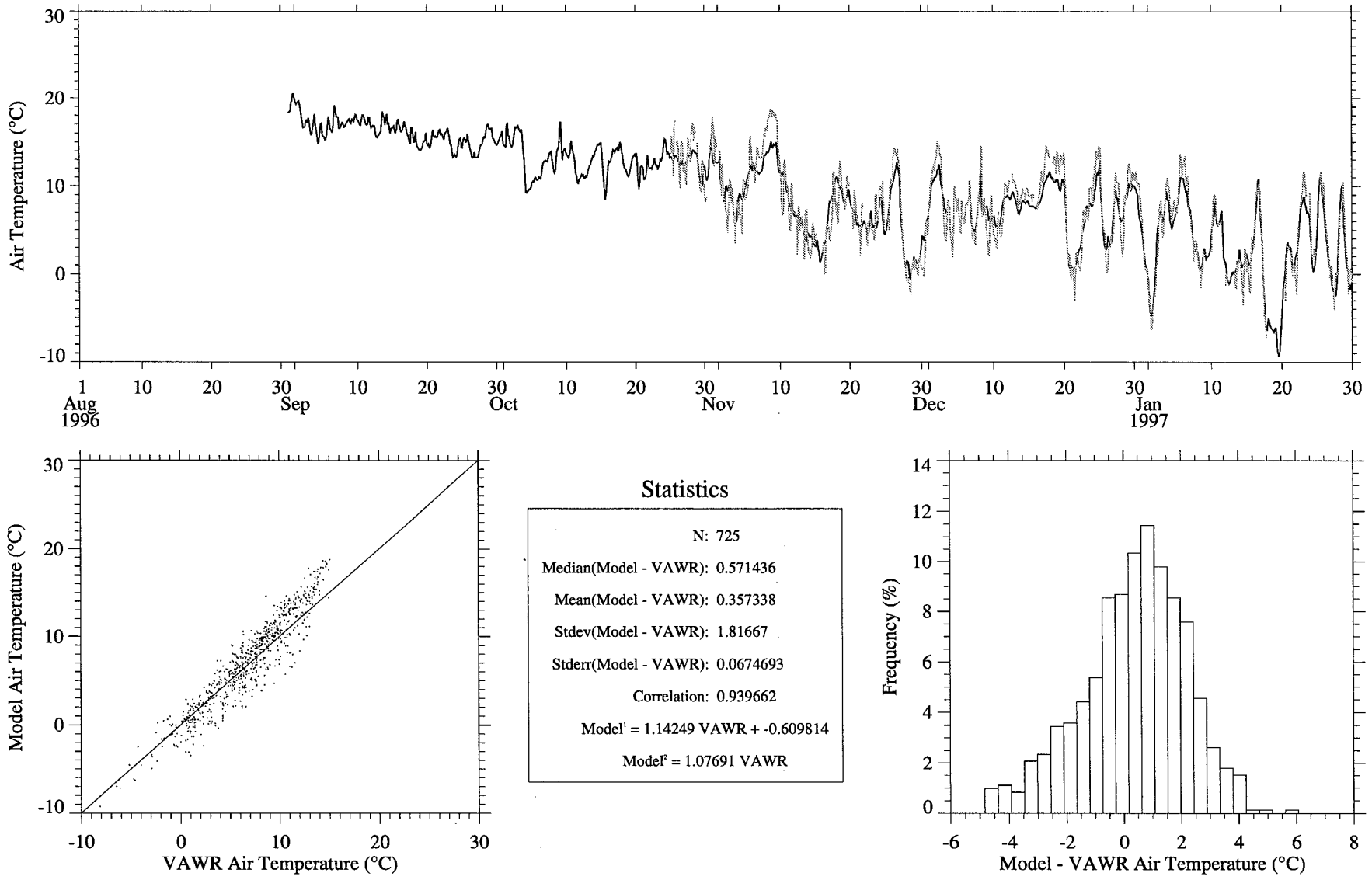

Figure A99. RUC Analysis (gray) vs. CMO VAWR 0704 (black) air temperature.

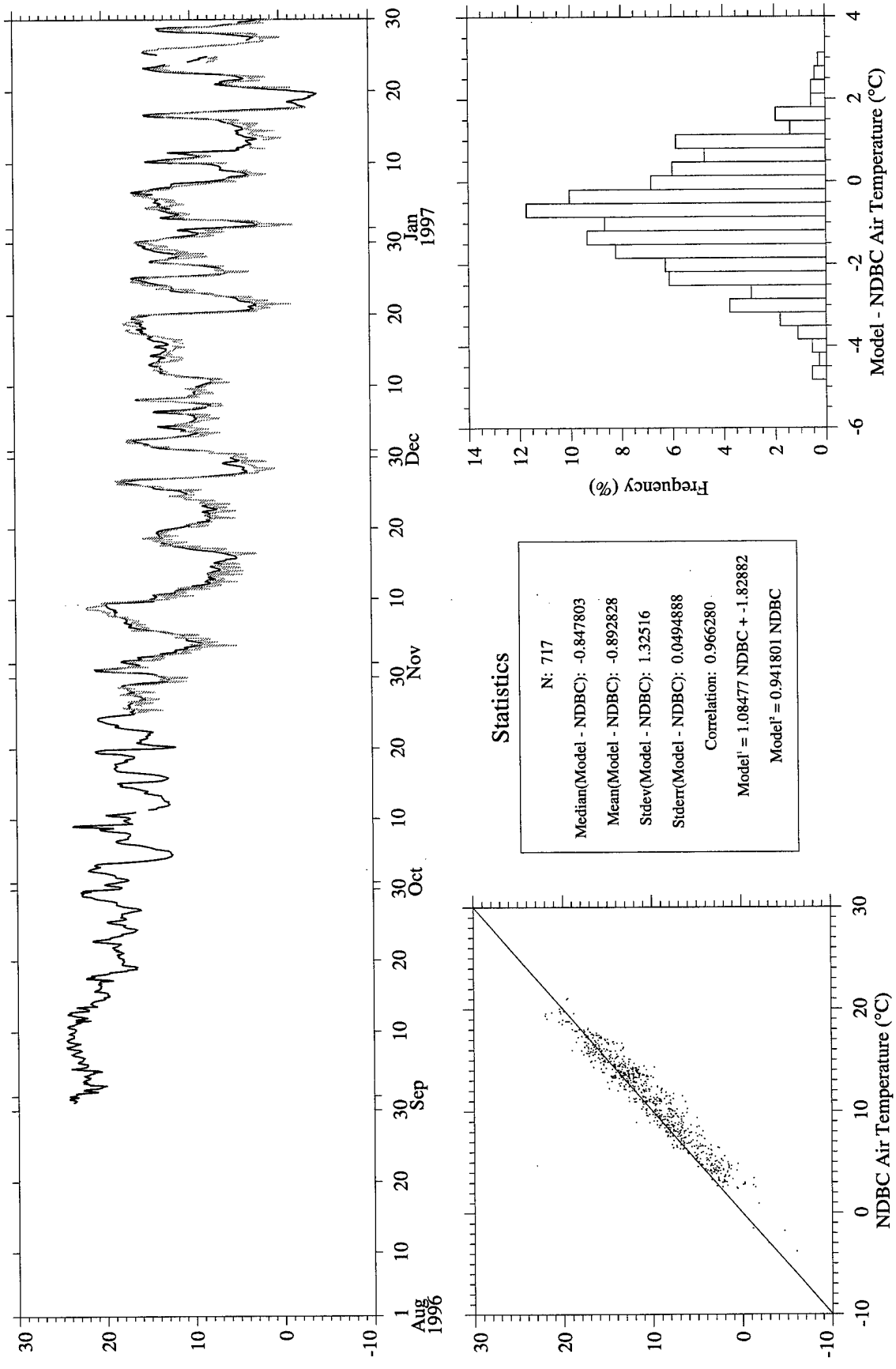

Figure A100. RUC Analysis (gray) vs. NDBC Buoy 44004 (black) air temperature.

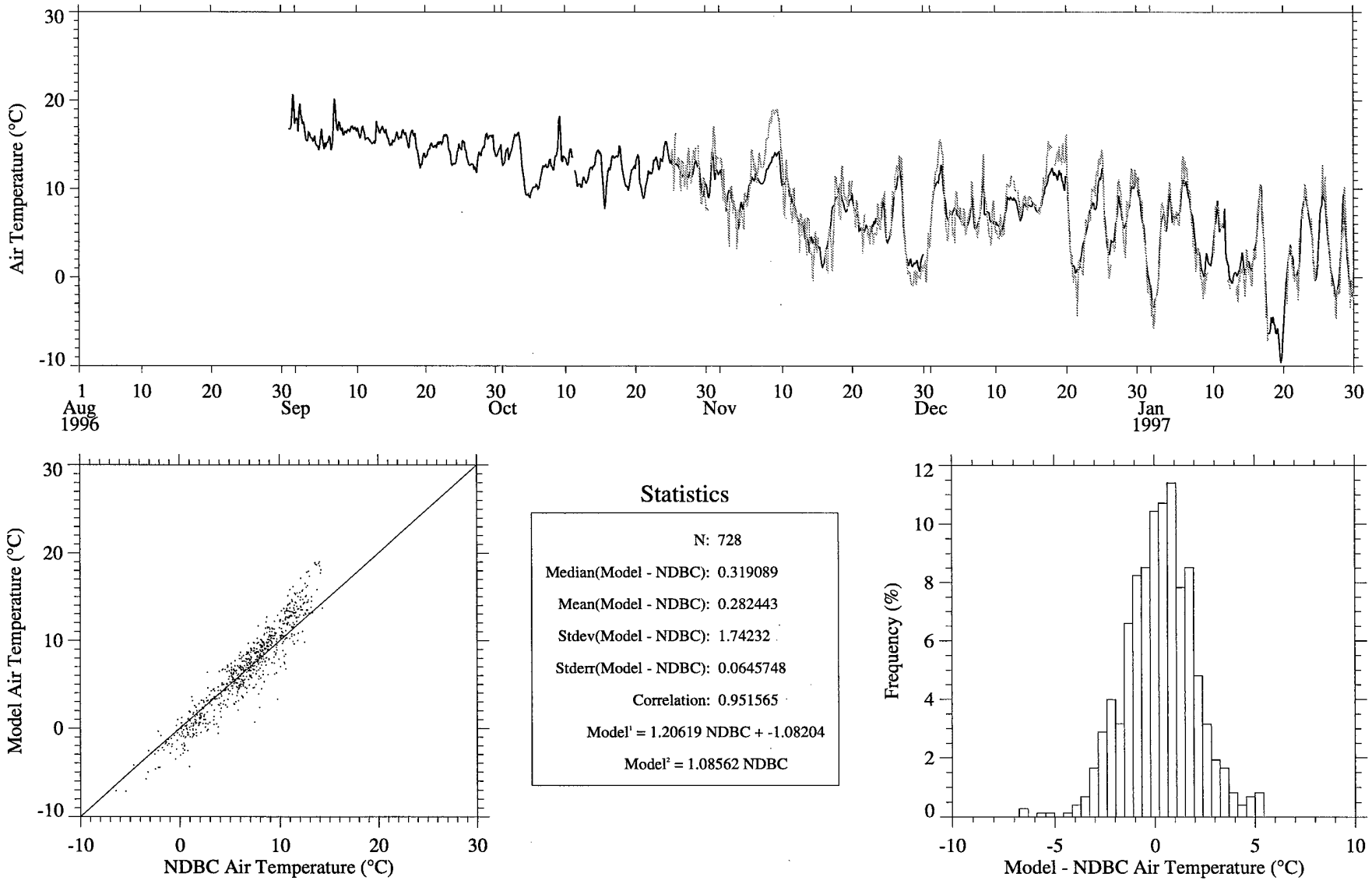

Figure A101. RUC Analysis (gray) vs. NDBC Buoy 44008 (black) air temperature.

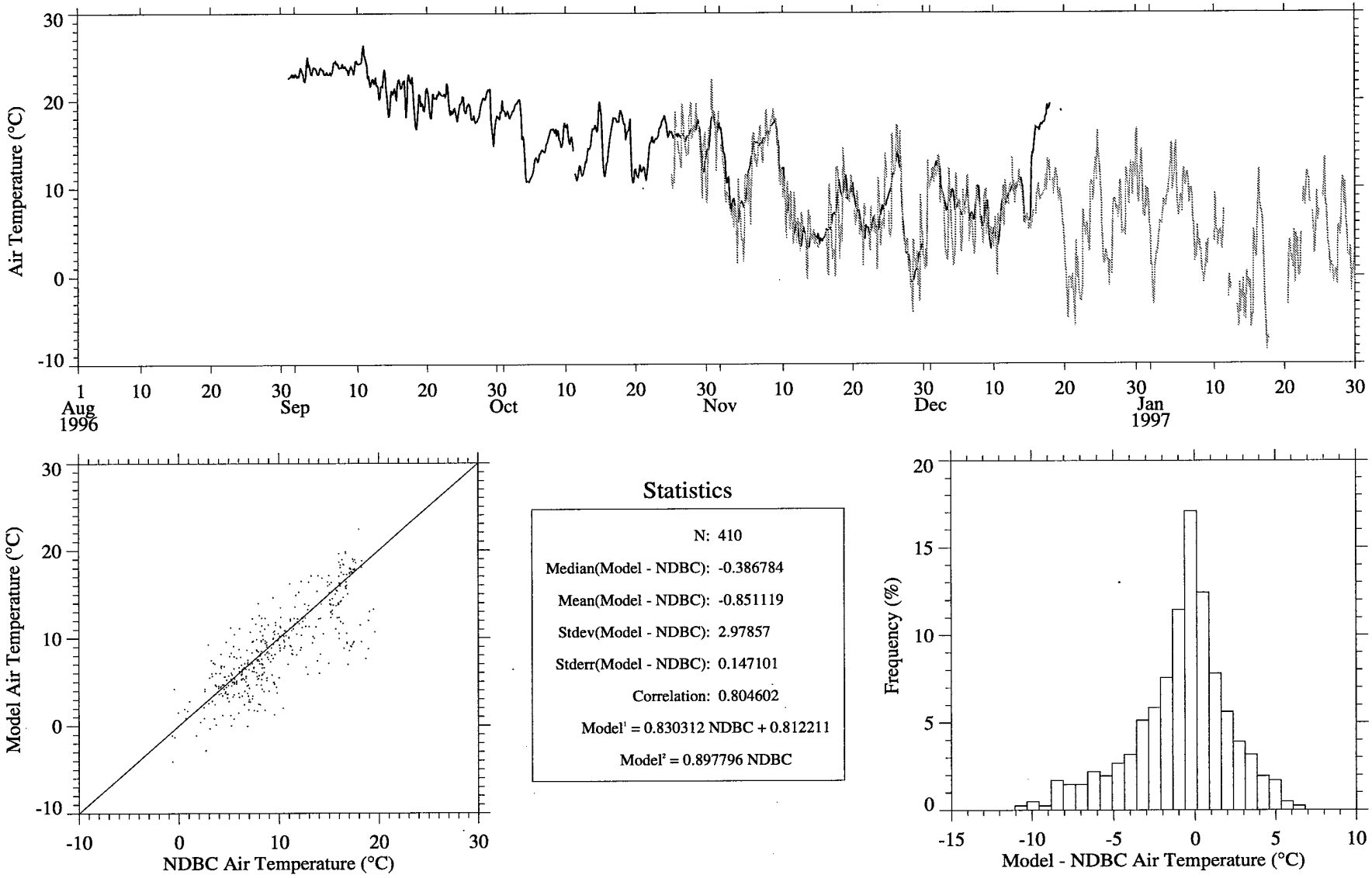

Figure A102. RUC Analysis (gray) vs. NDBC Buoy 44009 (black) air temperature.

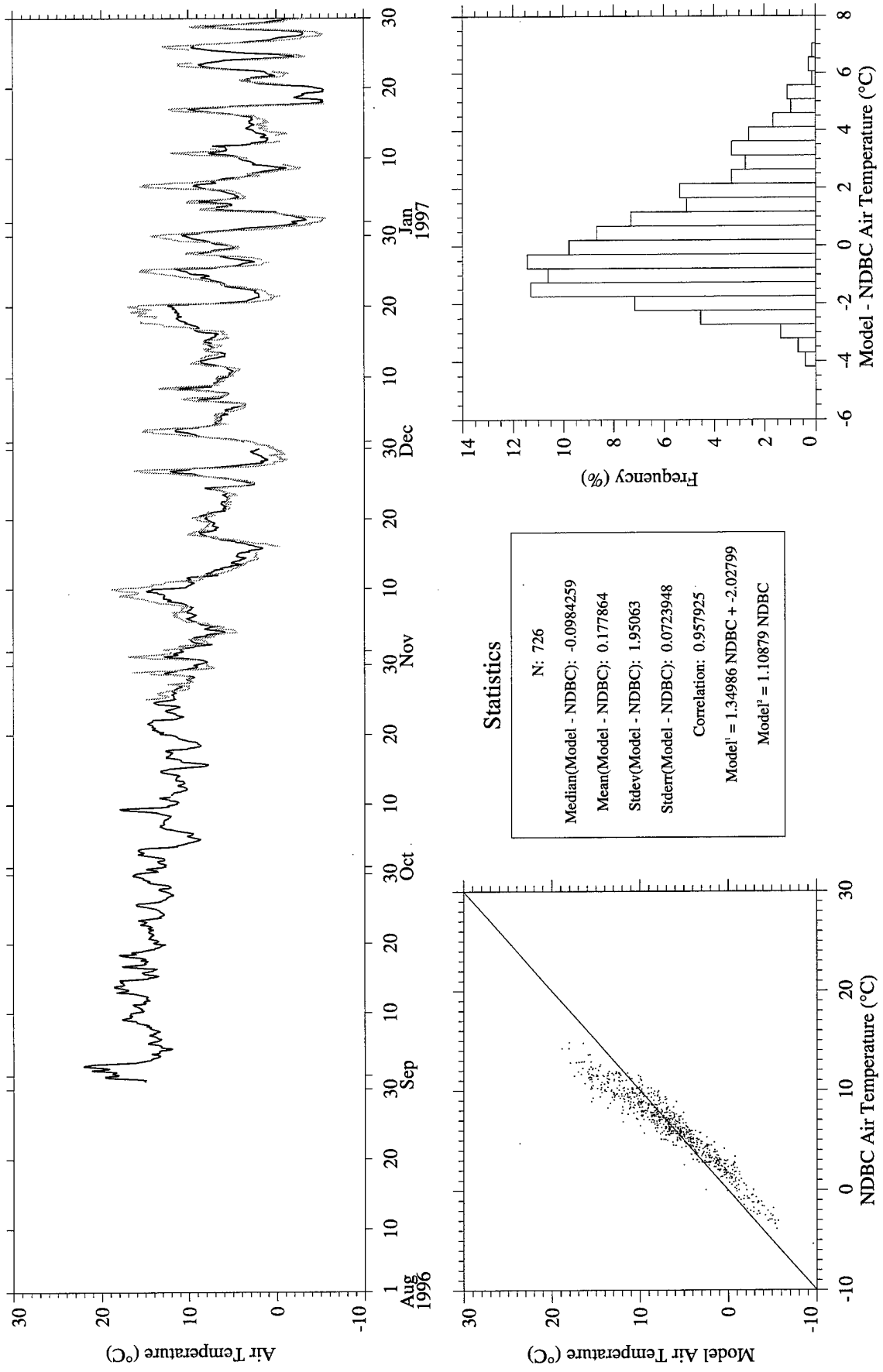

Figure A103. RUC Analysis (gray) vs. NDBC Buoy 44011 (black) air temperature.

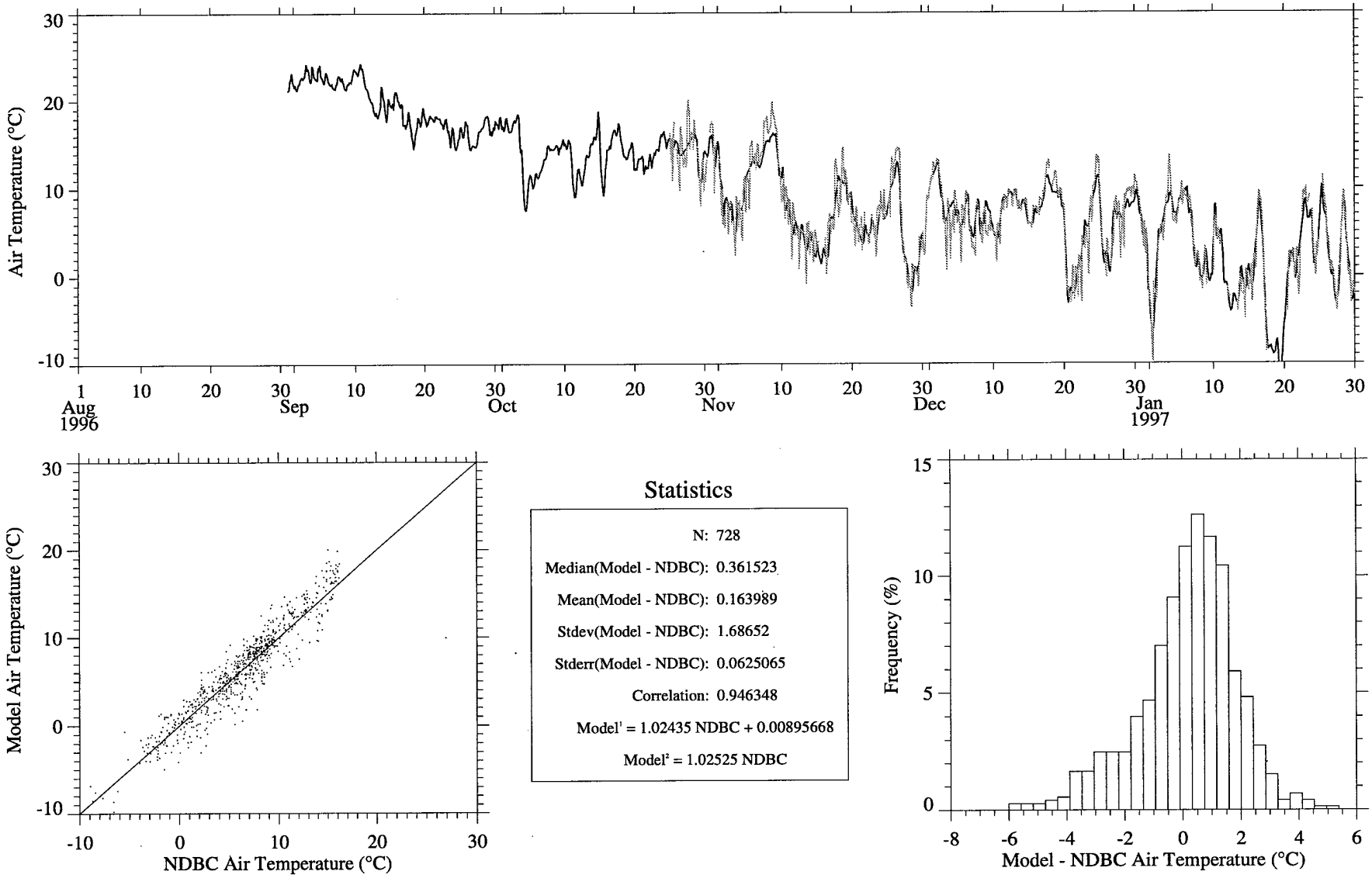

Figure A104. RUC Analysis (gray) vs. NDBC Buoy 44025 (black) air temperature.

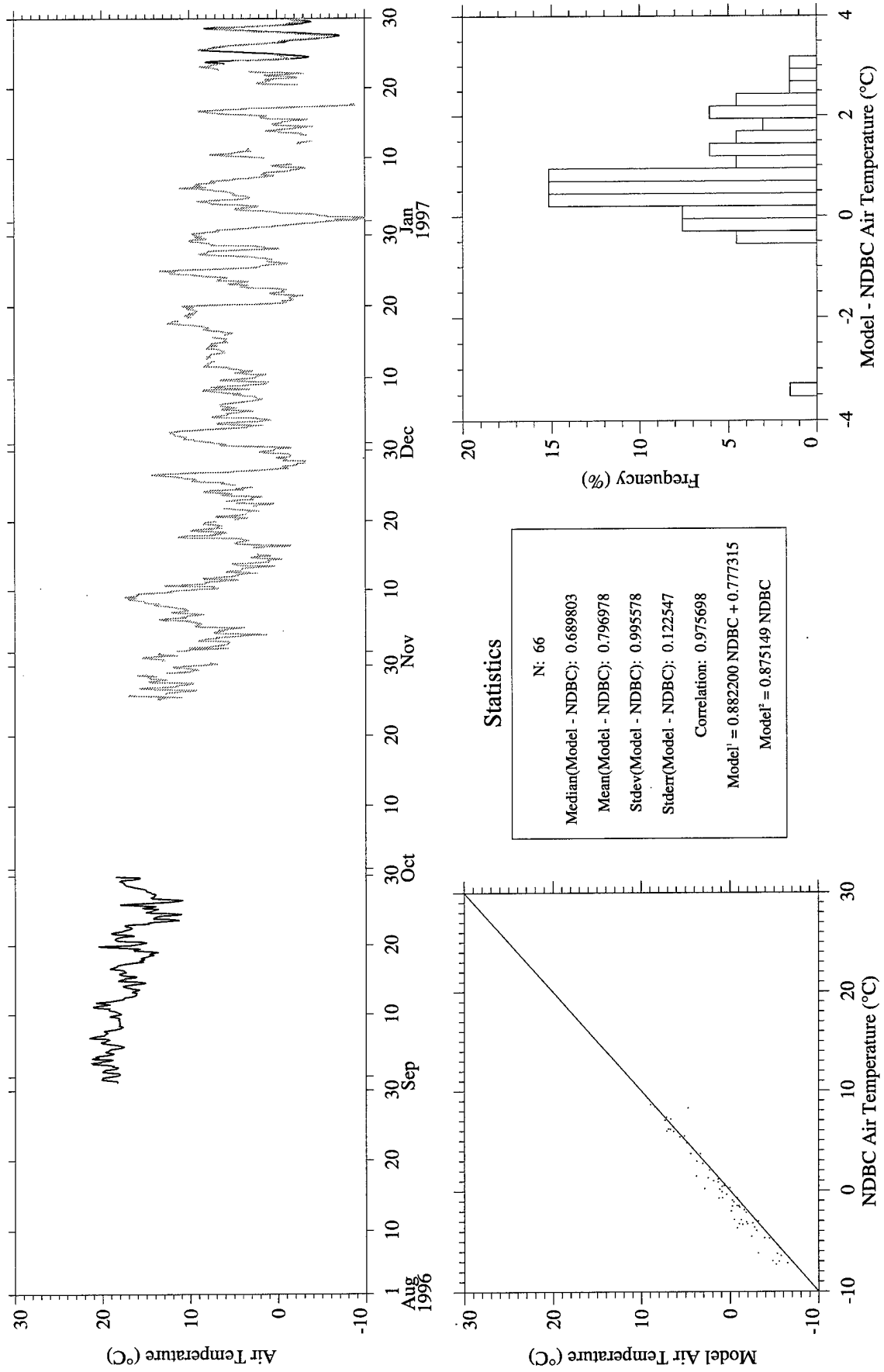

Figure A105. RUC Analysis (gray) vs. NDBC Buoy 44028 (black) air temperature.

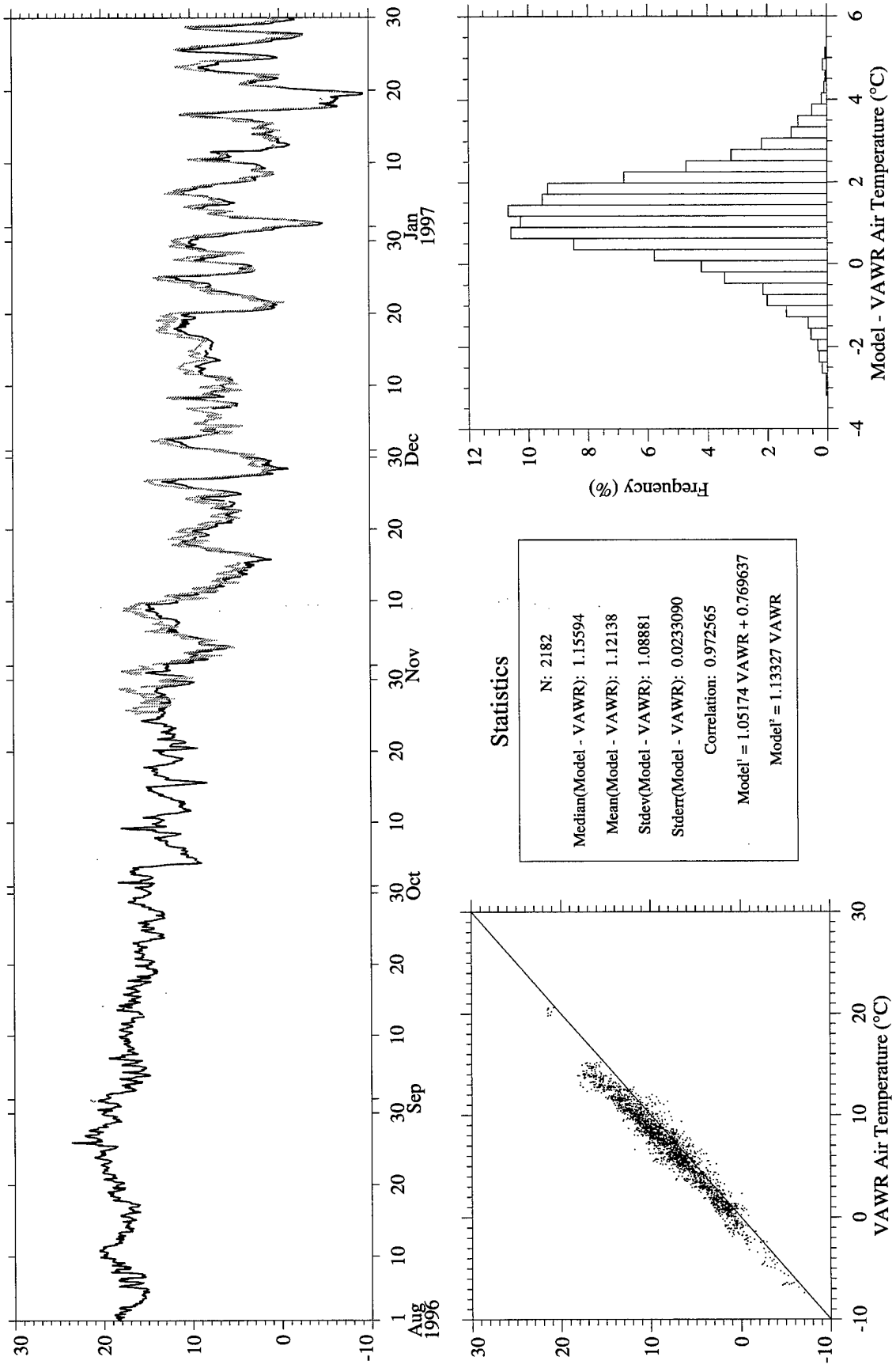

Figure A106. RUC Hourly (gray) vs. CMO VAWR 0704 (black) air temperature.

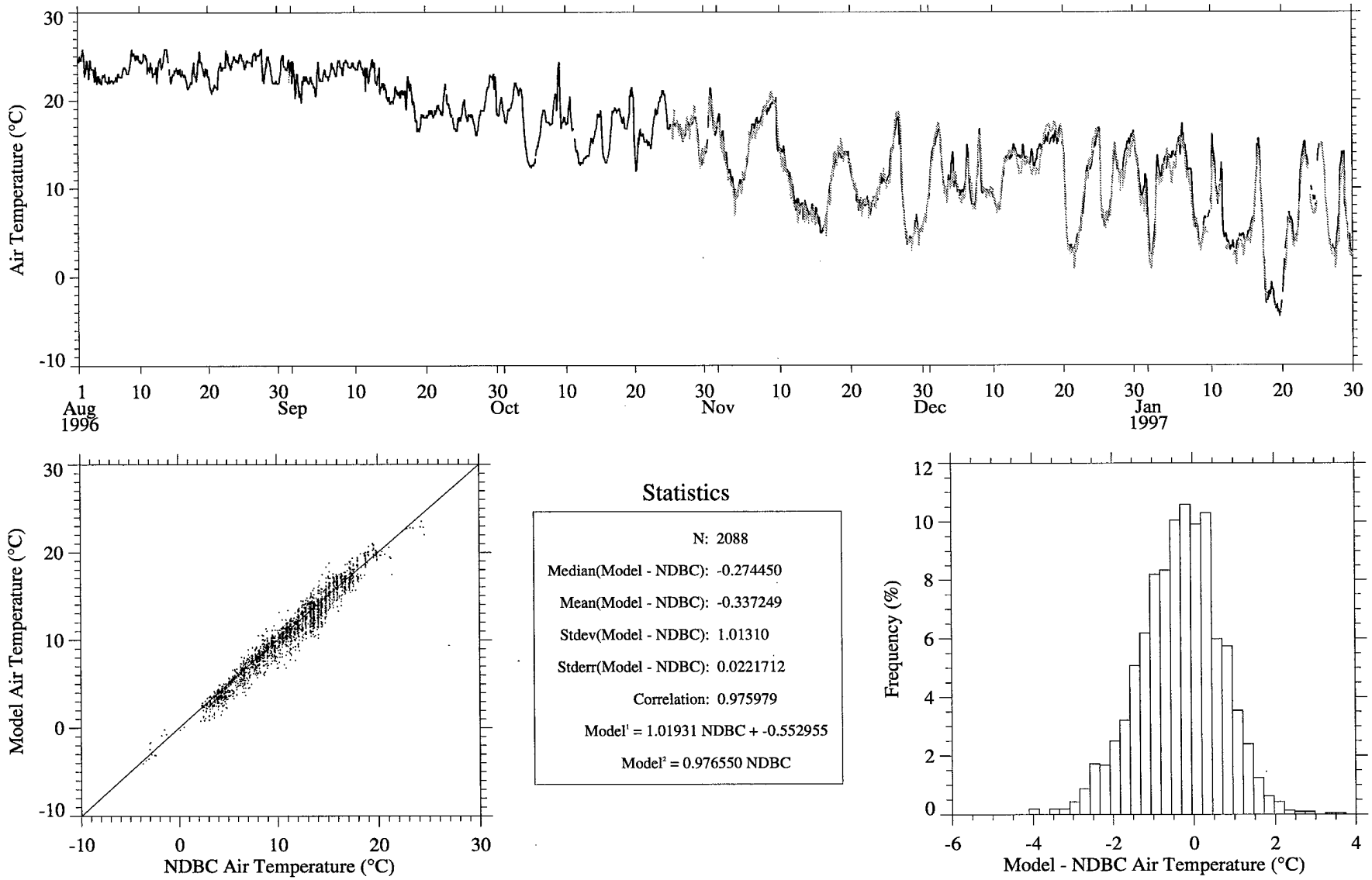

Figure A107. RUC Hourly (gray) vs. NDBC Buoy 44004 (black) air temperature.

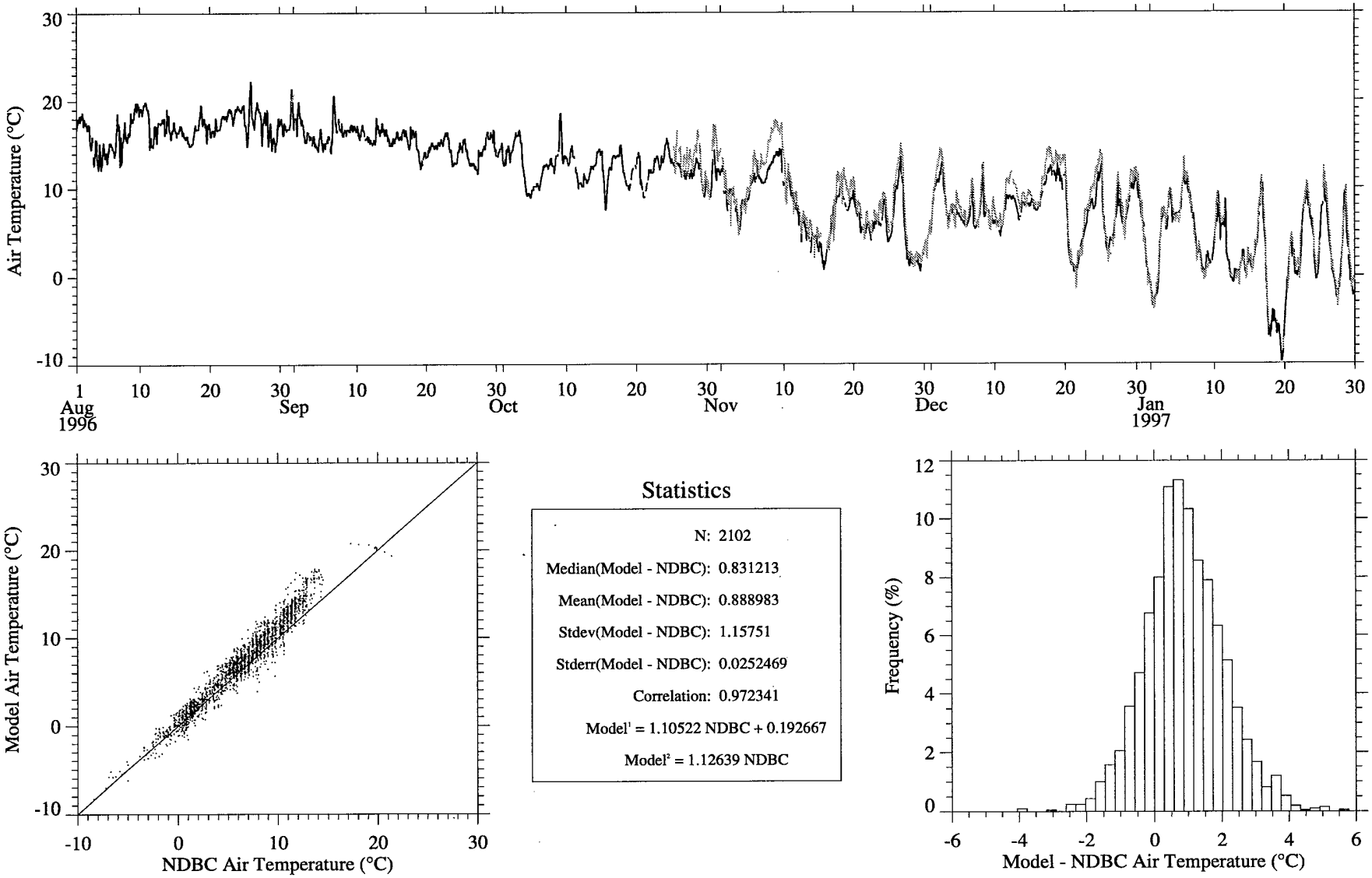

Figure A108. RUC Hourly (gray) vs. NDBC Buoy 44008 (black) air temperature.

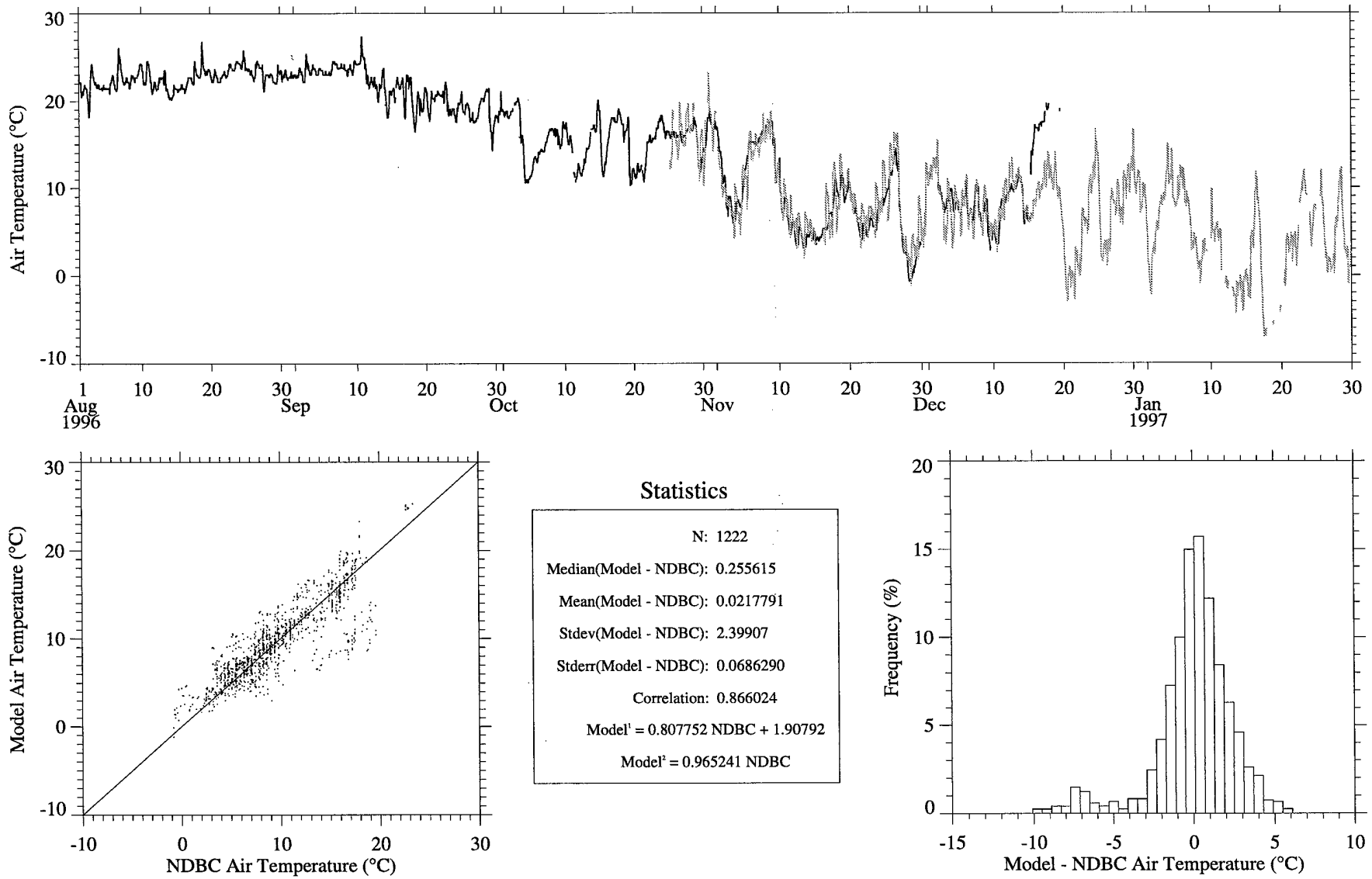

Figure A109. RUC Hourly (gray) vs. NDBC Buoy 44009 (black) air temperature.

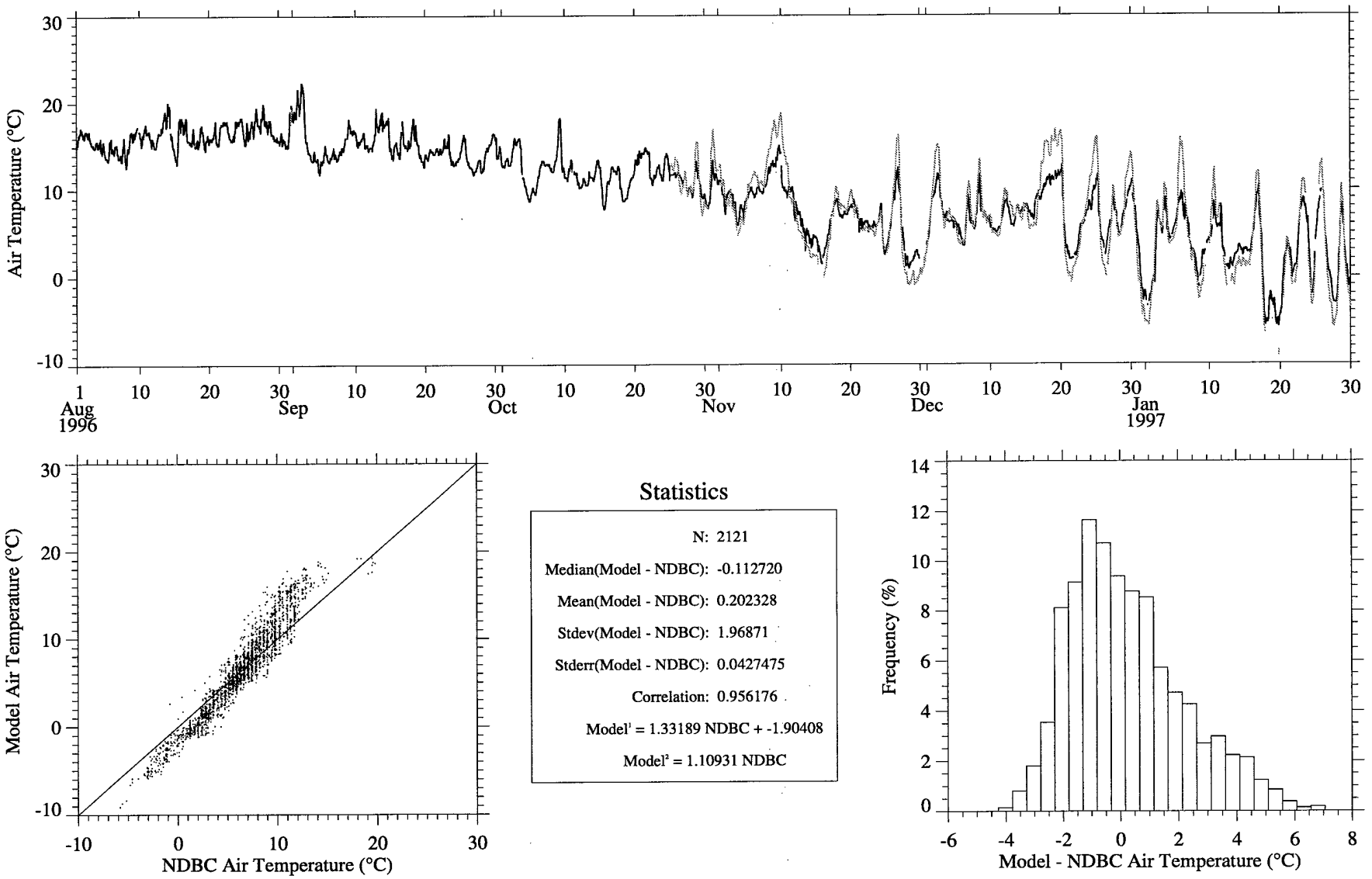

Figure A110. RUC Hourly (gray) vs. NDBC Buoy 44011 (black) air temperature.

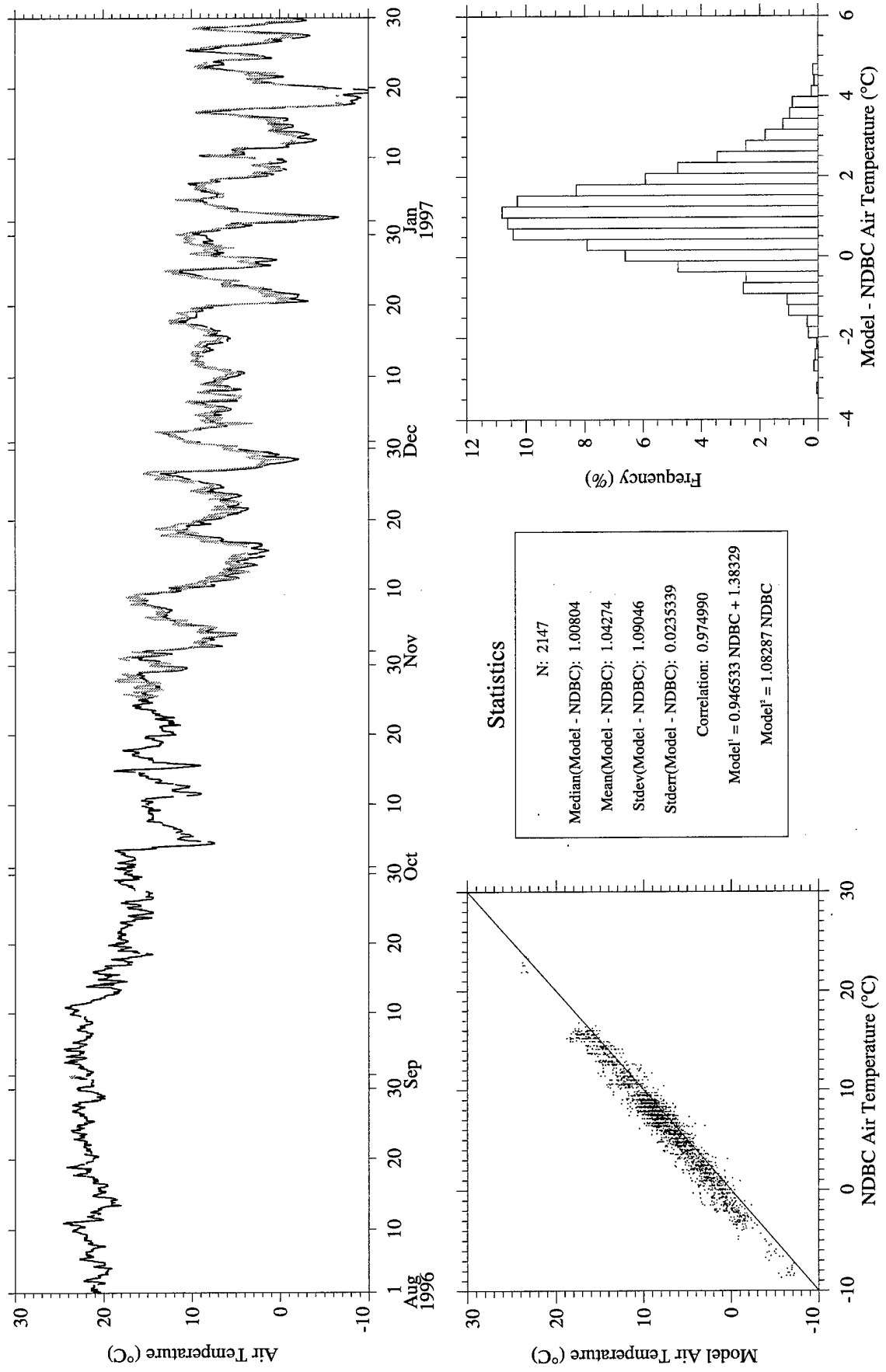

Figure A111. RUC Hourly (gray) vs. NDBC Buoy 44025 (black) air temperature.

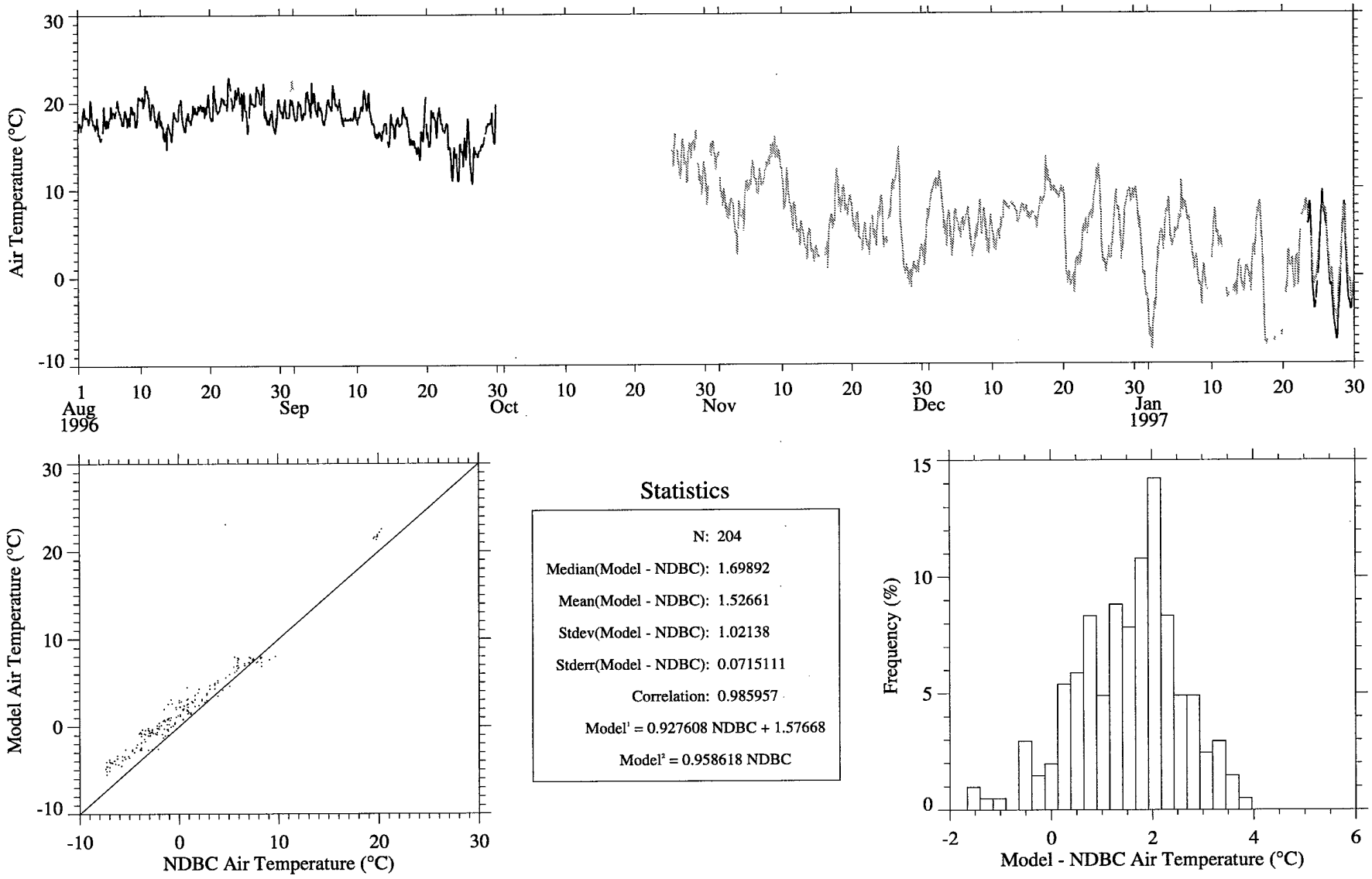

Figure A112. RUC Hourly (gray) vs. NDBC Buoy 44028 (black) air temperature.

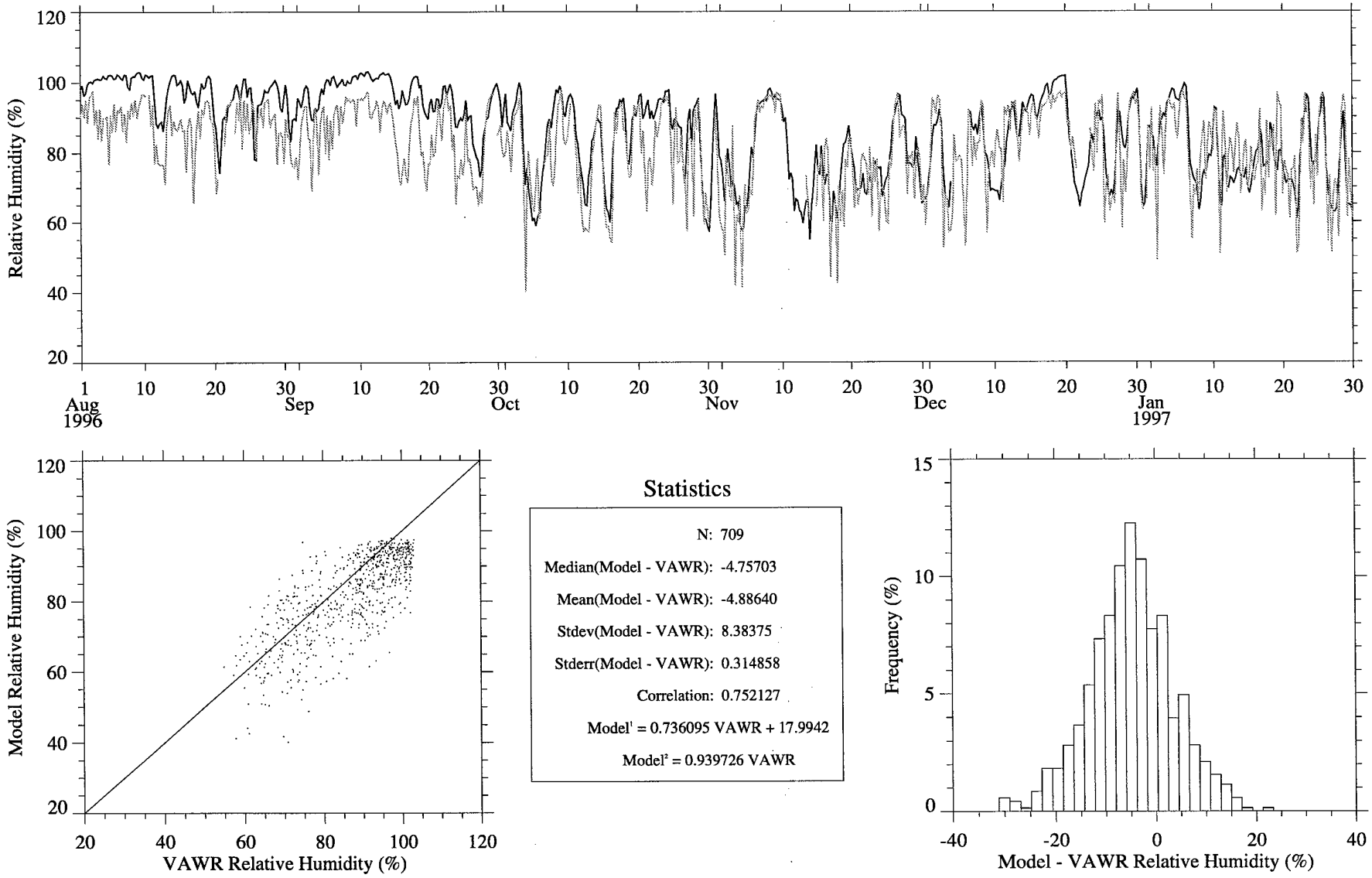

Figure A113. Eta (gray) vs. CMO VAWR 0704 (black) relative humidity.

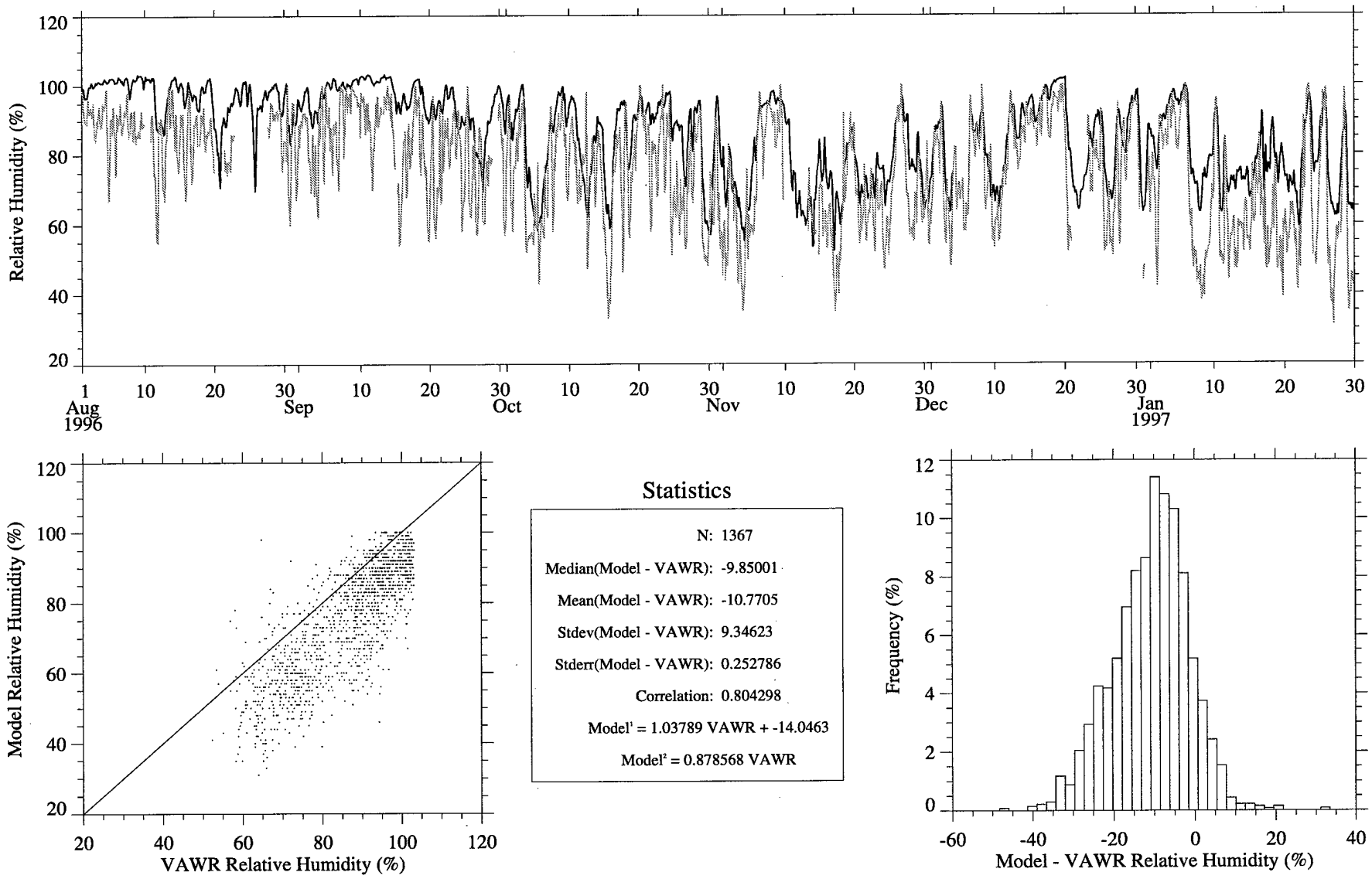

Figure A114. RUC (gray) vs. CMO VAWR 0704 (black) relative humidity.

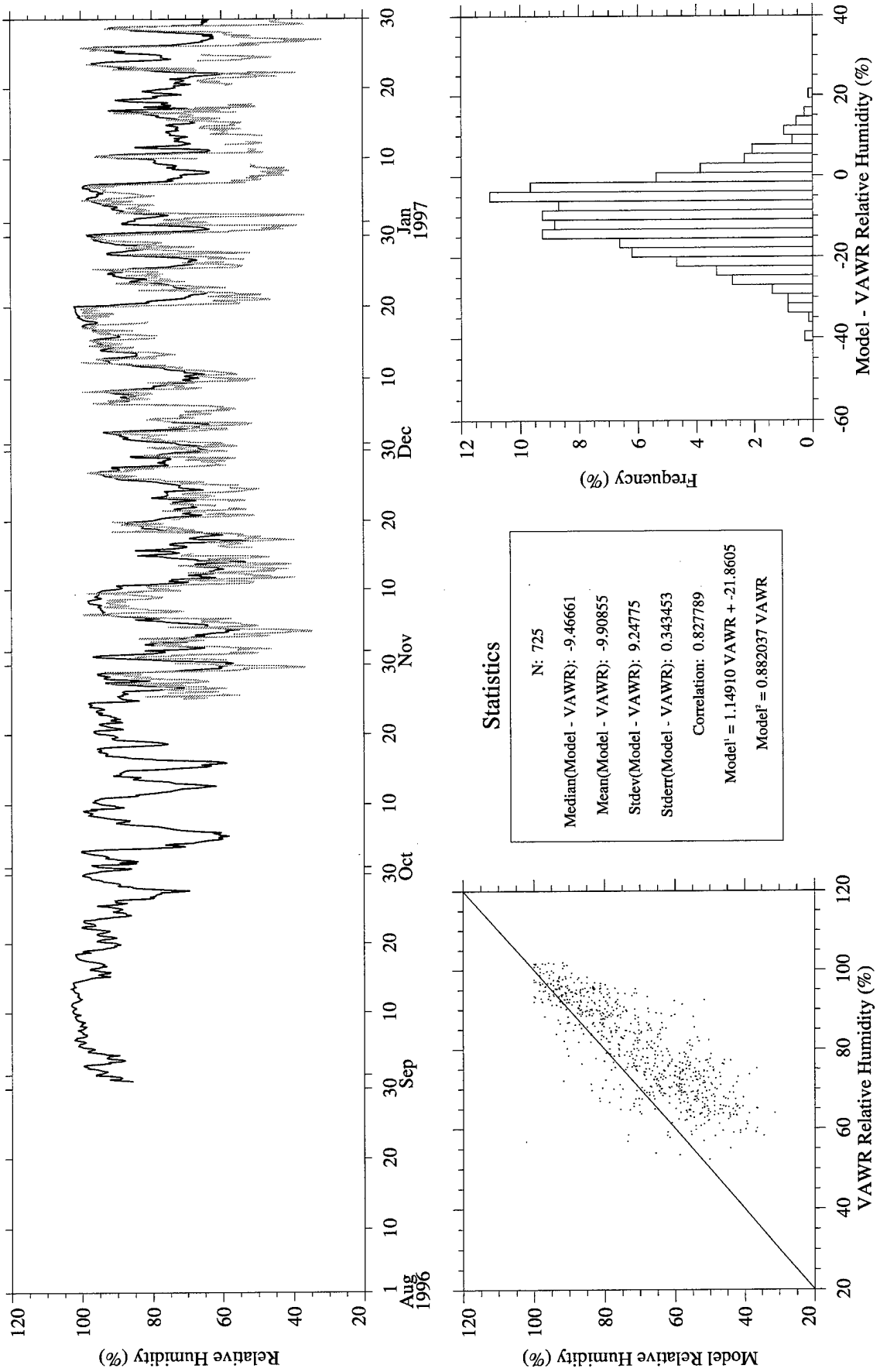

Figure A115. RUC Analysis (gray) vs. CMO VAWR 0704 (black) relative humidity.

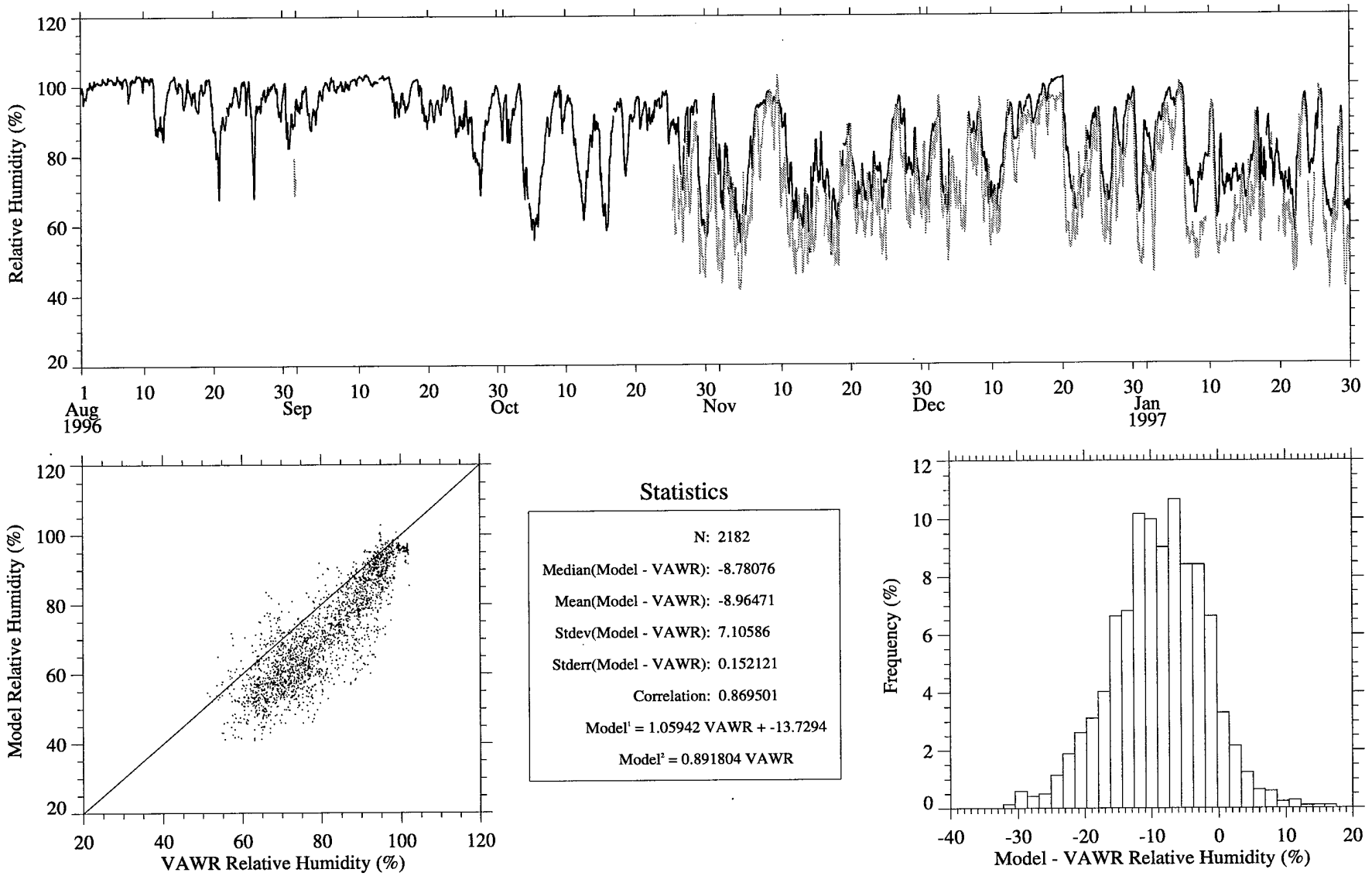

Figure A116. RUC Hourly (gray) vs. CMO VAWR 0704 (black) relative humidity.

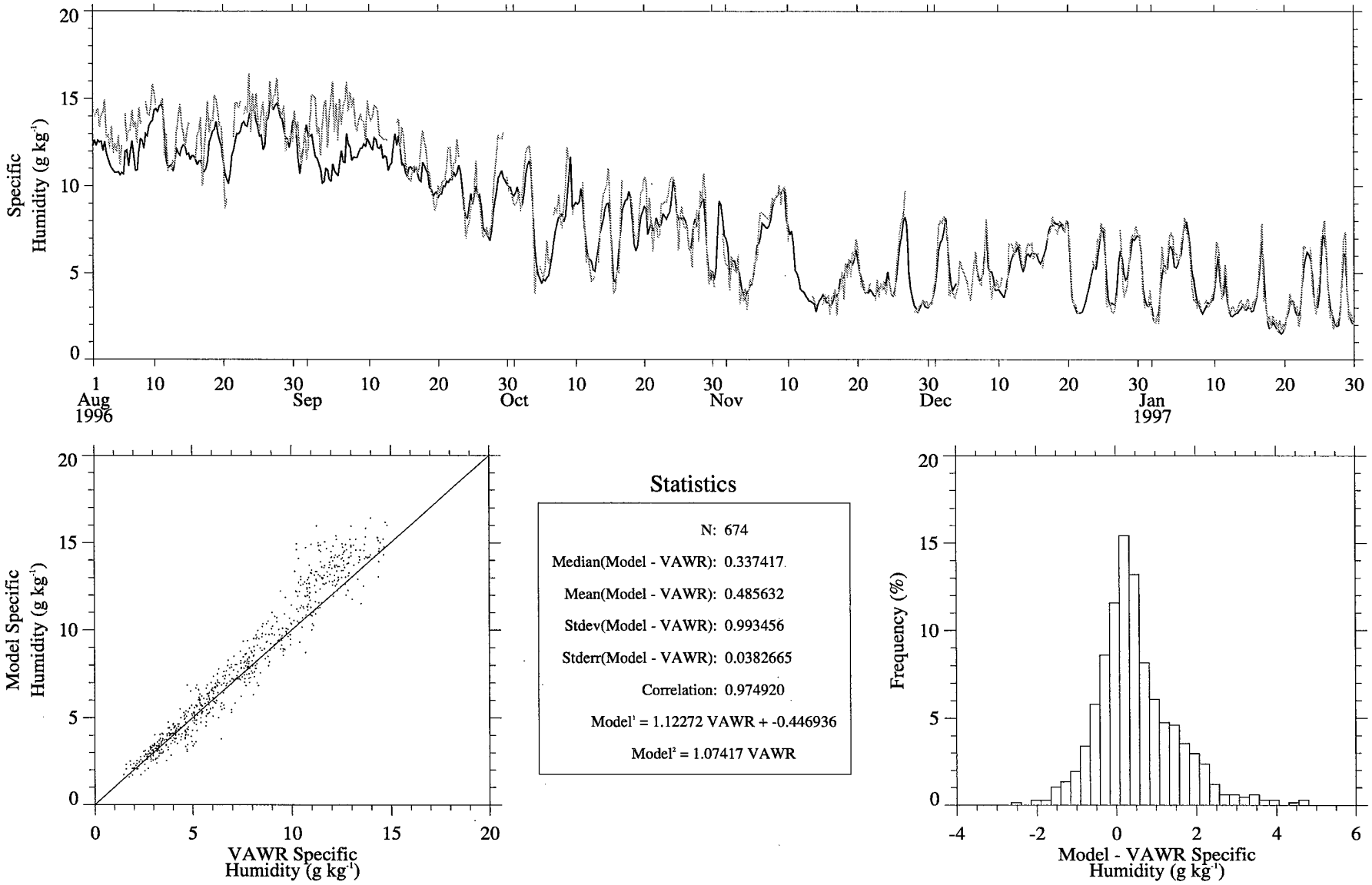

Figure A117. Eta (gray) vs. CMO VAWR 0704 (black) specific humidity.

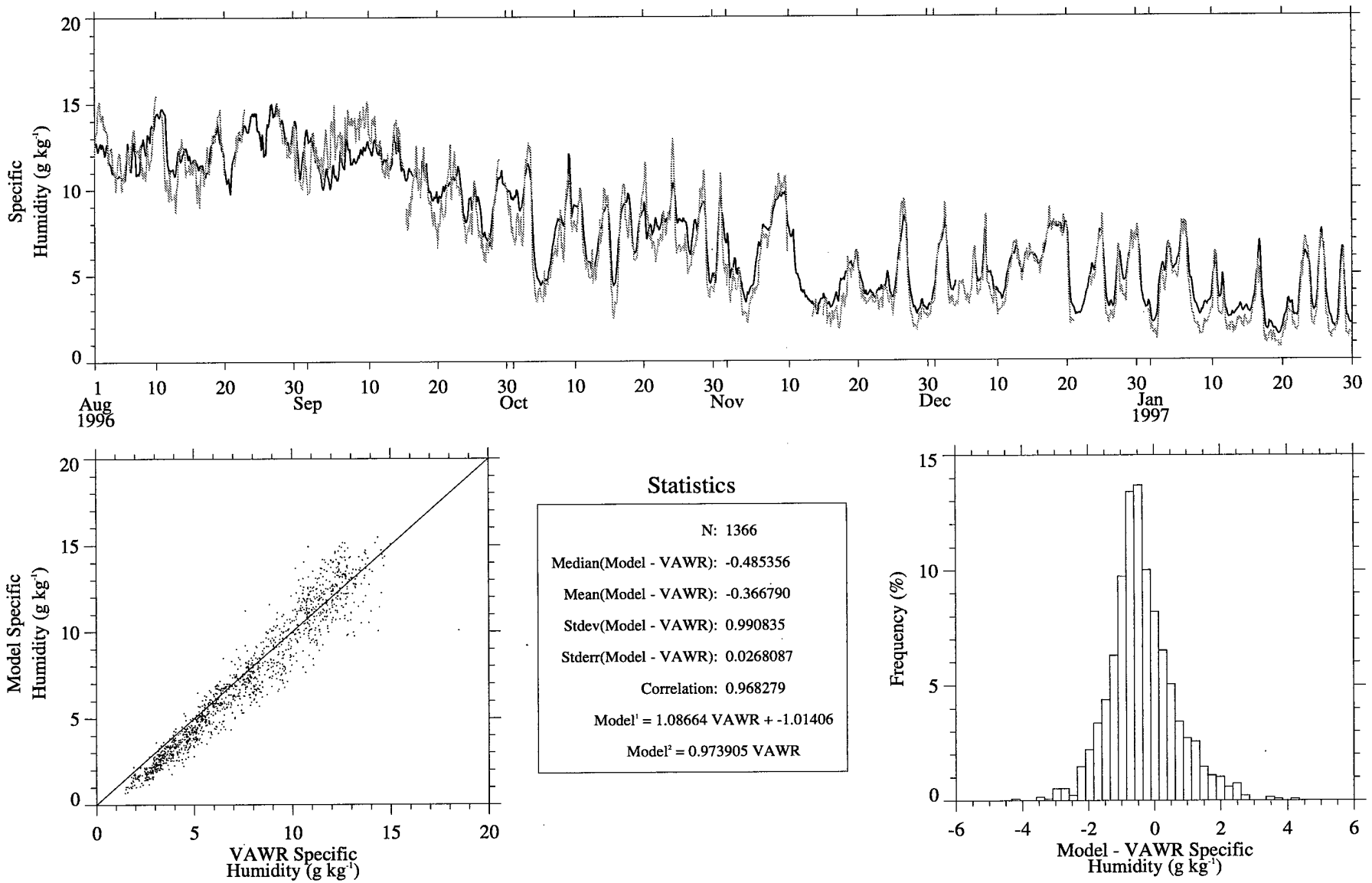

Figure A118. RUC (gray) vs. CMO VAWR 0704 (black) specific humidity.

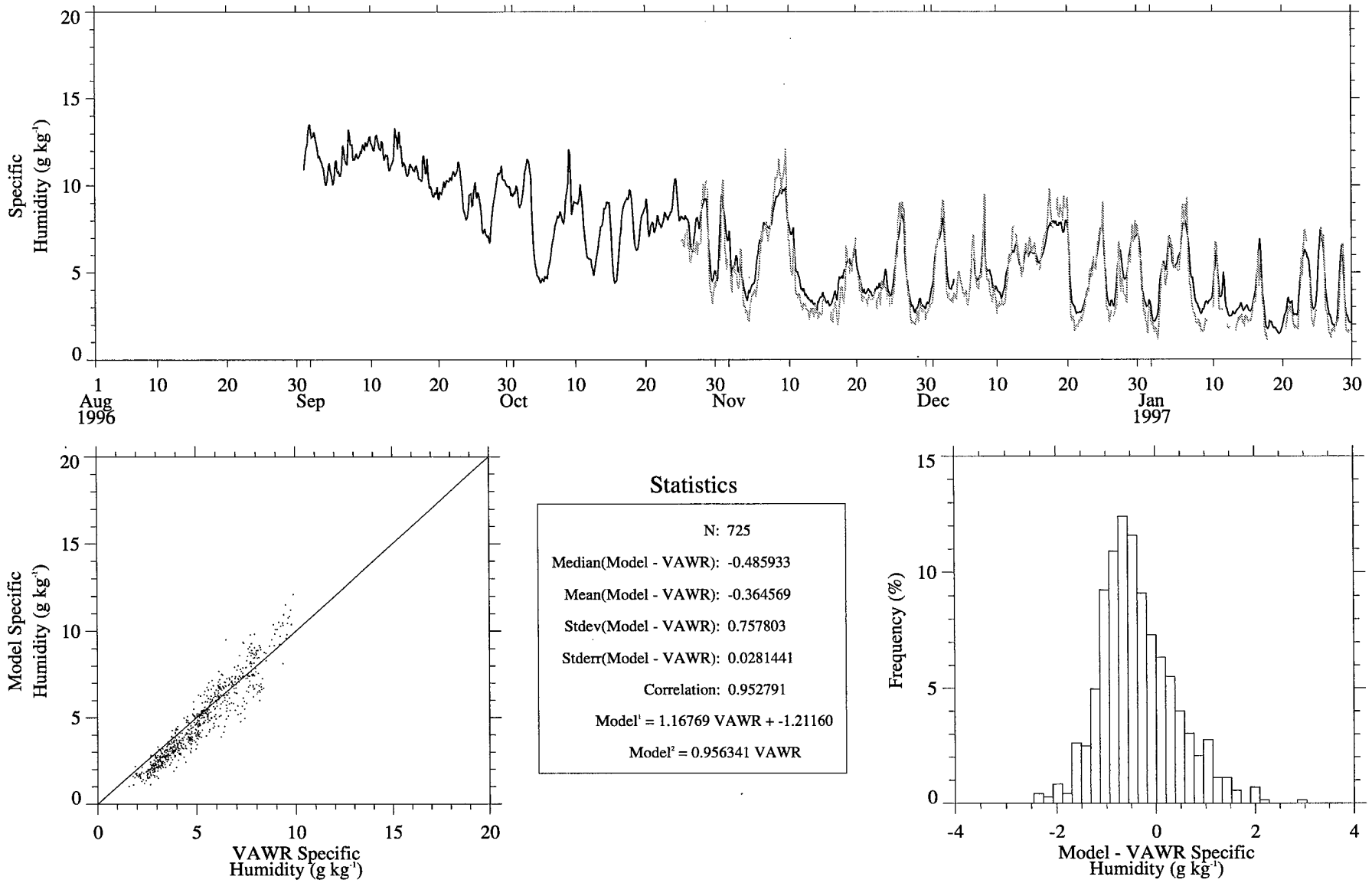

Figure A119. RUC Analysis (gray) vs. CMO VAWR 0704 (black) specific humidity.

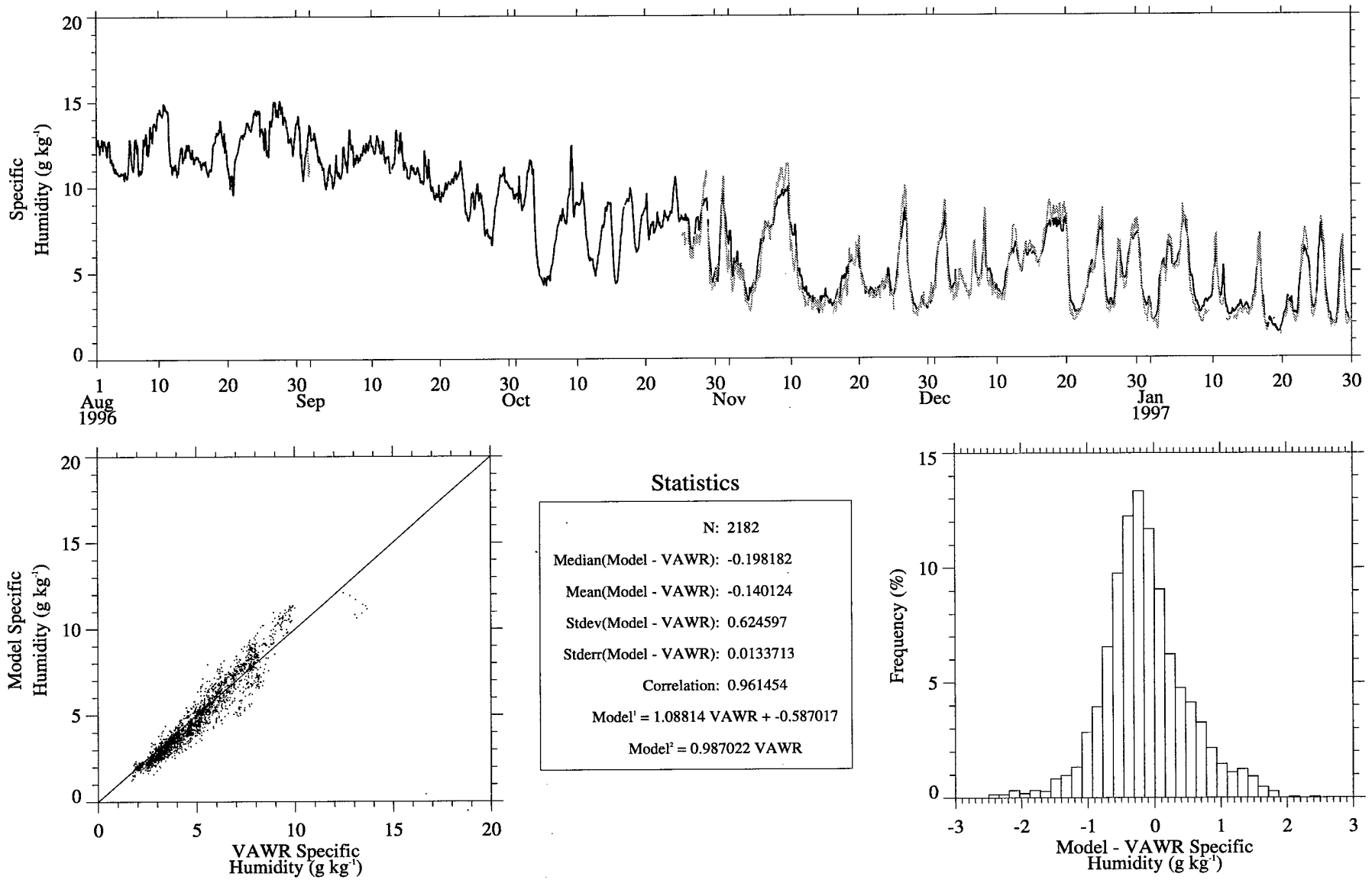

Figure A120. RUC Hourly (gray) vs. CMO VAWR 0704 (black) specific humidity.

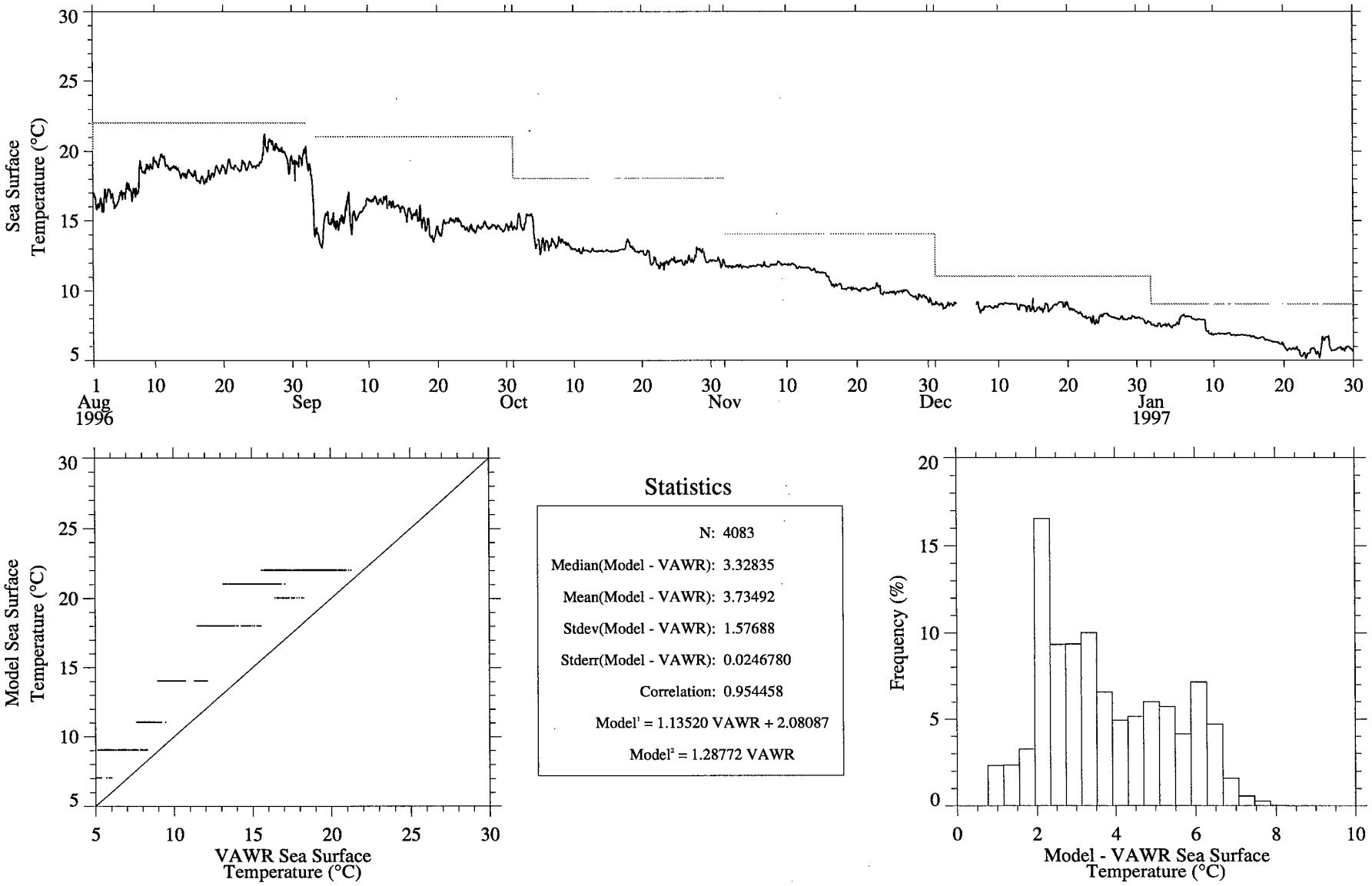

Figure A121. RUC Hourly (gray) vs. CMO VAWR 0704 (black) sea surface temperature.

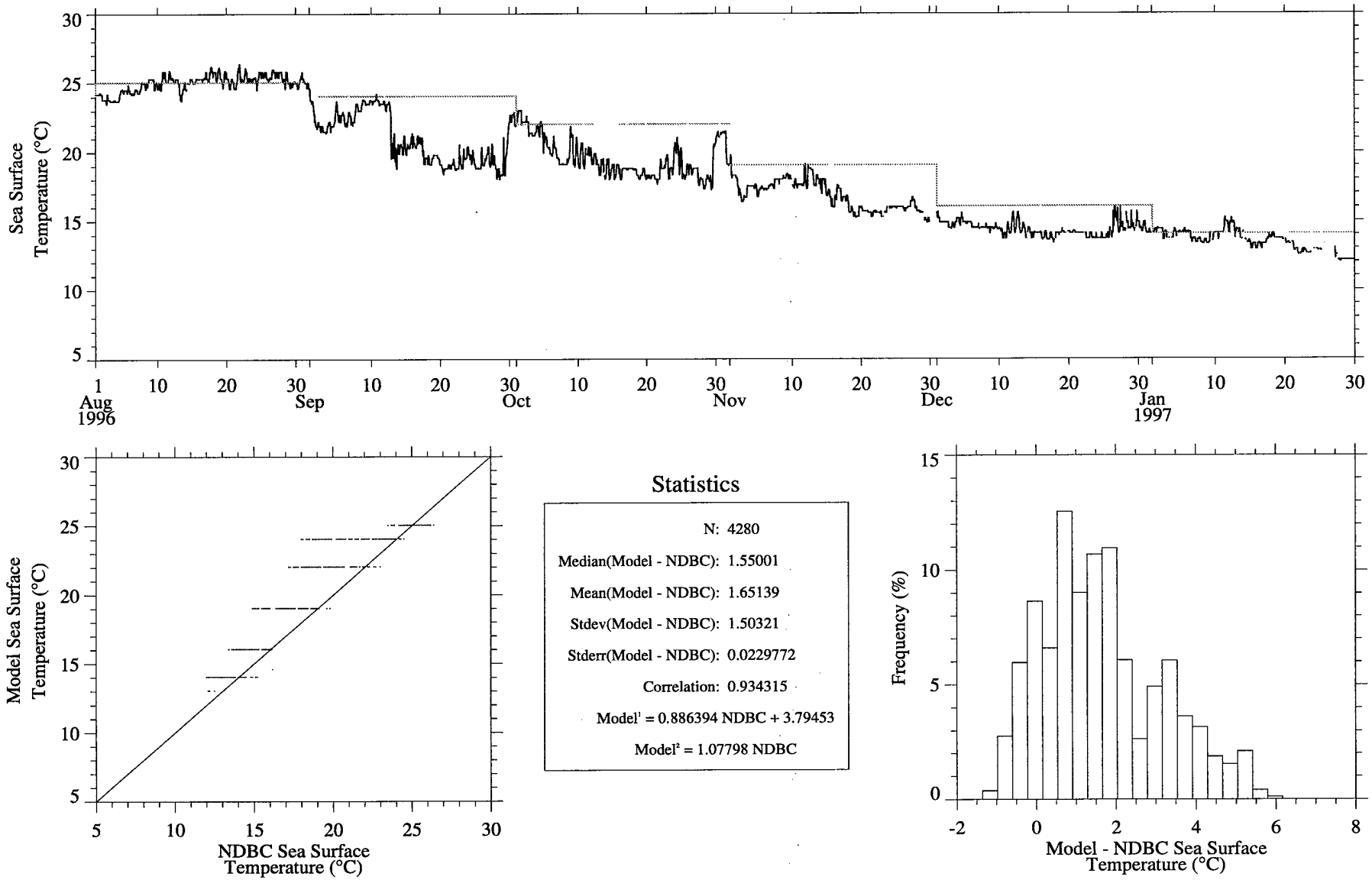

Figure A122. RUC Hourly (gray) vs. NDBC Buoy 44004 (black) sea surface temperature.

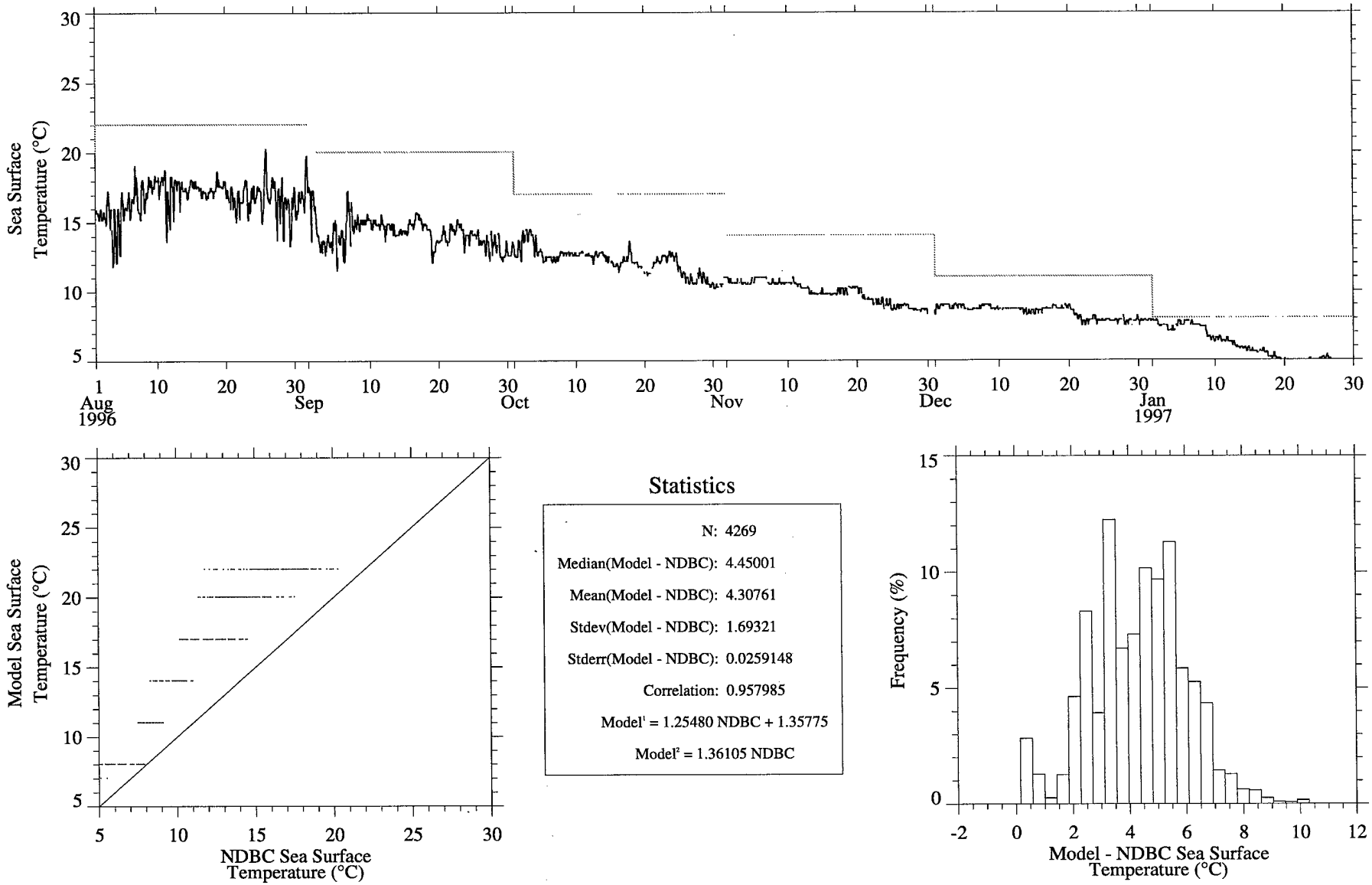

Figure A123. RUC Hourly (gray) vs. NDBC Buoy 44008 (black) sea surface temperature.

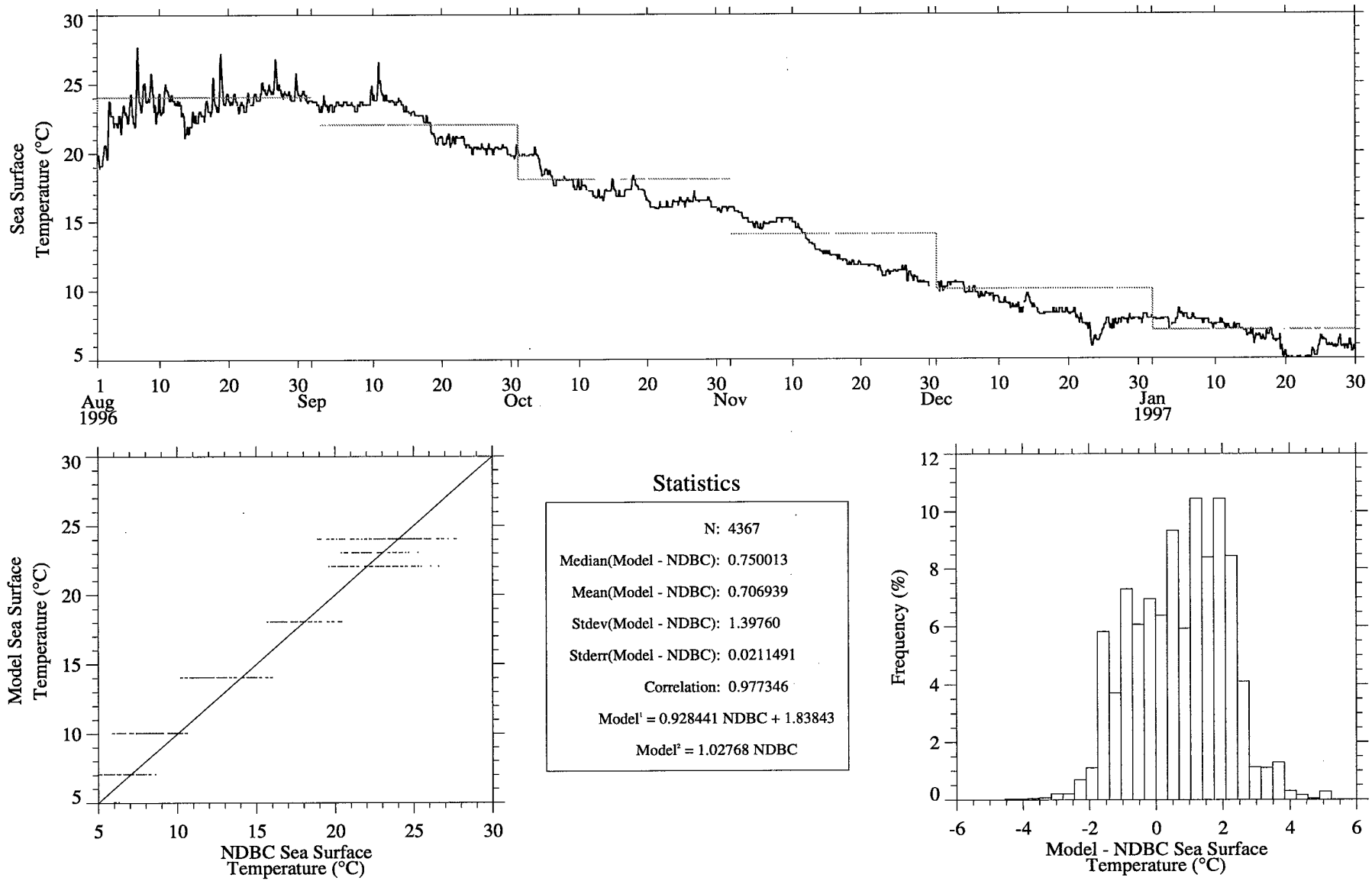

Figure A124. RUC Hourly (gray) vs. NDBC Buoy 44009 (black) sea surface temperature.

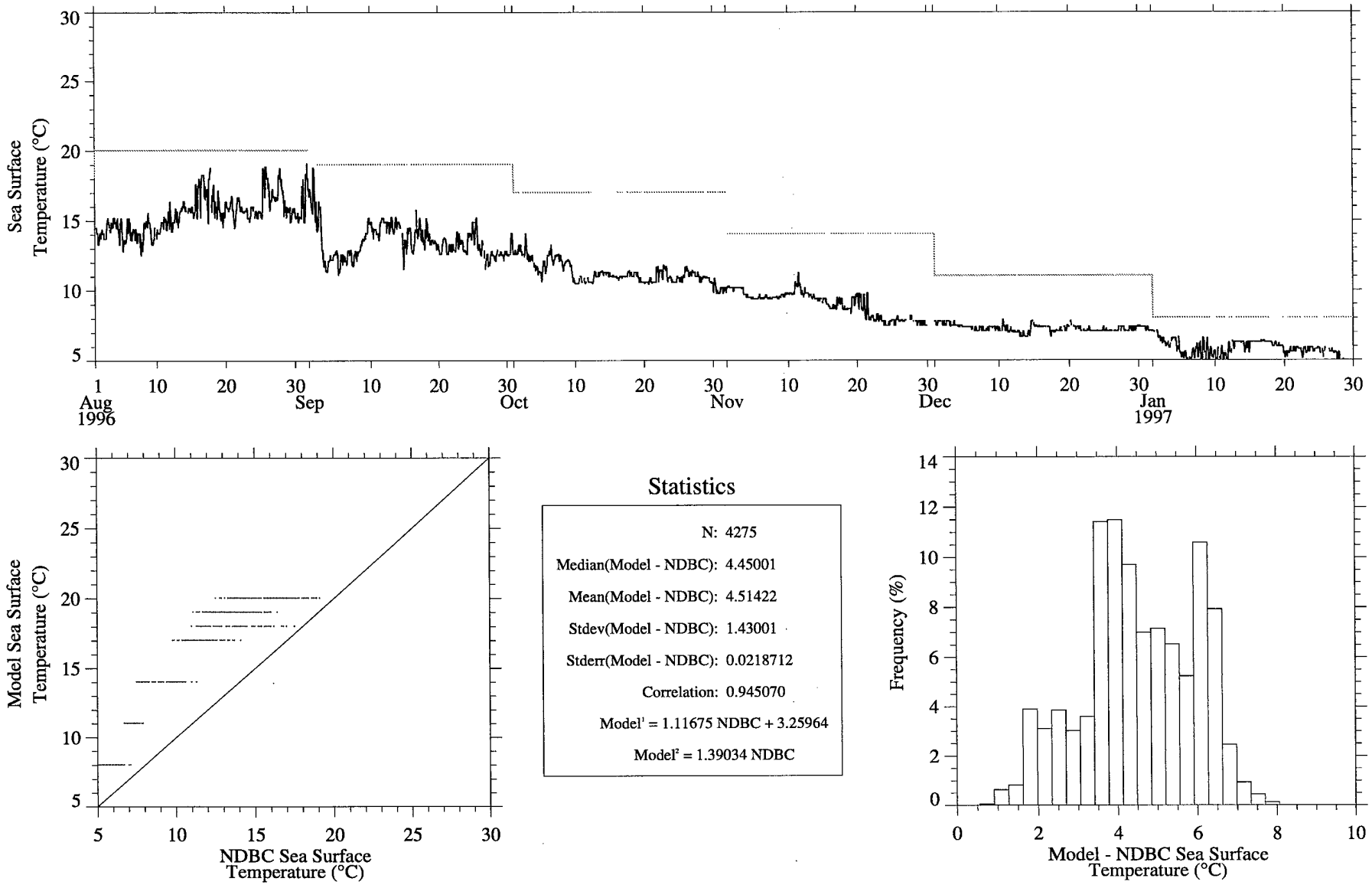

Figure A125. RUC Hourly (gray) vs. NDBC Buoy 44011 (black) sea surface temperature.

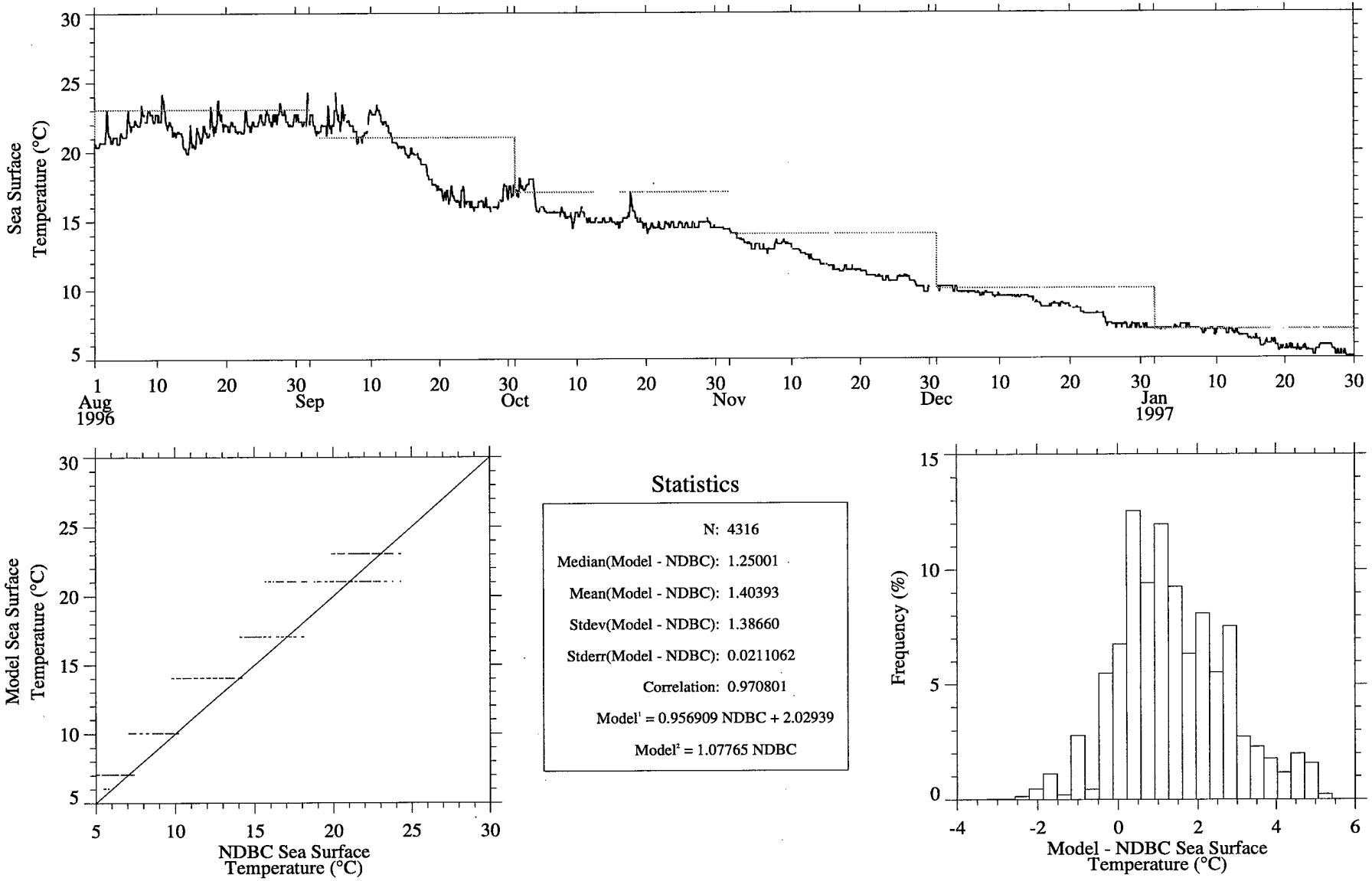

Figure A126. RUC Hourly (gray) vs. NDBC Buoy 44025 (black) sea surface temperature.

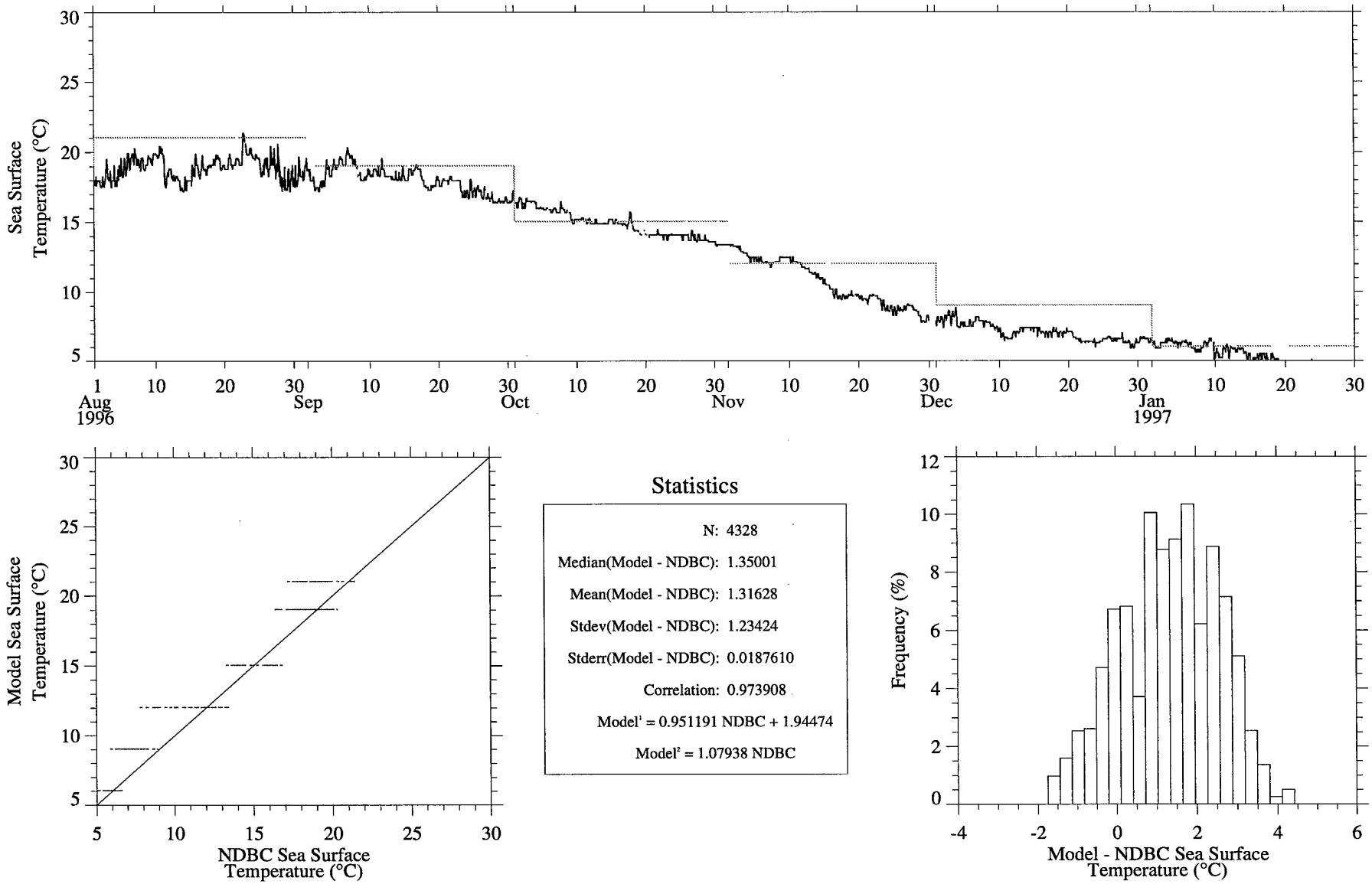

Figure A127. RUC Hourly (gray) vs. NDBC Buoy 44028 (black) sea surface temperature.

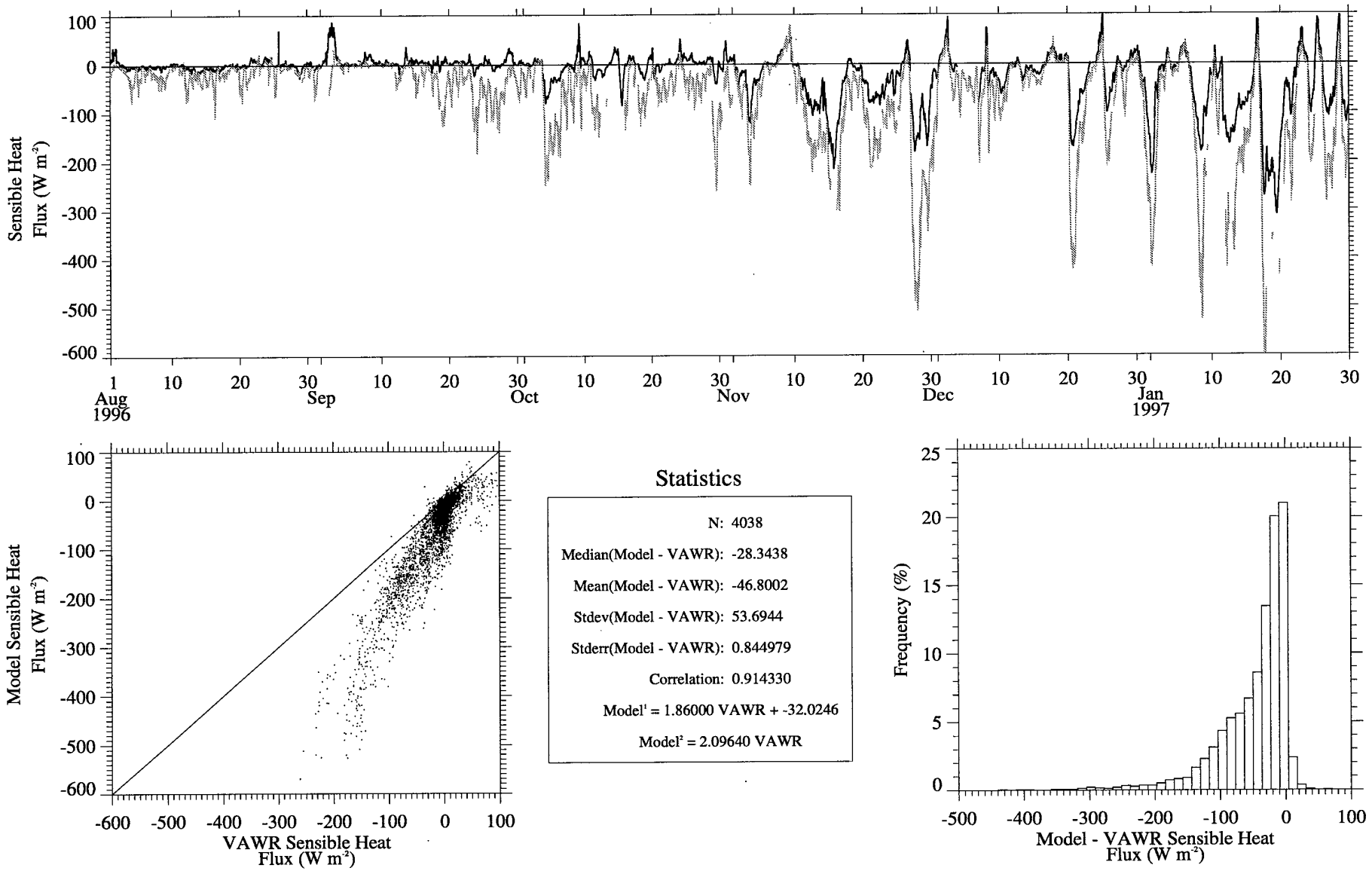

Figure A128. RUC Hourly (gray) vs. CMO VAWR 0704 (black) sensible heat flux.

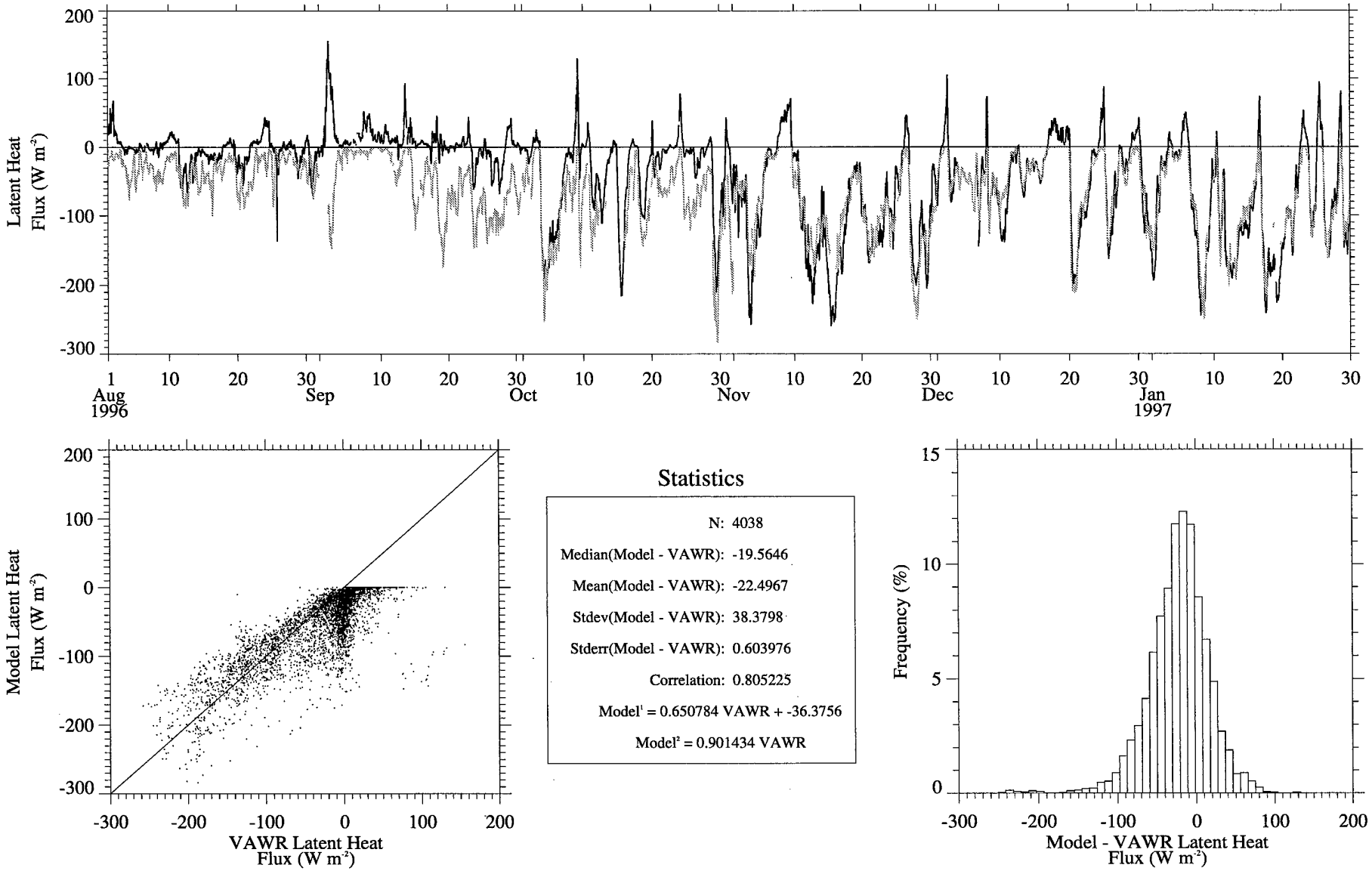

Figure A129. RUC Hourly (gray) vs. CMO VAWR 0704 (black) latent heat flux.

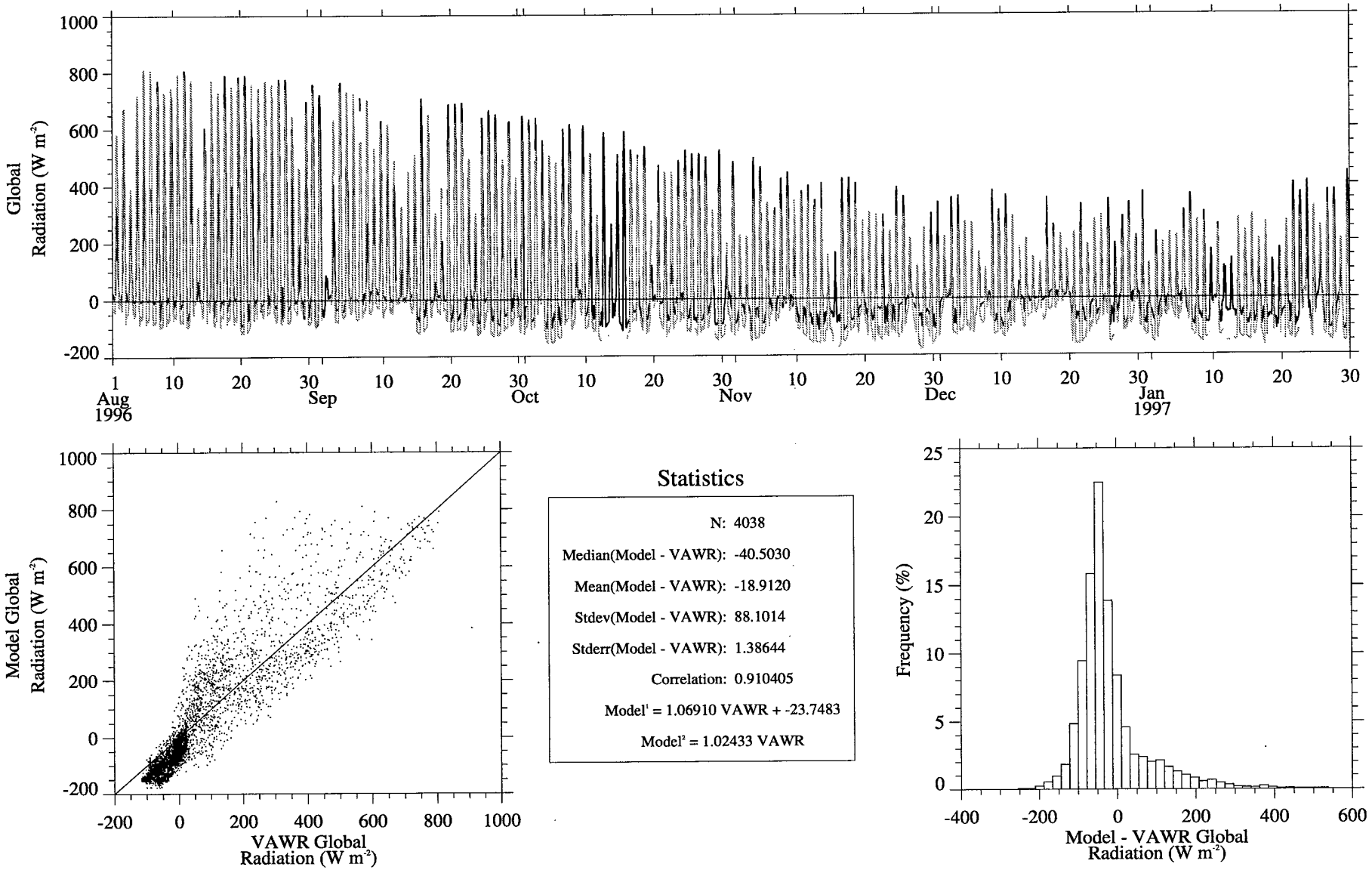

Figure A130. RUC Hourly (gray) vs. CMO VAWR 0704 (black) global radiation.

Appendix B: Comparison of CMO buoy and NDBC buoy 44008

Since NDBC buoy 44008 is only 90km to the east of the CMO central buoy, intercomparisons of wind speed, wind direction, barometric pressure, air temperature and sea surface temperature from these sites are presented here. Positive differences indicate that the observations from the NDBC buoy 44008 are greater or larger than those of the CMO buoy. The figures include a time series of the NDBC buoy 44008 and CMO central buoy variables, a scatterplot, a histogram of the differences and a statistics box. The statistics box displays the sample size, statistics of the [NDBC - CMO] difference (median, mean, standard deviation and standard error), the correlation coefficient and two linear regressions. The first linear regression is denoted by a superscript 1 and is a simple linear regression. The second is forced through the origin and is denoted by a superscript 2.

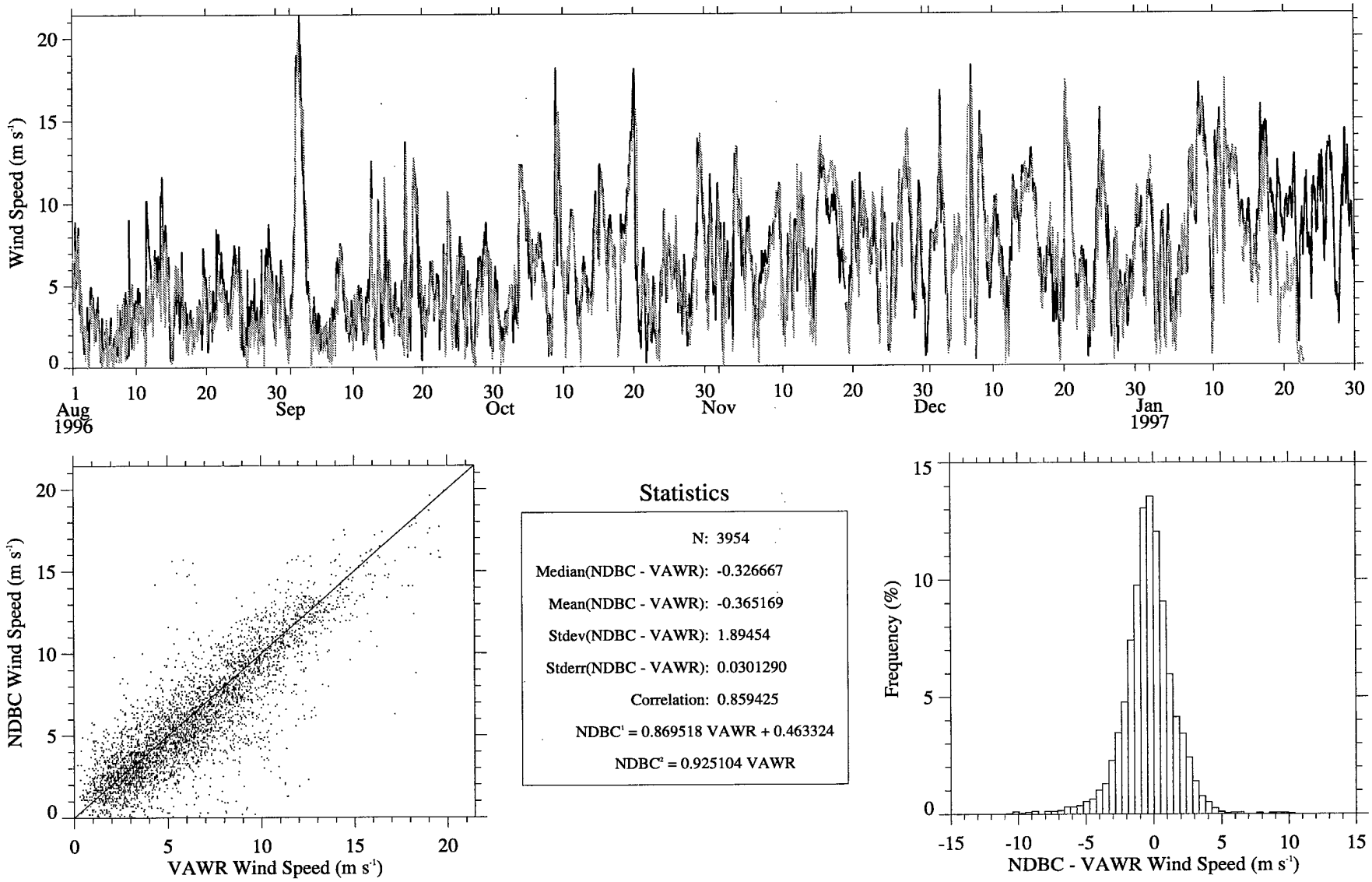

Figure B1. NDBC Buoy 44008 (gray) vs. CMO VAWR 0704 (black) wind speed.

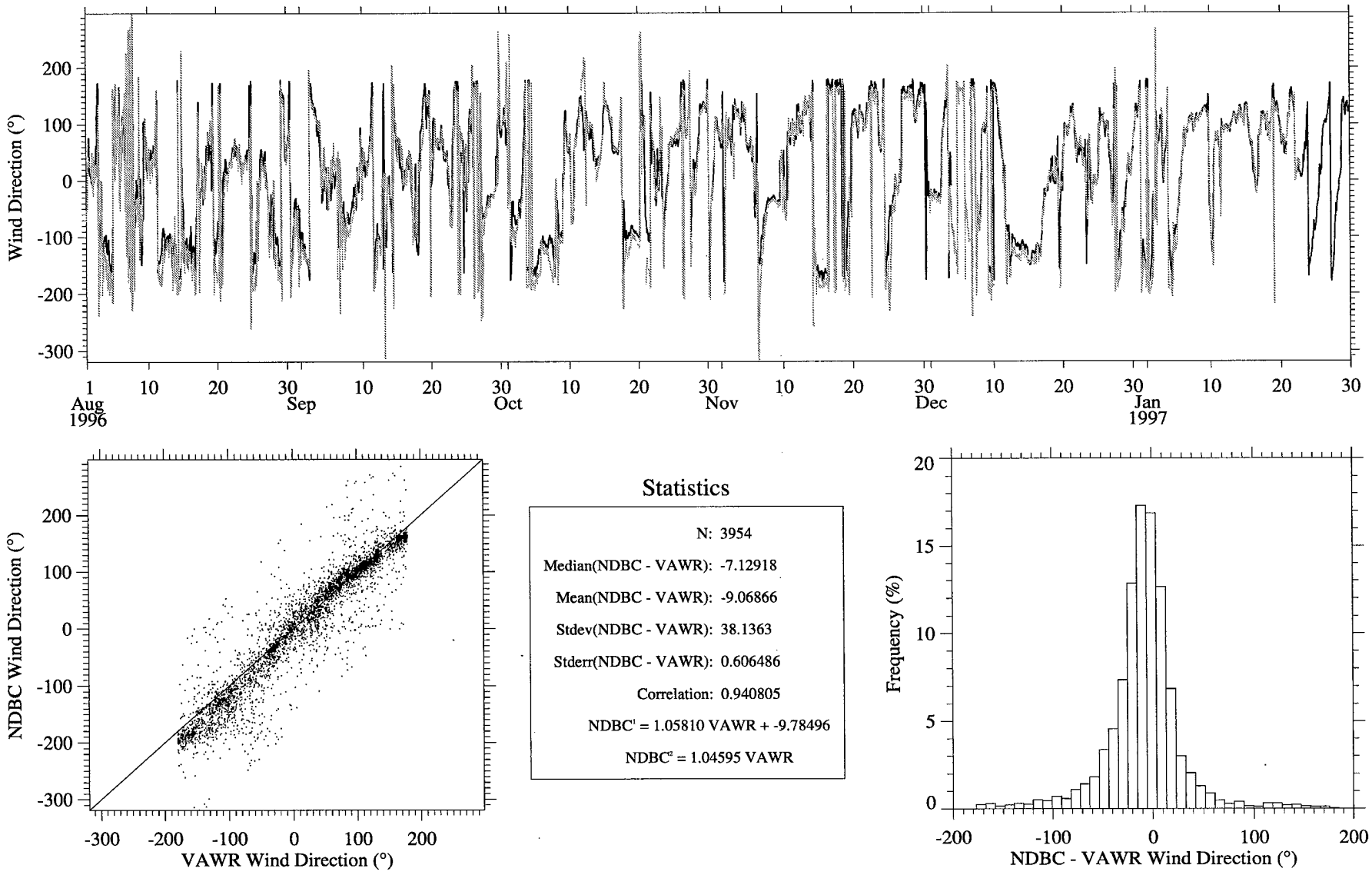

Figure B2. NDBC Buoy 44008 (gray) vs. CMO VAWR 0704 (black) wind direction.

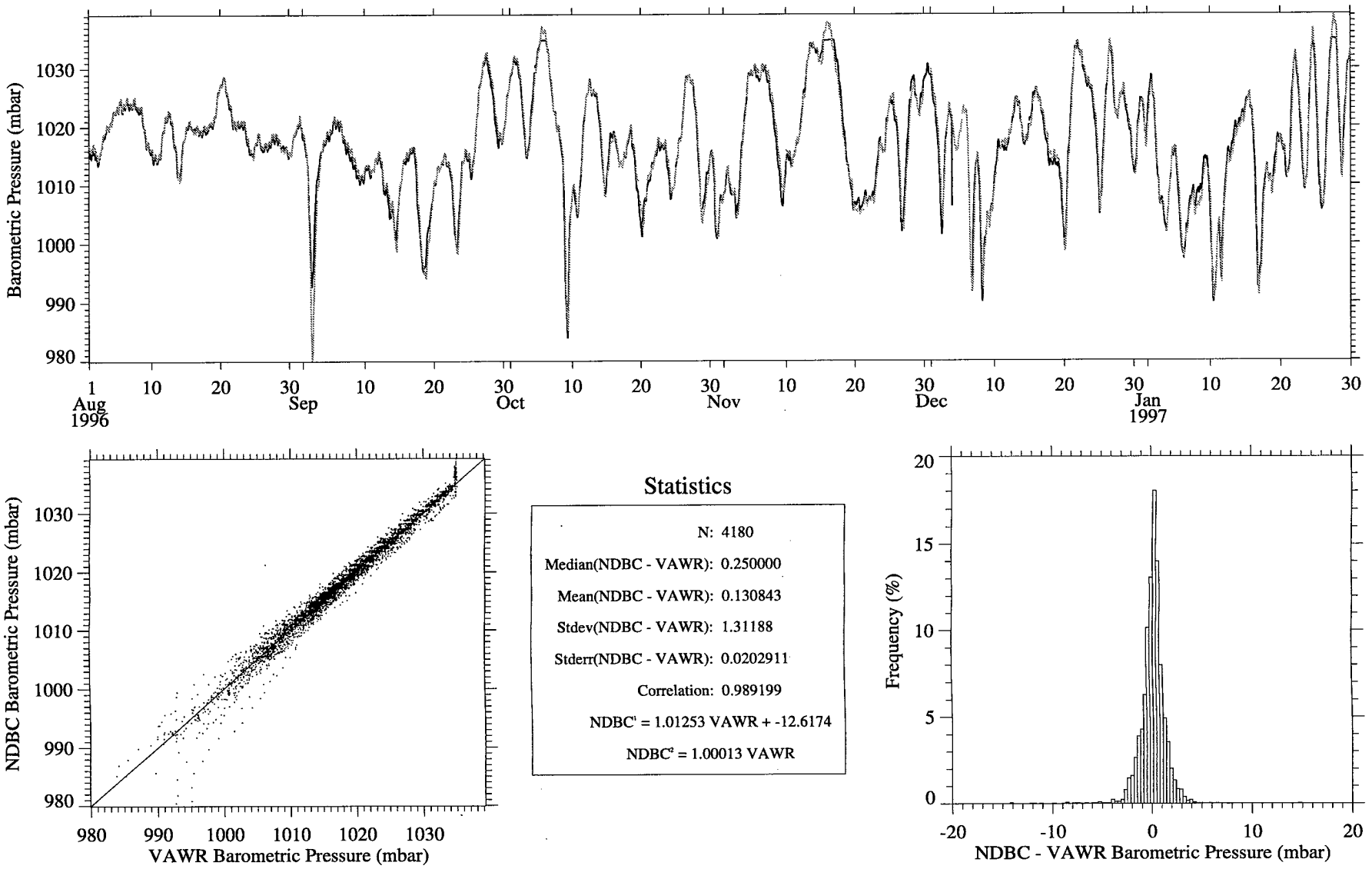

Figure B3. NDBC Buoy 44008 (gray) vs. CMO VAWR 0704 (black) barometric pressure.

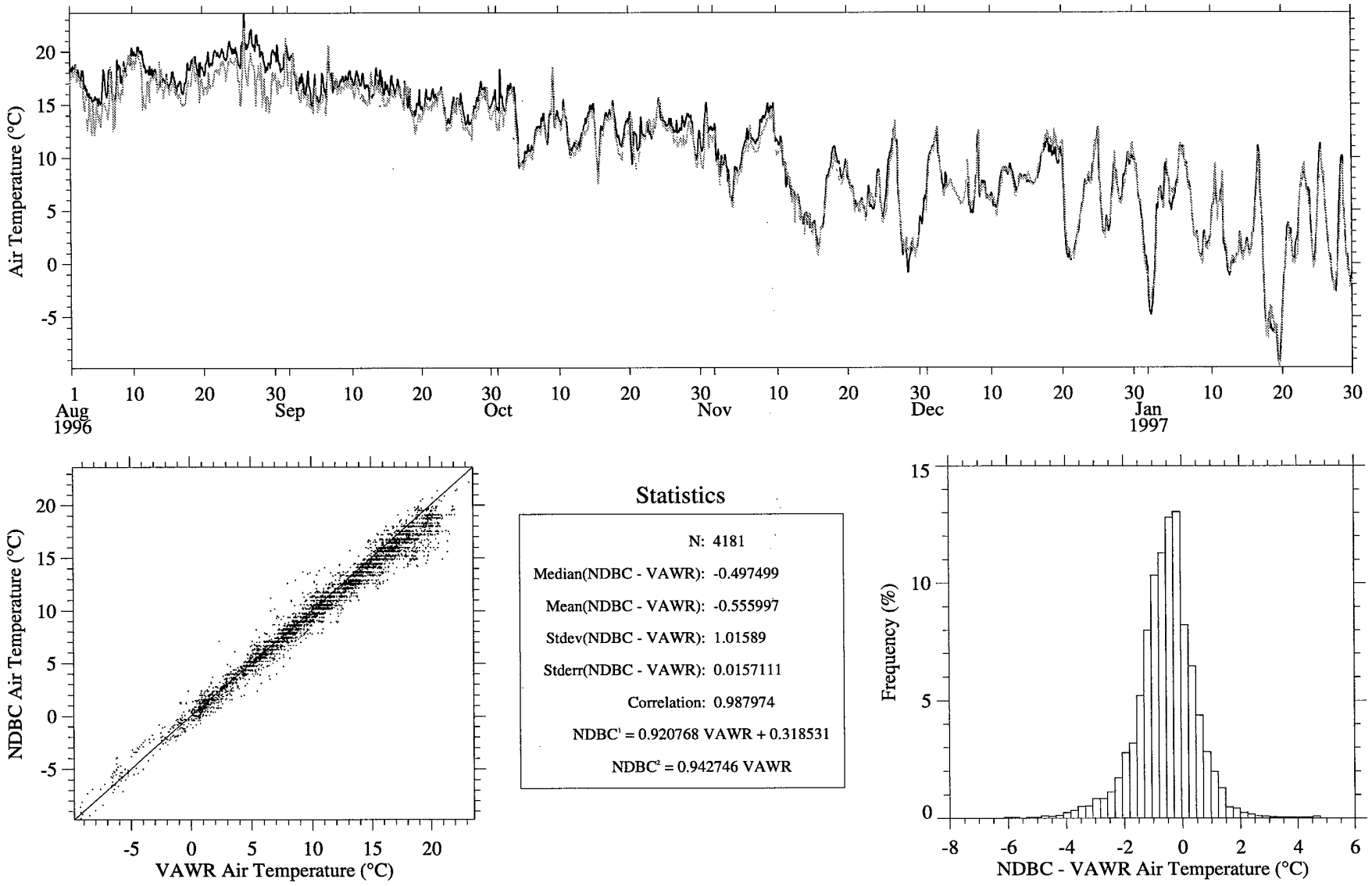

Figure B4. NDBC Buoy 44008 (gray) vs. CMO VAWR 0704 (black) air temperature.

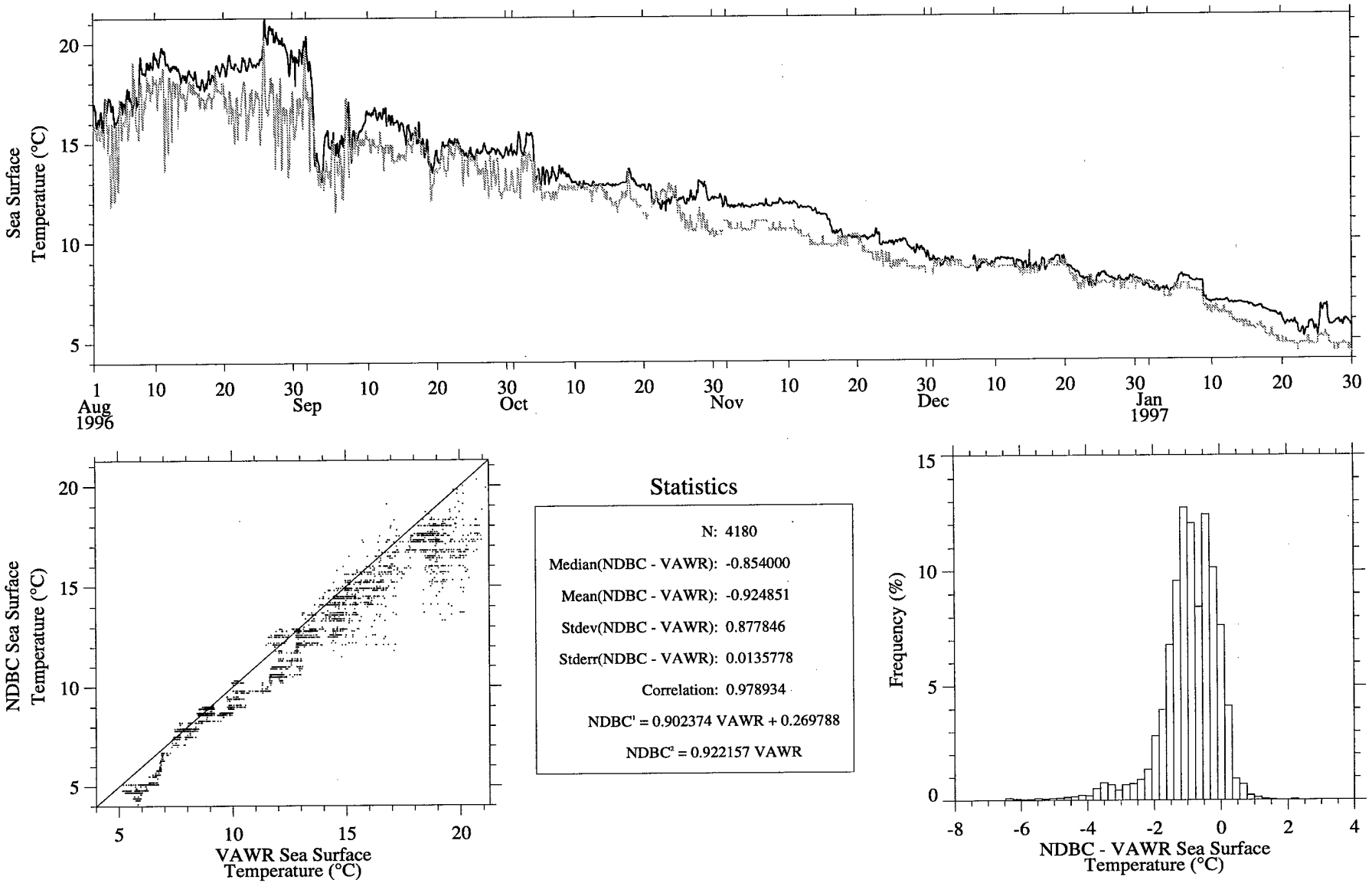

Figure B5. NDBC Buoy 44008 (gray) vs. CMO VAWR 0704 (black) sea surface temperature.

Appendix C: NetCDF formats for archived model data

Eta Model

The following is the NetCDF format (from the ncdump utility) of the Eta model archive file. This particular example is from the file 97022500eta.nc which is the Eta model data from the 25 February 1997 0000 model run. The data consists of the 0, 6, 12, 18 and 24 hour forecast data indexed by the dimension time.

```
netcdf 97022500eta {
dimensions:
        time = 5 ;
        y = 65 ;
        x = 93 ;
        nav = 1 ;
        nav_len = 100 ;
        accum = 2 ;

variables:
        char nav_model(nav, nav_len) ;
                nav_model:long_name = "navigation model name" ;
        long grid_type_code(nav) ;
                grid_type_code:long_name = "GRIB-1 GDS data representation type" ;
        char grid_type(nav, nav_len) ;
                grid_type:long_name = "GRIB-1 grid type" ;
        char grid_name(nav, nav_len) ;
                grid_name:long_name = "grid name" ;
        long grid_center(nav) ;
                grid_center:long_name = "GRIB-1 originating center ID" ;
        long grid_number(nav) ;
                grid_number:long_name = "GRIB-1 catalogued grid number" ;
        char earth_shape(nav, nav_len) ;
                earth_shape:long_name = "assumed earth shape" ;
        char x_dim(nav, nav_len) ;
                x_dim:long_name = "x dimension name" ;
        char y_dim(nav, nav_len) ;
                y_dim:long_name = "y dimension name" ;
        long Nx(nav) ;
                Nx:long_name = "number of points along x-axis" ;
        long Ny(nav) ;
                Ny:long_name = "number of points along y-axis" ;
        float La1(nav) ;
                La1:long_name = "latitude of first grid point" ;
                La1:units = "degrees_north" ;
        float Lo1(nav) ;
                Lo1:long_name = "longitude of first grid point" ;
                Lo1:units = "degrees_east" ;
        byte ResCompFlag(nav) ;
                ResCompFlag:long_name = "resolution and component flags" ;
        float Lov(nav) ;
                Lov:long_name = "orientation of the grid" ;
                Lov:units = "degrees_east" ;
        float Dx(nav) ;
                Dx:long_name = "x-direction grid length" ;
                Dx:units = "meters" ;
        float Dy(nav) ;
                Dy:long_name = "y-direction grid length" ;
                Dy:units = "meters" ;
        byte ProjFlag(nav) ;
                ProjFlag:long_name = "projection center flag" ;
        float Latin1(nav) ;
                Latin1:long_name = "first intersecting latitude" ;
                Latin1:units = "degrees_north" ;
        float Latin2(nav) ;
                Latin2:long_name = "second intersecting latitude" ;
                Latin2:units = "degrees_north" ;
        float SpLat(nav) ;
                SpLat:long_name = "latitude of the southern pole" ;
                SpLat:units = "degrees_north" ;
        float SpLon(nav) ;
                SpLon:long_name = "longitude of the southern pole" ;
                SpLon:units = "degrees_east" ;
```

```
        long time(time) ;
                time:units = "days" ;
                time:epic_code = 624 ;
        long time2(time) ;
                time2:units = "milliseconds since midnight" ;
                time2:epic_code = 624 ;
        float u(time, y, x) ;
                u:long_name = "u-component of wind at 10m" ;
                u:units = "meters/second" ;
                u:_FillValue = -9999.f ;
        float v(time, y, x) ;
                v:long_name = "v-component of wind at 10m" ;
                v:units = "meters/second" ;
                v:_FillValue = -9999.f ;
        float temp(time, y, x) ;
                temp:long_name = "temperature at 2m" ;
                temp:units = "degC" ;
                temp:_FillValue = -9999.f ;
        float rh(time, y, x) ;
                rh:long_name = "relative humidity at 2m" ;
                rh:units = "percent" ;
                rh:_FillValue = -9999.f ;
        float p(time, y, x) ;
                p:long_name = "pressure at surface" ;
                p:units = "mbar" ;
                p:_FillValue = -9999.f ;
        float psea(time, y, x) ;
                psea:long_name = "mean sea level pressure (ETA model reduction)" ;
                psea:units = "mbar" ;
                psea:_FillValue = -9999.f ;
        float precip(time, y, x) ;
                precip:long_name = "total precipitation over accumulation interval" ;
                precip:units = "kg/m^2" ;
                precip:_FillValue = -9999.f ;
        float precip_accum_times(time, accum) ;
                precip_accum_times:long_name = "precipitation accumulation interval" ;
                precip_accum_times:units = "hours" ;
                precip_accum_times:_FillValue = -9999.f ;
        float cin_sfc(time, y, x) ;
                cin_sfc:long_name = "surface convective inhibition" ;
                cin_sfc:units = "J/kg" ;
                cin_sfc:_FillValue = -9999.f ;
        float cape_sfc(time, y, x) ;
                cape_sfc:long_name = "surface convective available potential energy" ;
                cape_sfc:units = "J/kg" ;
                cape_sfc:_FillValue = -9999.f ;

// global attributes:
                :history = "created by gribtonc from HDS broadcast" ;
                :title = "NCEP Global Product Set" ;
                :Conventions = "NUWG" ;
                :version = 0. ;
                :model = "Eta" ;
}
```

RUC Model

The following is the NetCDF format of the RUC model archive file. This particular example is from the file `97022403ruc.nc` which is the RUC model data from the 24 February 1997 0300 model run. The data consists of the 0, 3, 6, 9 and 12 hour forecast data indexed by the dimension `time`.

```
netcdf 97022403ruc {
dimensions:
        time = 5 ;
        y = 65 ;
        x = 93 ;
        nav = 1 ;
        nav_len = 100 ;
        accum = 2 ;

variables:
        char nav_model(nav, nav_len) ;
                nav_model:long_name = "navigation model name" ;
        long grid_type_code(nav) ;
                grid_type_code:long_name = "GRIB-1 GDS data representation type" ;
        char grid_type(nav, nav_len) ;
                grid_type:long_name = "GRIB-1 grid type" ;
        char grid_name(nav, nav_len) ;
                grid_name:long_name = "grid name" ;
        long grid_center(nav) ;
                grid_center:long_name = "GRIB-1 originating center ID" ;
        long grid_number(nav) ;
                grid_number:long_name = "GRIB-1 catalogued grid number" ;
        char earth_shape(nav, nav_len) ;
                earth_shape:long_name = "assumed earth shape" ;
        char x_dim(nav, nav_len) ;
                x_dim:long_name = "x dimension name" ;
        char y_dim(nav, nav_len) ;
                y_dim:long_name = "y dimension name" ;
        long Nx(nav) ;
                Nx:long_name = "number of points along x-axis" ;
        long Ny(nav) ;
                Ny:long_name = "number of points along y-axis" ;
        float La1(nav) ;
                La1:long_name = "latitude of first grid point" ;
                La1:units = "degrees_north" ;
        float Lo1(nav) ;
                Lo1:long_name = "longitude of first grid point" ;
                Lo1:units = "degrees_east" ;
        byte ResCompFlag(nav) ;
                ResCompFlag:long_name = "resolution and component flags" ;
        float Lov(nav) ;
                Lov:long_name = "orientation of the grid" ;
                Lov:units = "degrees_east" ;
        float Dx(nav) ;
                Dx:long_name = "x-direction grid length" ;
                Dx:units = "km" ;
        float Dy(nav) ;
                Dy:long_name = "y-direction grid length" ;
                Dy:units = "km" ;
        byte ProjFlag(nav) ;
                ProjFlag:long_name = "projection center flag" ;
        float Latin1(nav) ;
                Latin1:long_name = "first intersecting latitude" ;
                Latin1:units = "degrees_north" ;
        float Latin2(nav) ;
                Latin2:long_name = "second intersecting latitude" ;
                Latin2:units = "degrees_north" ;
        float SpLat(nav) ;
                SpLat:long_name = "Latitude of the southern pole" ;
                SpLat:units = "degrees_north" ;
        float SpLon(nav) ;
                SpLon:long_name = "Longitude of the southern pole" ;
                SpLon:units = "degrees_east" ;
        long time(time) ;
                time:units = "days" ;
                time:epic_code = 624 ;
```

```
        long time2(time) ;
                time2:units = "milliseconds since midnight" ;
                time2:epic_code = 624 ;
        float u(time, y, x) ;
                u:long_name = "u-component of wind at 10m" ;
                u:units = "meters/second" ;
                u:_FillValue = -9999.f ;
        float v(time, y, x) ;
                v:long_name = "v-component of wind at 10m" ;
                v:units = "meters/second" ;
                v:_FillValue = -9999.f ;
        float temp(time, y, x) ;
                temp:long_name = "temperature at 2m" ;
                temp:units = "degC" ;
                temp:_FillValue = -9999.f ;
        float rh(time, y, x) ;
                rh:long_name = "relative humidity at 2m" ;
                rh:units = "percent" ;
                rh:_FillValue = -9999.f ;
        float p(time, y, x) ;
                p:long_name = "pressure at surface" ;
                p:units = "mbar" ;
                p:_FillValue = -9999.f ;
        float psea(time, y, x) ;
                psea:long_name = "mean sea level pressure (MAPS reduction)" ;
                psea:units = "mbar" ;
                psea:_FillValue = -9999.f ;
        float precip(time, y, x) ;
                precip:long_name = "total precipitation over accumulation interval" ;
                precip:units = "kg/m^2" ;
                precip:_FillValue = -9999.f ;
        float precip_accum_times(time, accum) ;
                precip_accum_times:long_name = "precipitation accumulation interval" ;
                precip_accum_times:units = "hours" ;
                precip_accum_times:_FillValue = -9999.f ;

// global attributes:
                :history = "created by gribtonc from HDS broadcast" ;
                :title = "RUC/MAPS model, from Forecast Systems Lab" ;
                :Conventions = "NUWG" ;
                :version = 0. ;
                :model = "RUC" ;
}
```

RUC Analysis

The following is the NetCDF format of the RUC Analysis archive file. This particular example is from the file `97022403rucanl.nc` which is the RUC Analysis from the 24 February 1997 0300 model run. The data consists of the analysis data only, which is indexed by the dummy dimension `record`.

```
netcdf 97022403rucanl {
dimensions:
        record = 1 ;
        x = 81 ;
        y = 62 ;
        nav = 1 ;
        nav_len = 100 ;

variables:
        char nav_model(nav, nav_len) ;
                nav_model:long_name = "navigation model name" ;
        long grid_type_code(nav) ;
                grid_type_code:long_name = "GRIB-1 GDS data representation type" ;
        char grid_type(nav, nav_len) ;
                grid_type:long_name = "GRIB-1 grid type" ;
        char grid_name(nav, nav_len) ;
                grid_name:long_name = "grid name" ;
        long grid_center(nav) ;
                grid_center:long_name = "GRIB-1 originating center ID" ;
        long grid_number(nav) ;
                grid_number:long_name = "GRIB-1 catalogued grid number" ;
        char earth_shape(nav, nav_len) ;
                earth_shape:long_name = "assumed earth shape" ;
        char x_dim(nav, nav_len) ;
                x_dim:long_name = "x dimension name" ;
        char y_dim(nav, nav_len) ;
                y_dim:long_name = "y dimension name" ;
        long Nx(nav) ;
                Nx:long_name = "number of points along x-axis" ;
        long Ny(nav) ;
                Ny:long_name = "number of points along y-axis" ;
        float La1(nav) ;
                La1:long_name = "latitude of first grid point" ;
                La1:units = "degrees_north" ;
        float Lo1(nav) ;
                Lo1:long_name = "longitude of first grid point" ;
                Lo1:units = "degrees_east" ;
        byte ResCompFlag(nav) ;
                ResCompFlag:long_name = "resolution and component flags" ;
        float Lov(nav) ;
                Lov:long_name = "orientation of the grid" ;
                Lov:units = "degrees_east" ;
        float Dx(nav) ;
                Dx:long_name = "x-direction grid length" ;
                Dx:units = "km" ;
        float Dy(nav) ;
                Dy:long_name = "y-direction grid length" ;
                Dy:units = "km" ;
        byte ProjFlag(nav) ;
                ProjFlag:long_name = "projection center flag" ;
        float Latin1(nav) ;
                Latin1:long_name = "first intersecting latitude" ;
                Latin1:units = "degrees_north" ;
        float Latin2(nav) ;
                Latin2:long_name = "second intersecting latitude" ;
                Latin2:units = "degrees_north" ;
        float SpLat(nav) ;
                SpLat:long_name = "Latitude of the southern pole" ;
                SpLat:units = "degrees_north" ;
        float SpLon(nav) ;
                SpLon:long_name = "Longitude of the southern pole" ;
                SpLon:units = "degrees_east" ;
        long time(record) ;
                time:units = "Julian days" ;
                time:epic_code = 624 ;
```

```
        long time2(record) ;
                time2:units = "milliseconds" ;
                time2:epic_code = 624 ;
        float pot(record, y, x) ;
                pot:long_name = "potential temperature" ;
                pot:units = "deg C" ;
        float hybl_bp(record, y, x) ;
                hybl_bp:long_name = "hybrid level 1 pressure" ;
                hybl_bp:units = "mbars" ;
        float hybl_condp(record, y, x) ;
                hybl_condp:long_name = "hybrid level 1 condensation pressure" ;
                hybl_condp:units = "mbars" ;
        float u(record, y, x) ;
                u:long_name = "east wind" ;
                u:units = "m/s" ;
        float v(record, y, x) ;
                v:long_name = "north wind" ;
                v:units = "m/s" ;
        float bp(record, y, x) ;
                bp:long_name = "mean sea level pressure (MAPS system reduction)" ;
                bp:units = "mbars" ;
        float pwater(record, y, x) ;
                pwater:long_name = "precipitable water" ;
                pwater:units = "kg/m^2" ;
        float cape(record, y, x) ;
                cape:long_name = "convective available potential energy" ;
                cape:units = "J/kg" ;
        float cin(record, y, x) ;
                cin:long_name = "convective inhibition" ;
                cin:units = "J/kg" ;

// global attributes:
                :history = "created by unpkgrb_to_ncdf from NCEP archive" ;
                :title = "RUC/MAPS model, from Forecast Systems Lab" ;
}
```

RUC Hourly

The following is the NetCDF format of the RUC Hourly archive file. This particular example is from the file `97022409rucflux.nc` which contains some of the RUC Hourly model data from the 24 February 1997 0600 model run. The data consists of the 3 hour forecast only, indexed by the dummy variable `record`. For this same model run, the files `97022407rucflux.nc` and `97022408rucflux.nc` were also archived. These two files contain the 1 and 2 hour forecasts from the same model run, respectively.

```
netcdf 97022409rucflux {
dimensions:
        record = 1 ;
        x = 81 ;
        y = 62 ;
        nav = 1 ;
        nav_len = 100 ;

variables:
        char nav_model(nav, nav_len) ;
                nav_model:long_name = "navigation model name" ;
        long grid_type_code(nav) ;
                grid_type_code:long_name = "GRIB-1 GDS data representation type" ;
        char grid_type(nav, nav_len) ;
                grid_type:long_name = "GRIB-1 grid type" ;
        char grid_name(nav, nav_len) ;
                grid_name:long_name = "grid name" ;
        long grid_center(nav) ;
                grid_center:long_name = "GRIB-1 originating center ID" ;
        long grid_number(nav) ;
                grid_number:long_name = "GRIB-1 catalogued grid number" ;
        char earth_shape(nav, nav_len) ;
                earth_shape:long_name = "assumed earth shape" ;
        char x_dim(nav, nav_len) ;
                x_dim:long_name = "x dimension name" ;
        char y_dim(nav, nav_len) ;
                y_dim:long_name = "y dimension name" ;
        long Nx(nav) ;
                Nx:long_name = "number of points along x-axis" ;
        long Ny(nav) ;
                Ny:long_name = "number of points along y-axis" ;
        float La1(nav) ;
                La1:long_name = "latitude of first grid point" ;
                La1:units = "degrees_north" ;
        float Lo1(nav) ;
                Lo1:long_name = "longitude of first grid point" ;
                Lo1:units = "degrees_east" ;
        byte ResCompFlag(nav) ;
                ResCompFlag:long_name = "resolution and component flags" ;
        float Lov(nav) ;
                Lov:long_name = "orientation of the grid" ;
                Lov:units = "degrees_east" ;
        float Dx(nav) ;
                Dx:long_name = "x-direction grid length" ;
                Dx:units = "km" ;
        float Dy(nav) ;
                Dy:long_name = "y-direction grid length" ;
                Dy:units = "km" ;
        byte ProjFlag(nav) ;
                ProjFlag:long_name = "projection center flag" ;
        float Latin1(nav) ;
                Latin1:long_name = "first intersecting latitude" ;
                Latin1:units = "degrees_north" ;
        float Latin2(nav) ;
                Latin2:long_name = "second intersecting latitude" ;
                Latin2:units = "degrees_north" ;
        float SpLat(nav) ;
                SpLat:long_name = "Latitude of the southern pole" ;
                SpLat:units = "degrees_north" ;
        float SpLon(nav) ;
                SpLon:long_name = "Longitude of the southern pole" ;
                SpLon:units = "degrees_east" ;
```

```
        long time(record) ;
               time:units = "Julian days" ;
               time:epic_code = 624 ;
        long time2(record) ;
               time2:units = "milliseconds" ;
               time2:epic_code = 624 ;
        float pot(record, y, x) ;
               pot:long_name = "potential temperature" ;
               pot:units = "deg C" ;
        float hybl_bp(record, y, x) ;
               hybl_bp:long_name = "hybrid level 1 pressure" ;
               hybl_bp:units = "mbars" ;
        float hybl_condp(record, y, x) ;
               hybl_condp:long_name = "hybrid level 1 condensation pressure" ;
               hybl_condp:units = "mbars" ;
        float u(record, y, x) ;
               u:long_name = "east wind" ;
               u:units = "m/s" ;
        float v(record, y, x) ;
               v:long_name = "north wind" ;
               v:units = "m/s" ;
        float bp(record, y, x) ;
               bp:long_name = "mean sea level pressure (MAPS system reduction)" ;
               bp:units = "mbars" ;
        float temp(record, y, x) ;
               temp:long_name = "surface air temperature" ;
               temp:units = "deg C" ;
        float Qs(record, y, x) ;
               Qs:long_name = "sensible heat flux" ;
               Qs:units = "W/m^2" ;
        float Ql(record, y, x) ;
               Ql:long_name = "latent heat flux" ;
               Ql:units = "W/m^2" ;
        float Qrad(record, y, x) ;
               Qrad:long_name = "global radiation" ;
               Qrad:units = "W/m^2" ;
        float prate(record, y, x) ;
               prate:long_name = "precipitation rate" ;
               prate:units = "kg/m^2/s" ;
        float nprecip(record, y, x) ;
               nprecip:long_name = "large scale precipitation (non-convective)" ;
               nprecip:units = "kg/m^2" ;
        float cprecip(record, y, x) ;
               cprecip:long_name = "convective precipitation" ;
               cprecip:units = "kg/m^2" ;
        float pwater(record, y, x) ;
               pwater:long_name = "precipitable water" ;
               pwater:units = "kg/m^2" ;
        float cape(record, y, x) ;
               cape:long_name = "convective available potential energy" ;
               cape:units = "J/kg" ;
        float cin(record, y, x) ;
               cin:long_name = "convective inhibition" ;
               cin:units = "J/kg" ;

// global attributes:
               :history = "created by unpkgrb_to_ncdf from NCEP archive" ;
               :title = "RUC/MAPS model, from Forecast Systems Lab" ;
}
```

Appendix D: Bibliography

Benjamin, S.G., 1989. An isentropic mesoα-scale analysis system and its sensitivity to aircraft and surface observations. *Monthly Weather Review.* **117**, 1586–1603.

Benjamin, S.G. and P.A. Miller, 1990. An alternative sea level pressure reduction and a statistical comparison of geostrophic wind estimates with observed surface winds. *Monthly Weather Review.* **118**, 2099–2116.

Benjamin, S.G., K.J. Brundage and L.L. Morone, 1994. The rapid update cycle. Part I: Analysis/model description. NOAA/NWS Technical Procedures Bulletin No. 416. 16 pp. [Available from National Weather Service, Office of Meteorology, 1325 East-West Highway, Silver Springs, MD 20910].

Black, T.L., 1994. The new NMC mesoscale Eta model: Description and forecast examples. *Weather and Forecasting.* **9**, 265–278.

Bleck, R. and S.G. Benjamin, 1993. Regional weather prediction with a model combining terrain-following and isentropic coordinates. Part I: Model description. *Monthly Weather Review.* **121**, 1770–1785.

Dévényi, D. and T.W. Schlatter, 1994. Statistical properties of three-hour prediction "errors" derived from the mesoscale analysis and prediction system. *Monthly Weather Review.* **122**, 1263–1280.

Miller, P.A. and S.G. Benjamin, 1992. A system for the hourly assimilation of surface observations in mountainous and flat terrain. *Monthly Weather Review.* **120**, 2342–2359.

Pan, Z., S.G. Benjamin, J.M. Brown and T. Smirnova, 1994. Comparative experiments with MAPS on different parameterization schemes for surface moisture flux and boundary-layer processes. *Monthly Weather Review.* **122**, 449–470.

Also, see *www.fsl.noaa.gov/frd-bin/MAPS.pubs.cgi* for a comprehensive bibliography for the RUC model.

Appendix E: WWW Resources

Unfortunately, there is no single source of information for describing, acquiring, decoding and using forecasting models. Relevant information is scattered far and wide. Here are a few links that will help you get started:

Model Information	
Forecast Systems Laboratory	*www.fsl.noaa.gov*
MAPS/RUC homepage at FSL	*www.fsl.noaa.gov/frd-bin/MAPS.homepage.cgi*
NCEP	*www.ncep.noaa.gov*
NCEP Environmental Modeling Center	*nic.fb4.noaa.gov:8000*
Instructions for downloading RUC data from the NIC	*www.fsl.noaa.gov/frd-bin/MAPS.rucinfo.cgi*
Comprehensive bibliography of RUC publications	*www.fsl.noaa.gov/frd-bin/MAPS.pubs.cgi*
On-line version of the RUC technical manual	*www.fsl.noaa.gov/frd-bin/tpbruc.cgi*
Change log for MAPS/RUCS	*www.fsl.noaa.gov/frd-bin/MAPS.60changelog.cgi*
LDM Information	
Unidata	*www.unidata.ucar.edu*
Overview of LDM from 1996 LDM Workshop	*www.unidata.ucar.edu/packages/ldm/ws/ws.html*
Data recovery from the IDD	*www.unidata.ucar.edu/data/recovery.html*
NetCDF Information	*www.unidata.ucar.edu/packages/netcdf/index.html*
Data Sources (FTP)	
NOAA Information Center	*nic.fb4.noaa.gov*
National Data Buoy Center	*seaboard.ndbc.noaa.gov*
GRIB	
GRIB manual	*nic.fb4.noaa.gov/pub/nws/nmc/docs/gribed1*
GRIB unpacking software	*nic.fb4.noaa.gov/pub/info*

Appendix F: Acronyms

AVN	Aviation model
CMO	Coastal Mixing and Optics Experiment
ECMWF	European Centre for Medium-Range Weather Forecasts
FOS	Family of Services
FTP	File Transfer Program
GOES	Geosynchronous Operational Environmental Satellite
IDD	Internet Data Distribution system
LDM	Local Data Manager
MAPS	Mesoscale Analysis and Prediction System
MRF	Medium Range Forecast model
NCEP	National Centers for Environmental Prediction
NDBC	National Data Buoy Center
NetCDF	Network Common Data Form
NEXRAD	Next Generation Weather Radar
NGM	Nested Grid Model
NIC	NOAA Information Center
NMC	National Meteorological Center
NOAA	National Oceanic and Atmospheric Administration
NWS	National Weather Service
RSM	Regional Spectral Model
RUC	Rapid Update Cycle model
TOGA COARE	Tropical Ocean Global Atmosphere Coupled Ocean-Atmosphere Response Experiment
UPS	Uninterruptible Power Supply
VAWR	Vector Averaging Wind Recorder
WHOI	Woods Hole Oceanographic Institution

DOCUMENT LIBRARY

Distribution List for Technical Report Exchange – February 1996

University of California, San Diego
SIO Library 0175C
9500 Gilman Drive
La Jolla, CA 92093-0175

Hancock Library of Biology & Oceanography
Alan Hancock Laboratory
University of Southern California
University Park
Los Angeles, CA 90089-0371

Gifts & Exchanges
Library
Bedford Institute of Oceanography
P.O. Box 1006
Dartmouth, NS, B2Y 4A2, CANADA

Commander
International Ice Patrol
1082 Shennecossett Road
Groton, CT 06340-6095

NOAA/EDIS Miami Library Center
4301 Rickenbacker Causeway
Miami, FL 33149

Research Library
U.S. Army Corps of Engineers
Waterways Experiment Station
3909 Halls Ferry Road
Vicksburg, MS 39180-6199

Institute of Geophysics
University of Hawaii
Library Room 252
2525 Correa Road
Honolulu, HI 96822

Marine Resources Information Center
Building E38-320
MIT
Cambridge, MA 02139

Library
Lamont-Doherty Geological Observatory
Columbia University
Palisades, NY z10964

Library
Serials Department
Oregon State University
Corvallis, OR 97331

Pell Marine Science Library
University of Rhode Island
Narragansett Bay Campus
Narragansett, RI 02882

Working Collection
Texas A&M University
Dept. of Oceanography
College Station, TX 77843

Fisheries-Oceanography Library
151 Oceanography Teaching Bldg.
University of Washington
Seattle, WA 98195

Library
R.S.M.A.S.
University of Miami
4600 Rickenbacker Causeway
Miami, FL 33149

Maury Oceanographic Library
Naval Oceanographic Office
Building 1003 South
1002 Balch Blvd.
Stennis Space Center, MS, 39522-5001

Library
Institute of Ocean Sciences
P.O. Box 6000
Sidney, B.C. V8L 4B2
CANADA

National Oceanographic Library
Southampton Oceanography Centre
European Way
Southampton SO14 3ZH
UK

The Librarian
CSIRO Marine Laboratories
G.P.O. Box 1538
Hobart, Tasmania
AUSTRALIA 7001

Library
Proudman Oceanographic Laboratory
Bidston Observatory
Birkenhead
Merseyside L43 7 RA
UNITED KINGDOM

IFREMER
Centre de Brest
Service Documentation - Publications
BP 70 29280 PLOUZANE
FRANCE

50272-101

REPORT DOCUMENTATION PAGE	1. REPORT NO. WHOI-97-02	2.	3. Recipient's Accession No.

4. Title and Subtitle
Acquisition, Description and Evaluation of Atmospheric Model Products for the Coastal Mixing and Optics Experiment

5. Report Date
March 1997

6.

7. Author(s) Mark F. Baumgartner and Steven P. Anderson

8. Performing Organization Rept. No.
WHOI-97-02

9. Performing Organization Name and Address

Woods Hole Oceanographic Institution
Woods Hole, Massachusetts 02543

10. Project/Task/Work Unit No.

11. Contract(C) or Grant(G) No.
(C) N00014-95-1-0339
(G)

12. Sponsoring Organization Name and Address

Office of Naval Research

13. Type of Report & Period Covered
Technical Report

14.

15. Supplementary Notes
This report should be cited as: Woods Hole Oceanog. Inst. Tech. Rept., WHOI-97-02.

16. Abstract (Limit: 200 words)

Numerical weather forecasting model products were acquired for use in the Coastal Mixing and Optics (CMO) Experiment to augment in situ observations of meteorological parameters (e.g., wind speed and direction, air temperature and relative humidity) at a moored array of buoys in the Middle Atlantic Bight. In this report, the Eta and Rapid Update Cycle (RUC) regional models are described and the two methods of acquisition via the Internet, the Internet Data Distribution (IDD) system and file transfer (FTP) from the NOAA Information Center's data server, are discussed. Processing and archival of the model data are also addressed. Data from the CMO central mooring and six National Data Buoy Center (NDBC) buoys in the Middle Atlantic bight were used to evaluate the accuracy of the model products. Comparisons between model and in situ wind speed, wind direction, barometric pressure, air temperature and sea surface temperature were possible for all seven of the buoys. Since no moisture measurement was made from the NDBC buoys, comparisons of relative and specific humidity were only possible at the CMO buoy. Sensible and latent heat fluxes and global (net) radiation from the models were compared to estimates of heat fluxes and net radiation from the CMO central buoy.

17. Document Analysis a. Descriptors
air-sea interaction
moored data
numerical weather forecasting models

b. Identifiers/Open-Ended Terms

c. COSATI Field/Group

18. Availability Statement
Approved for public release; distribution unlimited.

19. Security Class (This Report)
UNCLASSIFIED

20. Security Class (This Page)

21. No. of Pages
196

22. Price

(See ANSI-Z39.18) *See Instructions on Reverse*

OPTIONAL FORM 272 (4-77)
(Formerly NTIS-35)
Department of Commerce